BERICHTE
aus dem
INSTITUT FÜR MEERESKUNDE
an der
CHRISTIAN-ALBRECHTS-UNIVERITÄT
Nr. 265

Proceedings of the International COADS Winds Workshop, Kiel, Germany, 31 May - 2 June 1994

Editors:

Henry F. Diaz,

ans-Jörg Isemer

May 1995

DOI 10.3289/IFM_BER_265

ENT OF COMMERCE
TATES OF AMERICA

U.S. Department of Commerce
National Oceanic and Atmospheric Administration
Environmental Research Laboratories
Climate Diagnostics Center

Institut für Meereskunde • Kiel

NOTICE

Mention of a commercial product does not constitute an endorsement by NOAA/ERL. Use for publicity or advertising purposes, of information from this publication concerning proprietary products or the tests of such products, is not authorized.

Cover Panel: Northern winter season surface wind fields for the Atlantic and Indian Oceans. Color bar is for scalar winds, arrows denote vector mean winds; 10 m/s vector indicated by arrow above color scalar wind scale.

Acknowledgments

We are grateful to Vera Hebert and to Beverly O'Donnell for assistance in preparations for the workshop, and for helping all the participants with their travel needs and attending to many other logistical details. Craig Anderson helped with the editing process, which involved converting all of the individual manuscripts and styles to a uniform standard. We also thank Klaus Wolter and Scott Woodruff for careful reviews of the final volume of manuscripts.

The workshop was generously suppported by the Institut für Meereskunde of the University of Kiel, Germany, through a grant from the German Research Foundation project titled "Warmwatersphere of the Atlantic Ocean," and by a grant from the NOAA Office of Global Programs. The editors gratefully acknowledge their continuing support.

Contents

Part IV. Applications and Data Improvements

Workshop Participants

Dr. Rob Allan
Climate Impact Group
CSIRO Division of Atmospheric Research
PMB No 1
Mordialloc 3195 Victoria
AUSTRALIA
Phone: +61 3 586 7540
Fax: +61 3 586 7600
e-mail: rja@dar.csiro.au

Dr. Claus Böning
Institut für Meereskunde
Düsternbrooker Weg 20
D-24105 Kiel
GERMANY
Phone: +49 431 5973885
Fax: +49 431 565876
e-mail: cboening@meereskunde.uni-kiel.d400.de

Dr. Henry F. Diaz
NOAA/ERL/CDC (R/E/CD)
325 Broadway
Boulder, CO 80303
USA
Phone: +1 303-497-6649
Fax: +1 303-497-7013
e-mail: hfd@noaacdc.Colorado.edu

Mr. Joe D. Elms
Global Climate Laboratory
National Climatic Data Center
151 Patton Ave., Rm 120
Asheville, NC 28801-5001
USA
Phone: +1 704-271-4344
Fax: +1 704-271-4328
e-mail: jelms@ncdc.nOaa.gov

Dr. Joseph O. Fletcher
NOAA/ERL (R/E)
325 Broadway
Boulder, CO 80303
USA
Phone: +1 303-497-6000
Fax: +1 303-497-6951

Dr. Fredric A. Godshall
Science Applications International Corp.
EPA-ERL, 27 Tarzwell Drive
Narrangansett, RI 02874
USA
Phone: +1 401-782-3197
Fax: +1 401-782-3070

Dr. Sergey Gulev
Shirshov Institute of Oceanology RAS
Krasikova Str.,23
117218 Moscow, Russia
Phone: (095) 1291972, 2462889
Telex: 411968 OKEAN SU
Fax: (095) 1245983
e-mail: gulev.boba@omnet.com

Mr. Fernando Guzman
Ocean Affairs Division
World Weather Watch Department
World Meteorological Organization
41, Avenue Giuseppe-Motta
Case postale No 2300
CH-1211 Geneve 2
Switzerland
Phone: +41 22 7308111
Fax: +41 22 7330242

Dr. Donald Hansen
CIMAS
University of Miami
4600 Rickenbacker Causeway
Miami, FL 33149
USA
Phone: +1 305-361-4346
Fax: +1 305-361-4582
e-mail: hansen@ocean.aoml.erl.gov

Dr. Lutz Hasse
Institut fuer Meereskunde
Duesternbrooker Weg 20
D-24105 Kiel, Germany
Phone: +49 431 5973870
Fax: +49-431-565876
e-mail: lhasse@meereskunde.uni-kiel.d400.de

Dr. Hans-Jörg Isemer
GKSS - Research Center - Institute for Atmospheric Physics
Max Planck Strasse
D-21502 Geesthacht
GERMANY
Phone: +49 4152 871536
Fax: +49 4152 872020
e-mail: isemer@gkss.de

Dr. Lothar Kaufeld
Seewetteramt
Bernhard-Nocht Strasse 76
D-20359 Hamburg
GERMANY
Phone: +49 40 3190 8823
Fax: +49 40 3190 8803

Dr. Elizabeth Kent
James Rennell Centre for Ocean Circulation
Gamma House, Chilworth Research Centre
Chilworth, Southampton SO1 7NS
UNITED KINGDOM
Phone: +44 0703 766184
Fax: +44 0703 767507
e-mail: eck@unixb.nerc-southampton.ac.uk

Dr. Yochanan Kushnir
Lamont-Doherty Geological Observatory
Columbia University
Route 9W
Palisades, NY 10964
USA
Phone: +1 914-359-2900 ext. 669
Fax: +1 914 365-8736
e-mail: kushnir@lamont.ldgo.columbia.edu

Dr. Ralf Lindau
Institut fuer Meereskunde
Duesternbrooker Weg 20
D-24105 Kiel
GERMANY
Phone: +49 431 5973873
Fax: +49 431 565876
e-mail: hjisemer@meereskunde.uni-kiel.d400.de

Dr. Jose Maliekal
Department. of the Earth Sciences
SUNY College at Brockport
Brockport, NY 14420
USA
Phone: +1 716-395-2582
Fax: +1 716-395-2416
e-mail: jmalieka@acsprl.acs.brockport.edu

Dr. Mark L. Morrissey
Oklahoma Climatological Survey
University of Oklahoma
Sarkeys Energy Center, Suite 1210
100 East Boyd
Norman, OK 730190628
USA
Phone: +1 405-325-2541
Fax: +1 405-325-2550
e-mail: mmorriss@alliant.backbone.uoknor.edu

Prof. James J. O'Brien
Center for Ocean Atmosphere Prediction Studies
Mail Stop B-174 Room 012, Love Building
Florida State University
Tallahassee, FL 32306-3041, USA
Phone: +1 904-644-4581
e-mail: obrien@masig.fsu.edu

Mr. Xiaowei Quan
CIRES, CB 449
University of Colorado
Boulder, CO 80309-0449
USA
Phone: +1 303-492-5961
e-mail: qxw@noaacdc.colorado.edu

Mr. Heiner Schmidt
Seewetteramt
Bernhard-Nocht Strasse 76
D-20359 Hamburg
GERMANY
Phone: +49 40 3190 8822
Fax: +49 40 3190 8803
e-mail: heiner.schmidt@swa-m2.hamburg.bsh.d400.de

Dr. Arlindo M. da Silva
Data Assimilation Office
NASA/GSFC
7501 Forbes Blvd., Suite 200
Seabrook, MD 20706
USA
Phone: +1 301 805-7959
Fax: +1 301 805-7960
e-mail: dasilva@schemm.gsfc.nasa.gov

Mr. Geoff Smith
The Meteorological Office
Met O OP, Room 131
London Road
Bracknell, Berkshire RG12 2SZ
UNITED KINGDOM
Phone: + 44 0344 854627
Fax: +44 0344 856412
e-mail: jballentine@email.meto.govt.uk

Dr. Val R. Swail
Canadian Climate Centre
4905 Dufferin Street
Downsview, Ontario M3H 5T4
CANADA
Phone: (416) 739-4347
Fax: (416) 739-4297
e-mail: vswail@dow.on.doe.ca

Dr. Peter K. Taylor
James Rennell Centre for Ocean Circulation
Gamma House, Chilworth Research Centre
Chilworth, Southampton SO1 7NS
UNITED KINGDOM
Fax: +44 0703 767507
e-mail: pkt@unixb.nerc-southampton.ac.uk

Dr. Volker Wagner
Seewetteramt
Bernhard-Nocht Strasse 76
D-20359 Hamburg
GERMANY
Phone: +49 40 3190 8821
Fax: +49 40 3190 8803

Dr. M. Neil Ward
Hadley Centre for Climate Prediction and Research
Meteorological Office
London Road
Bracknell Berkshire RG12 2SY
UNITED KINGDOM
Phone: +44 344 856080
Fax: +44 344 854898
e-mail: mnward@email.meto.govt.uk

Dr. Erik Wishman
Museum of Archaeology
P.O. Box 478
N-4001 Stavanger
NORWAY
Phone: +47 51534140
Fax: +47 51531181

Mr. Scott D. Woodruff
NOAA/ERL (R/E/CD)
325 Broadway Boulder, CO 80303
USA
Phone: +1 303497-6747
Fax: +1 303-497-7013
e-mail: sdw@noaacdc.colorado.edu

Dr. Zhongxiang Wu
Dept. of Earth, Atmospheric, and Planetary Sciences
Massachusetts Institute of Technology
Cambridge, MA 02139
USA
Phone: 617-253-2290
Fax: 607-2536208
e-mail: zhong@newell3.mit.edu

Ms. Christine C. Young
National Oceanographic Data Center
Ocean Climate Laboratory - Rm 426
1825 Connecticut Ave., NW
Washington, DC 20235
USA
Phone; +1 202 606-1043
Fax: +1 202 606-4586
e-mail: ccy@nodc.noaa.gov

Preface

An *International COADS Winds Workshop* was held during 31 May to June 2, 1994 at the Institut für Meereskunde in Kiel, Germany. Financial support was provided by the National Oceanic and Atmospheric Administration (NOAA) through its Office of Global Programs, and from the German Research Foundation Project "Warmwatersphere of the Atlantic Ocean."

The workshop had as its main objective to evaluate the quality of the marine surface winds in the global surface marine data archive known as COADS (for Comprehensive Ocean-Atmosphere Data Set), and to ascertain the usefulness of the products derived from the basic wind measurements. Papers were solicited in the area of documentation of sources of observational errors and biases, on work done to evaluate past and current observational methods and data processing procedures, and to evaluate how useful the data set is for climatological and climate change studies. In addition, the organizers of the workshop hoped to gather input from a broad cross-section of COADS users to help improve future COADS Releases and products, to promote greater communication and to foster cooperation among COADS users.

Surface wind data are needed to calculate the fluxes of momentum, sensible and latent heat and water substance at the ocean-atmosphere interface. Thus, knowledge of the long-term behavior of the surface wind for the world oceans is critical for understading the causes of past variations in climate, as well as for predicting future climate behavior.

In particular, the following items were discussed at the workshop:
i) how best to determine and quantify temporal homogeneity; ii) methodology aimed at standardizing surface wind measurements from the voluntary observing fleet and from other observing platforms (e.g., moored and drifting buoys); iii) an evaluation of the sufficiency of spatial and temporal data coverage, i.e., to consider the question of sampling adequacy for various space and time scales; iv) the work being carried out to develop a uniform (dynamically consistent) data set of marine surface wind fields; and v) review what the record actually shows about large-scale surface wind variations during the past several decades, consider whether these changes are physically plausible, and what kinds of supplementary, corroborating evidence is available to evaluate changes in the mean surface wind fields over the oceans.

This proceedings volume is divided into four thematic sections. The first one provides some background material and a summary of current efforts to enhance the COADS. The second section deals with comparisons of the long-term behavior of marine surface winds with other wind indices derived from the independently observed sea level pressure field. A third section addresses itself to the question of accuracy of wind measurements at sea and compares different methods, such as wind estimation based on the state of the sea (through application of the Beaufort wind scale(s)), and from the reading of anemometer platforms onboard the ships. The last section deals with various methodologies being applied by different investigators to improve the accuracy and utility of the existing COADS wind observations.

A list, with addresses, of all the participants is included as part of this proceedings volume. We hope that the papers presented here will assist the greater COADS user community to make better and more informed use, not only of the COADS wind products, but also of the other atmospheric and oceanic variables available from the COADS data set.

Part I

Background Papers

The Importance of COADS Winds for Understanding Climate Change

J.O. Fletcher

Cooperative Institute for Research in Environmental Science (CIRES)
Boulder, Colorado USA

A quarter century ago S. Manabe and R. Weatherald published a one dimensional computation of surface warming from a doubling of CO_2: 3°C was their result. It was an interesting and useful result; but no one believed that all other factors remained constant or that all the feedback loops canceled.

A few years later an error bar of 1.5°C was added by a U.S. National Academy panel. It was a guess. Today the Intergovernmental Panel on Climate Change (IPCC) estimate is about the same and is being used to represent what is likely to happen in the real world. Does this mean that all other factors really do remain constant or that all the feedback loops cancel each other? Or is something wrong?

The first IPCC report was published four years ago and was accepted by most political authorities as gospel. For example, in 1992 the five democratic presidential candidates held a televised debate before the New Hampshire primaries. All five agreed that to reduce greenhouse warming effects the U.S. should commit to limiting CO_2 emissions by the year 2000 to 1990 levels. Two of the candidates called this, "the most important issue of our time."

The U.S. government has now made such a commitment. The enormous costs involved will impact such social needs as health care, education and child care, but, they have been convinced that there is no other choice if we are to avoid catastrophic climate changes, such as sea level rise and desertification of the American mid-continent. Costly legislation is now before the U.S. Congress to implement this policy, including using the tax code to force conversion of power generation from coal, which we have in vast reserve, to natural gas, which we have in limited reserves.

In the real world, we know that other factors are not constant. A look at observed behavior of climate tells us that changing strength of the atmospheric circulation is a very robust feature of climate change, and many factors are strongly influenced by wind strength. For example, evaporation over the ocean is proportional to wind speed and amounts to about 100 W/m^2. Only a 4% *decrease* in wind would decrease evaporative cooling of the ocean by 4 W/m^2, about equal to doubling of CO_2, thus adding to surface warming by a factor of two.

On the other hand, an *increase* of surface wind by 4% would increase evaporation by 4 W/m2 and just about cancel the greenhouse surface warming. The additional heat and moisture extracted from the ocean would be added to the mid-troposphere where rain is formed. If the increase in evaporation is more than 4%, it more than balances the radiative

effect of CO_2 doubling and the ocean is cooled, while the atmosphere is warmed more strongly.

What does the record show? Will the wind blow stronger or weaker in an enhanced greenhouse world? Fig. 1 shows the strength of the surface wind over the global tropics, 30°N to 30°S, for more than half a century. The first vital question: is the trend upward or downward and how does the magnitude compare with the 4% corresponding to CO_2 doubling? The graph also shows the main forcing factor for the Hadley Circulation, deep tropical convection, which heats the mid troposphere and transports mass upward. Since we have only about two decades of direct satellite observation of tropical convection I use as a proxy, the area of ocean warmer than 29°C.

This COADS record of the last sixty years says several things:

1. The trend (in surface wind and the index of tropical convection) is up. Other things do not remain constant.
2. The changes are large and strongly correlated with each other (both the size of the warm pool and the strength of the Hadley Circulation). The mean wind speed has increased by about 25% to 6.5 m/s and evaporation by a similar proportion, several times larger than the 4 W/m^2 associated with CO_2 doubling. The small arrow representing 4% is shown on the chart for comparison.
3. Contrary to the usual notion that the ocean and atmosphere cool or warm in the same direction, the opposite is true. Increasing wind speed extracts more heat by evaporation from the ocean and gives it by condensation to the atmosphere. The ocean as a whole is cooling, even though the size of the warm pool has been increasing. This infers that ocean circulation plays an important time variable role in maintaining the warm pool. COADS tells us that the wind increase has been greatest in the Northern Hemisphere during its winter. The Northern Hemisphere oceans show cooling. The Southern Hemisphere wind increase is less and sea surface temperature has warmed slightly.

These trends cannot continue indefinitely because a cooling ocean must eventually overcome a growing warm pool. We have here the essential element of an oscillating system, negative feedback and delayed response.

How is circulation strength related to rainfall over continents? Common sense would say that more evaporation and more moisture carried inland by stronger circulation means more precipitation inland. That is also what the record shows. The best and longest record for Central North America is the level of the Great Lakes. Over the last century and one half it has gone from high levels in the 1870s to low levels during the 1920s and 30s to high levels again in the 1980s, parallel to changes of wind strength. We call the mid-continental drought of the late 1920s and 30s the "dust bowl". By contrast, the 1980s and 90s have had much more rainfall.

In this revised scenario of increasing wind strength both of the greenhouse threats are gone: sea level does not rise because the ocean is losing heat, not gaining heat and snow on land is increasing, not decreasing. Mid continent desertification is related to weak rather than strong circulation.

We are left, however, with a big question. How long can the size of the warm pool and the circulation strength continue to increase while the global ocean is losing heat? It cannot continue indefinitely. Ocean transport of heat into the warm pool is necessary to maintain its large and increasing size and this must deplete heat storage at higher latitudes. COADS data shows that the last peak in circulation strength was about 1870 and when the trend changed, it was quite abrupt. I suggest that forecasting the end of the present increasing trend, with its regional climate changes, is the pressing challenge facing the climate research program.

Forecasting the size of the warm pool and strength of the circulation is the heart of the problem. Improving the surface wind data set will be a big help.

There are several questions that need attention:

Why don't GCM's give the right answer? How should they be improved?

A first order answer to this question is shown by the dashed line in Fig. 1 which represents the lowest level wind (990 mb) in G. Lau's four decade simulation using observed global SST. It says that even the expensive GFDL model does not simulate change on this time scale. There is no significant trend in the model results. Parameterization of tropical convection must be improved to simulate correctly the last half century before we can accept its prediction for the coming century.

How is this dynamic feedback loop related to the cloud/radiation feed back?

A first order answer is given by V. Ramanathan who used ERBE data to conclude that the cloud feedback is negative, together with other work based on COADS and other data that show that cloudiness has been increasing over the last half century. Both results would add to the negative feedback of the dynamic wind feedback loop but more investigation is needed.

How good an index is the size of the warm pool for representing the amount of deep convection ?

We now have about 3 decades of outgoing longwave radiation (OLR) and we should be able to compile a satellite record of deep convection for comparison.

Should we believe the wind record that yields these startling results?

Some would say no. Included in the ocean wind record are many possible biases that are difficult to evaluate. That is what this workshop aims to accomplish.

The first order question is: Is the wind trend up, down or zero? I believe that the trend is up and that the change of recent decades is more than 4%. If so, the greenhouse "threats" of sea level rise and mid continent audity have been grossly exaggerated.

As evidence of increasing circulation strength figures 2 and 3 show the ocean basin wide change in surface pressure and vector wind from 1950-70 to 1970-90 (from COADS). The coherence of the changes in pressure field and wind field is conspicuous.

Critics of the conclusion outlined above point to the many defects of COADS. Many are real. Many are exaggerated. The governing consideration is that we have no alternative description of the behavior of the global climate system over the century time scale. This description, though incomplete, is in glaring contrast to current assumptions about greenhouse warming and climate change on which costly policies are based. An important step was recently taken by Prof. James O'Brien at Florida State University. For the tropical areas for which his group produces the reference wind stress maps for TOGA he has extended the record backward in line to 1930, also incorporating more sophisticated quality control, interpolation and bias corrections such as has been suggested by C. Ramage and others. Figure 4 reflects this data set for comparison with Fig. 1. The trend is up! The change is large! All of the considerations outlined above apply!

Figure 1:

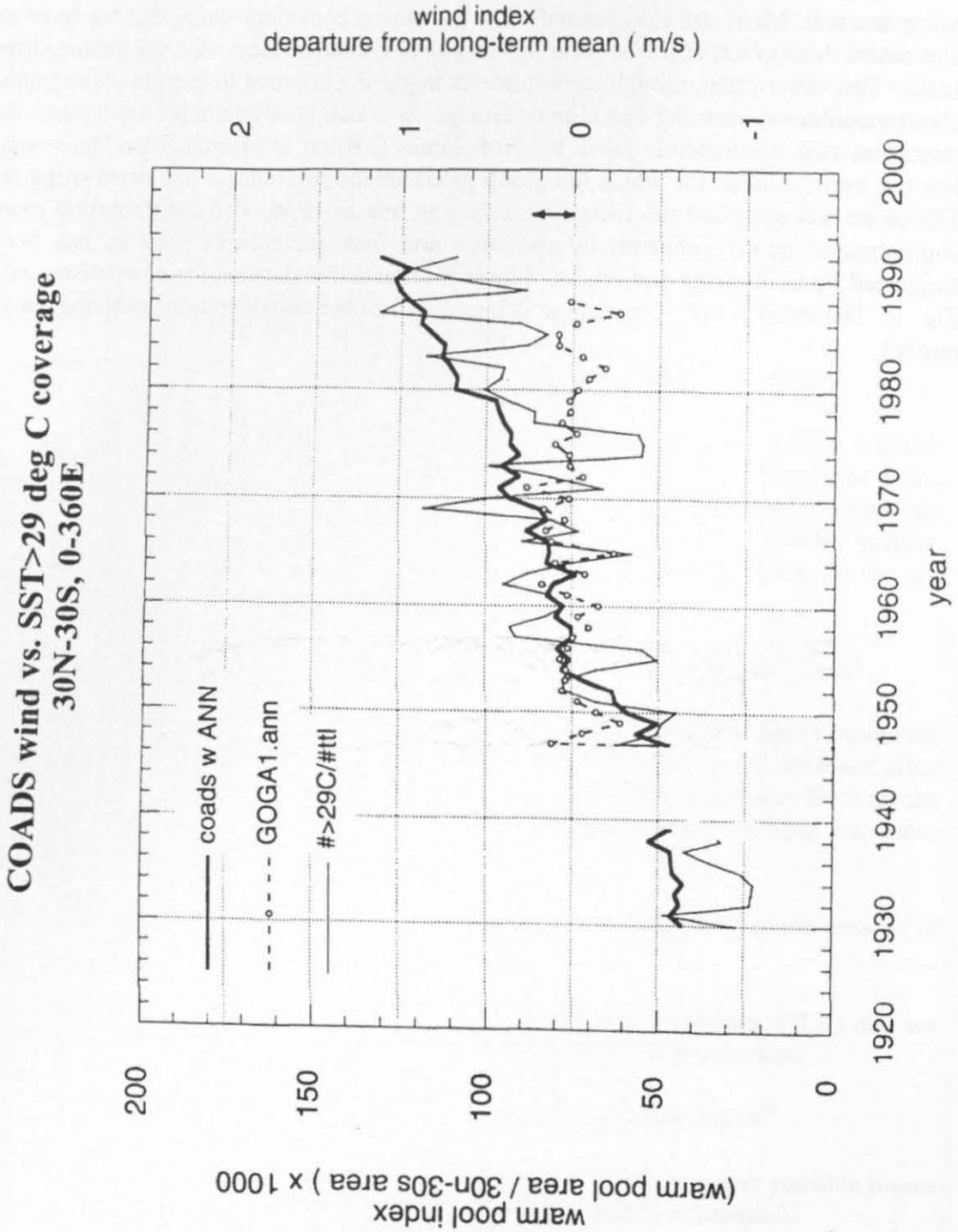
COADS wind vs. SST>29 deg C coverage
30N-30S, 0-360E
wind index
departure from long-term mean (m/s)
2
1
0
-1
coads w ANN
GOGA1.ann
#>29C/#ttl
200
150
100
50
0
warm pool index
(warm pool area / 30n-30s area) x 1000
1920
1930
1940
1950
1960
1970
1980
1990
2000
year

Figure 2:

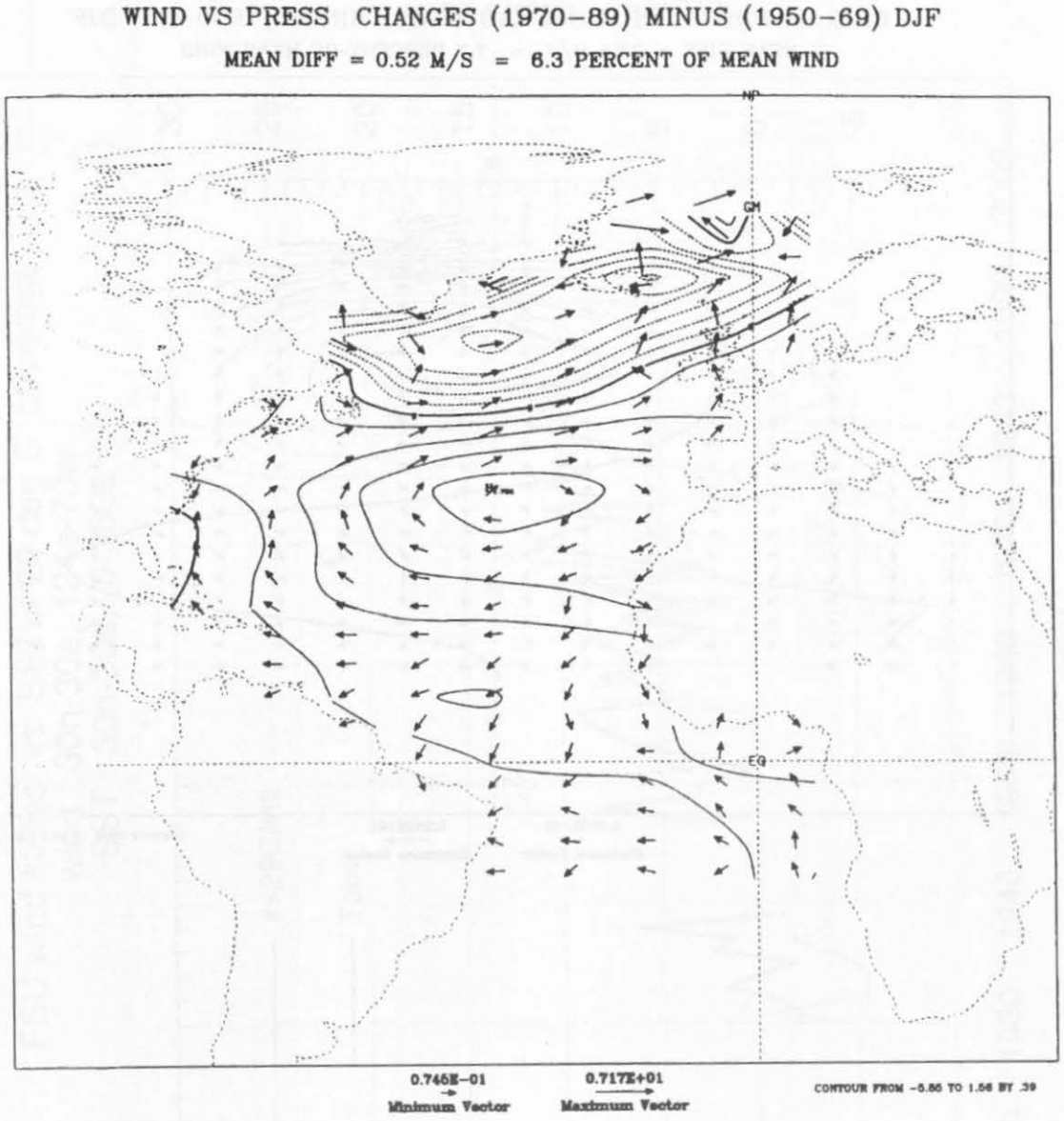
WIND VS PRESS CHANGES (1970–89) MINUS (1950–69) DJF
MEAN DIFF = 0.52 M/S = 6.3 PERCENT OF MEAN WIND
NP
GM
EQ
0.745E-01
Minimum Vector
0.717E+01
Maximum Vector
CONTOUR FROM -5.85 TO 1.56 BY .39

Figure 3:

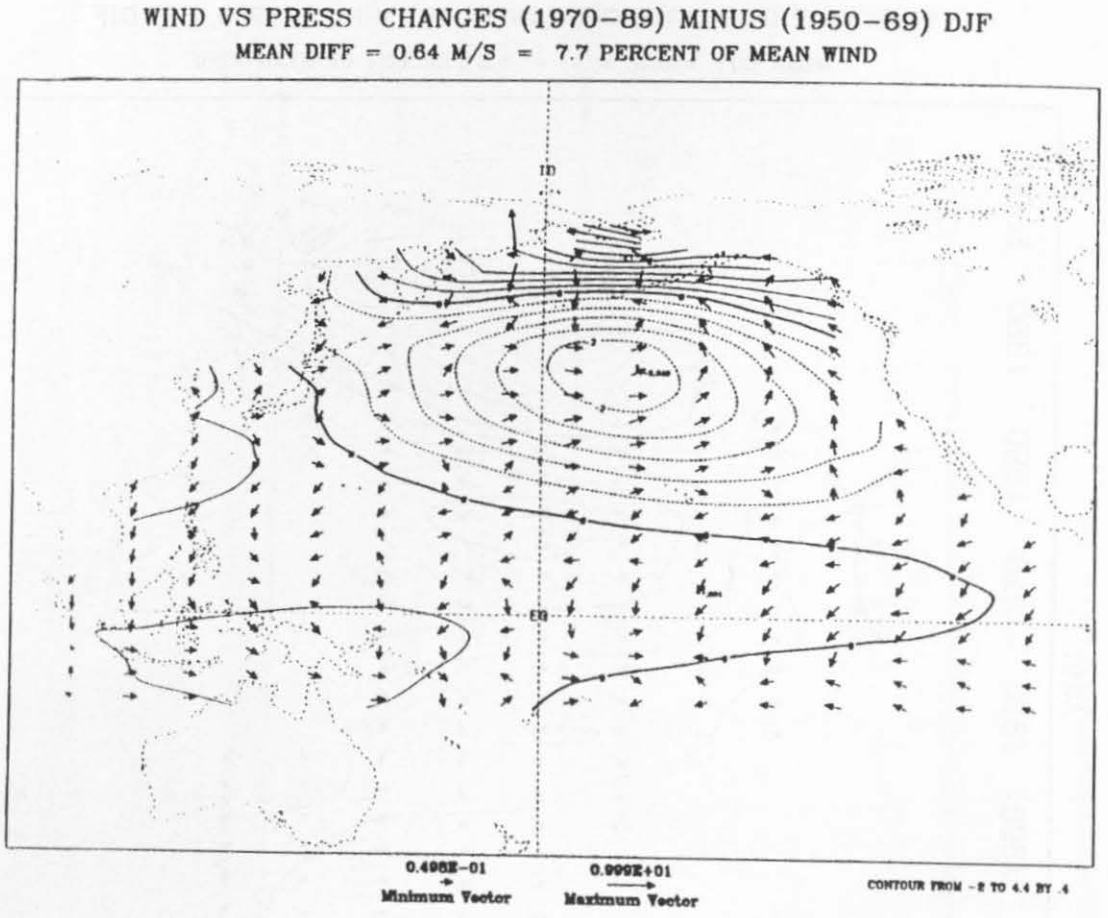
WIND VS PRESS CHANGES (1970–89) MINUS (1950–69) DJF
MEAN DIFF = 0.64 M/S = 7.7 PERCENT OF MEAN WIND
0.496E-01
Minimum Vector
0.999E+01
Maximum Vector
CONTOUR FROM -2 TO 4.4 BY .4

Figure 4:

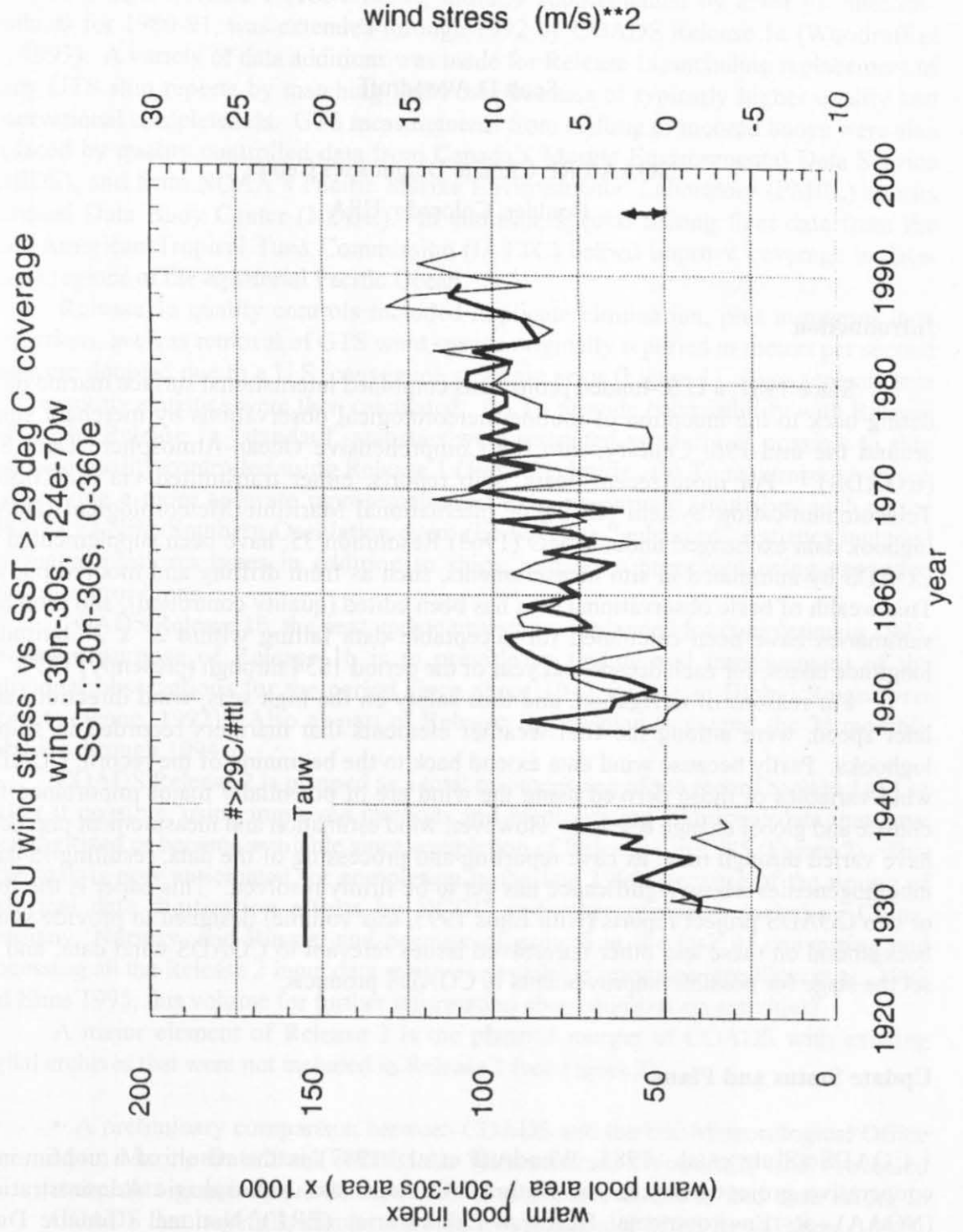
FSU wind stress vs SST > 29 deg C coverage
wind : 30n-30s, 124e-70w
SST : 30n-30s, 0-360e
#>29C/#ttl
Tauw
wind stress (m/s)**2
warm pool index
(warm pool area / 30n-30s area) x 1000
year
30
25
20
15
10
5
0
-5
-10
200
150
100
50
0
1920
1930
1940
1950
1960
1970
1980
1990
2000

COADS Project Report I: Update Plans and Unresolved Issues

Scott D. Woodruff

NOAA/ERL Climate Diagnostics Center
Boulder, Colorado USA

Introduction

Since 1981, a U.S.-funded project has combined international surface marine data, dating back to the inception of routine meteorological observations by merchant ships around the mid-19th Century, into the Comprehensive Ocean-Atmosphere Data Set (COADS).[1] For more recent years, ship reports, either transmitted via the Global Telecommunication System (GTS), or International Maritime Meteorological (IMM) logbook data exchanged under WMO (1963) Resolution 35, have been supplemented in COADS by automated in situ measurements, such as from drifting and moored buoys. This wealth of basic observational data has been edited (quality controlled), and monthly summaries have been calculated for acceptable data falling within 2° x 2° latitude-longitude boxes, for each decade and year of the period 1854 through (presently) 1992.

For reasons of navigation, and thus safety on the high seas, wind direction, and later speed, were among the first weather elements that mariners recorded in ships' logbooks. Partly because wind data extend back to the beginning of the record, COADS wind variables or those derived using the wind are of potentially major importance for climate and global change research. However, wind estimation and measurement practices have varied through time, as have reporting and processing of the data, resulting in data inhomogeneities whose significance has yet to be firmly resolved. This paper is the first of two COADS project reports (with Elms 1995, this volume) designed to provide some background on these and other unresolved issues relevant to COADS wind data, and to set the stage for possible improvements in COADS products.

Update Status and Plans

[1] COADS (Slutz et al., 1985; Woodruff et al., 1987) is the result of a continuing cooperative project between the National Oceanic and Atmospheric Administration (NOAA)—its Environmental Research Laboratories (ERL), National Climatic Data Center (NCDC), and Cooperative Institute for Research in Environmental Sciences (CIRES; joint with the University of Colorado)—and the National Science Foundation's National Center for Atmospheric Research (NCAR). COADS products are available from NCAR, or individual observations from NCDC.

COADS Release 1 (1854-1979), initially supplemented by a set of "interim" products for 1980-91, was extended through 1992 by COADS Release 1a (Woodruff et al., 1993). A variety of data additions was made for Release 1a, including replacement of many GTS ship reports by matching IMM data because of typically higher quality and observational completeness. GTS measurements from drifting or moored buoys were also replaced by quality controlled data from Canada's Marine Environmental Data Service (MEDS), and from NOAA's Pacific Marine Environmental Laboratory (PMEL) and its National Data Buoy Center (NDBC). In addition, special fishing fleet data from the Inter-American Tropical Tuna Commission (IATTC) helped improve coverage in data-sparse regions of the equatorial Pacific Ocean.

Release 1a quality controls included duplicate elimination, plus numerous data corrections, such as removal of GTS wind speeds originally reported in meters per second that were doubled due to a U.S. conversion software error (Figure 1). Two separate sets of 2° monthly statistics were then calculated: (a) To provide compatibility with Release 1 data, the Release 1a "standard" statistics were restricted as nearly as possible to ship data, and quality controlled using Release 1 (1950-79) limits. (b) To maximize coverage and provide a more accurate representation of extreme climate anomalies such as the 1982-83 El Niño/Southern Oscillation event (ENSO), the "enhanced" statistics included automated platform types in addition to ships, and were processed using expanded quality control limits.

COADS Release 1b, the next update milestone, is planned for completion in 1995. The main purpose of Release 1b is to provide an update and improvement of the individual observations for the period since about 1947 for use in Global Re-analysis projects (Jenne, 1992). Also as part of Release 1b, we plan to extend the 2° monthly statistics through 1994.

COADS Release 2 is planned as a total re-processing of the record back to 1854 or earlier if possible, using improved methods and incorporating additional data that have been digitized or become available since completion of Release 1 in 1985 (Figure 2). This large task is now anticipated for completion in the late 1990s because of the timing of historical data digitization efforts by NCDC and other countries including China, Germany, Norway, and Russia, and because of growth in the task of converting and processing all the Release 2 input data relative to available resources (see Elms et al., 1993 and Elms 1995, this volume for further information about digitization activities).

A major element of Release 2 is the planned merger of COADS with existing digital archives that were not included in Release 1 (see Figure 2):

- A preliminary comparison between COADS and the UK Meteorological Office Main Marine Data Bank (MDB) for selected areas (Woodruff, 1990) revealed more data generally in COADS, but also some reductions and data errors in COADS that hopefully can be resolved by inclusion of MDB data (Parker, 1992).
- Russia has provided its Marine Meteorological Data Set of ship data extending back to 1888 (1980-90 data were used for Release 1a), and drifting Arctic "ice island" data back to 1950.
- Germany hopefully will be able to provide records from the Seewetteramt Data Archive to replace Historical Sea Surface Temperature (HSST) Data Project

reports input to Release 1, because the WMO-defined HSST format (also used as input for HSST receipts from the Netherlands) lacked some subsidiary weather elements such as present weather and complete cloud fields.

Among possible processing improvements under consideration for Release 2 are proposed increases in the temporal and spatial resolution of statistical summaries for selected time periods, regions, and variables (e.g., 1° latitude x 1° longitude/sub-monthly), and separations of statistics to accommodate differences in data from different platform types (e.g., enhanced versus standard statistics) and times-of-day. In addition, improvements in quality control are planned to provide a more faithful representation of climatic extremes (see section below).

Unresolved Issues

This section is a general discussion of other important unresolved issues relevant to COADS winds, as well as other variables, that merit discussion in planning possible data or product improvements.

Spatial and temporal inhomogeneities

Changes in ship propulsion and routing (e.g., construction of the Suez and Panama Canals) account for many large variations since 1854 in global COADS data density (Figure 2; see also Woodruff et al., 1987). Less well documented, however, are changes in the time of reporting ship observations (Figure 3). A significant deficiency with the 1912-46 U.S. merchant marine data, which only came to light as the data started to be keyed at NCDC, is that observers were instructed to make logbook entries only once a day at 1200 UTC. Regrettably, corresponding teletype messages that may have been reported more frequently in some areas were discarded at NCDC (Elms et al., 1993).

Scientific measurements from moored and drifting buoys have helped expand spatial and temporal coverage for recent decades, although areas such as the tropical Pacific and the Southern Ocean are still under-sampled. However, combination of ship and buoy data in statistical summaries may also introduce unwanted sampling biases. For example, NDBC moored buoys reporting hourly around the coastal U.S. would likely dominate the statistics for those 2° boxes, except that they were reduced to 3-hourly resolution before inclusion in the Release 1a enhanced statistics.

Changes in instrumentation and observing practices

A survey in this volume of documented procedures for U.S. merchant mariners (Elms 1995, this volume) shows that changes have occurred in procedures for estimating and reporting Beaufort force, or later a wind speed equivalent in knots. For example, the verbal descriptions that accompanied tables for Beaufort force changed (or even were omitted in some years) in gradual transition to the change in estimation of wind speed using sail capacity to that using sea state.

Significant data inhomogeneities also may have arisen from variations in anemometer type and location relative to the evolving size and construction of ships. Compounding all these problems, there is believed to have been a steady upward trend in

the ratio of measured to estimated winds (Ramage, 1987). A corresponding positive trend in scalar wind speed, or at least part of that trend, has been widely attributed to such artificial influences (e.g., Ramage, 1987; Wright, 1988; Cardone et al., 1990). These include application of the "old" Beaufort equivalence scale made effective by WMO after 1946, but also applied retrospectively for conversion to knots or meters per second of most winds thought to have been originally reported as a Beaufort force code (e.g., "re bracketing" of HSST receipts; see p. K28 of Slutz et al., 1985).

Cardone et al. (1990) illustrated that different source "decks" (as assigned by NCDC) may exhibit significant differences in wind data, depending on the makeup and processing history of each deck (see also Woodruff, 1990). Based on comparisons for selected areas (see Figure 1), GTS ship wind speed observations from the former USSR (reported in meters per second) appear to average about 2 knots higher than those from other countries (generally reported in knots). However, more study is warranted before definite conclusions can be drawn from this selective comparison, and separations for other countries might also prove illuminating. Similarly, IATTC fishing boat (estimated or measured) wind speed data have a pronounced bias toward weaker speeds in comparison to the Release 1a enhanced statistics (Figure 4). This is probably explained largely by the preference for tuna fishermen to seek out calmer wind areas, plus the effects of an anemometer height of approximately 10 m (F. Miller, personal communication). Thus although the IATTC data appear to reflect actual wind conditions, they were omitted from Release 1a enhanced statistics to avoid calm wind biases.

Introduction of automated platform types into COADS creates new possibilities for data inhomogeneities, applicable to wind data starting about 1970 with the advent of moored buoy measurements (Figure 5; see also Wilkerson and Earle, 1990; Pierson, 1990; Radok, 1991). Considering for example only the issue of wind averaging period (nominally 10 minutes for ships), two subsets of PMEL data were included in Release 1a: (a) daily averages from Equatorial Pacific Ocean Climate Studies (EPOCS) moored buoys and low-elevation islands; and (b) Tropical Ocean-Global Atmosphere (TOGA) Program TAO ATLAS moored buoys, with wind averaging periods varying from 1-24 hours (in addition, ATLAS data were not necessarily synchronized on regular synoptic hours, and for earlier instrumentation packages different averaging periods and report times were used for different variables originating from a single buoy).

Similarly, NDBC hourly moored buoy wind data have been averaged over periods of 8-10 minutes, with anemometer heights ranging from 3.7-13.8 m, and either vector or "scalar" averaging depending on the instrument package (Gilhousen, 1987; Woodruff et al., 1991). NDBC and other groups internationally have begun experimentation with wind speed and direction sensors on new drifting buoy designs, and some countries already report these data over GTS. Because of concerns about the experimental nature of this new instrumentation, as well as the size of drifting buoys relative to sea state, wind data from drifting buoys were excluded from the Release 1a enhanced statistics.

Quality control problems

"Trimming" in COADS refers to the process of flagging individual observations that exceed upper and lower quality control limits defined for each 2° box and month, and excluding them from the trimmed 2° monthly summaries (note that the existing summaries have combined wind data without respect either to the original directional compass or to whether the wind speed was estimated or measured; see Morrissey, 1990). For Release 1, the trimming limits were set at the 3.5σ level using three climatological periods (1854-1909; 1910-49; 1950-79). As shown by, e.g., Wolter et al. (1989) and Wolter (1992), the 3.5σ limits have proven overly restrictive for extreme climate anomalies such as the 1982-83 ENSO. For Release 1a, the 1950-79 trimming limits were expanded to 4.5σ for the enhanced statistics; but 3.5σ was used for the standard statistics to provide greater compatibility with Release 1.

However, a more complex set of quality control problems applies to wind data, including a lower-bound of zero on wind speed, than to univariate quantities such as temperatures and pressure. COADS wind trimming is currently performed by testing both the u and v components (calculated from individual observations of wind speed and direction) against upper and lower limits for u and v. If either u or v exceeds its limits, the wind components (and speed) are flagged and omitted from monthly summaries. The feasibility of a bivariate test for trimming wind is under consideration for Release 2, as well as possible general improvements in the procedure for all variables (e.g., checks for consistency with respect to "local," as well as climatological, conditions in time and space).

Metadata from individual marine reports

This section discusses wind-related metadata (information about data) available in individual marine reports (the next section describes metadata available from external sources, and issues arising in attempting to join the two metadata sources).

a) Wind direction indicator

NCDC's (1968) Tape Data Family-11 (TDF-11) formed the core of COADS Release 1 data for 1854-1969. TDF-11 contained a wind direction indicator specifying the original compass code: 36-point, 32-point, 16 of 36-point, or 16 of 32-point. Additional wind direction indicator values have been defined in COADS to accommodate HSST 8-point data and high resolution automated measurements.

b) Wind speed indicator (i_W; WMO code 1855)

Modern ship GTS and IMM data contain i_W, which indicates whether wind speed was estimated or measured, and whether it was reported in meters per second or knots (the reduction in precision from reporting winds in whole meters per second, as recommended by WMO, instead of whole knots, should be noted; see Woodruff et al., 1991). Only starting in 1982 was i_W included in its present form in WMO's IMM formats. Although i_W may have been standardized in GTS data after 1963 (Cardone et al., 1990), its availability also depends on the date on which individual GTS receiving centers started saving that information. For example, the units part of the i_W information was apparently omitted from basic GTS data collected by NOAA's National

Meteorological Center (NMC), the primary GTS source for COADS since 1980, until 9 May 1984.

Many of the early card decks included in TDF-11 contained little or no explicit information about wind speed observing method or reporting units, although we may be able to estimate indicator settings from documentation (e.g., the earliest decks clearly consist only of Beaufort estimates). Since it was designed after the 1963 IMM format, the TDF-11 wind speed indicator had only two settings: blank for "not measured" and 0 for "measured," such that the former also includes the meaning "unknown." Unfortunately, this ambiguous indicator is still in use in the current NCDC archival format (TD-1129), which is also the COADS format currently distributed by NCDC, although it has been supplemented by an "original wind speed units indicator" whose presence presumably allows reconstruction of i_W when reported. Additional wind indicator flag settings have been defined in the current Long Marine Report (LMR.6) format for COADS individual observations in an attempt to provide users with a single indicator that incorporates both historical and modern information (Table 1).

c) Automated report metadata

As discussed above, wide differences have existed in instrumentation and reporting by US. moored buoys (e.g., PMEL and NDBC); internationally, even greater differences may exist. Similar to the situation with ship data, the availability of metadata from buoy reports may vary depending on the source and age of the data. Using NDBC moored buoy reports for example, anemometer height is included starting February 1985, and about 1988 fields were added for anemometer method (scalar or vector) and wind averaging period.

Linkage with metadata from external sources

WMO Publication 47 (1955 and later) describes many characteristics of individual ships participating in the WMO Voluntary Observing Program (VOP); unfortunately, WMO Pub. 47 is available only in paper form until 1973 (P. Dexter, personal communication). In addition, NOAA's National Weather Service (NWS) maintains some ship information, and other sources of information may exist (e.g., insurance companies).

At least in its current form, WMO Pub. 47 (and presumably the NOAA ship list) can be linked to individual ship reports only by matching the ship radio call sign. Due possibly to ship call sign errors either in the external lists or the individual ship reports, Wilkerson and Earle (1990) found that many ships apparently participating in the VOP were neither in WMO Pub. 47 nor in the NOAA list. In fact, a variety of format and data source problems impacts the availability of call sign or any form of platform ID in individual marine reports (Figure 6). In addition, some countries have elected to include a national ship number instead of the call sign in IMM reports (see Woodruff et al., 1992). Figure 6 also illustrates the availability of report metadata indicating the recruiting country or flag nationality of each ship report, which could facilitate intercomparison of national observing and reporting practices.

For drifting and moored buoys, WMO has expanded its *Operational Newsletter* for the World Weather Watch and Marine Meteorological Services to include some general information about the parameters reported by individual buoys. However, the *Operational Newsletter* currently lacks instrumentation details (e.g., anemometer types

and heights). In addition, NDBC periodically updates a publication (NDBC, 1993) that lists instrument packages used aboard each of its moored buoys (and other platform types). As suggested by Woodruff et al. (1991), an internationally sanctioned repository of metadata for automated platform types appears to be highly desirable in digital form (WMO and NDBC metadata for automated platform types apparently are not yet available in digital form, in contrast to WMO Pub. 47 since 1973).

Conclusions

COADS wind data are impacted by many complex and interrelated issues, such as highlighted in this paper, that will take substantial time and resources to resolve. For example, it is only with the vigorous cooperation of the international community that we can hope to significantly improve spatial and temporal coverage through digitization of historical logbooks. Research into variations in observing practices and instrumentation, not only for wind data but for other variables such as sea surface temperature, should be significantly advanced by easily usable digital files of external metadata for ships and automated platform types; WMO (1955-) Publication 47 and its *Operational Newsletter* should provide starting points for development of such products. For historical data, national and international instructions to mariners through time, such as discussed in the companion paper by Elms (1995) this volume, may need to be made more widely available.

Problems of a more technical or operational nature may also warrant closer attention and better coordination at the international or national level, perhaps through creation of a working group of marine data focal points as discussed in Woodruff et al. (1993). Following are a few such key issues whose resolution should help improve data and metadata quality for future COADS updates, and thus enhance the prospects for research using marine wind data:

- Because of differences between the ship GTS and IMM formats, as well as variations in handling the basic GTS and IMM data by different nations and sources, substitution among duplicates appears critical in order to obtain the best quality data and metadata. For example, ship radio call signs, which are usually included in GTS data, provide the linkage between individual marine reports and external ship metadata (e.g., WMO Pub. 47). However, the call sign was not included in IMM format until 1982, and some countries may still include national ship numbers in their IMM data. Unfortunately, substitution of fields among duplicates is a complicated process because there are frequently multiple duplicate reports, all of which should be compared for differences and relative information quality before creating a single composite report. Thus identification of composite reports and the source of their constituent fields becomes a further issue related to quality control. The simplest solution, in addition to providing report fields indicating when composites have been created, may be to retain the duplicate-rich input for further analysis as needed.

• Similarly, experience has clearly shown that permanent retention of original input data sets before conversion into common data formats is highly desirable. For example, errors have now been found in data converted from the original TDF-11 card decks, but not all of the original card deck data are available in digital form, and some of these data are probably slated for destruction should ongoing data recovery efforts be derailed.[2]

• The wind speed indicator (e.g., for estimated/measured) and other report metadata fields may need to be improved in usability and reliability. NCDC should ensure that wind speed indicator information is being accurately retained in its archival formats, at least through permanent retention of original input data sets. It should also be noted that questions have been raised about whether observers aboard US.-recruited ships have a clear understanding of how to properly encode the wind speed indicator, since spot checks of US. keyed data archived at NCDC have shown a higher proportion of measured winds, than was expected by the NOAA/NWS marine observations program (V. Zegowitz, personal communication).

Acknowledgments. I am grateful to S. Lubker and K. Wolter for preparation of the figures; and, in addition to the editors, to J. Elms, R. Jenne, S. Lubker, U. Radok, K. Wolter, and S. Worley for comments and discussion. The NOAA/ERL portion of COADS update activities has been funded in part by the NOAA Climate and Global Change program.

References

Cardone, V.J., J.G. Greenwood, and M.A. Cane, 1990: On trends in historical marine wind data. *J. Climate*, **3**, 113-127.

Elms, J.D., 1995: COADS project report II: Early data digitization and U.S. code history. *Proceedings, International COADS Winds Workshop* (this volume).

Elms, J.D., S.D. Woodruff, S.J. Worley, and C. Hanson, 1993: Digitizing Historical Records for the Comprehensive Ocean-Atmosphere Data Set (COADS). *Earth System Monitor*, **4**, No. 2, 4-10.

---

[2] NCDC years ago stored images of punched cards on 16 mm film using the Film Optical Sensing Device Input to Computer (FOSDIC), prior to disposal of the actual punched cards. The FOSDIC was also used to read card images from film and convert them to digital data (i.e., ASCII or EBCDIC) on 1/2" magnetic tape. Unfortunately, the digital tapes were not adequately maintained, as was discovered when attempts were made to migrate them to modern media. However, at the time of this report, 16 mm film and a FOSDIC to read it are believed to still exist, and funding was obtained to recover the film to digital media.

Gilhousen, D.B., 1987: A field evaluation of NDBC moored buoy winds. *J. Atmos. Oceanic Technol.*, **4**, 94-104.

Jenne, R.L., 1992: The importance of COADS for Global Reanalysis. *Proceedings of the International COADS Workshop, Boulder, Colorado, 13-15 January 1992.* H.F. Diaz, K. Wolter, and S.D. Woodruff, Eds., NOAA Environmental Research Laboratories, Boulder, CO, 9-15.

Morrissey, M.L., 1990: An evaluation of ship data in the equatorial western Pacific. *J. Climate*, **3**, 99-112.

NCDC (National Climatic Data Center), 1968: *TDF-11 Reference Manual.* NCDC, Asheville, NC.

NDBC (National Data Buoy Center), 1993: *NDBC Data Availability Summary* (1801-24-02, Rev. H). NDBC, Stennis Space Center, MS, 141 pp.

Parker, D.E., 1992: Blending of COADS and UK Meteorological Office marine data sets. *Proceedings of the International COADS Workshop, Boulder, Colorado, 13-15 January 1992.* H.F. Diaz, K. Wolter, and S.D. Woodruff, Eds., NOAA Environmental Research Laboratories, Boulder, CO, 61-72.

Pierson, W.J., 1990: Examples of, reasons for, and consequences of the poor quality of wind data from ships for the marine boundary layer: Implications for remote sensing. *J. Geophys. Res.*, **95**, 13313-13340.

Radok, U., 1991: Anemometer height effects in ship/buoy wind discrepancies? *Differences Within and Among Surface Marine Datasets.* NOAA Environmental Research Laboratories, Boulder, CO, 43-48.

Ramage, C.S., 1987: Secular change in reported wind speeds over the ocean *J. Climate Appl. Meteor.*, **26**, 525-528.

Slutz, R.J., S.J. Lubker, J.D. Hiscox, S.D. Woodruff, R.L. Jenne, D.H. Joseph, P.M. Steurer, and J.D. Elms, 1985: *Comprehensive Ocean-Atmosphere Data Set; Release 1.* NOAA Environmental Research Laboratories, Boulder, CO, 268 pp. (NTIS PB86-105723).

Wilkerson, J.C. and M.D. Earle, 1990: A study of differences between environmental reports by ships in the Voluntary Observing Program and measurements from NOAA buoys. *J. Geophys. Res.*, **95**, 3373-3385.

Wolter, K., 1992: Sifting out erroneous observations in COADS—the trimming problem. *Proceedings of the International COADS Workshop, Boulder, Colorado, 13-15 January 1992.* H.F. Diaz, K. Wolter, and S.D. Woodruff, Eds., NOAA Environmental Research Laboratories, Boulder, CO, 91-101.

Wolter, K., S.J. Lubker, and S.D. Woodruff, 1989: Trimming—a potential error source in COADS. *Trop. Ocean-Atmos. Newslett.*, **No. 51**, 4-7.

Woodruff, S.D., 1990: Preliminary comparison of COADS (US) and MDB (UK) ship reports. *Observed Climate Variations and Change: Contributions in Support of Section 7 of the Scientific Assessment of Climate Change of Working Group 1 of the IPCC*, D. Parker, Ed., WMO/UNEP publication.

Woodruff, S.D., S.J. Lubker, and M.Y. Liu, 1992: Updating COADS—Problems and opportunities. *Proceedings of the International COADS Workshop, Boulder, Colorado, 13-15 January 1992.* H.F. Diaz, K. Wolter, and S.D. Woodruff, Eds., NOAA Environmental Research Laboratories, Boulder, CO, 19-36.

Woodruff, S.D., R.J. Slutz, R.L. Jenne, and P.M. Steurer, 1987: A comprehensive ocean-atmosphere data set. *Bull. Amer. Meteor. Soc.*, **68**, 1239-1250.

Woodruff, S.D., S.J. Lubker, R.G. Quayle, U. Radok, and E.D. Doggett, 1991: *Differences Within and Among Surface Marine Datasets.* NOAA Environmental Research Laboratories, Boulder, CO, 216 pp.

Woodruff, S.D., S.J. Lubker, K. Wolter, S.J. Worley, and J.D. Elms, 1993: Comprehensive Ocean-Atmosphere Data Set (COADS) Release 1a: 1980-92. *Earth System Monitor*, **4**, No. 1, 1-8.

WMO (World Meteorological Organization), 1955-: *International List of Selected, Supplementary and Auxiliary Ships.* WMO No. 47, Geneva, Switzerland.

WMO (World Meteorological Organization), 1963: *Fourth World Meteorological Congress Abridged Report with Resolutions.* WMO No. 142, Geneva, Switzerland.

WMO (World Meteorological Organization), 1965: *Technical regulations,* WMO No. 49, (Appendix F, Suppl. No. 4), Geneva, Switzerland.

WMO (World Meteorological Organization), 1975: *Technical regulations,* WMO No. 49, Geneva, Switzerland.

Wright, P.B., 1988: On the reality of climatic changes in wind over the Pacific. *J. Climatol.*, **8**, 521-527.

Table 1: Expanded wind speed indicator (WI) settings as defined in the current Long Marine Report (LMR.6) format, corresponding to available values from TDF-11 ("—" indicates no corresponding information). Also shown are the resultant mappings into WI of corresponding wind speed metadata from original IMM and GTS formats; in many cases these mappings occurred through conversion first into the TDF-11 indicator, and then into LMR.6 (see also Table 6 of Woodruff et al., 1991)

		International Maritime Met. (IMM)			
LMR.6 WI	TDF-11	1963*	1968*	1982(i_W)**	GTS(i_W)***
0=m/s, estimated	-	-	-	6/0	6/0
1=m/s, measured	-	-	-	7/1	7/1
3=knot, estimated	-	-	-	6/3	6/3
4=knot, measured	-	-	-	7/4	7/4
5=Beaufort force	-	6?	6?	-	-
6=est./unknown	not meas.	-	6?	-	-
7=measured	meas.	-	7?	-	-
8=high resolution	-	-	-	-	-

* The 1963 IMM punched card format was defined by WMO (1965) in a standard and a supplementary version ("for exchange of cards with deviating codes or additional data"). For the 1968 IMM format, WMO (1975) revised both the standard and supplementary versions. This table shows the mapping to WI of approximately corresponding fields defined in the two standard versions; additional fields were available in the two supplementary versions. Note that original IMM receipts prior to about 1985 are no longer available at NCDC, thus wind metadata were retained only as converted into the TDF-11 indicator (question marks indicate that the method used to convert IMM metadata into TDF-11 indicator values is not known).

** Two possible mappings, because in some cases i_W (see text) may have been retained only as converted through the TDF-11 indicator (e.g., "6/0" indicates that the resultant WI was 6 if retained only through the TDF-11 indicator, and 0 otherwise).

*** Two possible mappings, depending on when i_W (see text) information was available in each GTS source. Using NMC data for example (see discussion in text), "6/0" indicates that the resultant WI was 6 prior to 9 May 1984, and 0 starting on that date.

Figure 1: GTS ship wind speeds averaged for selected 10 Marsden Squares in the North Atlantic, North Pacific, and Mediterranean: 79, 80, 122, 123, 141, 142, 184, 185, 199, 200, 217, and 252. Curves shown for USSR and all other data are displaced possibly due to biases from reporting wind in meters per second versus knots (see text). The effect of a U.S. conversion software error is also strongly evident during February-June 1984.

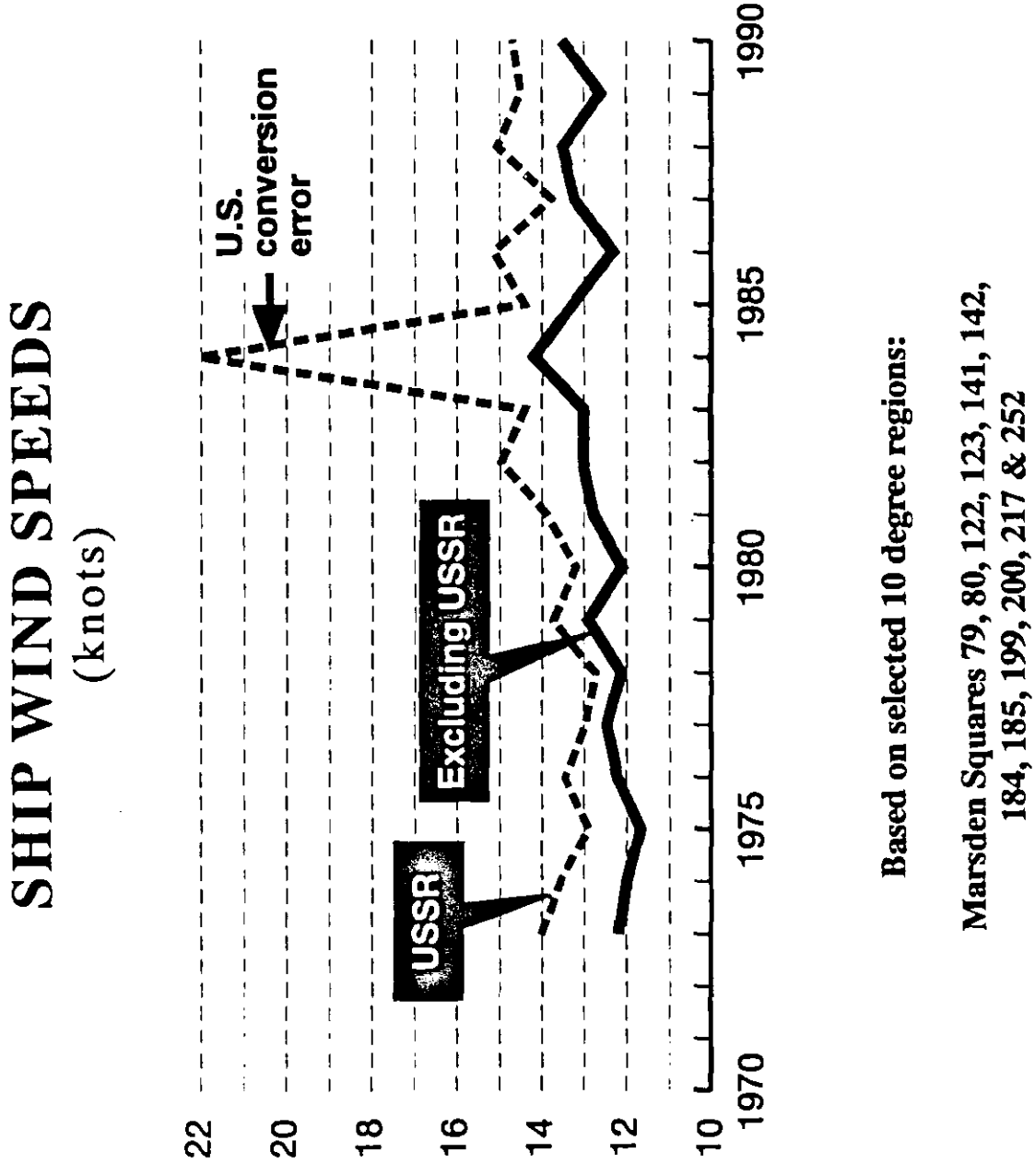

Figure 2: Annual global marine reports after duplicate elimination (curve) for COADS Release 1 through 1979, continued by Release 1a through 1992. Horizontal lines span the time periods for data now being collected and digitized, or proposed for future digitization (*), with the approximate numbers of reports shown in millions (M) or thousands (K) (Elms et al., 1993). Also listed are major existing digital data inputs proposed for inclusion in Release 2 or following Release 2. Labeled ticks along the upper horizontal axis mark the starting years for Release 1a, and those planned for Release 1b (1947) and Release 2 (1854, or earlier).

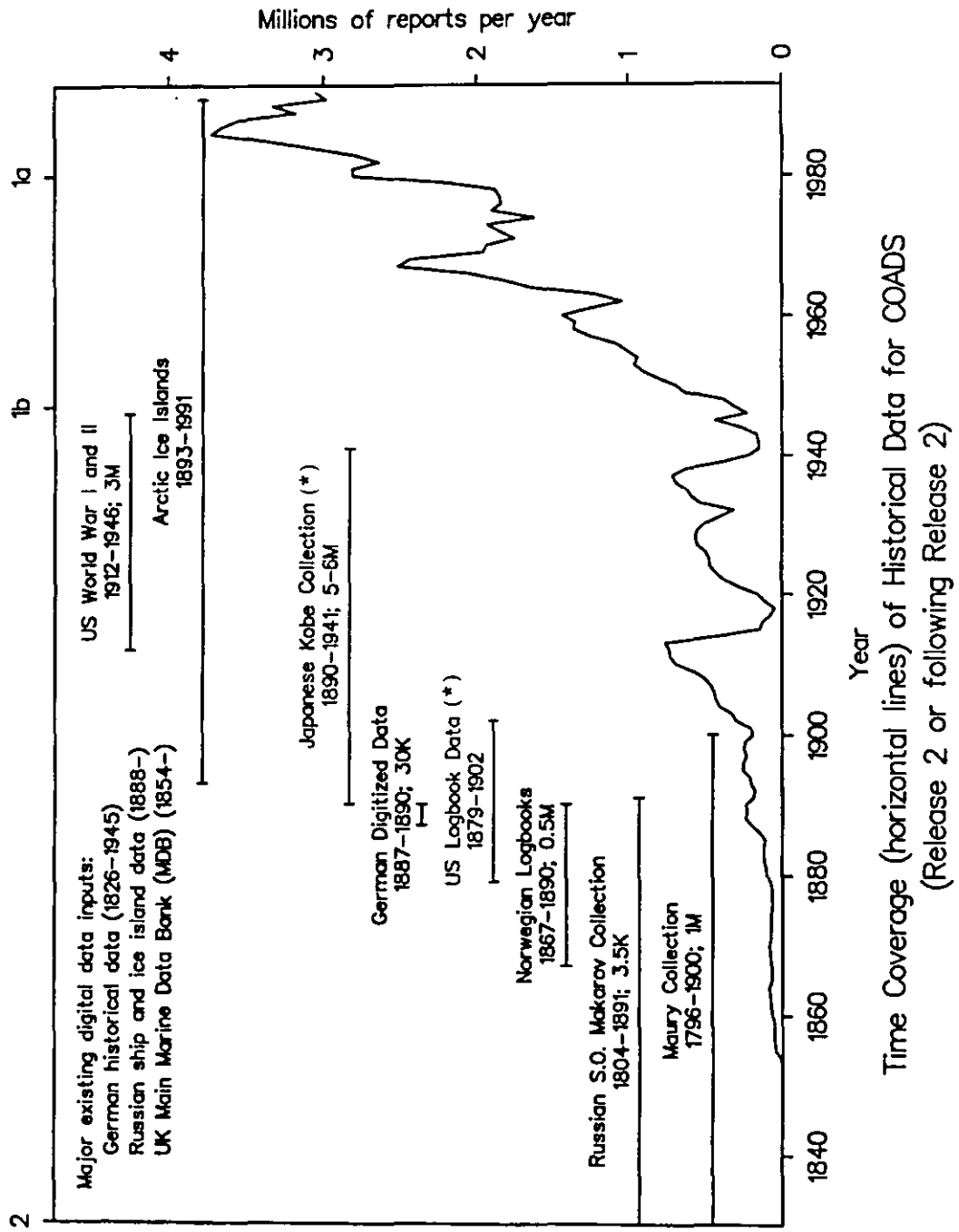

Figure 3: COADS Release 1 (upper) versus the UK Meteorological Office MDB (lower): annual percentages of total ship reports recorded at each UTC hour in 10° box number 200 (Marsden Square 122) west of the U.S. (because the division between two hours corresponds to 25%, a given bar may extend across four such divisions). The concentration of reports in COADS at hour 21 around 1900 has been traced to deck 192 (Deutsche Seewarte Marine), which was excluded from MDB (figure from Woodruff, 1990).

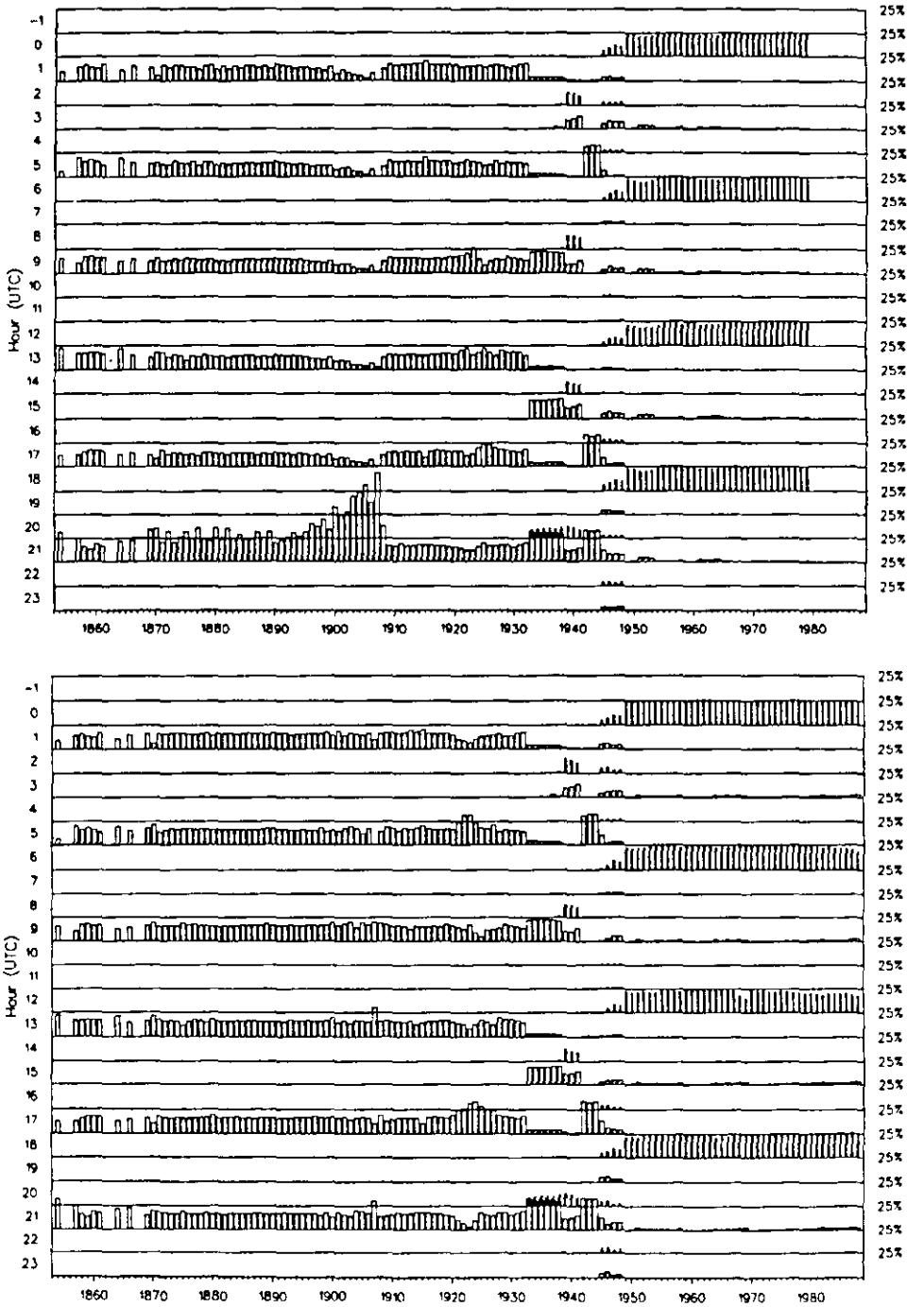

Figure 4: Average of 1980-92 monthly differences between the mean of scalar wind from the Release 1a enhanced statistics, minus that from IATTC special fishing fleet data (meters per second). Note that IATTC wind data were excluded from the Release 1a enhanced statistics.

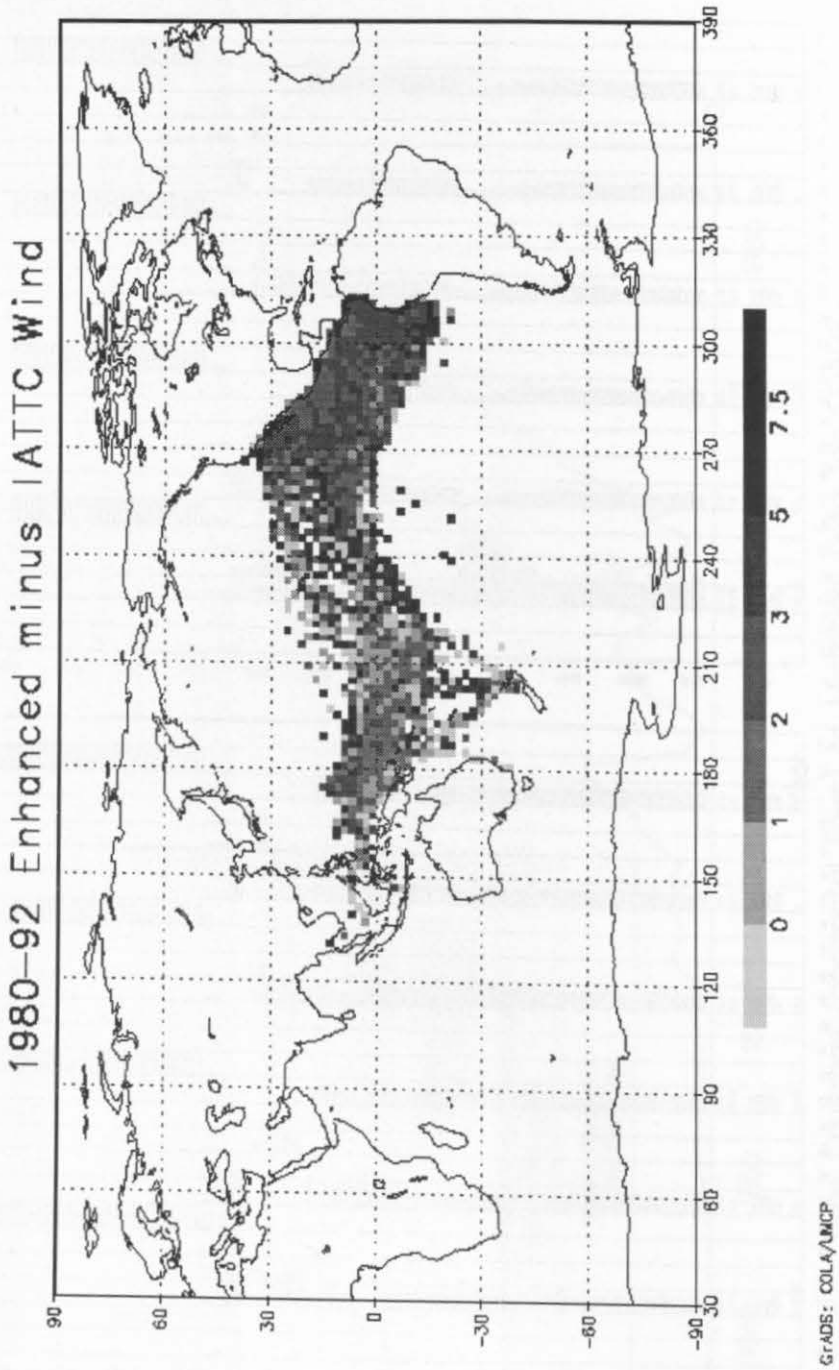

Figure 5: Annual average of 1980-92 monthly average differences between the Release 1a enhanced minus standard mean of scalar wind (meters per second). In many cases, negative differences (> -2 m/s) in 2° boxes around the U.S. coastline and across the equatorial tropical Pacific correspond to NDBC and PMEL moored buoy locations. Positive differences (< 5 m/s, but rarely above 2 m/s) arise from relaxation of the trimming limits to 4.5σ (figure from Woodruff et al., 1993).

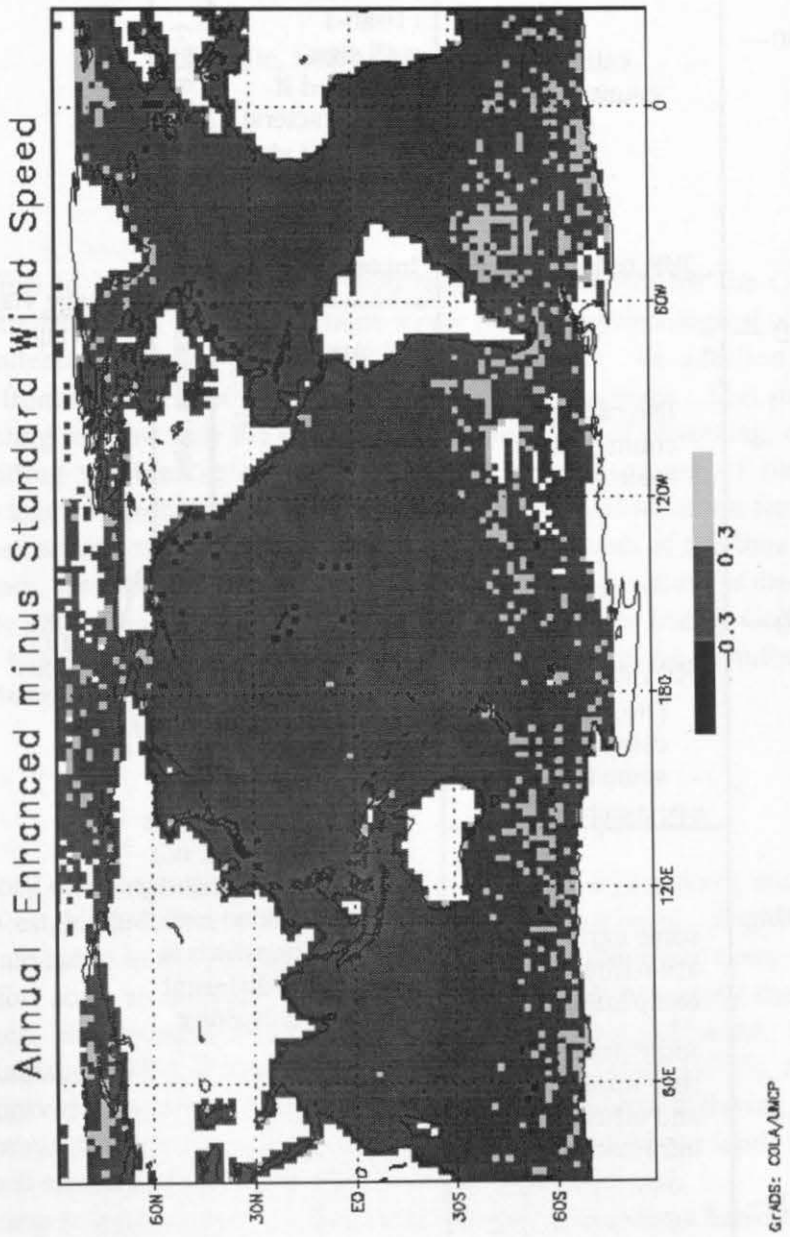

Figure 6: Approximate availability through time of ship radio call sign or other ID information, of wind indicator information (i_W) and of recruiting country code and ship flag nationality, from IMM (logbook) versus GTS data. Also shown is the availability of annual metadata from WMO (1955-) Publication 47. (Note: There were also IMM format revisions in 1987 and 2 November 1994 that did not impact the availability of fields shown here.)

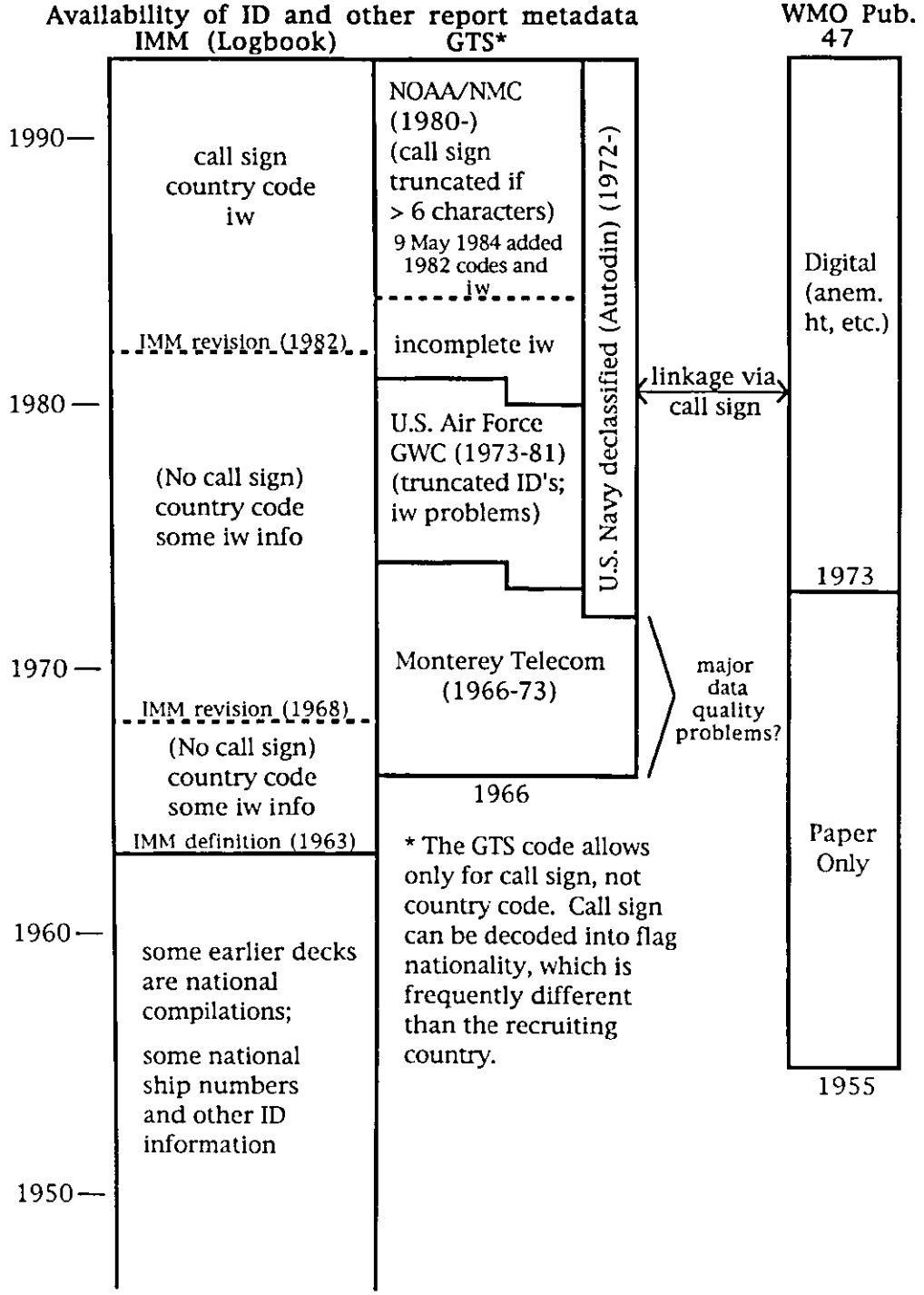

COADS Project Report:

Early Data Digitization and United States Code History

Joe D. Elms

National Climatic Data Center, NOAA

Asheville, North Carolina USA

Abstract

In an effort to better establish an historical metadata file for the COADS project, a complete set of U.S. instructions to the marine meteorological observer has been collected, for the period 1903 to the present. In addition, some instructions from the late 1800's were also found in the archives. This provides some interesting insights into the practices and procedures of observing, coding, and transmitting weather information during a given segment of time. It occasionally takes a combination of inspecting the original observation forms and published instructions to determine the conventional practices of the time. With regard to winds, a history of the U.S. observing and coding practices is discussed, as well as the digitizing of early marine observations from the Maury Collection, which were basically collected before the common usage of the Beaufort wind scale.

Introduction

The history of the Beaufort wind scale, its evolution, adaptations, and usage are very difficult to establish and verify, as with most historical events. Slightly different facts and slants are noted in the literature and it is certainly evident that every ship's crew using the Beaufort scale to estimate surface wind speeds, did not apply the scale in a consistent manner. Numerous accounts on the subject have been published. Some good references are Ramage (1982), Kinsman (1969), Cook (1989), Smith (1925), and Garbett (1926) which provide important historical, although somewhat differing, facts and insights. It is always difficult to ensure exact factual truths and, in our work to establish the COADS winds metadata file, this has proven to be especially true.

In beginning to digitize the U.S. Merchant Marine observations between 1912 and 1946, it was quickly realized that it was necessary to know what guidance (instructions) was given to the observer at the time the observations were being recorded. It was critical to know what the coding and observing practices were and how they evolved over time. This information was needed so that proper digitizing procedures could be established

and so that accurate documentation would be available for future users and for converting the digitized records correctly to a common format compatible with COADS. First efforts were to collect only those editions of instruction to the marine meteorological observers of the U.S. Weather Bureau for the period 1912 through 1946 which covered the data periods being digitized at NCDC. An agreement was later reached with the Chinese National Oceanographic Data Center to digitize the Maury Collection, which consists basically of U.S. collected observations between 1820 and 1860, (the original Maury Collection is located at the National Archives, with a microfilm copy maintained at NCDC; it contains some observations from as early as 1792 and as late as 1900). This prompted us to locate as many earlier editions as possible, together with any additional publications or documentation that could provide guidance.

In an Earth System Monitor article (Elms et al., 1993) describing digitizing efforts in support of COADS including the project at NCDC for the 1912 - 1946 U.S. Merchant Marine observations, a table was developed based on the instructions issued from the late 1800s through 1949. This illustrated examples of changes in the codes and observing practices for the basic elements. The focus of this study is restricted to winds only, but with an expanded time horizon from the earliest available records of wind information to the present.

Important Dates

As mariners began to enter, in their ship's log, the strength and direction of the winds they encountered, they had to devise a somewhat uniform system for recording the information. As early as 1626, Captain John Smith published a list of names given to winds (Smith, 1925) which, somewhat surprisingly, are not very different from those used by Beaufort in 1806 when he first entered his scale into his ship's log. Lamb (1991) republished some wind terms which were first published by Defoe in 1704, and used by English sailors of the period; they too are similar to those later jotted down by Beaufort. In 1771 William Falconer published a glossary of technical sea terms which helped further standardize the reporting of customary terms. The East India Company, which had been sailing between England and India since 1599, appointed Alexander Dalrymple as hydrographer in 1779. Dalrymple had devised a 1-12 wind scale based on engineer John Smeaton's work with windmills. He entered this scale in an unpublished treatise entitled "Practical Navigation" and a synopsis of the wind scale also appears in some letterpress volumes now housed in the Library of Congress. Dalrymple later provided the information to Beaufort in 1805 (Cook, 1989).

In 1806, Beaufort first entered his adaptation of the Dalrymple wind scale (1-13) in his log, plus a notation for weather. As he advanced in the British Navy, he was able to bring the wind scale and weather notation into general use, and in 1838 the British Navy officially adopted the Beaufort wind scale (Garbett, 1926). The Beaufort scale was adopted for general use in the Merchant Marine by the Maritime Congress being held in London in 1874, with some modifications first recommended by the Maritime Congress held in 1872. In 1947, the International Meteorological Organization held a conference in Washington, D.C., and agreed to start reporting wind velocities in knots on January 1, 1949. However, the wind reports were still very closely linked to the Beaufort scale, as

is still the case today for most estimated wind speeds. Increase in size and height of vessels over the past century may also have biased the estimated wind speeds.

Changes in U.S. Wind Codes and Observing Practices

In the Maury Collection prior to the mid-1870s, most of the wind reports (generally three per day - first, middle and latter) provide prevailing direction, often with a descriptive term, in the remarks section, similar to the terminology used in the Beaufort scale (e.g. brisk wind, fresh breeze, etc.). There is doubt as to what period of the day is referred to with "first", "middle", and "latter". Oliver and Kington (1970) and the minutes from the 1853 Brussels Conference (Maury, 1854) indicate that these terms represent the 8 hours prior to 4 a.m., noon, and 8 p.m. However, the U.S. "instructions to the observer" from 1876 indicate that they represent the prevailing conditions 8 hours before 8 a.m., 4 p.m. and midnight. Although Oliver et al. and Maury indicated the same eight hour periods of the day, it is not clear from existing documentation the order they were entered on the observing form. Oliver and Kington state that daily entries were made in the logbook for the previous 24 hours meaning the "first part" was the period 1200-2000 hours, the "middle part" 2000-0400 hours, and the "latter part" 0400-1200 hours, meaning all three entries were for periods prior to the time the ship's position was established for the date of the observation. In contrast Maury wrote in the minutes from the Brussels Conference that "The direction and force of the wind should be regularly entered at 4 A.M., noon, and 8 P.M. The force and direction entered should be that which has been most prevalent during the eight preceding hours". This would seem to indicate that the "first part" represented 2000 (previous day) - 0400 hours, the "middle part" 0400-1200 hours, and the "latter part" 1200-2000 hours. To add to the confusion some of the observational logbooks in the Maury Collection contained a note at the bottom that read "Enter the wind for the point of the compass from which it has MOST PREVAILED for the eight hours" and a few even noted "Whether the day commences at noon or midnight, always call from noon to 8 P.M. First Part". This matches the explanation provided by Oliver and Kington (1970). It cannot be established from the observational forms (logbooks) which country originated them and no documentation was located indicating individual country practices or how they evolved over time. It is probable all observers did not follow a common procedure in entering data, thus adding more uncertainty to the data collection.

Although the U.S. merchant marine vessels did not generally begin to report wind force using the Beaufort scale until after the mid-1870s, it appears that U.S. Navy ships began doing so in the 1850s. If feasible and it can be proven to be scientifically sound, we propose to convert the descriptive terms found in the Maury reports to a Beaufort number, which can then be converted to a wind speed. In a majority of cases, the descriptive terms are exactly the same as, or very close to, the Beaufort descriptive terms. However, there are those terms such as "declining wind", "strong winds", "good wind", etc., which cannot be cross referenced and converted to a Beaufort number. It must be stressed that, before any conversions are performed, a significant amount of research must be conducted to ensure valid procedures are followed. Under all circumstances, we must ensure that the original entries are not lost.

It is uncertain at this point if the wind directions reported in the Maury Collection are magnetic or true. Again, much more work is required in this area to document the common practice during this era. From the minutes of the 1853 Maritime Conference held in Brussels (Maury, 1854), the following statements were included: "The direction of the wind is the magnetic direction, with due allowances for appearances caused by the motion of the vessel. It is the direction of the wind which has prevailed for the last 8 hours. It should be expressed to the nearest point of the compass". They also agreed that "The force of the wind should be expressed in figures. The nomenclature of Admiral Beaufort was adopted". However, as noted in the above paragraph, the Merchant Marine reports in the Maury Collection did not conform to this recommendation until approximately the mid-1870s; therefore, we cannot assume that the reported wind directions were magnetic, although it is highly likely they were, because of the information needed to correct them to a true direction.

A lineage of instructions provided to the U.S. Marine observers from the mid-1800s until the present appears in Table 1 with details on when coding and observing practices changed with regards to wind direction and speed. Instructions published between the 1880s and 1910 included the Beaufort scale (0-12) with the description of the wind force as related to the use of sails. However, the wind scale noted in miles per hour was similar to the WMO Beaufort conversion to knots (adopted in 1947) up through force 4; somewhat lower between force 5 and 9; but much higher for force 10 and above (reference figure 1). From 1898 through 1924 the published speeds associated with the Beaufort scale were somewhat higher than what would later become known as the WMO convention of mean equivalent wind speeds (WMO,1970) for all Beaufort forces. However, the scale that was published between 1898 and 1924 for forces 10-12 was considerably lower than the instructions published in the 1880s. By 1910, those in the U.S. preparing the instructions for the observer realized they had a problem, as most of the ships were no longer sailing vessels. As a result, they simply dropped any reference to sails and only maintained the word description and equivalent velocities in both statute and nautical miles per hour.

In 1925, the U.S. issued another edition of instructions to the marine observers. In this issue, and the one to follow in 1929, the equivalent wind velocities were presented in meters per second and statute miles per hour. These equivalent wind speeds were those used by the British since 1906 and which were later adopted by the IMO in 1947. To aid the observer in estimating the winds, new descriptive terms were added, one specifically for use on land and a second which was again based on a mode of estimating the wind speed aboard a sailing vessel. By 1938 a different approach was instituted. They again dropped the equivalent wind speed and added descriptive terms based on the state of the sea, but with a few caveats. The descriptions only went through force 5, as they theorized that sea heights generated above force 5 were generally near storm centers where rapid changes of duration and velocity would not permit the sea to reach a state of equilibrium with respect to the wind. The instructions also indicated that, to use this method, the ship had to be in the open sea and the sea surface had to be in a state of equilibrium (no appreciable current, and the wind direction and speed had to remain essentially constant for a sufficient length of time).

Based on the International Meteorological Code adopted by the IMO, Washington, D.C., in 1947, wind directions were to be reported in tens of degrees and

speeds in knots. However, the new instructions provided a description of the sea state for each Beaufort number (0-12) and a coded value in knots corresponding to each Beaufort number. This coded value is the one used to convert all Beaufort Force winds in COADS, except for two relatively small data sources which were converted using a slightly different conversion. This conversion only differed by 1 or 2 knots, in 7 Beaufort categories, from the 1947 IMO convention.

With regard to the Beaufort force, the U.S. continued to provide the same instructions from 1949 through 1981, with the exception of 1949 when they published a code value in knots. Pictures of the state of the sea were then published in 1982 for Beaufort forces 3-12 as guidance. Forces 0-2 only carried a description. However, with each photograph a wind speed, rounded to the nearest 5 knots, was inserted into the lower section of the photograph except for force 5 which displayed two photographs, one at 18 knots and a second at 20 knots. In 1992, the Instructions were again revised and color photographs of the state of the sea were published for each Beaufort force (0-12) with only the wind speed range inserted below each photograph.

Summary

Many of the observing practices and changes to those practices have introduced numerous biases to the data. By identifying where these have been introduced, through researching the historical documentation and analyzing the digitized data, it is believed that many of these biases can be identified and adjusted sufficiently to where the wind record contained within COADS will prove most beneficial to ocean research, especially climate and global change studies. We have just begun to identify the U.S. coding and observing practices with this study, yet much more effort is needed to investigate those of all maritime nations.

References

Cook, A.S., 1989: Alexander Dalrymple's appointment as East India Company hydrographer in 1779 and his "Instructions to Captains' for a new system of chart compilation", 13th Annual Conference on the History of Cartography, Amsterdam and the Hague, June 26 to July 1.

Elms, J.D., S.D. Woodruff, S.J. Worley, and C.S. Hanson, 1993: Digitizing Historical Records for the Comprehensive Ocean-Atmosphere Data Set (COADS), Earth System Monitor, Vol. 4, No. 2.

Garbett, L.G., 1926: Admiral Sir Francis Beaufort and the Beaufort Scales of Wind and Weather, Quarterly Journal of the Royal Meteorological Society, Vol. 52, London.

Kinsman, B.,1969: OCEANS, Vol. 2, No. 2, Who Put the Wind Speed in Admiral Beaufort's Force Scale?

Lamb, H., and K. Frydendahl, 1991: Historical Storms of the North Sea, British Isles and Northwest Europe, Cambridge University Press.

Maury, M.F., 1854: Maritime Conference Held at Brussels, for Devising a Uniform System of Meteorological Observations at Sea, August and September, 1853, Wind and Current Charts, Explanations and Sailing Directions, Sixth Edition, Philadelphia.

Oliver, J., and J.A. Kington, 1970: The Usefulness of Ships' Log-books in the Synoptic Analysis of Past Climate, Weather, Vol. 25, No. 12., Royal Meteorological Society.

Ramage, C.S., 1982: Observations of Surface Wind Speed in the Ocean Climate Data Set, Tropical Ocean - Newsletter, No. 13.

Smith, H.T., 1925: Marine Meteorology, History and Progress, The Marine Observer, Vol. II, No. 15.

World Meteorological Organization, 1970: The Beaufort Scale of Wind Force (Technical and operational aspects), Reports on Marine Science Affairs, Report No. 3, Geneva.

Table 1:

EXAMPLES OF CHANGES IN U.S. CODES & OBSERVING PRACTICES

Instructions Edition		Wind Speed	Wind Direction
Edition	Year		
Instructions attached to form	pre-1870's	Descriptive Terms	32 point scale, Magnetic or True?
	1880's	Beaufort Force	32 point scale, mean magnetic direction
	1898		32 point scale, true direction
H.O. Pub 119	1903		
Circular M			
1st Edition	1906		
2nd	1908		
3rd	1910		
4th	1925	Added new descriptions	
5th	1929		
6th	1938	Word descriptions Force 0-5	DD+33=gustiness, DD+67=squalls
7th	1941		
Provisional	1949	Knots	36 Point scale
8th	1950		
9th	1954		
10th	1959		
11th	1963		
12th	1964		
NWS Observing Hand-book #1			
1st Edition	1969		
	1971		
	1974, rev		
	Jan, '82	Sea state photos, Force 3-12	
	Jul, '91	Color photos, Force 1-12	
	Nov, '94 (code change)		

Figure 1:

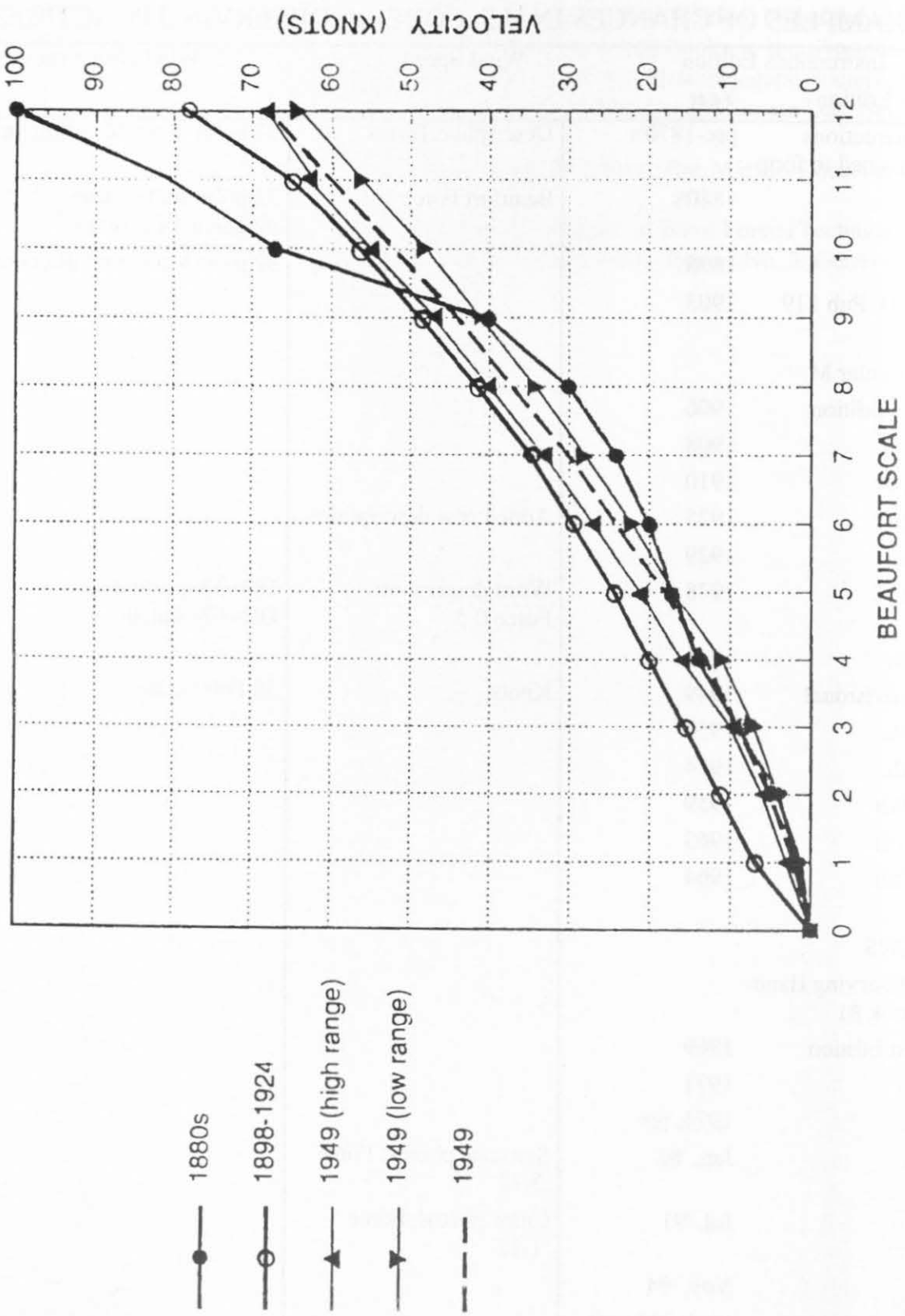
VELOCITY (KNOTS)
100
90
80
70
60
50
40
30
20
10
0
0 1 2 3 4 5 6 7 8 9 10 11 12
BEAUFORT SCALE
1880s
1898-1924
1949 (high range)
1949 (low range)
1949

Part II

Evaluation of Long-Term Changes

Near-Global MSLP Since 1871: A Source for COADS Wind Validation

Robert J. Allan

Climate Impact Group,
CSIRO Division of Atmospheric Research,
Melbourne, Victoria,
Australia.

Introduction

Recent research emphases on the enhanced greenhouse effect and climatic variability has seen the development of quality controlled global historical data compilations covering land and sea surface temperatures (including integrated sets), precipitation and clouds. However, no such global to near-global coverage is available with regard to parameters indicative of near-surface atmospheric circulation. At present, long-term monthly mean sea level pressure data sets cover 85°N-15°N, 0°E-5°W (1899-1991) (see Bradley et al., 1994) and 15°S-60°S, 0°E-5°W (1911-1989) (Jones, 1991). Shorter global to regional compilations are available (see Jones and Wigley, 1988; Jones, 1991; Barnett and Jones, 1992; Bradley et al., 1994), but they do not have the temporal coverage necessary to resolve the range of decadal-multidecadal fluctuations in climate that are evident in other historical data sets.

Efforts are currently underway to redress the above situation with the construction of a unique near-global monthly sea level pressure (MSLP) compilation using both land and ship observed data and covering the period since 1871 (Allan, 1993). A preliminary version of this MSLP set has been used to examine the long-term nature of relationships indicative of the El Niño Southern Oscillation (ENSO) phenomenon. Results from analyses of the historical instrumental period using the MSLP data have identified decadal-multidecadal global scale fluctuations in ENSO and the climate system. Periods or epochs with different ENSO and MSLP characteristics should also be evident in variables such as surface wind fields that are indicative of atmospheric circulation patterns. In fact, assuming a simple geostrophic relationship with the new near-global MSLP data would allow the calculation of a proxy field for near-surface winds, which could be used as a check on the validity of land or Comprehensive Ocean-Atmosphere Data Set (COADS) ship observed wind fields. In the latter case, this would aid in efforts to develop a quality controlled historical oceanic near-surface wind data compilation.

This paper outlines the current status of the new near-global MSLP compilation, some analyses with a preliminary version of this product, and its potential as a check for historical ship wind reconstruction's based on experience with studies in the Indian Ocean region.

Data Sources and Methods

Historical station level pressure from land stations and MSLP data from ships across the globe were obtained from World Weather Records (Smithsonian Institute, 1944; WeatherDisc Associates, 1990), Lockyer (1908); Reseau Mondial (1910-34); Berlage, (1957, 1966); Schove and Berlage (1965); Jones (1991); COADS (Woodruff et al., 1987); Allan et al. (1991); Young (1993) and Allan and D'rrigo (1995) (Figure 1). Additional records were extracted from numerous manuscripts held by various meteorological services and reports in old meteorological journals. Station level pressure data were reduced to MSLP, and all the resulting MSLP time series were checked and corrected where necessary using a three stage process. In the first stage, each of the individual time series were detrended linearly and the annual cycle removed; the data were then examined for spurious data points, jumps and trends. The second stage of quality control involved cross checking spatially, with the construction of station differences between each time series and neighboring time series used to highlight spurious data points, jumps and trends. Monthly mean gridded data were then derived from the point measurements of MSLP that had undergone the first two stages of quality control, and contoured to form spatial fields of monthly MSLP since 1871. A third and final stage was the subjective checking of each contoured monthly MSLP field against long-term monthly climatologies for obvious spatial inhomogeneities.

Applications

Preliminary MSLP correlation studies of ENSO and the climate system

A preliminary version of the MSLP dataset was the basis for correlation analyses examining the spatial and temporal pattern of ENSO/anti-ENSO teleconnections through relationships between Darwin and global MSLP observations since 1879 (Allan, 1993). Darwin MSLP was used instead of a Southern Oscillation Index (SOI), because a running/sliding correlation (set at 21 years in this case) between the two MSLP stations most often used to form a SOI (Tahiti and Darwin) showed that the correlation structure has changed on multidecadal time frames (Figure 2). In fact, the strong out of phase relationship between these stations, that is common to more recent epochs and is the basis of persistence forecasts, was not evident over the full period of record (1876-1990). In order to test the wider responses of ENSO during the historical period, and given the indications in Figure 2, the preliminary MSLP data set was divided initially into five 21-year periods centered around the years 1921-41, when ENSO was apparently weaker than at any other time in the record. The validity of partitioning the data into these five different periods was supported by a number of papers in the literature which have documented the marked weakening and even 'breakdown' of correlation's between ENSO and rainfall over the globe during the 1920s-30s period.

Figures 3, 4 and 5 show the three most differing epochs in terms of ENSO characteristics during the historical record. Both the earliest (1879-99) and the most recent (1963-83) epochs display the type of coherent and robust patterns indicative of the

distribution and extent of ENSO impacts. However, the 1921-41 period (Figure 4) shows a more fragmented pattern, with the major regions in both Indo-Australasia and the southeastern Pacific being very much weaker and contracted in spatial extent. Thus it would seem that regions of ENSO influence over the globe wax and wane on decadal-multidecadal time scales. The correlation patterns derived from the MSLP set should also reflect changes in other oceanic and atmospheric variables such as broad scale wind patterns. This could be assessed if a global near-surface wind compilation covering the historical period was produced.

Potential as a check for historical ship wind reconstructions: Indian Ocean experience

Significant research has been conducted on historical data observations over the Indian Ocean-Australian region during the austral summer (JFM) (Allan and Lindesay, 1991, 1993; Lindesay and Allan, 1992, 1993; Allan et al., 1995). These studies show different spatial responses in atmospheric circulation/wind, MSLP, sea surface temperature (SST) and cloudiness on inter-annual to multidecadal time scales. Confidence in the observed surface wind data analyzed in the above studies was increased by a comparison of observed winds and those derived from MSLP gradients under a geostrophic assumption (Ward, 1991, 1992). Despite potential biases in ship winds due to changing observer practices, the studies of Ward (1991, 1992) have indicated that data problems relating to observed ship winds tend to be least over the Indian Ocean basin when compared to other ocean regions. However, wind reconstructions using existing MSLP data gradients also need to be examined with care due to potential problems with the MSLP observations in some ocean basins. Preliminary analyses in Allan et al. (1995) suggest that, apart from periods of sparse observations, MSLP data problems in the Indian Ocean region are most acute at high latitudes along the far southern historical ship tracks. Some of these problems are easily identified, as they show up as distinct outliers in MSLP time series. Others are less obvious, and require careful quality control efforts to identify them.

Conclusions

Studies with a preliminary version of a new global MSLP data set have revealed fluctuations in ENSO and the climate system that should also be detectable in surface wind fields. In addition, efforts to produce high quality surface wind field data from sources such as COADS ship observations would benefit substantially from comparisons with geostrophically derived surface wind fields calculated from a high quality MSLP compilation. As noted in Allan (1993) and this study, examinations of historical global MSLP data and the development of a more comprehensive global MSLP compilation are in progress. The ultimate aim is to produce an MSLP data set comparable in quality to the Global sea-Ice and Sea Surface Temperature (GISST) compilation produced by the United Kingdom Meteorological Office (UKMO).

Acknowledgments

This work contributes to the CSIRO Climate Change Research Program and is part funded through Australia's National Greenhouse Research Program. Thanks are due to Dr. Phil Jones for making available numerous MSLP station files from the Climatic Research Unit, University of East Anglia's collections; Dr. Kenneth Young for providing his reconstructed MSLP station data; and Dr. Jim Salinger for the extension and recovery of data in the New Zealand Meteorological Service archives.

References

Allan, R.J., 1993: Historical fluctuations in ENSO and Teleconnection structure since 1879: Near-global patterns. *Quaternary Australasia*, 11: 17-27.

Allan, R.J. and Lindesay, J.A., 1991: Modulation of summer rainfall in southern Africa and Australia with teleconnection patterns across the Indian Ocean. In International Conference on the Physical Causes of Drought and Desertification, Abstracts, (ed. B.G. Hunt), Melbourne University. (AMOS publication 7). Bureau of Meteorology, Melbourne.

Allan, R.J., Nicholls, N., Jones, P.D. and Butterworth, I.J., 1991: A further extension of the Tahiti-Darvin SOI, early ENSO events and Darvin pressure. *J. Climate*, 4: 743-749.

Allan, R.J. and Lindesay, J.A., 1993: Multidecadal fluctuations in the climate system over the Indian Ocean region. 4th International Conference on Southern Hemisphere Meteorology and Oceanography, Hobart, Tasmania, 29 March-2 April, 1993.

Allan, R.J., Lindesay, J.A., and Reason, C.J.C. (1995). Multidecadal variability in the climate system over the Indean Ocean region during the austral summer. *J. Climate* (in press).

Allan, R.J. and D'Arrigo, R.D., 1995: 'Persistent' ENSO sequences: How unusual was the recent El Niño? (In review)

Barnett, T.P. and Jones, P.D., 1992: Inter-comparison of two different Southern Hemisphere sea level pressure datasets. *J. Climate*, 5: 93-99.

Berlage, H.P., 1957: Fluctuations in the General Atmospheric Circulation of more than One Year, their Nature and Prognostic Value. Mededlingen en Verhandelingen No. 69, Koninklijk Meteorologische Instituut, Staatsdrukkerijs-Gravenhage, The Netherlands, 152 pp.

Berlage, H.P., 1966: The Southern Oscillation and World Weather. Mededlingen en Verhandellngen No. 88, Koninklijk Meteorologische Instituut, Staatsdrukkerijs-Gravenhage, The Netherlands, 152 pp.

Bradley, R.S., Ahem, L.G. and Keimig, F.T., 1994: A computer-based atlas of global instrumental climate data. *Bull. Amer. Meteor. Soc.*, 75: 35-41.

Jones, P.D., 1991: Southern Hemisphere Sea Level Pressure Data: An Analysis and Reconstructions Back to 1951 and 1911. *Int. J. Climatol.*, 11: 585-607.

Jones, P.D. and Wigley, T.M.L., 1992: Antarctic gridded sea level pressure data: An analysis and reconstruction back to 1957. *J. Climate*, 1: 1199-1220.

Lindesay, J.A. and Allan, R.J., 1992: Teleconnection patterns across the Indian Ocean and summer rainfall in Australia and southern Africa. In Technical Programme Abstracts of the 27th International Geographical Congress, pp. 372, Washington, August 1992.

Lindesay, J.A. and Allan, R.J., 1993: Summer rainfall modulation in southern Africa and northern Australia with inter-annual fluctuations over the Indian Ocean. 4th International Conference on Southern Hemisphere Meteorology and Oceanography, Hobart, Tasmania, 29 March-2 April, 1993.

Lockyer, N., 1908: Monthly Mean Values of Barometric Pressure for 73 Selected Stations over the Earth's surface. Solar Physics Committee, London, 97 pp.

Reseau Mondial, 1910-34: British Meteorological and Magnetic Year Book Part V. H.M. Stationary Office, London.

Schove, D.J., and Berlage, H.P., 1965: Pressure Anomalies in the Indian Ocean Area, 1796-1960. *Pure Appl.. Geophys.*, 61: 219-231.

Smithsonian Institute, 1944: World Weather Records, Smithsonian Miscellaneous Collections, Vol. 79, Smithsonian Institute, Washington, DC, 1199 pp.

Ward, M.N., 1991: Worldwide ocean-atmosphere surface fields in Sahel wet and dry years using provisionally corrected surface wind data. Climate Research Tech. Note No. 20 [Available from the National Meteorological Library, Meteorological Office, Bracknell, Berkshire, UK].

Ward, M.N., 1992: Provisionally corrected surface wind data, worldwide ocean-atmosphere surface winds, and Sahelian rainfall variability. *J. Climate*, 5: 454-475.

WeatherDisc Associates, 1990: World Monthly Surface Station Climatology (TD9645). On World WeatherDisc: Climate data for the planet Earth. - Version 2.0., Seattle, Washington.

Woodruff, S.D., Slutz, R.J., Jenne, R.L. and Steurer, P.M., 1987: A Comprehensive Ocean-Atmosphere Data Set. *Bull. Amer. Meteor. Soc.*, 68: 1239-1250.

Young, K.C., 1993: Detecting and Removing Inhomogeneities from Long-Term Monthly Sea Level Pressure Time Series. *J. Climate*, 6: 1205-1220.

Figure 1: Maximum distribution of land and ship observations of MSLP used in the new global monthly MSLP data compilation

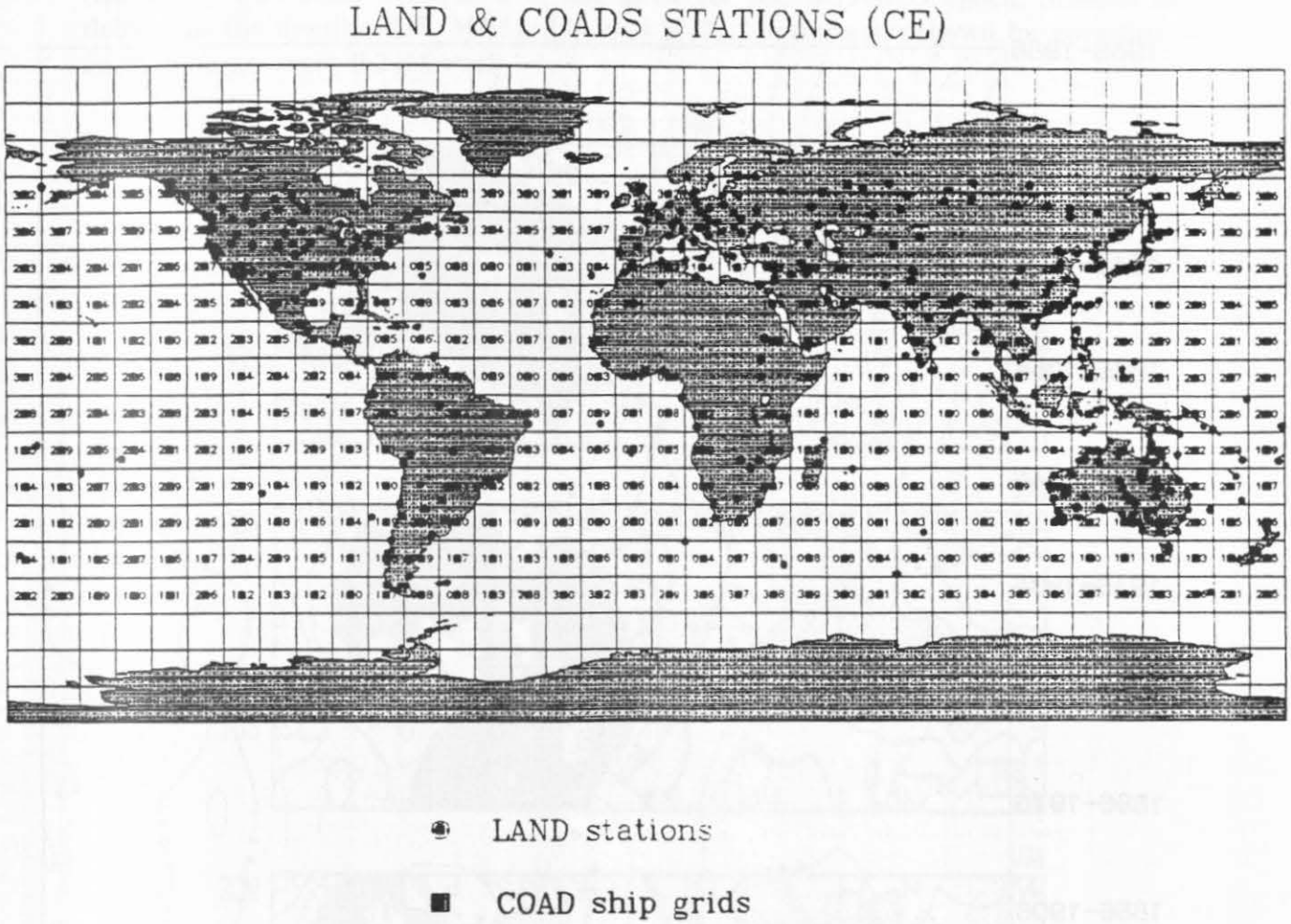

Figure 2: 21 year running/sliding monthly correlations between Darwin and Tahiti MSLP since 1876. Areas of negative correlation significant at the 95% level are shaded.

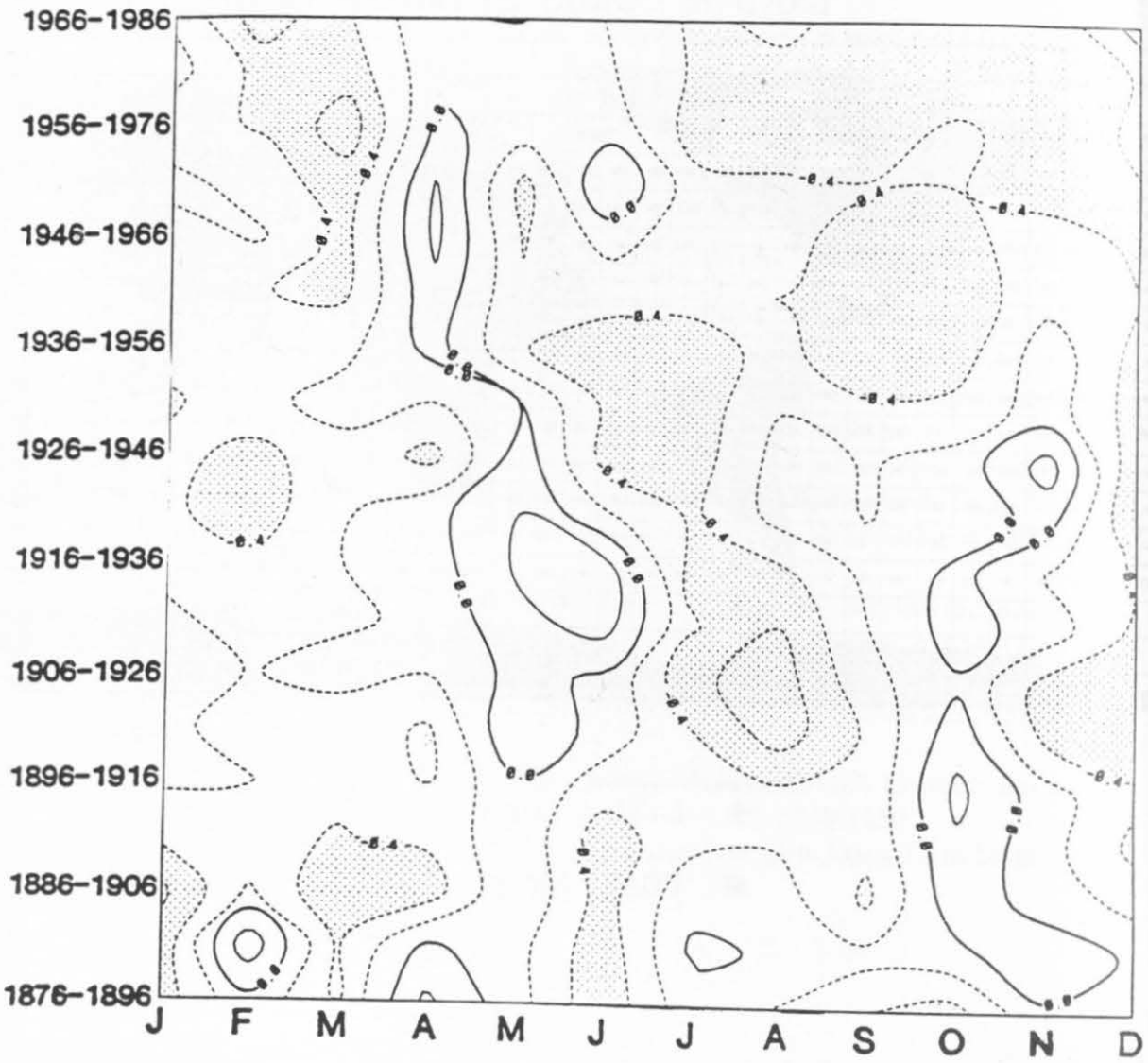

Figure 3: Seasonal analysis of regions of significant (at the 95% level) positive (shaded) and negative (stippled) correlation between mean sea level pressure (MSLP) at Darwin (Australia) and other stations over the globe for the 1879-1899 epoch. Seasons are defined as the months DJF, MAM, JJA and SON. Contours are shown for correlation coefficients at every 0.2 interval.

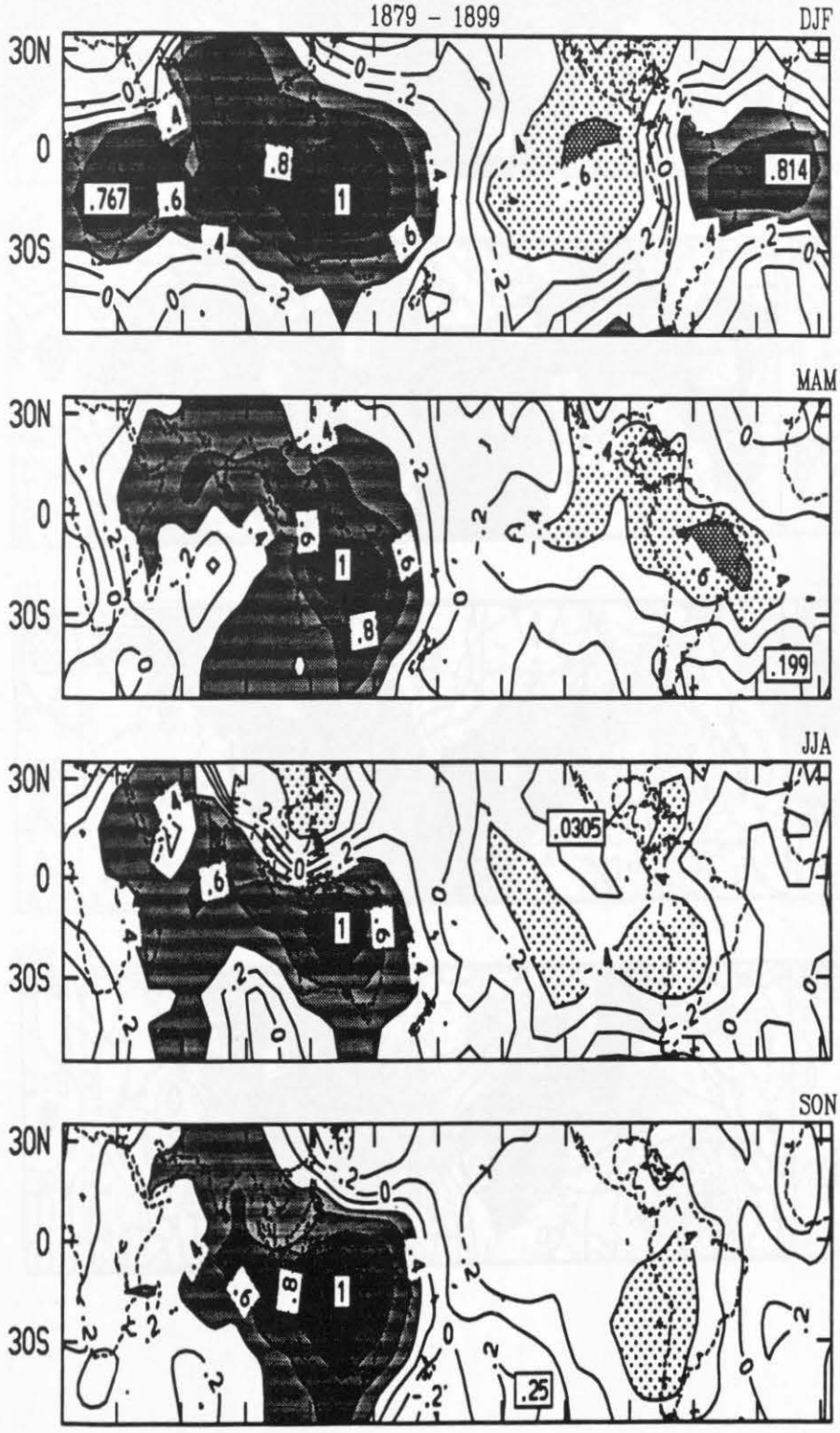

Figure 4: As in Figure 3, except for the 1921-1941 epoch.

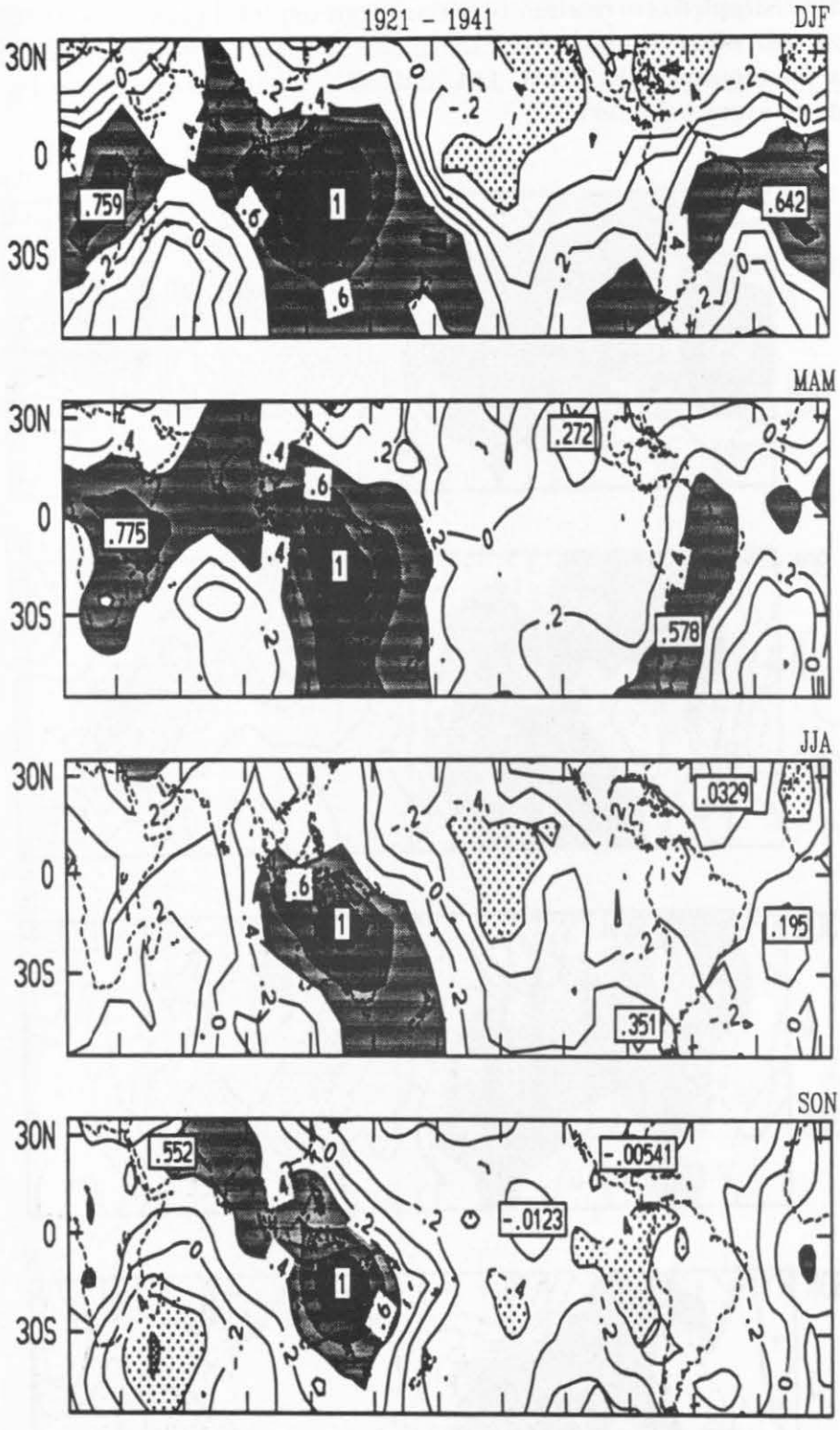

Figure 5: As in Figure 3, except for the 1963-1983 epoch.

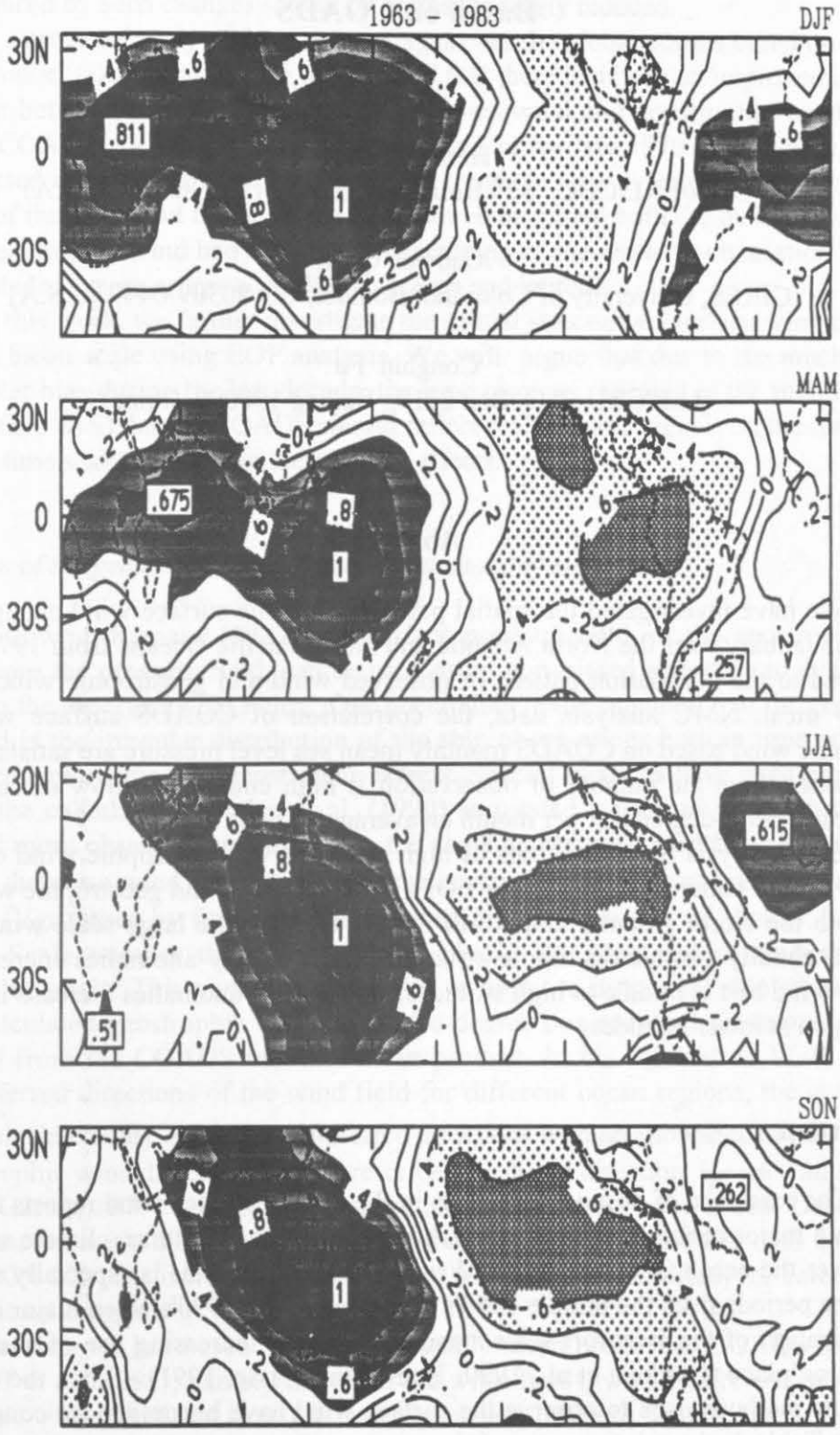

Marine Surface Wind Changes During 1978-1992: An Estimation Based on COADS

Henry F. Diaz
(NOAA/ERL/CDC, 325 Broadway, Boulder CO 80303, U.S.A)

Xiaowei Quan
(CIRES, University of Colorado, Boulder, CO 80309-0449, U.S.A)

Congbin Fu
(IAP/CRL, P.O. Box 2718, Beijing 100080, China)

Abstract

We have investigated the spatial pattern of marine surface wind changes for the month of January over the North Atlantic and North Pacific Oceans from 1978 to 1992. Compared to the correlation pattern of observed wind and geostrophic wind based on monthly mean NMC analysis data, the correlation of COADS surface winds with geostrophic wind based on COADS monthly mean sea level pressure are satisfactory over the regions where the number of observation is high enough to allow more than five observations per 4-degree box per month on average.

EOF analysis for the regions of high observed vs. geostrophic wind correlation produce similar patterns of the leading EOFs in the observed and geostrophic wind fields. Over both the North Atlantic and North Pacific Oceans, the large-scale wind changes exhibit a zonally symmetric dipole structure, i.e. westerly anomalies increase in the westerly wind belt at middle to high latitudes, and easterly anomalies increase in the trade wind region at lower latitudes.

Introduction

The existence of observational bias in the marine surface wind reports from ships has been a major concern when using such data to detect long-term climate signals and trends over the ocean (Ramage, 1987; Wright, 1986). The bias is especially significant during the periods from the middle 1960's to the end of the 1970's when major changes in the application of the Beaufort scale standards and the increasing use of anemometers were taking place (Cardone et al., 1990; Isemer and Hasse, 1991). Since the end of the 1970's, the methods used to observe the surface wind have become more consistent. As shown in Table 1, the relative ratio of the number of anemometer measurements versus those based on Beaufort estimation has increased by less than ten percent during the 10 years from 1980 to 1989. This is relatively small compared to about a forty percent

percent change during the previous 13 years 1965 to 1977. Consequently, the systematic biases induced by such changes should be correspondingly reduced.

In a previous study of the zonal averages over the global oceans based on COADS interim product (Diaz et al., 1992), we showed that there had been an improvement in the agreement between zonal components of observed wind and geostrophic wind derived from the COADS sea level pressure field starting in the late 1970's. The improvement was reflected in closer agreement of the linear trends in area-average indices for January and July of the two wind fields. In the Northern Hemisphere both the observed wind and derived geostrophic wind had shown a strengthening of the westerly circulation although the magnitude is more or less according to season and latitude.

In this work, we further investigate the spatial structure of surface wind change at the ocean basin scale using EOF analysis. We will argue that due to the much smaller anemometer bias during the last decade, the time changes revealed in the monthly mean ocean surface wind data of COADS should reflect real climatic signals on the interannual to decade time scale, rather than the artificial effects.

Evaluation of the geostrophic wind method with monthly mean data

Following Ramage (1987), the surface pressure field, or the geostrophic wind derived from the pressure field, can be used as an non-biased reference to evaluate the changes in the observed wind fields. One uncertainty in the calculation of the geostrophic wind field is the irregular distribution of the ship observations both in time and space. Another concern is the non-geostrophic effects. Several methods have been proposed to improve the calculation. Lindau et al. (1990) suggested a method in which they first calculated mean observed wind direction, the angle between the base-line connecting two ships and the mean wind direction (β) and the geostrophic wind component normal to the base-line (Vgn); then by fitting sinusoidal functions to the curves of Vgn vs. β for each Beaufort Scale number they were able to obtain the geostrophic wind speed and ageostrophic angle. This method was devised to apply to individual ship reports. Ward (1992) calculated geostrophic wind using two-degree box seasonal mean pressure field converted from the COADS monthly mean product. In his calculation Ward deduced some preferred directions of the wind field for different ocean regions, the geostrophic wind is calculated only along these preferred directions with an allowance of $\pm 20^{\circ}$ shift of the geostrophic wind direction from a prescribed preferred direction. He used an empirical formula (Garrat, 1977) to include the effect of friction on the wind speed. Deser (1993) used regression method to determine the friction term and she noted that over the tropical Pacific (20N-20S) the inclusion of the friction term is more important for calculation of the meridional component.

The data we have used here is the monthly mean product of COADS Release-1a (Woodruff et al., 1993), namely the observed wind fields, which were compared to the geostrophic wind calculated from the monthly surface pressure field in 4x4 degree boxes, assuming only simple geostrophic balance. In the following we first give an evaluation of our geostrophic wind calculations.

Ideally, the surface pressure field used to calculate the geostrophic wind should be observed simultaneously with the surface wind. However, this condition is not often able to be satisfied in many parts of the ocean by the network of ship observations. The use of monthly mean values will induce errors in the calculated geostrophic winds and weaken its correlation to the observed wind due to arbitrarily shifting the time of the observations within a month and the positions within a box. In order to evaluate how much this kind of error will affect our results, we have made similar calculations using the NMC analysis data of both twice daily and monthly mean products. The twice daily data used to calculate the geostrophic wind covers 90 days from December 1, 1991 to February 28, 1992 providing a total of 180 time points for each grid point. The monthly mean data set covers 84 months from January 1985 to December 1991.

The correlations between the observed wind and geostrophic wind are shown in Figure 1. High correlation patterns are obtained for both zonal and meridional wind components. When the monthly mean data is used, the correlations are still high over most of the extra tropical oceans for the zonal wind component but they are significantly reduced for the meridional wind component. Since the NMC daily analysis are generally complete for each grid point, the difference between the correlation patterns of daily data and monthly mean data actually describes the effect of removing the short time and small spatial scale eddies. It is clear that for the purpose of using geostrophic wind to estimate the change of wind speed or the full vector wind field, it would be better to use the data with daily time resolution. Since the smaller scale eddies have a greater impact on the relative accuracy of the derived meridional geostrophic wind component, data that are capable of resolving these scales of atmospheric motions are necessary to get a good representation of the meridional wind by its geostrophic component.

Comparing the pattern of correlation coefficients between the observed wind and geostrophic wind based on COADS monthly mean (Figure 2) to that of NMC monthly mean, we note that most of the NMC monthly mean correlation can be reproduced by COADS in the North Atlantic and North Pacific Oceans for the zonal wind component. Within these regions the number of observations is high enough to allow at least one data per month per box, and the number of observations range from 5 to 291 per month per box (see figure 2b of Diaz et al., 1992). In the Southern Hemisphere the high correlations in the correpsonding NMC monthly data are not reproduced by the COADS data, because there are much fewer observations in the southern oceans. For the meridional wind component the coverage of high correlation is even more reduced with the COADS monthly mean.

We have included a friction term in the calculation of geostrophic wind and found that the inclusion of this term has only a minor impact on the correlation patterns. We conclude that the largest source of error affecting the correlation pattern between geostrophic and observed wind comes from the distribution and number of observations.

The spatial structure of changes of the zonal wind over the northern mid-latitude oceans

To verify the wind changes shown in the time series of zonal means (Diaz et al., 1992), the spatial structure of the changes of surface zonal wind over the North Atlantic (70N-10N) and Northern Pacific (60N-10N) Oceans are further examined by means of

EOF analysis. The geostrophic wind and observed wind show similar spatial and temporal patterns of change during the last decade.

North Atlantic Ocean (10N-70N)

The EOF-1 patterns of the observed and geostrophic wind fields over the North Atlantic Ocean are shown in Figures 3a & b. The north-south dipole of the North Atlantic Oscillation is the most significant feature in the behavior of both wind fields. One amplitude center is at 55N with another of opposite sign at 30N while the zero line tilts from 50N in the west to the 38N in the east. Figure 3c shows the time series of the projections of the observed wind and geostrophic wind on its EOF-1 mode, i.e. the time series of the PC-1s, respectively. The strongest signal in the EOF-1 patterns may be contributed mostly by the interannual variations in the wind field. Although comparatively weaker to the interannual variability, an upward trend in the PC time series of this mode can still be observed. An increase of westerly anomalies in the middle and high latitudes (40N-65N) is shown together with an increase of easterly anomalies in the mid-to-low latitudes (10N-40N). The two PC-1 time series agree with each other very well as shown by the high value (0.94) of their correlation coefficient. In the EOF-2 of the observed wind (Figure 4a), centers of the maximum amplitude of the change are found at the latitudes of zero amplitude in its EOF-1 mode. This observed mode is well reproduced by the EOF-3 of the geostrophic wind (Figure 4b). Time series of both the PC-2 of observed wind and PC-3 of geostrophic wind show increasing values which corresponding to an intensification of these modes (Figure 4c).

North Pacific Ocean (10N-60N)

The EOF-1 mode of observed wind over the North Pacific Ocean also shows a dipole structure. A positive center of maximum variability is located at about 25N latitude while a negative one is at 50N and the zero line at about 40N. This mode is reproduced by the EOF-2 of the geostrophic wind (Figure 5a & b). The time series of the PCs of these two modes show good agreement, with a correlation coefficient of $r = 0.90$ (figure 5c). The low frequency trends appear to be in greater agreement than the interannual variations. The westerly anomalies have intensified at 50N and easterly anomalies have intensified at 25N during the last decade. The reason for the EOF-1 geostrophic wind not being able to represent the EOF-1 of observed wind is due to much larger variability in the geostrophic wind at the low latitudes. When we calculate the EOFs for the latitudes from 20N to 60N, the EOF-1 of observed wind is well reproduced by the EOF-1 of geostrophic wind (Figure 6a & b) and the correlation coefficients of the two PC-1's is 0.67 with their linear trend being almost the same value (Figure 6c).

Surface wind changes during 1979-92

Figure 7 shows the time series of the regional means of the zonal wind components of 1979-92. Regions are chosen according to two requirements: (i) presence of high geostrophic vs. observed wind correlation coefficients, and (ii) region encompassing the maximum centers of variability in the EOF-1 modes in the North Atlantic and North Pacific. The areas chosen for Figure 7 and the trends and their t-test values are listed in Table-2. The largest observed increase of the surface zonal wind is the westerly anomalies over the mid-latitude North Atlantic. The linear trend is about 0.3

m/s per year. The westerly anomalies over the mid-latitude North Pacific showed a linear trend of about 0.1 m/s per year. Within the low latitude regions, the easterly anomalies over the subtropical North Pacific and subtropical North Atlantic Oceans, the linear trends are smaller but of similar magnitude, about 0.2 m/s per year.

Conclusions

Using the geostrophic wind field as a non-biased reference, we have analyzed the surface wind change during the period 1978-92 based on the COADS Release-1a monthly mean product. The validation of the method is evaluated by comparing the pattern of geostrophic vs. observed wind correlation coefficient calculated from COADS monthly mean to those calculated from both of the NMC twice daily analysis and its monthly means. The latter ones are considered to be the optimum fields based on currently available data. The pattern of correlation coefficient of the NMC monthly means are well reproduced by COADS data for both the zonal and meridional wind components over the oceans where the number of observations are high enough to allow more than five data per box per month on average. High correlation values between u and ug cover extensive oceanic areas only for the zonal wind components. The meridional geostrophic wind calculated from the monthly mean pressure field exhibits good correlation compared to its observed counterpart only over small ocean regions. Thus, the geostrophic wind is not useful for evaluating the changes in observed meridional wind using the available monthly mean data, although its use may be adequate for this purpose, provided higher data densities are available.

Results of both the EOF analysis and regional means are consistent with the results based on zonally averaged wind data. The monthly mean zonal wind for January displays a clear signal that westerlies over the mid-latitude North Atlantic and mid-latitude Pacific oceans and easterlies over the northern subtropical oceans have strengthened in the past decade. The largest increases are observed over the North Atlantic Ocean with a linear trend of about 0.3 m/s per year. The linear trend is about 0.1 m/s per year over the North Pacific Ocean, and about 0.2 m/s per year over the subtropical Atlantic and subtropical Pacific oceans. The signals in the observed wind are well reproduced in the geostrophic wind field for zonal means, regional means and leading EOF modes. On such basis, we conclude that an increase of the January surface zonal wind observed from 1979-92, is likely a real climatic signal, rather than the result of artificial biases.

Acknowledgments

The NMC data made available by Kathy Smith, and Sandy Lubker of CIRES provided much technical support for extraction and manipulation of COADS data.

References

Cardone, V.J., J.G. Greenwood, and M.A. Cane 1990: On trend in the historical marine wind data. *J. Climate*, 3, 113-127.

Deser, C. , 1993: Diagnosis of the Surface Momentum Balance over the Tropical Pacific Ocean, *J. Climate*, 6, 64-74

Diaz, H. F., C. Fu, and X. Quan, 1992: A Comparison of Surface Geostrophic Wind with COADS ship Wind Observations, Proc. International Workshop, Boulder, Colorado, 13-15 January 1992, 131-141.

Garrat, J. R., 1977: Review of drag coefficients over oceans and continents. *Mon. Wea. Rev.*, 105, 915-929.

Isemer, H.-J. and L. Hasse, 1991: The scientific Beaufort equivalent scale: Effects on wind statistics and climatological air-sea flux estimates in the North Atlantic. *J. Climate*, 4, 819-836.

Lindau, R., H.-J. Isemer, and L. Hasse, 1990: Toward Time-Dependent Calibration of Historical Wind Observations at Sea, Tropical Ocean-Atmosphere Newsletter, Spring 1990, 7-12

Ramage, C. R., 1987: Secular changes in reported surface wind speeds over the ocean, *J. Appl. Meteor.*, 26, 525-528.

Ward, M. N., 1992: Provisionally Corrected Surface Wind Data, Worldwide Ocean-Atmosphere Surface Fields, and Sahelian Rainfall Variability, *J. Climate*, 5, 454-475

Woodruff, S.D., S.J. Lubker, K. Wolter, S.J. Worley, and J.D. Elms, 1993: Comprehensive Ocean-Atmosphere Data Set (COADS) Release-1a: 1980-92, *Earth System Monitor*, Vol 4, No. 1.

Wright, P.B., 1986 Problems in the Use of Ship Observations for the Study of Interdecadal Climate Changes. *Mon. Wea. Rev.*, 115, 1028-1034

Table 1: Ratio of number of Voluntary Observing Fleet ships with anemometers to total number of ships:

Year	Ratio(%)
1980	42.7
1981	42.8
1982	42.8
1983	43.7
1984	45.3
1985	45.5
1986	47.3
1987	46.7
1988	46.5
1989	48.7

Table 2: Percentage of the explained variance with each of the first 5 EOF's

	N. Atlantic		N.Pacific	
EOF-#	u	gu	u	gu
1	34.43	22.26	40.29	25.61
2	18.68	15.70	27.22	20.78
3	14.25	11.89	6.58	10.58
4	8.26	9.76	6.15	8.64
5	7.98	7.93	4.72	7.97

Table 3: Linear Trend of Surface Zonal wind over Selected Regions:

Region	Trend(u) m/s/yr	t-test value	Trend(gu) m/s/yr	t-test value
North Atlantic				
I: (60N-44N, 60W-0)	0.31	1.58	0.36	-1.69
II:(28N-12N,70W-10W)	-0.19	-1.71	-0.28	1.54
North Pacific				
III:(52N-32N,130E-120W)	0.11	1.14	0.16	1.54
IV:(28N-8N, 130E-120W)	-0.18	-2.53	-0.22	-2.09

n−2=12 α=0.1 tα=1.782

Table 4: Changes of the zonal wind between 1979-85 and 1986-92

	1979-85	1986-92	1979-92	
u(m/s)				Δ u/u %
Region				
I	3.27	5.63	4.45	53.0
II	-4.13	-5.46	-4.80	27.7
III	3.22	4.41	3.82	31.2
IV	-3.70	-5.55	-4.62	40.0
gu(m/s)				Δ gu/gu %
Region				
I	4.75	7.42	6.09	43.8
II	-6.46	-8.39	-7.42	26.0
III	4.02	5.40	4.71	29.3
IV	-6.57	-8.79	-7.86	28.9

Figure 1a: Correlation coefficient of observed vs. geostrophic wind for NMC twice daily analysis, zonal wind component

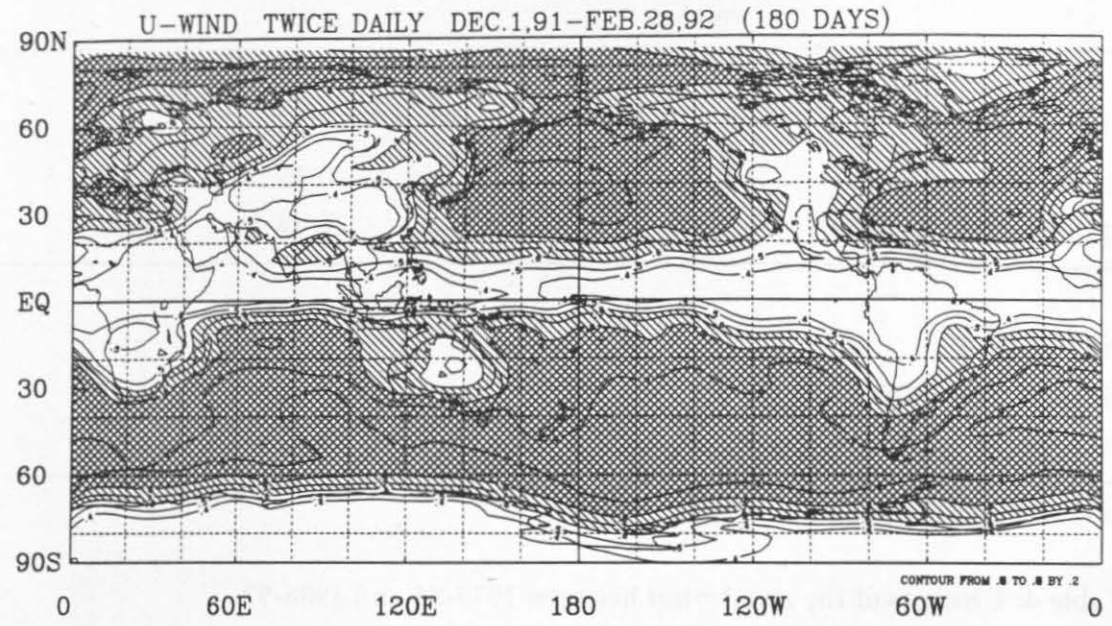

Figure 1b: Correlation coefficient of observed vs. geostrophic wind for NMC twice daily analysis, meridional wind component

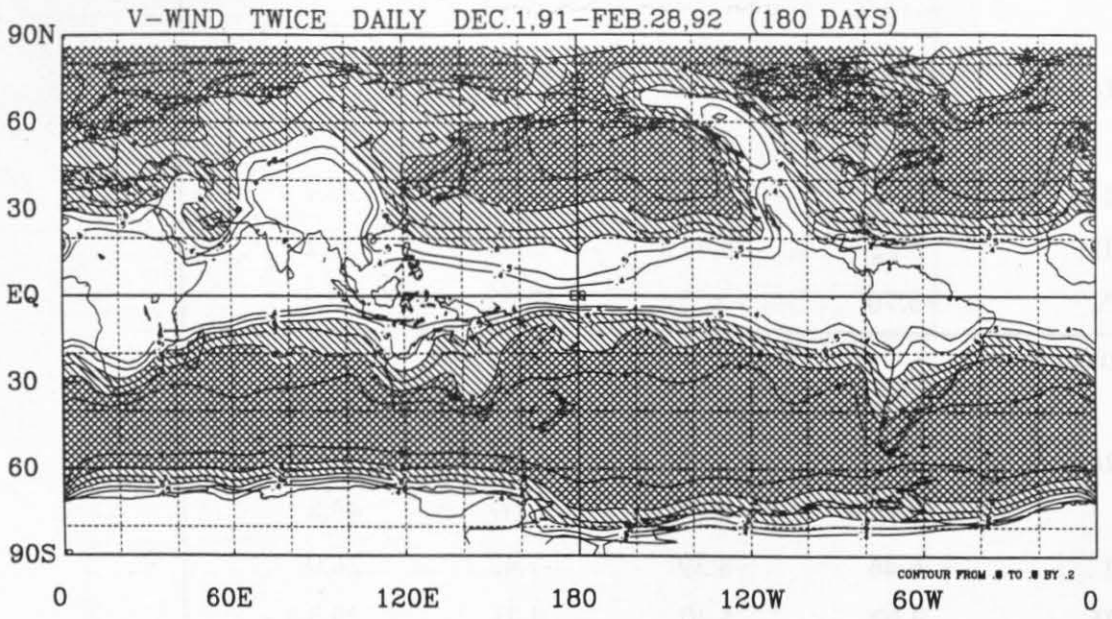

Figure 1c: Correlation coefficient of observed vs. geostrophic wind for NMC monthly mean, zonal wind component.

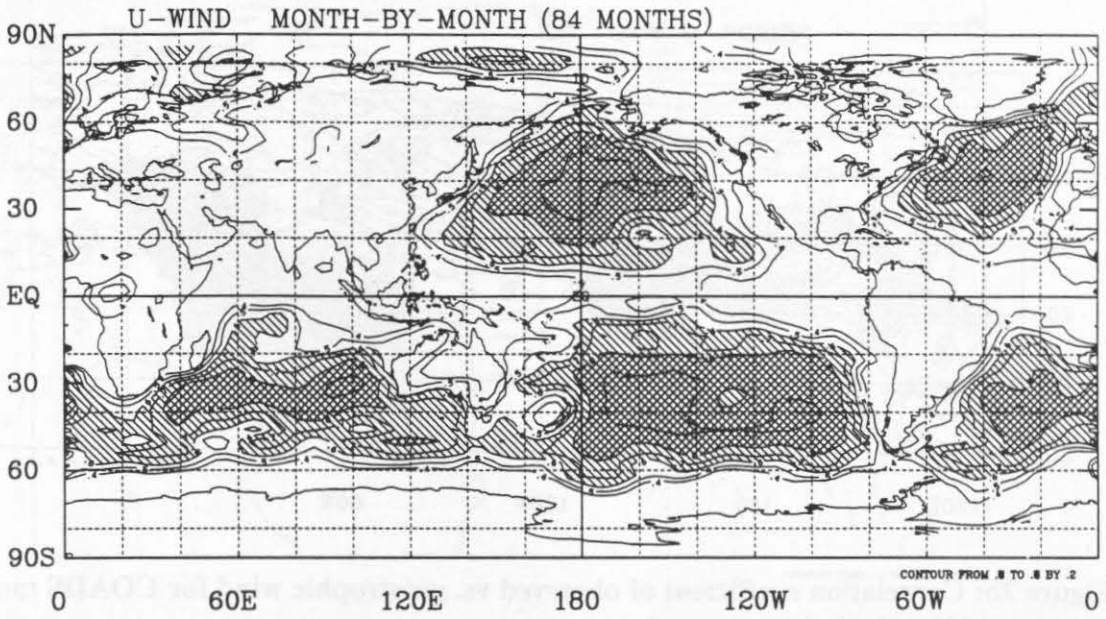

Figure 1d: Correlation Coefficient of observed vs. geostrophic wind for NMC monthly mean, meridional wind component.

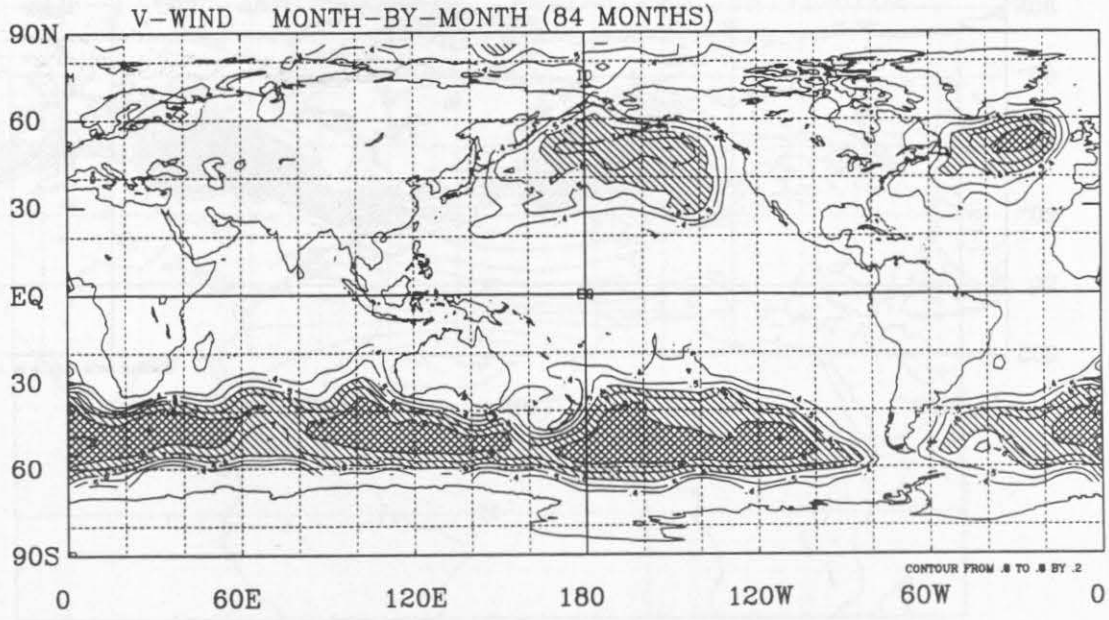

Figure 2a: Correlation coefficient of observed vs. geostrophic wind for COADS monthly mean, zonal wind component

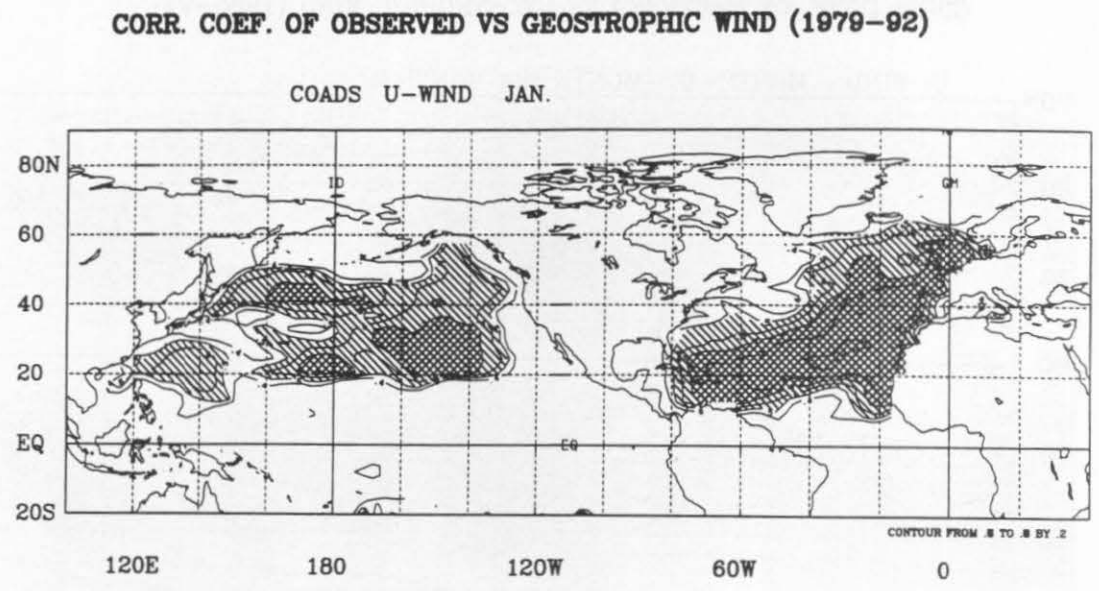

Figure 2b: Correlation coefficient of observed vs. geostrophic wind for COADS monthly mean, meridional wind component.

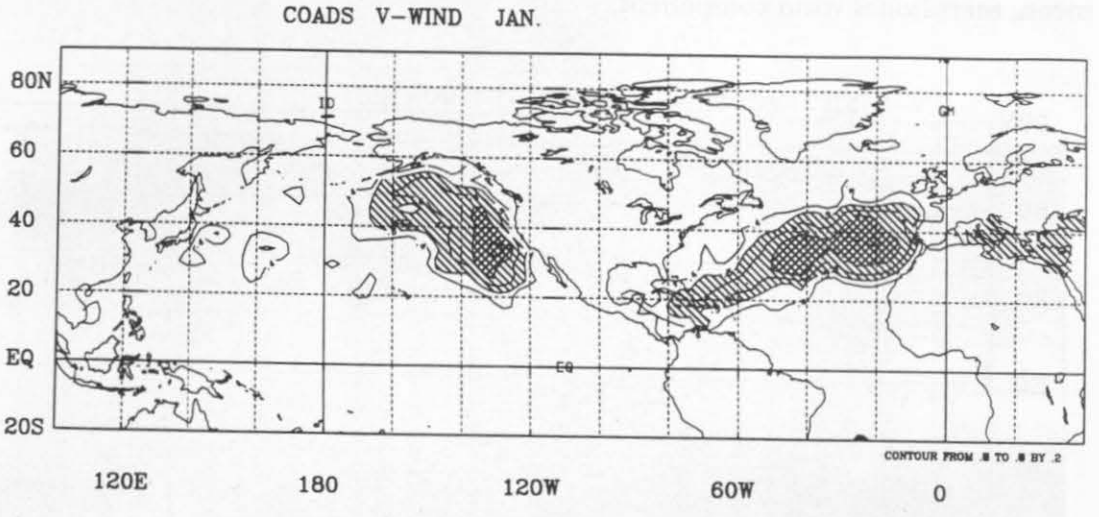

Figure 3a: EOF-modes of the surface zonal wind field over the North Atlantic Ocean (70N-10N): EOF-1 of the observed wind

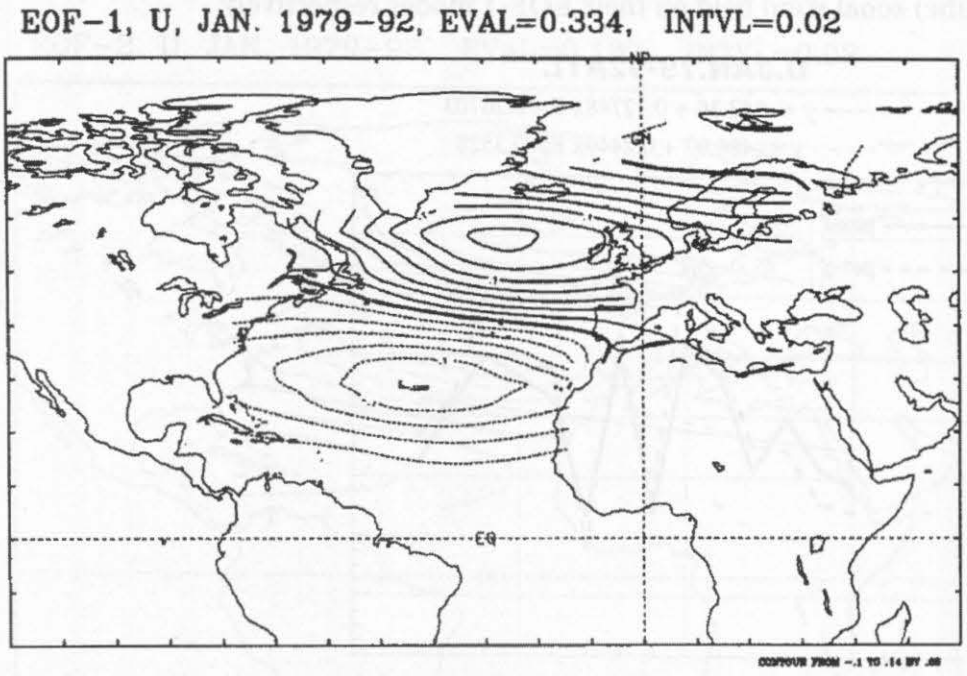

Figure 3b: EOf-modes of the surface zonal wind field over the North Atlantic Ocean (70N-10N) EOF-1 of the geostrophic wind.

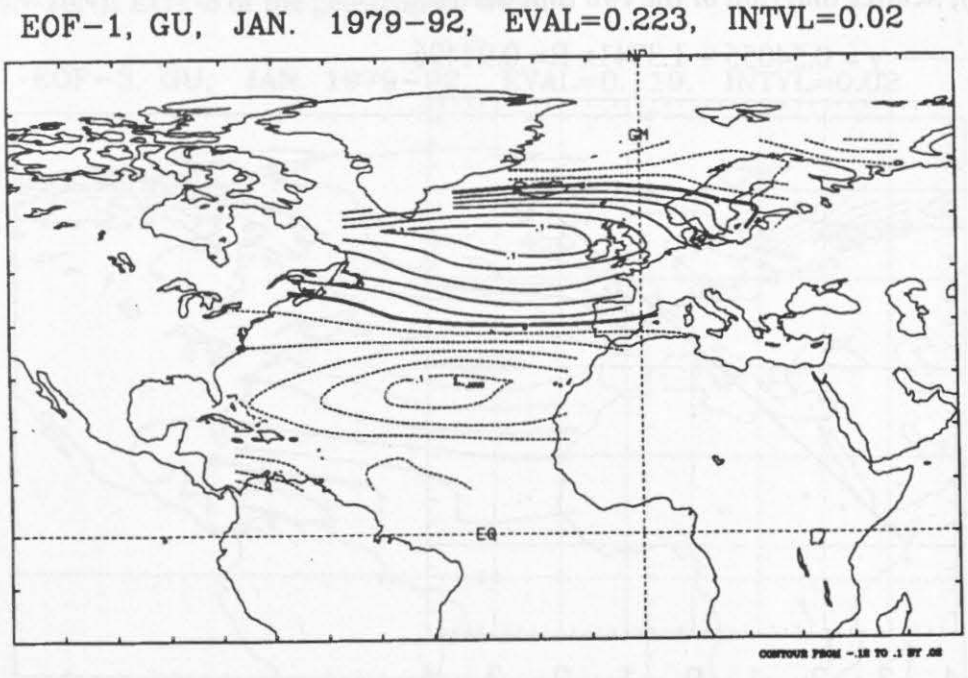

Figure 3c: EOF-modes of the surface zonal wind field over the North Atlantic Ocean (70N-10N); Time series of the projection of the ovserved (solid line) and geostrophic (dashed liine) zonal wind field on their EOF-1 modes respectively.

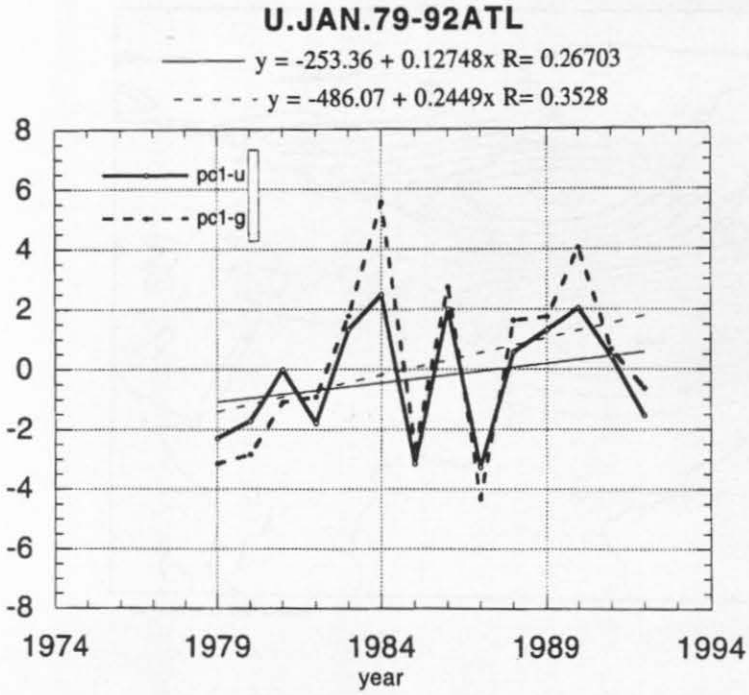

Figure 3d: EOF-modes of the surface zonal wind field over the North Atlantic Ocean (70N-10N); Scatter diagram of the two time series.

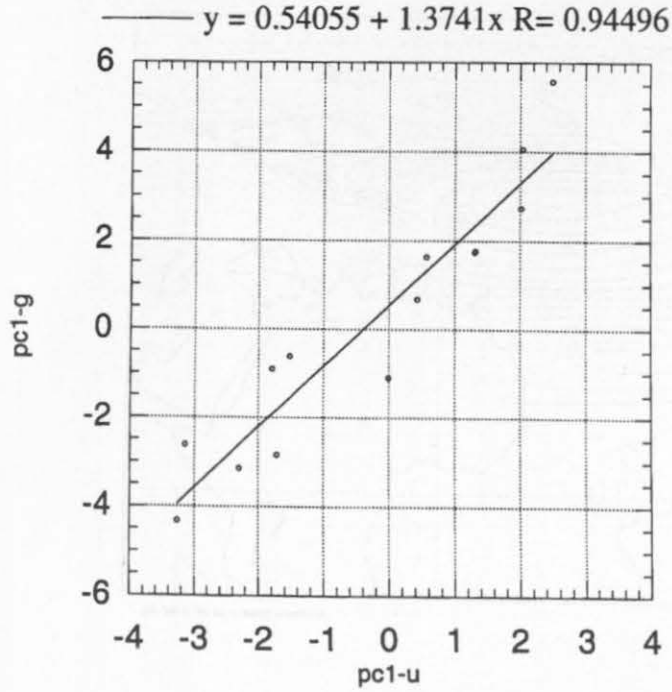

Figure 4a: EOF-modes of the surface zonal wind field over the North Atlantic Ocean (70N-10N); EOF-2 of the observed wind

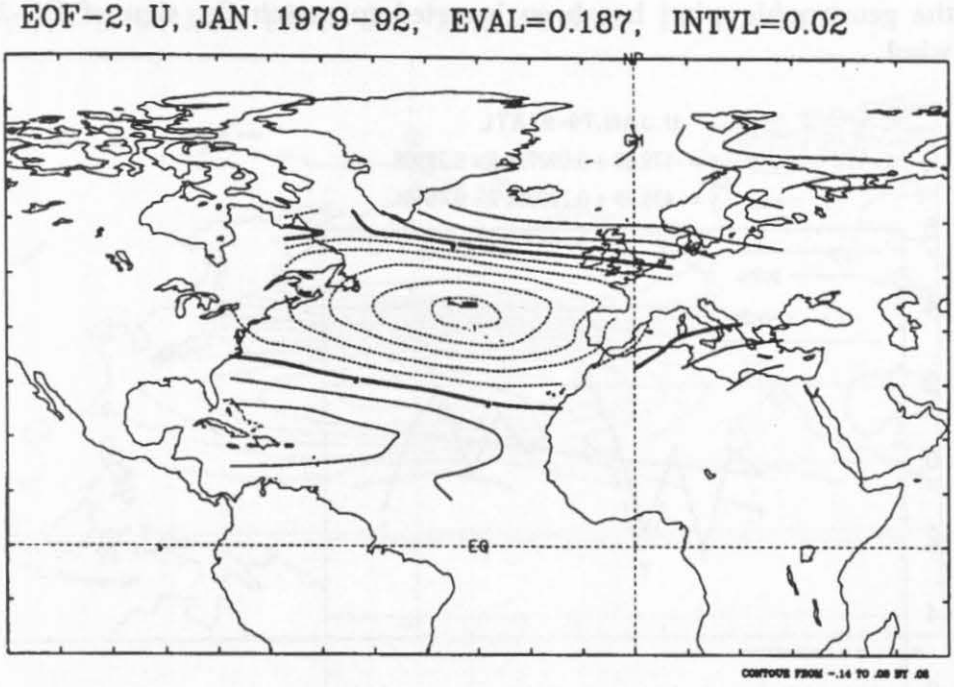

Figure 4b: EOF-modes of the surface zonal wind field over the North Atlantic Ocean (70N-10N); EOF-3 of the geostrophic wind.

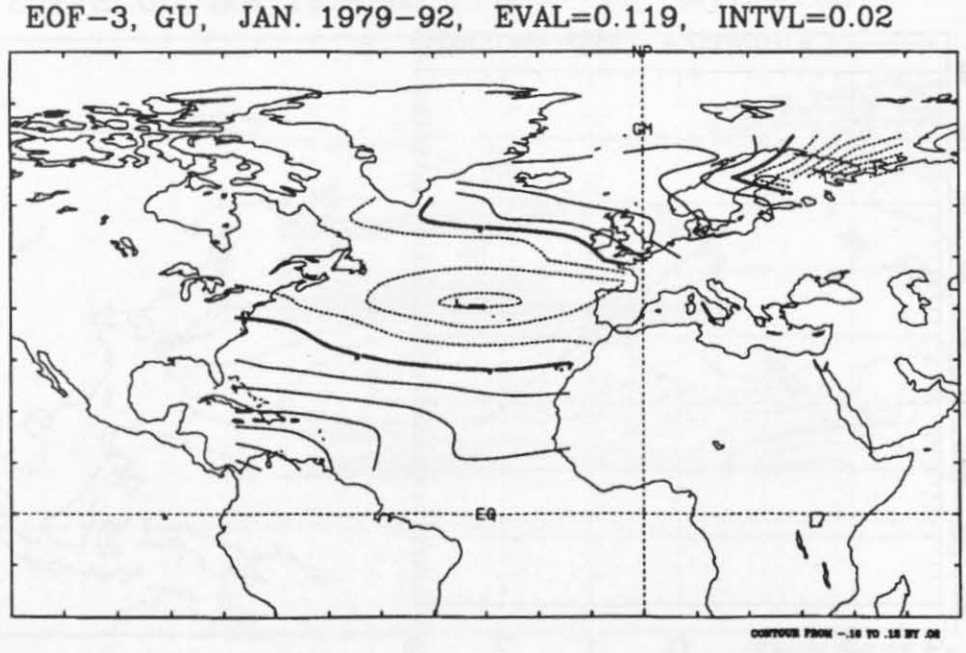

Figure 4c: EOF-modes of the surface zonal wind field over the North Atlantic Ocean (70N-10N); time series of the projection of the observed zonal wind field on its EOF-2 mode (solid line) and the geostrophic zonal wind field on its EOF-3 mode (dashed line), PC-3 of the geostrophic wind has been inverted to match the sign of PC-2 of the observed wind

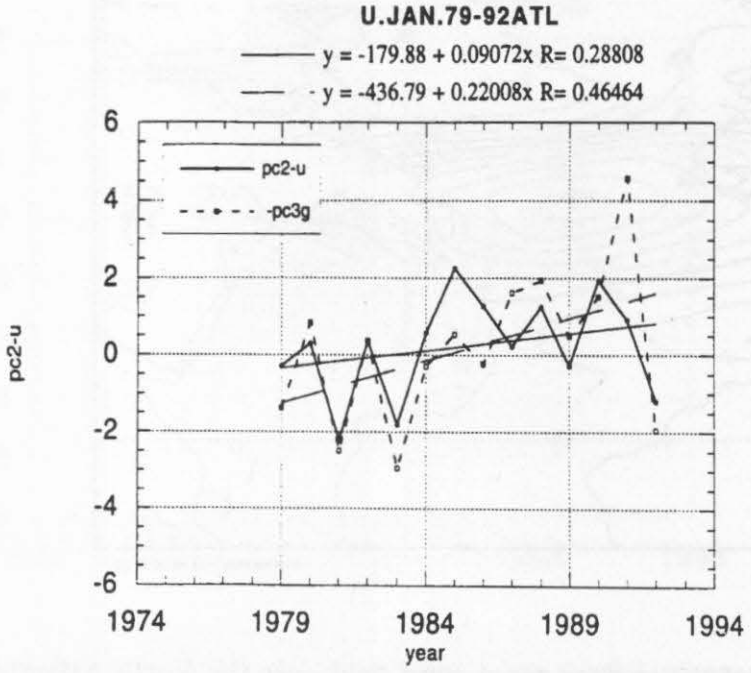

Figure 4d: EOF-modes of the surface zonal wind field over the North Atlantic Ocean (70N-10N); Scatter diagram of the two time series

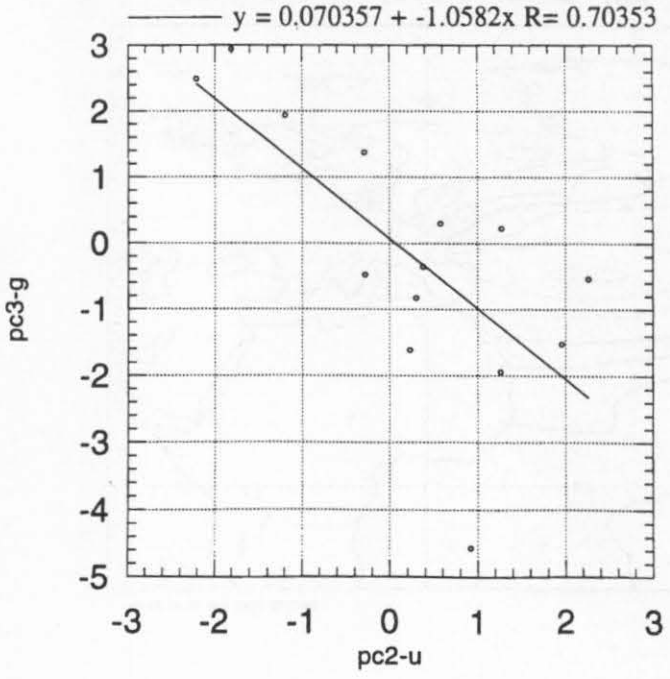

Figure 5a: EOF-modes of the surface zonal wind field over the North Pacific Ocean (60N-10N); EOF-1 of the observed wind

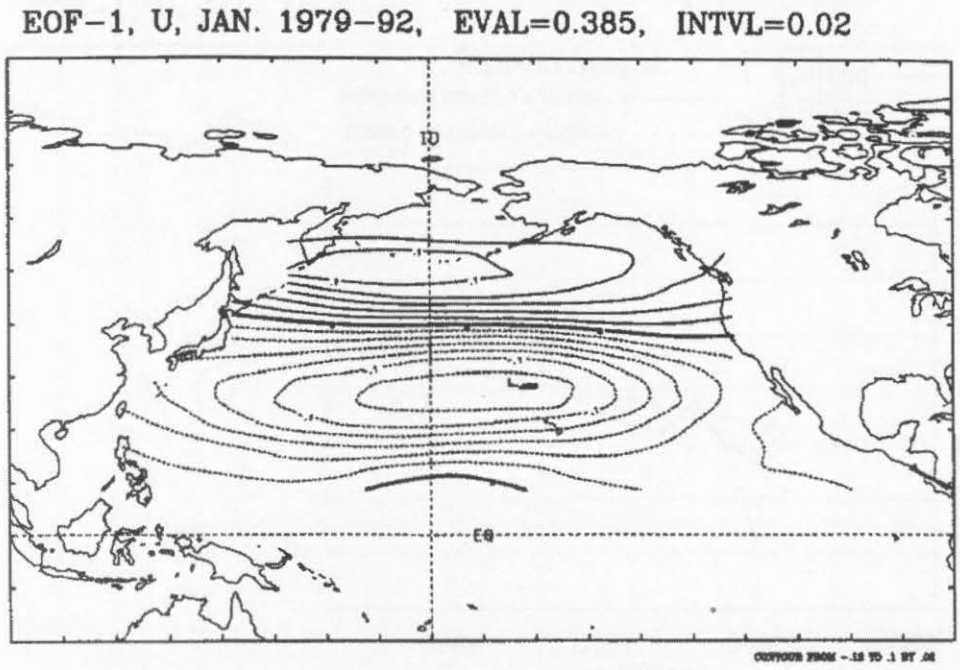

Figure 5b: EOF-modes of the surface zonal wind field over the North Pacific Ocean (60N-10N); EOF-2 of the geostrophic wind

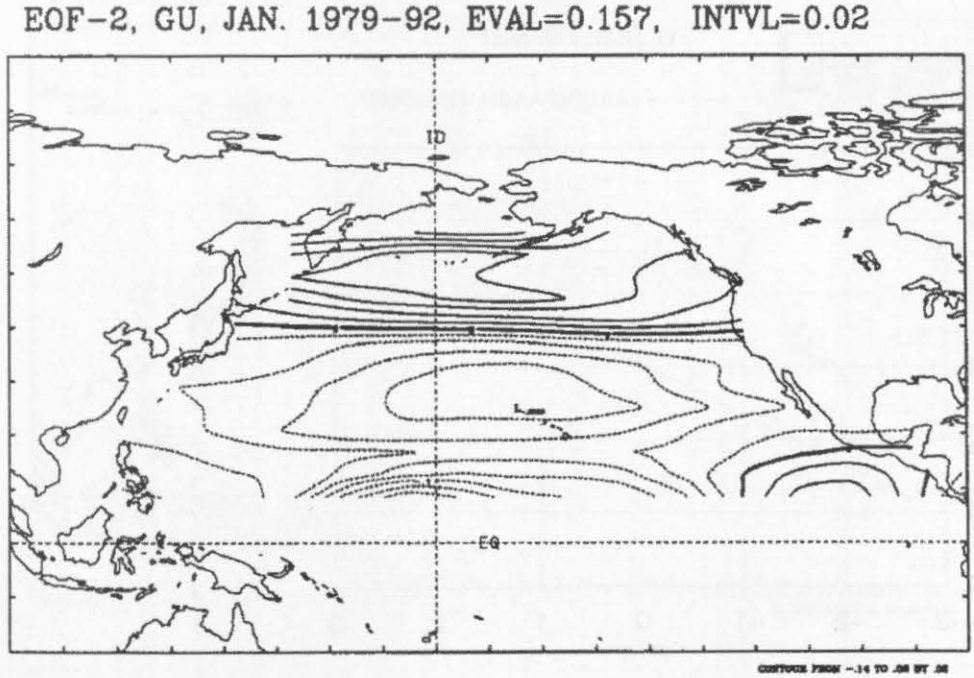

Figure 5c: EOF-modes of the surface zonal wind field over the North Pacific Ocean (60N-10N); time series of the projection of the observed wind field on its EOF-1 mode (solid line) and the geostrophic wind field onits EOF-2 mode (dashed line).

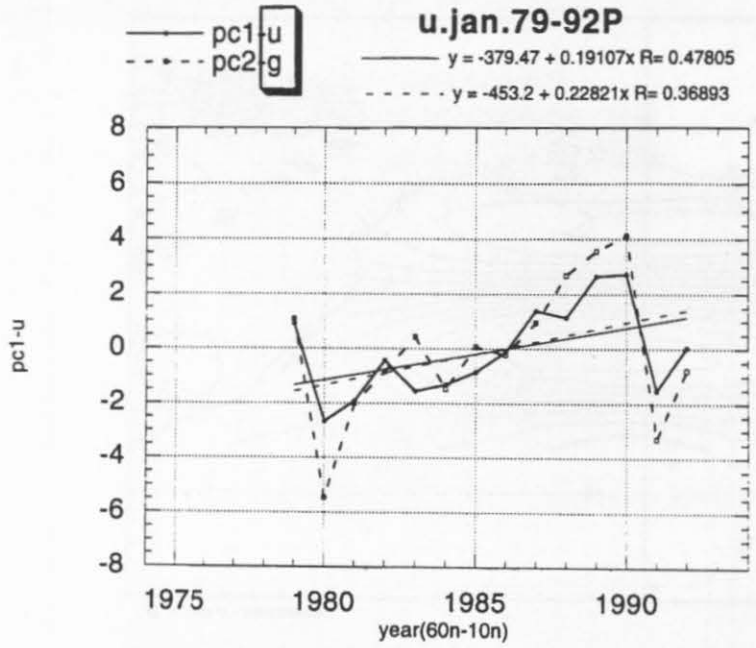

Figure 5d: EOF-modes of the surface zonal wind field over the North Pacific Ocean (60N-10N); Scatter diagram of the two time series.

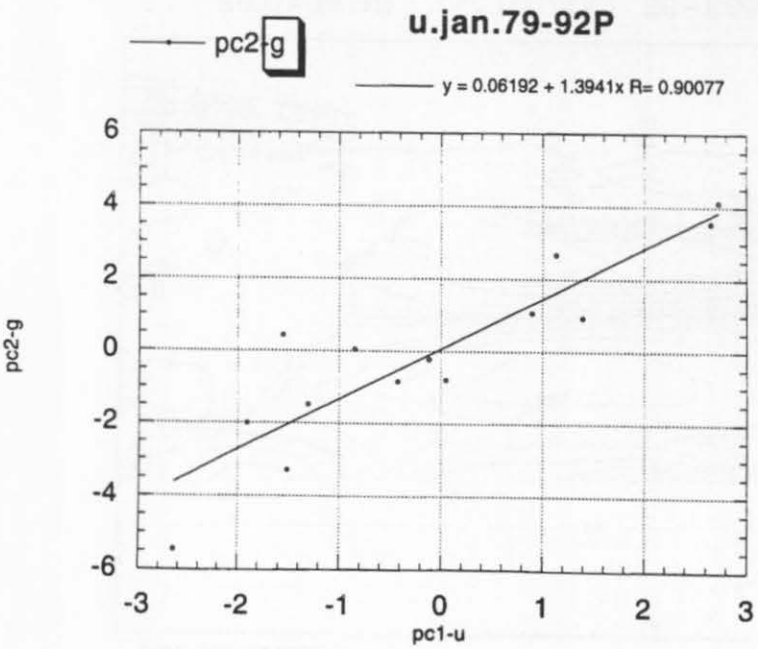

Figure 6a: EOF-modes of the surface zonal field over the North Pacific Ocean (60N-20N); EOF-1 of the observed wind.

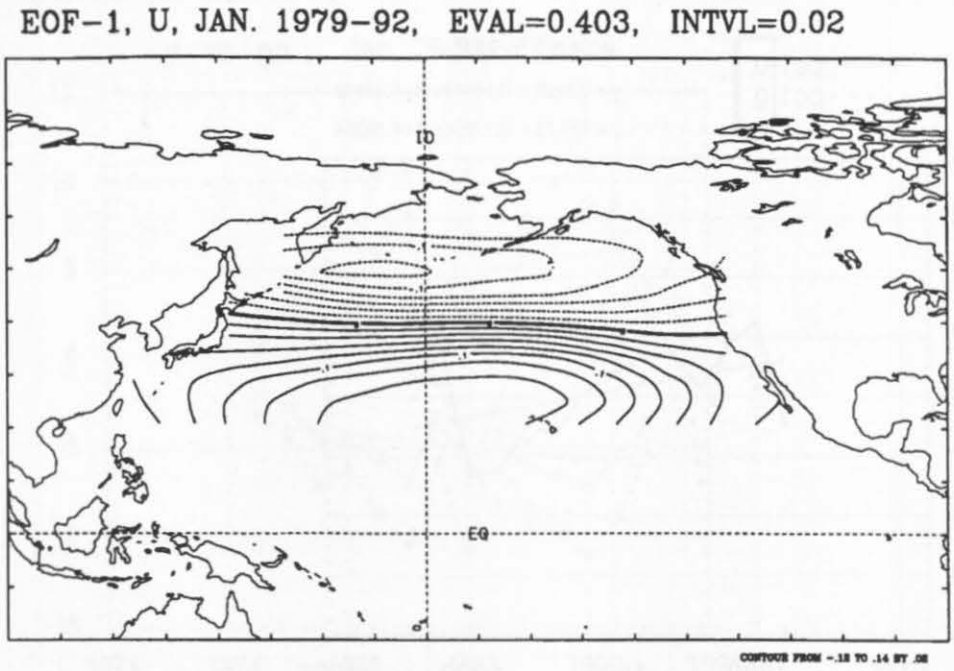

Figure 6b: EOF-modes of the surface zonal wind field over the North Pacific Ocean (60N-10N); EOF-1 of the geostrophic wind.

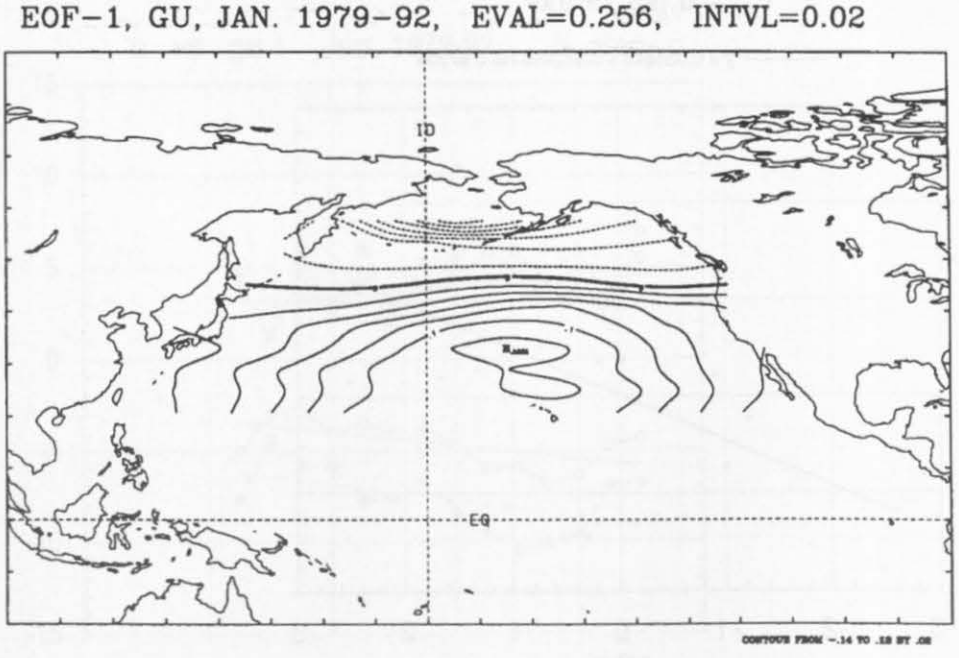

Figure 6c: EOF-modes of the surface zonal wind field over the North Pacific Ocean (60N-10N); time series of the projection of the observed (solid line) and geostrophic (dashed line) zonal wind field on their EOF-1 modes respectively.

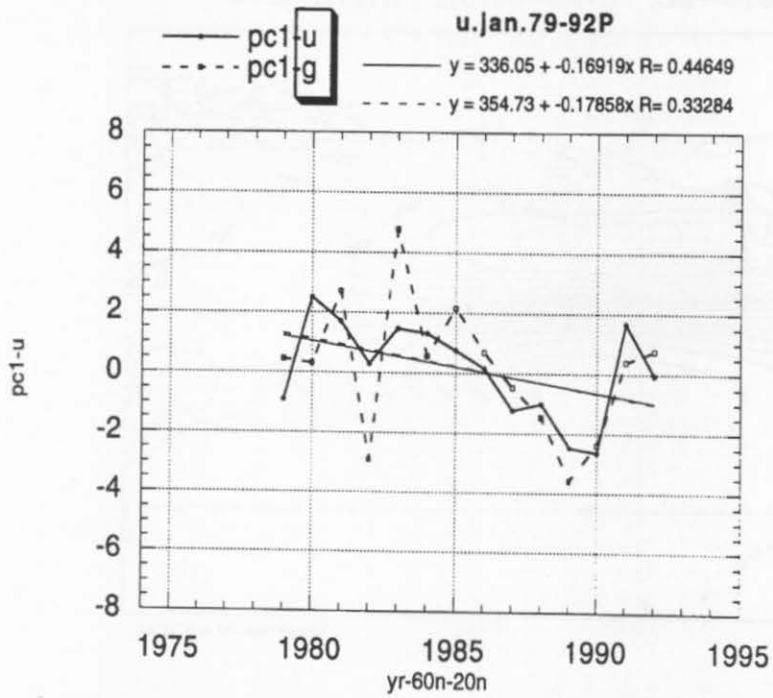

Figure 6d: EOF-modes of the surface zonal wind field over the North Pacific Ocean (60N-10N); Scatter diagram of the two time series.

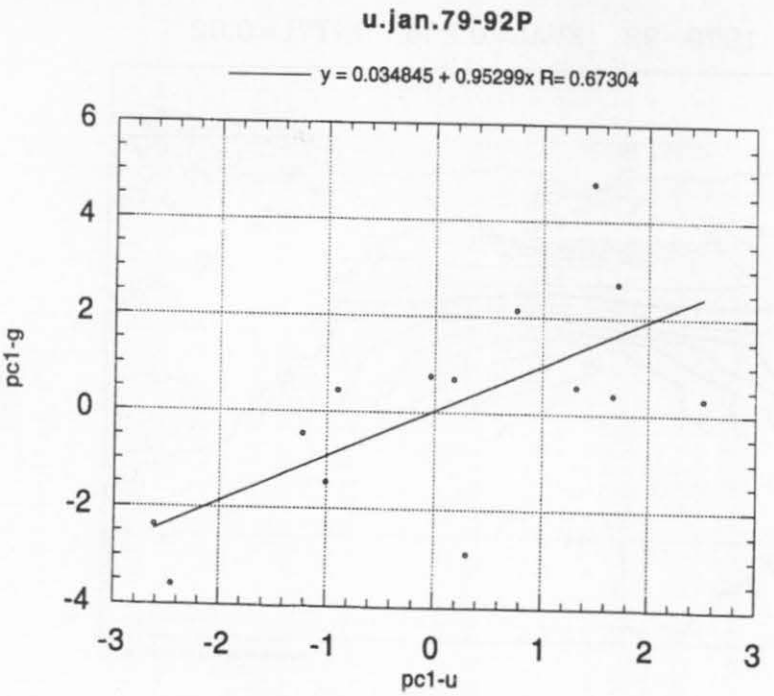

Figure 7a: Time series of the regional means of the surface zonal wind over North Atlantic, solid lines for observed wind, dashed lines for geostrophic wind, see Table 3 and 4 and text for details.

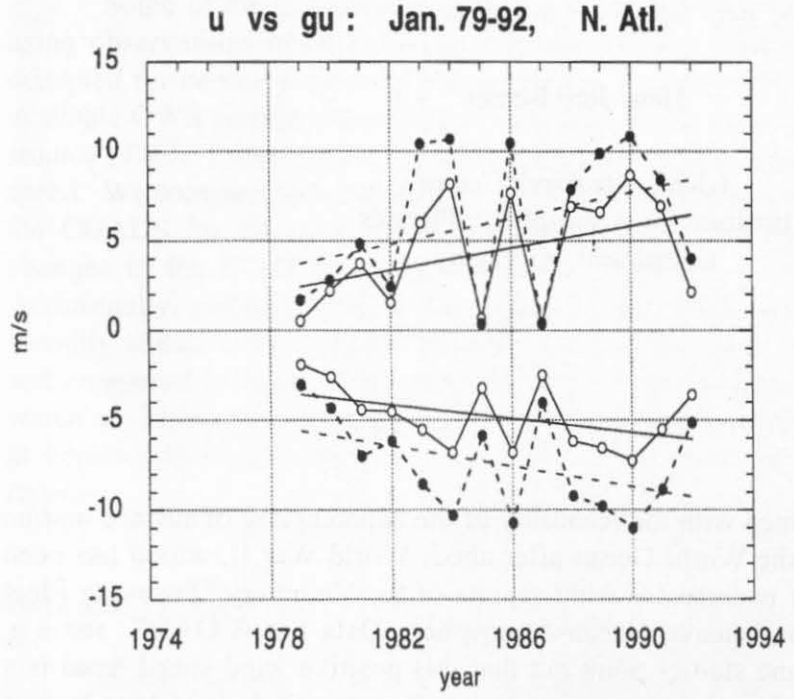

Figure 7b: Time series of the regional means of the surface zonal wind over North Pacific, solid lines for observed wind, dashed lines for geostrophic wind, see Table 3 and 4 and text for details.

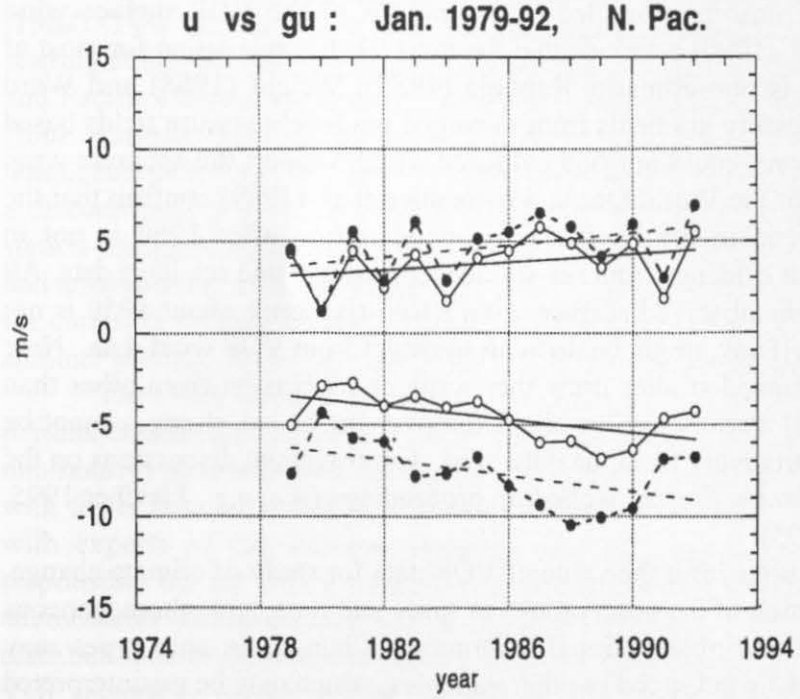

Trends in Marine Surface Wind Speed: Ocean Weather Stations versus Voluntary Observing Ships

Hans-Jörg Isemer

GKSS - Research Centre
Institute for Atmospheric Physics
Geesthacht, Germany

Introduction

This study is concerned with the reliability of the apparent rise of surface marine wind speed over much of the World Ocean after about World War II, which has been identified from data sets of uncorrected wind reports of the Voluntary Observing Fleet (VOF), such as the Comprehensive Ocean-Atmosphere Data Set (COADS, see e.g. Woodruff et al., 1987). Some studies point out that this positive wind speed trend is a true climate signal or is at least partly real, and that estimates of derived heat budget variables such as latent heat flux have changed accordingly in the mentioned period (e.g., Bunker 1980, Whysall et al. 1987, Flohn et al. 1990, 1992). Others indicate that observed wind trends, also in earlier records, are mainly an artefact produced by e.g. changing observational methods. From very detailed investigations of the VOF surface wind records itself, Cardone et al. (1990) conclude that the most likely explanation for most of the observed wind trends is non-climatic. Ramage (1987), Wright (1988) and Ward (1992), using horizontal pressure gradients from averaged sea level pressure fields based on VOF pressure observations, could not find evidence which support the apparent wind trends in different regions of the World Ocean. Posmentier et al. (1989) confirm that the apparent positive wind trend in the Pacific trade wind region after 1960 is not in accordance with independent evidence from sea surface temperature and sea level data. All these studies suggest that the observed surface wind speed rise since about 1950 is not real, and that the real trend, if any, might be difficult to detect from VOF wind data. Note especially, that i) the mentioned studies draw their critical conclusion from other than measured wind data, and ii) a real wind speed change over the ocean, if any, cannot be estimated or bounded quantitatively from the data used. Controversial discussions on the subject may also be found in the present workshop proceedings (see, e.g., Fletcher 1995, and Hansen and Bezdek 1995).

A number of restrictions limit the value of VOF data for study of climate change, especially irregular distribution of the observations in space and time, and inhomogeneous or unknown measurement and observational techniques. Changes in ship types may introduce changes in reported wind speed or other variables, which may be misinterpreted as climate signals. Additionally, the VOF data contain a mixture of Beaufort estimates

and anemometer measurements, which are not necessarily compatible. The ratio of Beaufort estimates to measurements varies with time, thus introducing additional time dependent artefacts into the time series of VOF-based marine wind speed.

Some of the deficiencies in the VOF records may be at least partly avoided by using observations made at Ocean Weather Stations (OWS) which were permanently occupied for certain periods by Ocean Station Vessels (OSV). In this study, we use all available OWS surface meteorological records, which are of appropriate length for trend studies (Table 1 and Figure 1), and calculate multiyear trends of monthly scalar wind speed. We compare these results with trends calculated from VOF records extracted from the COADS for the same OWS regions in order to verify or disproof the apparent changes in the COADS, and to specify an estimate of the real wind trend, if any. Additionally, radiosonde data from some of the OWSs are considered and trends of monthly scalar wind speed on pressure levels in the lower troposphere are investigated and compared to those of the surface winds. This comparison with independent data, which are based on a completely different measurement technique, is performed in order to obtain additional confidence in the trend results of the OWS surface wind speed records.

Data and Methods

Surface Reports from Ocean Weather Stations

The Ocean Weather Station surface data used in this study were obtained from the National Climatic Data Centre (NCDC) at Asheville, NC, U.S.A. A complete overview of all OWS data available at NCDC and the data processing involved is given by Diaz et al. (1987). Two different periods are covered by the OWS records: 1) the *earlier* period, starting at the end of the 1940s and ending in the early 1970s (13 stations in the Atlantic and Pacific Ocean), and 2) the *later* period from the mid 1970s to the end of the 1980s (four stations only in the Atlantic Ocean). For details see Table 1. The only homogeneous record covering the full length of both periods is at OWS M. Unfortunately, a discontinuity at OWS C in the mid-1970s, when the national responsibilities for this station changed leading to a significant change in ship type, and, hence, flow distortion and anemometer level, that makes this record doubtful for studies of wind changes over the complete 40 year record. OWS T in the Pacific Ocean was occupied only during the summer periods. Here, data from May to October of each year are considered.

The OWS monthly wind records (except at OWS T) are continuous in time for the periods considered. Usually, three-hourly (in some periods and at some stations even one-hourly) meteorological surface observations were performed on OSVs. Subperiods with fewer data still contain at least two observations per day on average. Discussions with experts of the different national weather services and institutes, which were responsible for the OSVs, yield that wind reports from OSVs are exclusively based on anemometer measurements, not on Beaufort estimates. We find this confirmed by the distributions of reported wind speed analysed from the NCDC files, which in contrast to VOF records do not show a predominance of the equivalent wind speeds of the Beaufort equivalent wind scale.

A very limited number of individual vessels have been used by the European countries (20 vessels total, but only 10 at the same time), Canada (four vessels total, but only two at the same time), Japan (between two and six vessels at the same time) and the former Soviet Union (six vessels). Moreover, some of the mentioned vessels are of the same type with identical ship dimensions and anemometer levels. The United States of America used a much larger number of vessels from their Coast Guard fleet. However, most of these cutters belong to only four different classes with almost identical ship dimensions.

The following two features restrict the value of OWS records: 1) Available OWS data are limited to periods after World War II, and, 2) only a small number of Ocean Weather Stations were occupied, all of them in the extratropical North Atlantic and North Pacific Oceans.

COADS-MSTG Wind Speeds

The Monthly Summary Trimmed Group (MSTG) version of Release 1 and Release 1a of the COADS (see Woodruff 1995 in this volume) is used. This version consists of individual monthly means of meteorological surface variables, defined on a regular 2° x 2° longitude/latitude grid net for the World Ocean. We use scalar wind speed from this record throughout this study. Note, that the averages were calculated from both anemometer measurements and Beaufort estimates. OSV reports are mixed with the VOF reports in the COADS. Hence, for comparison with the OWS trends, time series of wind speed for local OWS areas are extracted from COADS MSTG, which are based on data from a 3° x 3° grid box area centered on the nominal OWS positions, but excluding the central gridpoint of this area, because a large fraction of the individual reports within this central 2° grid point stem from the OSVs. For presentation of the large-scale trend features (Figure 2) individual monthly means for 10° x 10° Marsden Squares (MS) are formed from all 2° grid averages inside a MS by unweighted averaging.

Radiosonde Data at Ocean Weather Stations

Individual twice-daily radiosonde (RS) ascents made onboard of OSVs in the Atlantic Ocean were obtained from the British Meteorological Office and from NCDC (see Diaz et al., 1987). These records provide wind speed and direction, air temperature and humidity on both standard pressure levels and additional levels. Compared to the surface wind records the OSV RS data are more irregularly distributed in time, with larger gaps and somewhat different periods covered. Upper-air time series at OWSs M, A, B, C, D, I, J, L are used here. For comparison with the surface wind speed trends we calculate trends of upper air wind speed on standard pressure levels between 950 and 700 hPa. Unfortunately, pressure levels with continuous data coverage vary from station to station. For example, at OWS A, wind speed at 900, 850, 800 and 700 hPa are nearly continuously available while, at OWS B, the lowest reliable level with enough data for trend studies is 800 hPa. However, in general three or four levels between the surface and 700 hPa with enough data for trend investigations are available per station.

Methods

Monthly and Annual Time Series

Individual monthly means of scalar wind speed are calculated from the OWS surface wind speeds and also from the upper air pressure level wind data in order to obtain a comparable data form as is available from COADS MSTG. The annual cycle is extracted by applying a 25 point Hamming filter. This filter is used instead of forming conventional anomalies in order to avoid aliasing (see, e.g., Edwards 1987).

Trend Statistics

We will restrict ourselves to linear trends in the time series using the simple model

$$w(t) = a + b*t + e_w , \qquad (1)$$

where time, t, is the independent variable, and w(t) is monthly wind speed. The coefficient of linear regression against time, b, is obtained from an unweighted linear fit to the monthly wind speed time series. e_w is the deviation from the resulting trend line. Student's t - test is used to test $b \neq 0$ against the null hypothesis $b = 0$. The aim of this study is to look for changes within periods of typically 20 years, or more. We applied (1) and the t - test to both monthly anomalies and annual averages of scalar wind speed. Although, trend results from both data forms show mostly small numerical differences, both methods give essentially the same results, especially, the significance test results are the same in general. Hence, only results based on monthly filtered data are given throughout the paper.

Results

The Large-scale Picture from COADS

The large-scale coherent picture for the tropical and northern parts of the Pacific and Atlantic Oceans is that of an apparent significant positive trend of scalar wind speed (Figure 2), typically of order 0.2 to 0.4 m/s per decade. Only two out of 45 MS in the Atlantic Ocean, and one out of 96 MSs from the Pacific Ocean show a significant negative trend. Highest positive trends exceed 0.6 m/s per decade west of Norway and around the southern coast of Greenland in the Atlantic Ocean, and around the Indonesian islands and in the western Bering Sea in the Pacific Ocean. Especially the time series from the region between 50° and 60°N in the Atlantic Ocean do not indicate a significant change of surface wind speed.

Surface Wind Speed Trends at Ocean Weather Stations from 1949 to 1972

Results of trend analysis of the OSV series at OWSs are given for the longest reliable periods available (Figure 3). The only OWS with a significant positive wind speed trend is OWS M off the Norwegian coast with a linear 0.45 ± 0.33 m/s per decade increase of wind speed from 1949 to 1975. Also, for the whole period available the positive wind speed trend is significantly different from zero at this station. All other stations show a non-significant wind speed change, or, at OWSs I, J in the Atlantic Ocean, and for the summer time series of OWS T in the Pacific Ocean, even a significant negative trend. Figure 3 suggests that in the North Atlantic Ocean between 30°N and 70°N there is no significant trend of surface wind speed except for two limited areas. West of Ireland, two stations indicate a decrease, while, between Norway and Iceland, one station indicates a strengthening of surface wind speed.

Comparison with VOF Data from COADS

The trend results for the OWS areas from the COADS-MSTG (Figure 3) agree in general with the results of the respective MS they are extracted of (Figure 2). Exceptions are found at OWSs B and C. All OWS areas in the Pacific Ocean show an apparent significant increase of surface wind speed. In the Atlantic Ocean, the northernmost station area (OWS M) and the southern areas D, E and K show an apparent significant rise of wind speed, in the other areas, except at OWS A, wind speed apparently did not change significantly. These areas are situated between 50° and 60°N. OWS A is the only area with a significant decrease of surface wind speed as apparent from COADS-MSTG.

Comparison of the OWS results with the VOF results from COADS-MSTG (Figure 3) indicates that at all stations, except at OWS A in the Atlantic Ocean, the VOF trends are more positive (or less negative, respectively) than the OWS trends. For a qualitative comparison three types of trend results might be considered, significantly positive, significantly negative and nonsignificant changes. In these terms, agreement between OWS and VOF results are obtained only at OWSs B and C (nonsignificant changes) and at OWS M (significantly positive).

Surface Wind Speed Trends at Ocean Weather Stations from 1976 to 1989

In the later period, none of the four stations with available OSV data in the Atlantic Ocean shows a significant change of surface wind speed while at three stations (C, L, R) the COADS-MSTG data indicate a significant increase of surface wind speed (Figure 4). Agreement between both data records, indicating no significant wind speed change, is obtained only at OWS M.

Upper Air Wind Speed Trends at Ocean Weather Stations

The intention here is not to detail the vertical structure of wind changes at all stations but to check whether the surface wind changes in the OSV records are supported by those in the lower troposphere from the OSV radiosonde (RS) records. At all stations and both periods investigated here, trend results show a high degree of vertical

homogeneity. As an example, Table 2 depicts trend results for all available levels from the surface up to 700 hPa at OWSs A and C. At both stations wind speed tended to decrease in the lower troposphere, however, only at OWS A is this trend significantly negative at 850 hPa and higher levels. OWS A is the only station among those investigated here with a significant trend in lower tropospheric wind speed, and this trend is negative. At this station the decrease of wind speed with time grows monotonically with height from the surface up to 800 hPa and shows little change higher at 700 hPa. This feature suggests the following physically meaningful interpretation. The significant decrease of wind speed in the lower free troposphere outside the planetary boundary layer (PBL), which is presumably controlled by the change of the large-scale pressure gradient, might have been weakened by an opposite trend of physical processes inside the PBL (e.g. a change of frictional forces, stability, or advection). For all stations with available RS data, trend results of the two lowest pressure levels are compared to the surface results in Figure 5. At all stations in both periods the trends of the upper air winds do not contradict those of the surface winds. If the trend at the surface and that at the lowest available pressure level indicate different signs, both are never significantly different from zero (Table 2). Especially noteworthy is that there is no significant positive trend of wind speed at either station in either period at either pressure level below 700 hPa.

Summary and Conclusion

There is no significant increase of monthly surface scalar wind speed, derived from anemometer measurements performed regularly onboard of Ocean Station Vessels (OSV) at extratropical Ocean Weather Stations (OWS) in the North Atlantic and North Pacific Oceans, in the period from the late 1940s to the early 1970s. The only exception is at OWS M off the Norwegian coast at 66°N & 2°E. Here, an increase of surface wind speed of $+0.30 \pm 0.18$ m/s per decade for the period 1949 to 1989 is observed. However, this result at OWS M is strongly dependent on the chosen period. Excluding the years 1950 to 1953, which show anomalous low wind speeds, changes the trend result to insignificant (not detailed here). Also, for the *later* period after 1975, no significant change in surface wind speed is detectable in the OSV records at four OWSs in the North Atlantic Ocean.

Wind speed in the lower troposphere, derived from radiosonde ascents at North Atlantic Ocean OWSs, support the trend results of the surface anemometer measurements. At these stations, there is no significant positive trend of wind speed at either station in either period at either pressure level below 700 hPa detectable. The only significant trend signal is a wind speed decrease at OWS A between Iceland and Greenland in the period 1949 to 1972 (Table 2).

The COADS-MSTG wind records, which are based on a mixture of Beaufort estimates and anemometer measurements from VOF ships, show, in general, a more positive (or less negative) wind speed trend at the OWS areas compared to the OSV records. This is true for both the earlier and later periods. Exceptions are found in the north-western part of the Atlantic Ocean at OWSs A, B and C, in the period from the late 1940s to the early 1970s. The COADS-MSTG winds show a significant increase in the *earlier* period at the southern Atlantic Ocean OWSs (D, E, K) and, in particular, at all

Pacific Ocean OWSs, and at three out of four OWSs in the *later* period (1976 to 1989) in the Atlantic Ocean.

The OSVs provide for a much more reliable data set than the VOF, especially with respect to homogeneity of the measurement technique. Therefore, the significant positive wind speed trends in the COADS-MSTG records from the OWS areas have to be judged as questionable. This leads to the conclusion that COADS-MSTG in particular, and presumably VOF records in general, seem to be an unreliable data source for detection of interdecadal wind speed trends.

There is a number of possible reasons for artefacts in the VOF wind speed records which may lead to the apparent wind speed rise. These include the gradual change from estimation technique to measurements on VOF ships. However, artefacts are likely to be hidden also in the record of Beaufort estimates itself. Observers on VOF ships from different nations seem to have followed quite different observation rules leading to systematic differences in the "national" Beaufort equivalent scales (e.g. Isemer 1992, Lindau 1995). A change of the national contributions to VOF data sets like the COADS would inevitably lead to artificial wind speed changes providing that only one scale is used to transfer Beaufort estimates back into wind speed (as is common practice today). The merging of different national or international data decks into one data set, where the individual decks cover different time periods of the overall record, may consequently contaminate the homogeneity of the entire data set. The latter reason may have caused at least part of the unrealistic positive wind speed trend in the COADS-MSTG especially at OWSs in the Pacific Ocean. Until discrepancies, which are as striking as those in the OSV and VOF time series of wind speed at OWS P (see Figure 6), can be removed from the VOF records, results on wind climate change from uncorrected VOF wind data should be interpreted with utmost care.

This study does not rule out that parts of the World Ocean may have seen a strengthening of surface wind speed. It is, however, stressed that uncorrected VOF data records are an unreliable tool to detect and quantify them. The large-scale coherent picture of wind speed increase which can be derived from e.g. the COADS-MSTG (Figure 2) is not likely to represent the real distribution of wind speed changes over the oceans, both qualitatively and quantitatively.

Acknowledgements

Most of the data processing and the calculations were performed while the author was affiliated with the Institut für Meereskunde, Kiel, Germany. Financial support through the research project SFB 133, "Warmwassersphäre des Atlantiks" is gratefully acknowledged.

References

Bunker, A.F., 1980: Trends of variables and energy fluxes over the Atlantic Ocean from 1948 to 1972. *Mon.Wea.Rev.*, 108, 720-732.

Cardone, J.S., J.G.Greenwood and M.A.Cane, 1990: On trends in historical marine wind data. *J.Climate*, 3, 113-127.

Diaz, H.F., C.S.Ramage, S.D.Woodruff, and T.S.Parker, 1987: Climatic Summaries of Ocean Weather Stations. U.S. Department of Commerce, NOAA,ERL,CIRES, Boulder, Colorado, USA. 48 pp plus tables and maps.

Edwards, H.B., 1987: Sampling theory applied to measurement and analysis of temperature for climate studies. *J. Climate Appl.Meteor.*, 26, 731-736.

Fletcher, J.O., 1995: The importance of COADS winds for understanding climate change. In: Proceedings of the International COADS Winds Workshop, Kiel, Germany, 31 May - 2 June, 1994 (this volume).

Flohn, H., A.Kapala, H.R.Knoche and H.Mächel, 1990: Recent changes of the tropical water and energy budget and of midlatitude circulations. *Climate Dyn.*, 4, 237-252.

Flohn, H., A.Kapala, H.R.Knoche and H.Mächel, 1992: Water vapour as an amplifier of the greenhouse effect: new aspects. *Meteorol. Zeitschrift*, N.F.1, 122-138.

Hansen, D.V. and H.F. Bezdek, 1995: Testing winds against other variables from COADS. In: Proceedings of the International COADS Winds Workshop, Kiel, Germany, 31 May - 2 June, 1994 (this volume).

Isemer, H.-J., 1992: Comparison of estimated and measured marine surface wind speed. In: Diaz, H.F. et al., (Ed.): Proceedings of the international COADS workshop, Boulder, Colorado, 13-15 January 1992, p 143-158.

Lindau, R., 1995: A new Beaufort equivalent scale. In: Proceedings of the International COADS Winds Workshop, Kiel, Germany, 31 May - 2 June 1994 (this volume).

Posmentier, E.S., M.A.Cane and S.E.Zebiak, 1989: Tropical Pacific climate trends since 1960. *J.Climate*, 2, 731-736.

Ramage, C.S., 1987: Secular change in reported surface wind speeds over the ocean. *J.Clim.Appl.Met.*, 26, 525-528.

Ward, M.N, 1992: Provisionally corrected surface wind data, world-wide ocean-atmosphere surface fields, and Sahelian rainfall variability. *J.Climate*, 5, 454-475.

Whysall, K.D.B., N.S.Cooper and G.R.Bigg, 1987: Long-term changes in the tropical Pacific surface wind field. *Nature*, 327, 216-219.

Wright, P.B., 1988: On the reality of climatic changes in wind over the Pacific. *J.Climatol.*, 8, 521-527.

Woodruff, S.D., 1995 : Project Report I : Update plans and unresolved issues. In: Proceedings of the International COADS Winds Workshop, Kiel, Germany, 31 May - 2 June 1994 (this volume).

Woodruff, S.D., R.J.Slutz, R.L.Jenne and P.M.Steurer, 1987: A comprehensive ocean-atmosphere dataset. *Bull.Amer.Meteor.Soc.*, 68, 1239-1250

Table 1: List of Ocean Weather Stations in the Atlantic and Pacific Oceans, data periods with reliable data, nominal locations number of individual OWS wind reports available from the NCDC files for the reliable periods, and responsible countries. Data periods are identified by the first and last month/year combination

OWS	Period	Location	Reports	Countries
M	1/49/12/89	66N/ 2E	107171	N,NL
A	10/47-12/73	62N/33W	76828	US,F,N,NL,UK
B	1/49-7/73	56.5N/51W	71864	US
C	1/49-12/73	52.5N/35.3W		US
	7/75-12/89	52.5N/35.5W	118270	USSR
D	10/49-12/72	44N/41W	68398	US
E	10/49-12/72	35N/48W	67327	US
I	4/50-1/53	59N/19W		
	8/54-11/74	59N/19W	6886	NL,UK
J	4/50-12/74	52.5N/20W	74914	F,NL,UK
K	7/49-12/74	45N/16W	70274	F,NL,UK
L	10/75-12/89	57N/20W	35191	F,UK
R	12/76-12/85	47N/17W	24027	F
P	1/50-6/81	50N/145W	90061	CAN
N	7/46-11/50	30N/140W		
	1/54-12/72	30N/140W	69225	US
V	4/55-12/71	34N/164E	47964	US
T*	6/49-10/70	29N/135E		
	6/78-10/81	29N/135E	38472	JAP

* OWS T was occupied only during the summer seasons. Data from June to October of each year are used.

Table 2: Trend statistics of surface and upper air wind speed at OWSs A and C. Periods are 19848-1970 at OWS A and 1949-1973 at OWS C. d is the 95% confidence interval for b, and $P(t_b)$ is the t-probability of significance (in %) for $b \neq 0$. Units of b and d are m/s per decade.

OWS/Level	b	d	$P(t_b)$
OWS A			
Surface	-0.14	0.28	68
900 hPa	-0.24	0.41	76
850 hPa	-0.35	0.32	96.4
800 hPa	-0.49	0.34	99.2
700 hPa	-0.42	0.39	96.4
OWS C			
Surface	-0.10	0.23	60
850 hPa	+0.05	0.44	19
800 hPa	-0.23	0.48	67
750 hPa	-0.39	0.45	91
700 hPa	-0.36	0.52	84

Figure 1: Locations of Ocean Weather Stations in the Atlantic and Pacific Oceans.

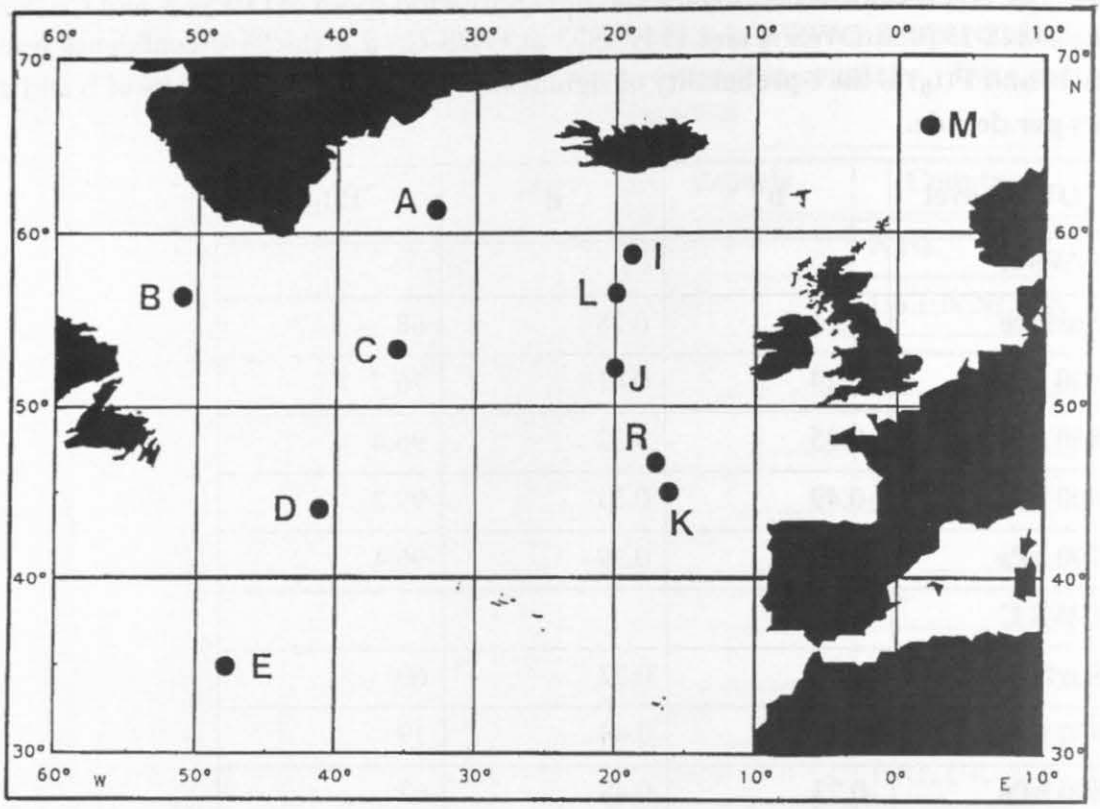

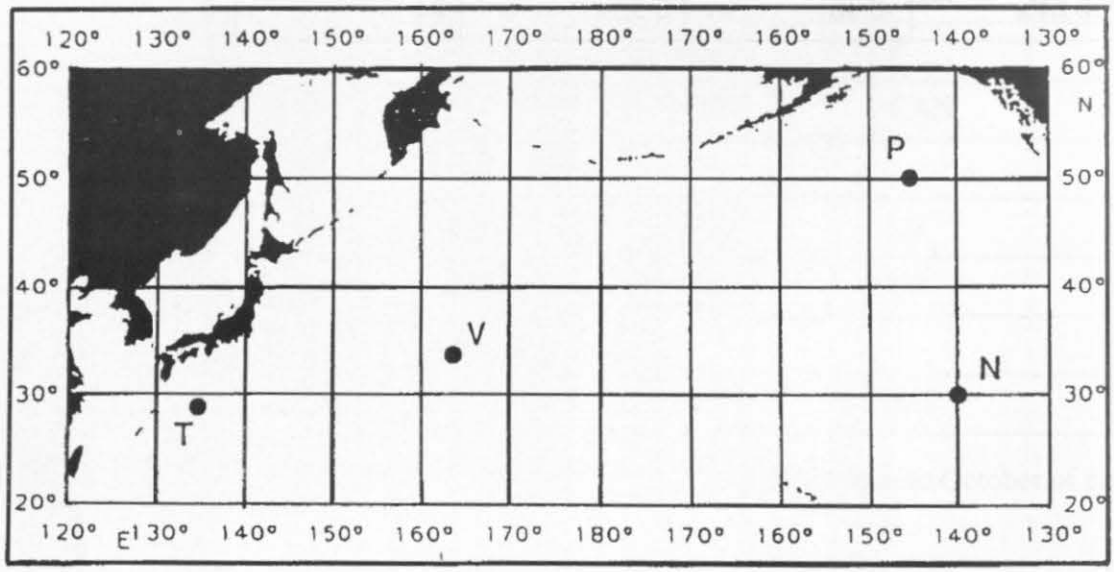

Figure 2a: Apparent linear trend of scalar wind speeds [cm/s per decade] in the Atlantic Ocean, based on the MSTG.2 version of COADS. Only significant trend results (at the 5% error level) are plotted, Marsden Squares (MS) with non-significant trends contain only the sign of the linear trend. MSs with insufficient data coverage for calculating a meaningful trend are left blank. Note that the author is thoroughly convinced that this result from the COADS dataset is largely influenced by non-climatic reasons and does not give the distribution of the real wind trend over the oceans.

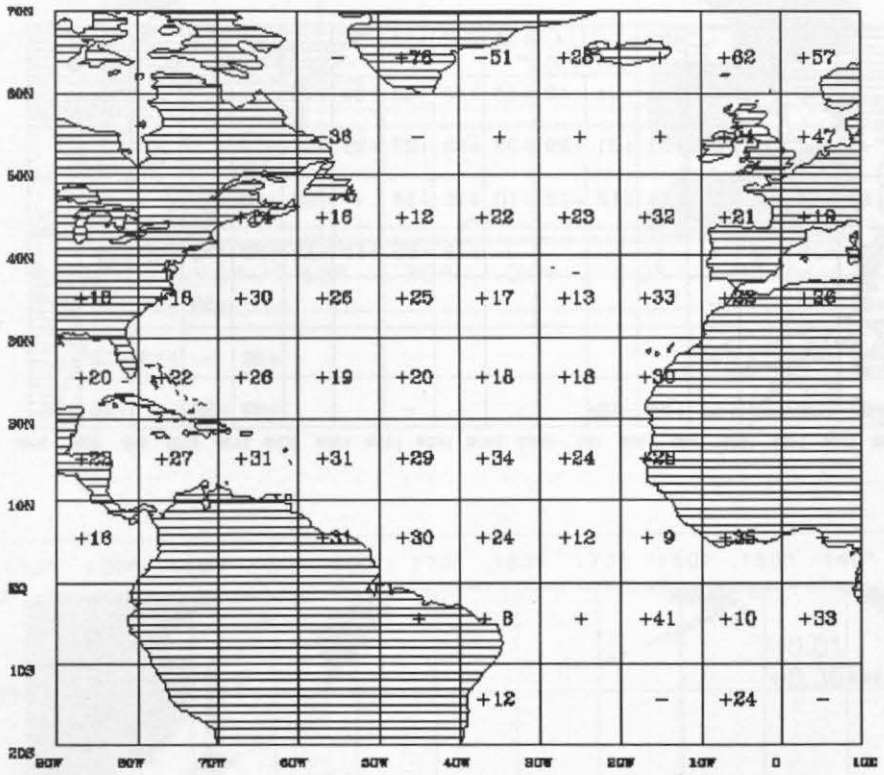

Figure 2b: As in Figure 2a, but for the Pacific Ocean.

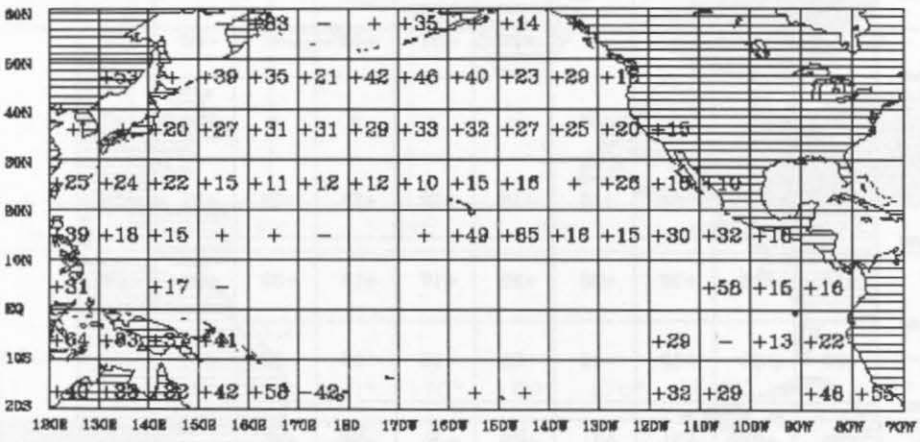

Figure 3: Linear trends of surface wind speed [m/s per decade] in the earlier period (late 1940's to early 1970's) at OWSs M, A, B, C, D, E, I, J, K in the Atlantic Ocean, and at OWSs P, N, V, T in the Pacific Ocean. The upper number of the two, given for each station, is the OSV result, the lower one the VOF result from COADS-MSTG. One, two and three stars indicate level of significance at 5%, 1% and 0.1% error levels respectively. No star indicates random result.

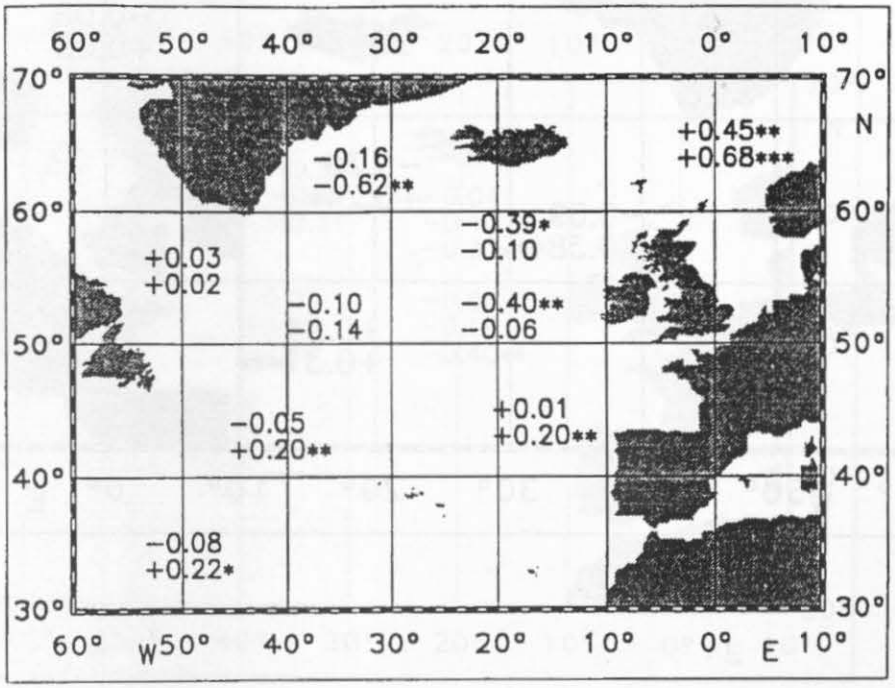

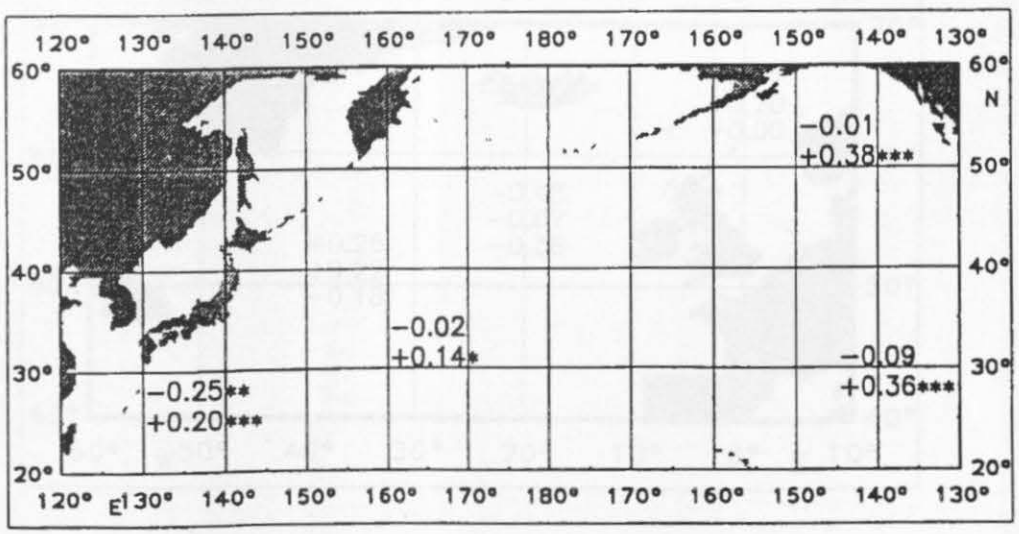

Figure 4: As in Figure 3, but trend results at OWSs in the Atlantic Ocean in the recent period (mid 1970's to the late 1980's).

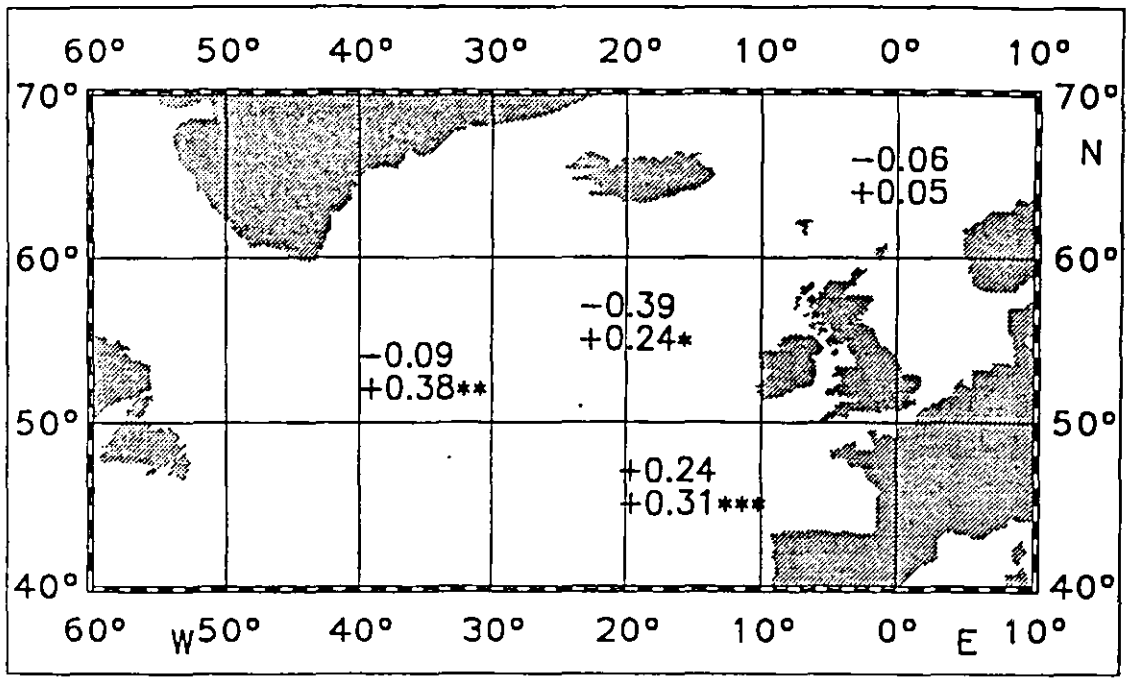

Figure 5: As in Figure 3, but linear trends of surface and upper-air wind speeds at OWSs in the Atlantic Oceans for the early period (a) and the later period (b). Three numbers are given for each station considered, indicating the trend at the surface (bottom) and in the two lowest pressure levels with available data.

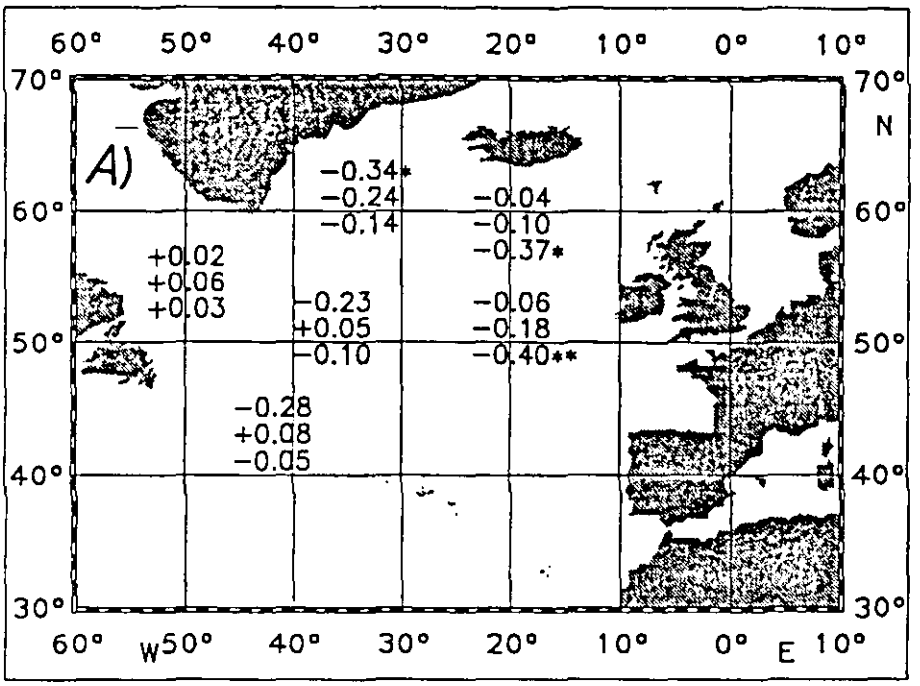

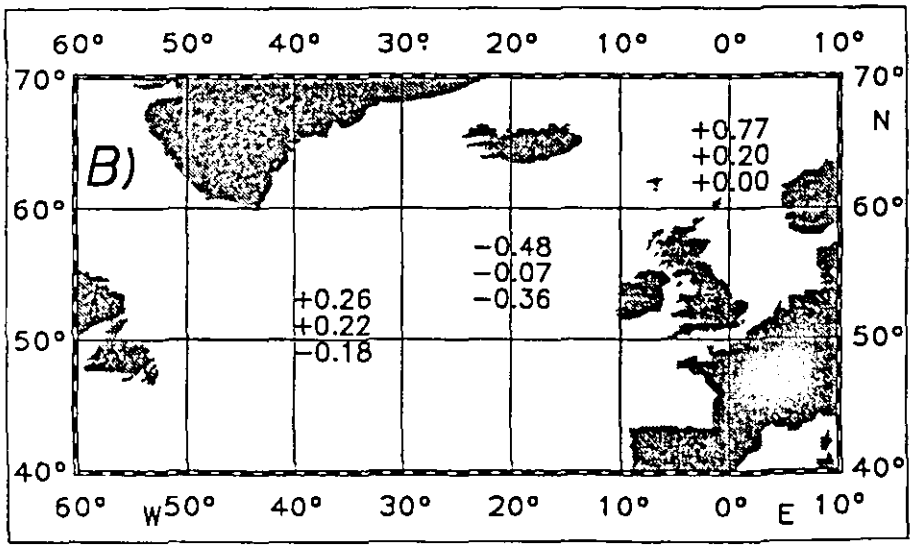

Figure 6: Time series of annual wind speed anomalies [m/s] at OWS P calculated from the OSV record (top) and from the COADS-MSTG record (bottom). The linear trend in the OSV record is -0.02 m/s per decade, a purely random result, while the COADS-MSTG record indicates a trend of +0.52 m/s per decade, highly significant at the 0.01% error level. The latter is considered as non-real.

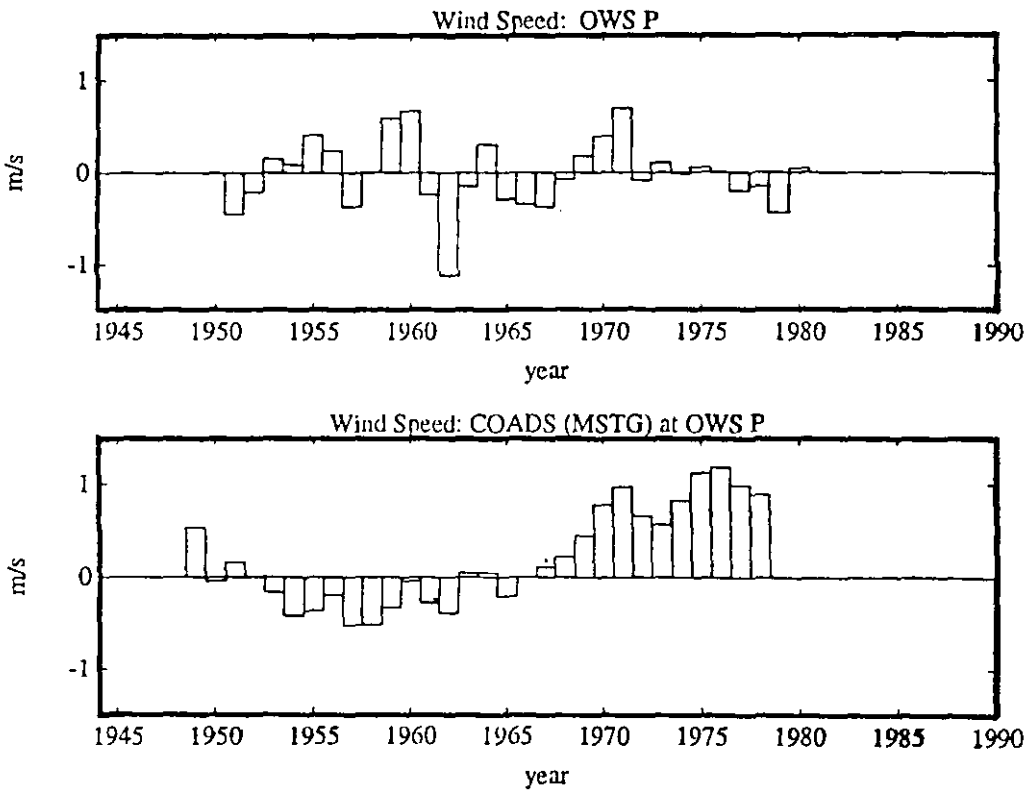

Testing Winds Against Other Variables from COADS

Donald V. Hansen

University of Miami
Cooperative Institute for Marine and Atmospheric Studies
4600 Rickenbacker Causeway
Miami, Florida 33149

Hugo F. Bezdek

National Oceanic and Atmospheric Administration
Atlantic Oceanographic and Meteorological Laboratory
4301 Rickenbacker Causeway
Miami, Florida 33149

Introduction

Several investigators have noted and commented on the appearance of multi-decadal secular trends in surface wind speed records from COADS summaries (as well as the data sets from which these summaries are derived) for various eras and areas. Most commonly, secular increases have been reported (Ramage, 1987; Wright, 1988; Cardone et al., 1990; Isemer and Hasse, 1991), and are dismissed as artifacts of the observing system. In some cases secular decreases have been reported (Cardone et al., 1990; Ward, 1992). Some investigators also interpret the apparent trends as indicative of real changes in air-sea interaction processes (Bunker, 1980; Whysall et al., 1987; Flohn and Kapala, 1989).

In applying the COADS for the North Atlantic Ocean from the period 1951-1987 to investigations for the NOAA Atlantic Climate Change Program, we too noticed a prevalence of secular increase over much of the region for this period. The secular increase is most evident in the monthly mean scalar wind speeds. Figure 1 shows the monthly time series of wind speed from the COADS summary for an exemplary two-degree square in the central subtropical Atlantic, and the secular trend line derived of a linear least square fit to the time series of monthly mean speeds. We decided to investigate more closely the prevalence and reality of this apparent secular increase of winds.

Approach

We chose to revisit, within the confines of the COADS summaries, the question of whether the apparent increase of wind speed in the COADS summaries is indicative of a true climate variation or an artifact of the observing system, by applying consistency tests to other variables contained in the COADS summaries. We selected data from the COADS trimmed file covering the North Atlantic region illustrated in Figure 2. These 359 two-degree by two-degree squares from COADS were chosen for completeness of the monthly mean time series during the 37-year period 1951-1987. They also are sufficiently distant from coasts to enable computation of sea level pressure gradients across each, in anticipation that these gradients will be an important ancillary variable. To provide some regional discrimination, we divided the data into high, middle, and low latitude zones for analyses, using cuts at 30°N and 40°N.

Linear least square fits to the monthly mean wind speed data, as exemplified by Figure l, were made for all of the 359 two-degree by two-degree squares. The secular trend of wind speed was positive in 97 percent of the two-degree squares of latitude greater than 40°N, and 99 percent of those of less than 40°N. For samples the size of those from our three regions, the non-parametric sign test indicates a median value greater than zero at 95 percent or higher confidence level for 58 percent or more positive values. A secular increase evidently is essentially ubiquitous in data from the region shown in Figure 2. The exemplary illustration of Figure 1 shows the median value, 2.6 cm s^{-1} yr^{-1}, for the entire region.

The most important ancillary variable obtainable from the COADS summaries is the sea level pressure gradient, from which an often fictitious but useful variable, the sea level geostrophic wind, can be computed. As the geostrophic wind computed from the monthly mean sea level pressure from the COADS summaries is intrinsically a vector average, it must be compared to the average component winds, or their modulus, from COADS. These vector averages can, of course, be quite different from the scalar average wind speed. The ratio of the modulus of the vector-averaged wind to the scalar average wind speed, sometimes called the directional steadiness, provides a convenient measure of their similarity or dissimilarity. This information is coded into Figure 2. The large area with directional steadiness less than 0.55 indicates considerable dissimilarity between the scalar and vector-averaged winds, and possibly also their secular trends. The linear least square fit procedure was applied also to the time series of moduli of the vector-averaged winds. The ranges of secular changes found for the vector-average winds were very similar to those found for scalar wind speed. In the high and low latitude bands, moreover, there is again a preponderance of positive values, 91 and 96 percent, respectively. The median values of the secular increase of vector winds are only one-half and one-third those of the scalar wind speed but they are significantly non-zero. In the mid-latitude band, however, the values of secular change of vector average wind are almost equally divided between positive and negative, for a median near zero. In this region the secular increase of wind speed does not carry over into the vector mean winds.

To seek support for the reality of the secular increase of vector-averaged wind, we defined estimators

$$\frac{\partial}{\partial t} w_v = \frac{\partial W_v}{\partial G}\frac{\partial G}{\partial t} + \frac{\partial W_v}{\partial \theta}\frac{\partial \theta}{\partial t}, \qquad (1)$$

and

$$\frac{\partial}{\partial t} \alpha = \frac{\partial \alpha}{\partial G}\frac{\partial G}{\partial t} + \frac{\partial \alpha}{\partial W_v}\frac{\partial W_v}{\partial t} + \frac{\partial \alpha}{\partial \theta}\frac{\partial \theta}{\partial t}, \qquad (2)$$

in which W_V and G denote the monthly vector averaged and geostrophic wind moduli, a, the angle between the observed vector averaged and the geostrophic wind, and q, the air-sea difference of virtual potential temperatures. Functional forms for $\partial W_v / \partial G,$, etc., were derived from a combination of the models of Rossby and Montgomery (1935) and Luthardt and Hasse (1981), and evaluated using regional mean values from the COADS summaries. Equations 1 and 2 were then evaluated for each two degree square using values of $\partial G / \partial t, \partial \theta / \partial t$, etc. obtained by the same linear least square fit procedure as was used for Figure l, etc.

Results

The procedure outlined above provides a set of estimations of wind changes consistent with changes in related variables that were compared to the COADS summaries of observations. The results were generally negative. Median values of the secular trend of vector-averaged winds estimated using (1) were different (less than) from their observed counterparts in the COADS at a 95 percent confidence level in both the high and low latitude bands. In fact, neither was different from zero with 95 percent confidence. The estimation of the secular change of geostrophic departure angle, with the apparent secular increase of vector average wind included among the estimators, was found to be significantly different from that observed in the northern band, but not significantly different in the southern band. In both cases, however, the secular trend of the geostrophic departure angles for the wind observations are not significantly different from zero.

Thus, we failed to find support among the other variables in the COADS summaries for the reality of the secular increase of the vector averaged winds and, by implication, the even larger increases of the scalar wind speeds during the past four decades. A primary conclusion is that considerable caution is advised in application of the COADS summaries to problems of decadal and longer-term climate studies. Furthermore, within the confines of the COADS summaries, possibilities for improving the data appear to be very limited. During the past decade most progress has been made by investigators working with data sets antecedent to COADS. More such efforts could be encouraged by making the carefully edited data from which the COADS summaries were made available in convenient form. Periodic reissues of the summaries should be made in step with progress in improving the quality of the historical data to support research on real climate variations.

References

Bunker, A. F., 1980: Trends of variables and energy fluxes over the Atlantic Ocean from 1948 to 1972. *Mon. Wea Rev.*, 108, 720-732.

Cardone, V. J., J. G. Greenwood, and M. A. Cane, 1990: On trends in historical marine data *J. Climate*, 3, 113-127.

Flohn, H., and A. A. Kapala, 1989: Changes of tropical sea-air interaction processes over a 30-year period. *Nature*, 338, 244-246.

Isemer, H.-J., and L. Hasse, 1991: The scientific Beaufort equivalent scale: Effects on wind statistics and climatological air-sea flux estimates in the North Atlantic Ocean. *J. Climate*, 4, 819-836.

Luthardt, H., and L. Hasse, 1991: On the relationship between surface and geostrophic wind in the region of the German Bight. Beitr. Phys. Atmos., 54, 222-237.

Ramage, C. S., 1987: Secular change of wind speeds over the ocean. *J. Climate Appl. Meteor.*, 26, 525528.

Rossby, C. G., and R. B. Montgomery, 1935: The layer of frictional influence in wind and ocean currents. Papers in Physical Oceanography and Meteorology, MIT and Woods Hole Oceanographic Institution.

Ward, M. M., 1992: Provisionally corrected surface wind data, worldwide ocean-atmosphere surface fields, and Sahelian rainfall variability. *J. Climate*, 5, 454-475.

Whysall, K D. B., N. S. Cooper, and G. R. Bigg, 1987: Long-term changes in the tropical Pacific wind field. *Nature*, 327, 216-219.

Wright, P. B., 1988: On the reality of climate changes in wind over the Pacific. *J. Climatology*, 8, 521-527.

Figure 1: Monthly mean values of surface wind speed in COADS summary for a two-degree square having its southwest corner located at 26 N, 46 W. Speed values are in cm s^{-1} for the years 1951-1987. Dark line denotes result of linear least square fit to data with slope 2.6 cm s^{-1} yr^{-1}.

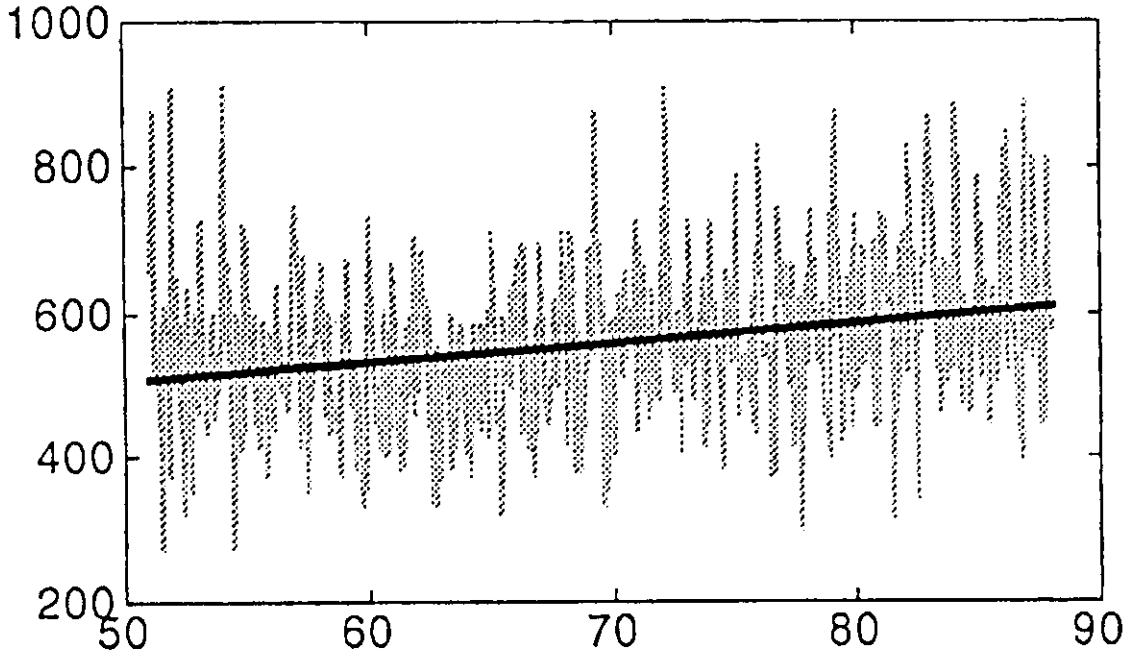

Figure 2: Map of two-degree squares from which COADS data were used in this investigation. Gray tones indicate intervals of directional steadiness, W_V/S: dark gray, .95-.75; intermediate gray, .75-.55; light gray, .55-.35.

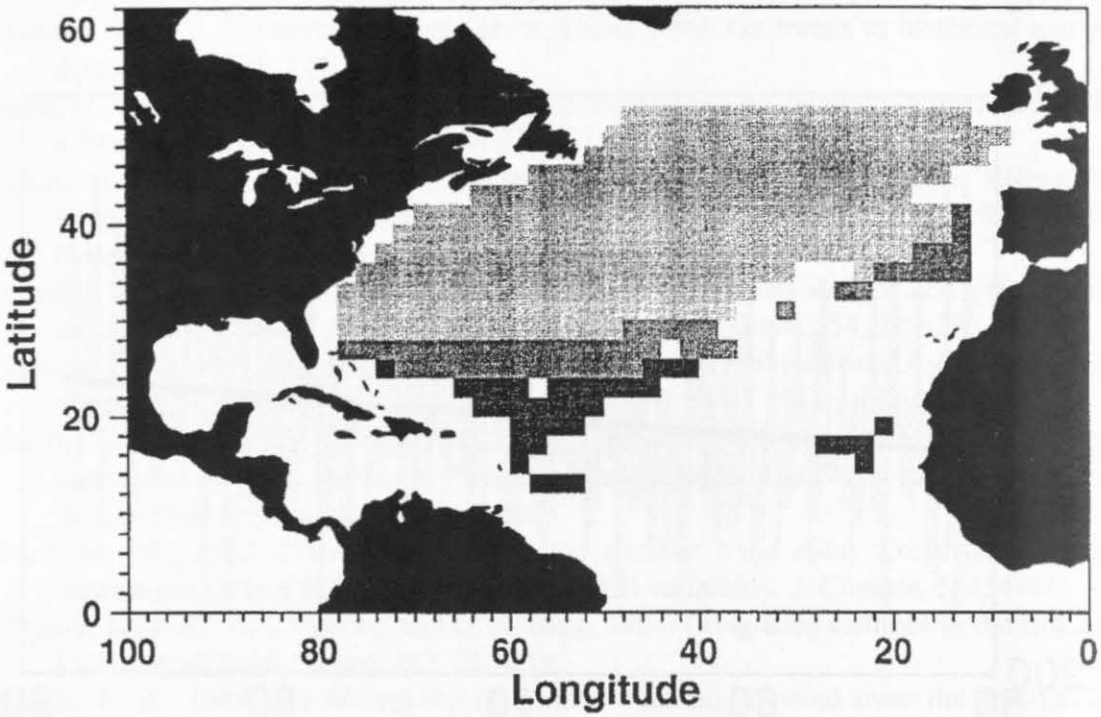

Dynamical Constraints for the Analysis of Sea Level Pressure and Surface Wind Over the World Ocean

Yochanan Kushnir and Alexey Kaplan

Lamont Doherty Earth Observatory of Columbia University
Palisades, NY 10964, U.S.A.

Introduction

In the study of climate and its variability the interaction between the atmosphere and ocean is of particular interest due to the time scales it entails. Fortunately, one of the most comprehensive sources of data for climate research is that of marine observations collected over more than a century by ocean-going vessels, mostly through a voluntary effort of mariners under the guidance of different national weather services. The archive of these reports, which is known as COADS (Woodruff et al., 1987), has been extremely useful to climate research. Of the variables observed routinely over the oceans, sea level pressure and surface wind are important for determining the forcing of the ocean by the atmosphere and for monitoring ocean-atmosphere interaction. Evidence to their importance in the study of climate variability can be found in numerous diagnostic studies early and more recent (e.g., Namias, 1965; Namias and Cayan, 1981; Wallace and Jiang, 1987; Cayan, 1992a, b; Deser, 1993; Kushnir, 1994). Many modeling studies have used these variables to determine the necessary forcing fields and evaluate the model performance.

The present study is part of our effort to construct a dynamically constrained statistical analysis of the monthly averaged sea level pressure (SLP) and surface wind fields of COADS. Such an analysis enables the minimization of the errors involved in the monthly averaged ship reports. It also provides a controlled way to interpolate and extrapolate data in regions of missing information. This paper outlines the methodology of the analysis and the construction of a simplified momentum balance for the oceanic boundary layer to be applied in the course of analysis.

Methodology

The goal of our analysis project has been to construct a monthly time history of the SLP and surface wind fields over the world ocean from the turn of the century to the present. Our analysis does not compete with the operational products coming from numerical weather prediction centers with their state-of-the-art assimilation techniques, but rather enables the handling of the early part of the data record before the advent of comprehensive upper level and satellite data. Thus we have planned to achieve our goal

by using the 2° monthly summaries in COADS and linear statistical techniques. The proposed analysis procedure will enable filling up some gaps in the record and more importantly minimize the errors in the representation of monthly averages in COADS (for a comprehensive discussion of the sources of such errors, see Trenberth et al., 1992).

The statistical analysis procedure we wish to apply to the 2° monthly summaries in COADS is based on the variational approach first outlined by Sasaki (1970). The analysis involves the minimization of a "cost function" S that is a function of the analyzed field $\mathbf{a}(\mathbf{x},t)$ ($\mathbf{x}$ being the location in space and t is time). Thus the analysis is a solution to the condition:

$$\frac{\partial S(\mathbf{a})}{\partial \mathbf{a}} = 0 \qquad (1)$$

In Sasaki's original work the cost function included the constraint that while the analysis stays close to observations (hereafter denoted as $\mathbf{o}$), its variables also obey a dynamic relationship. The degree of constraining the analyzed variables can be varied from the requirement that they obey the dynamic relationship exactly (so-called a "strongly constrained" analysis), or just in a general sense (a "weakly constrained" analysis). Schematically the cost function for a weakly constrained analysis can be written as:

$$S = \frac{1}{2}\{(\mathbf{o}-\mathbf{Ta})'\mathbf{E}_o^{-1}(\mathbf{o}-\mathbf{Ta}) + (\mathbf{Ma})'\mathbf{E}_m^{-1}(\mathbf{Ma}) + SC\} \qquad (2)$$

where ' denotes a transpose operation, $\mathbf{T}$ is a transformation matrix that interpolates the analyzed field to the observation point, and $\mathbf{M}$ is a matrix representing the dynamic constraints, i.e., a model written as:

$$\mathbf{Ma}=0 \qquad (3)$$

(Note that we have assumed that both the transformation $\mathbf{T}$ and the dynamic model are linear.) The matrices $\mathbf{E}_O$, $\mathbf{E}_m$ are the error covariance matrices associated with the observations and dynamic model, respectively. In the strong constraint problem the error covariance matrix $\mathbf{E}_m$ is replaced by a Lagrangian multiplier that is determined in the minimization process. The quantity SC symbolizes a statistical constraint applied to the analysis (such as a requirement that the large scale structure of the variability is close to its long-term statistical properties). This constraint helps fill gaps in the record provided we have information on the behavior of the data covariance matrix there.

An initial attempt to assess the feasibility of such approach was presented by us in the previous COADS Workshop (Kushnir et al., 1992). That pilot study focused on a tropical Pacific data set that was spatially complete and temporally continuous. In that study we used the linear momentum balance of Zebiak (1990) to constrain the data. This constraints entail a linear balance between the pressure gradient force, the coriolis force, and friction. Symbolically this balance can be written as:

$$f\mathbf{k}\times\mathbf{V}_s = -\rho^{-1}\nabla p + \mathbf{F} \qquad (4)$$

where friction F is parameterized as proportional to the wind vector ("Rayleigh" friction):

$$\mathbf{F} = -\varepsilon\mathbf{V}_s \qquad (5)$$

Here $\mathbf{V}_S$ is the surface wind vector, p is sea level pressure, ε is the Rayleigh friction coefficient, f is the coriolis factor, and ρ is the surface air density. When performing the analysis wind and pressure deviations from climatology were considered, and ρ was taken from climatology. Extending the pilot study outside of the tropical Pacific requires the reassessment of the simple, linear momentum balance (1). This discussion is concerned mainly with this issue.

To determine the feasibility of a linear momentum balance in constraining the wind and SLP fields two data sets were utilized:

• A monthly averaged, global 1000 mb ECMWF analysis (uninitialized) from 1980 to 1989. This data set includes the geopotential height, air temperature and winds (vector averaged and scalar averaged) on a 2.5° grid resolution.

• A 43-year integration of the NOAA/GFDL general circulation model with SST specified from observations 1946-1988. This data set included the 990 mb geopotential height, winds and temperature. In addition and as will be explained later, we included the 940 mb level wind (second model level from the surface). This data set has a resolution of 7.5° in longitude and ~4.25° in latitude.

In using these data the pressure gradient term in (4) was replaced by the geopotential gradient. Aside from that we have also made a comparable estimate with the more noisy and gappy COADS SLP and winds to assure that the results obtained for the above two data sets are in general agreement with COADS.

Determining the Parameters of Linear Dynamical Constraints

The issue of the agreement of observed pressure and wind data with the linear momentum balance has been addressed in several previous studies (Zebiak, 1990; Allen and Davey, 1993; Deser, 1993). In these studies attempts were made to asses the error in the balance when applied to tropical Pacific winds and/or to determine the free parameter in the balance, i.e., the Rayleigh friction coefficient ε. Results from these studies were quite satisfactory in statistical terms, i.e., in the statistical sense the monthly mean circulation in the tropics agrees with the balance. In the present study we extended the approach to the entire world ocean (excluding high latitude areas that are generally covered by sea ice) in an effort to determine the optimal value for ε.

The problem of finding the Rayleigh friction coefficient is of regressing the net geostrophic balance on the wind vector. Deser (1993) showed that if the regression is performed in the zonal and meridional directions separately, using the *climatological* values for surface winds and SLP, the coefficient of the zonal momentum balance differs significantly from that of the meridional momentum balance. Deser further argued that this difference is the result of the vertical structure of the wind vector in the planetary

boundary layer (PBL) and the fact that the simple linear balance {(4), (5)} fails to represent the friction vector correctly as the vertical derivative of the wind stress.

Applying the same approach to the *anomalous* winds and 1000 mb height values from the ECMWF analysis we find that the difference in the Rayleigh parameters of the zonal and meridional balances holds for all latitude belts (Fig. la). Moreover the friction parameter displays a distinct latitudinal structure. This behavior is emulated also by the GFDL model (Fig. lb, where the model monthly mean frictional force is taken from its history files and regressed against the model 990 mb vector wind). Note that the GCM parametrizes the friction as the vertical derivative of wind stress, the latter assumed to be proportional to the vertical wind shear i.e.,

$$\mathbf{F} = \frac{\partial}{\partial z}(K\frac{\partial \mathbf{V}}{\partial z}) \tag{6}$$

where K is a stability dependent eddy viscosity coefficient (see Gordon and Stern, 1982).

The availability of GCM data allows us to examine more carefully the directional dependence of ε., or more precisely, the effect of a more careful parameterization of friction in terms of wind. Using low level (~990 mb) model wind $\mathbf{V}_S$ and the wind at the next level above the ground (~940 mb) $\mathbf{V}_u$ we can write the following approximation to the friction vector **F** in (4):

$$\mathbf{F} = -\varepsilon_1 \mathbf{V}_s + \varepsilon_2(\mathbf{V}_u - \mathbf{V}_s) \tag{7}$$

This formulation assumes that the stress at the surface is proportional to the low level wind and the stress at the top of the lowest model layer is proportional to the difference between the wind vectors at the two levels. Using this formulation and regressing the monthly mean model friction separately on the x and y components of the monthly average total wind vector we obtain similar values for the values of ε_1 and ε_2. (Fig. 2). These results confirm the explanation offered by Deser (1993). Their application to the problem of analyzing surface winds and SLP from COADS is however not straight forward since we do not have observations of the wind above the surface layer.

The latitudinal dependence of ε could be attributed to at least two factors:

- Changes in the vertical structure of the PBL with latitude (e.g., PBL depth that is implicit in the coefficients both in (5) and (7)).
- The non linearity in the surface stress usually expressed in terms of a drag coefficient parameterization:

$$\vec{\tau}_s = \rho C_D w_s \mathbf{V}_s \tag{8}$$

where w_s is the surface wind speed.

It is possible to address the latter factor in the context of our linear approach, by substituting the instantaneous value of w_s by its climatological value $\overline{w}_s$. This approach was tested by regressing the geostrophic balance calculated from the ECMWF data

against the value of $\overline{w}_s\mathbf{V}$ as a function of latitude (Fig. 3). Results show that the new regression coefficient stays much more constant with latitude than the one in the old formulation (Fig. la). The value of the new coefficient is still dependent on the direction, with the meridional balance coefficient about twice as large as the zonal balance coefficient. These new coefficient can also be used to parameterize the frictional force **F** by writing:

$$\mathbf{F} = -\alpha\overline{w}_s\mathbf{V}_s \qquad (9)$$

remembering that different α's are used in the zonal and meridional directions, respectively.

Estimating the Errors in the Linear Constraints

Examination of the error in the linear balance can be done by substituting the ECMWF "observations" of wind and 1000 mb heights into the linear momentum balance, and calculating the residual. We have to remember however that the monthly means were calculated from uninitialized analyses and thus may still exhibit some data related errors. Figure 4 represents the rms error of the linear balance (4) with friction parameterized as in (5) using latitudinally and directionally dependent values for ε. The balance error increases with latitude and is largest north of ~50°N. A more revealing way of judging the quality of the balance is to examine the ratio between the rms residual of the frictional balance and that of the geostrophic balance. This is shown in Fig. 5 for two cases, one with a Rayleigh friction parameterization and the other with the so-called "drag coefficient" parameterization (9). In the latter case we used a globally fixed a with values of $1.9\text{x}10^{-6}$ for the zonal balance and $3.1\text{x}10^{-6}$ for the meridional balance. Both methods for parameterizing friction offer an improved representation of the momentum balance in the extratropics. In the tropics the results are strongly sensitive to data errors (a 1 ms^{-1} error in wind speed could result from a small, ~0.4 m error in geopotential height). This can be verified by comparing with a similar figure calculated from a fit to the GFDL model data (Fig. 6). Here the tropics do not stand out as very different form the rest of the globe.

Summary and Additional Considerations

The feasibility of using a linear momentum balance to constrain sea level pressure and wind in a variational analysis procedure was assessed by fitting the balance equations to data. Adding linear drag to the geostrophic balance improves the constraints for SLP and winds by reducing the error. This is shown clearly with model data and only partly successfully with assimilated data. To better assess the applicability of these constraints one would have to compare the ECMWF data with the results of a full variational analysis according to (1). We are planning to take this approach in the near future.

The error fields calculated based on the data (Fig. 5) reveal a zonal asymmetry that could be attributed to other terms neglected in the linear model. In particular, effects of

stability in the PBL, as well as the effect of transient motions, were not included. Including these effects in a linear model is another level of complication that should be addressed in future research.

References

Allen, M. R. and M. K. Davey, 1993: Empirical parameterization of tropical ocean atmosphere coupling: The "Inverse Gill problem". J. Climate, 6, 509-530.

Cayan, D. R., 1992a: Latent and sensible heat flux anomalies over the northern oceans: Driving the sea surface temperature. J. Phys. Oceanogr., 22, 859-881.

Cayan, D. R., 1992b: Latent and sensible heat flux anomalies over the northern oceans: The connection to monthly atmospheric circulation. J. Climate, 5, 354-369.

Deser, C., 1993: Diagnosis of the surface momentum balance over the tropical Pacific Ocean. J. Climate, 6, 64-74.

Deser, C. and M. L. Blackmon, 1993: Surface climate variations over the North Atlantic Ocean during winter: 1900-1989. J. Climate, 6, 1743-1753.

Gordon, C. T. and W. F. Stern, 1982: A description of the GFDL global spectral model. *Mon. Wea. Rev.*, 110, 625-644.

Kushnir, Y., 1994: Interdecadal variations in North Atlantic sea surface temperature and associated atmospheric conditions. *J. Climate*, 7, 141-157.

Kushnir, Y., S. E. Zebiak, M. A. Cane and R. L. Tagett, 1992: Towards a dynamically constrained analysis of sea level pressure and winds. Proceedings of the International COADS Workshop, 13-15 January 1992, Boulder, CO., H. F. Diaz, K. Wolter and S. D. Woodruff (eds.), U.S. Department of Commerce/NOAA-ERL, 201-209.

Namias, J., 1965: Short period climatic fluctuations. *Science*, 147, 696-706.

Namias, J. and D. R. Cayan, 1981: Large-scale air-sea interactions and short period climate fluctuations. *Science*, 214, 869-876.

Sasaki, Y., 1970: Some basic formalisms in numerical variational analysis. *Mon. Wea. Rev.*, 98, 875-883.

Trenberth, K. E., J. R. Christy and J. W. Hurrell, 1992: Monitoring global monthly surface temperature. *J. Climate,* 12, 1424-1440.

Wallace, J. M. and Q.-R. Jiang, 1987: On the observed structure of interannual variability of the atmosphere/ocean climate system. *Atmospheric and Oceanic Variability*, H. Cattle, ed., Royal Meteorological Society, 17-43.

Woodruff, S. D., R. J. Slutz, R. L. Jenne and P. M. Steurer, 1987: A comprehensive ocean-atmosphere data set. *Bull. Amer. Meteor. Soc.*, 68, 521-527.

Zebiak, S. E., 1990: Diagnostic studies of Pacific winds. *J. Climate*, 3, 1016-1031.

Figure 1: The regression coefficient between the geostrophic balance residual for anomalous 1000 mb height and wind values, and the anomalous wind vector over the world ocean, based on: a) ECMWF analysis using the months December, January, and February from 1980 to 1989. b) GFDL GCM using the same month but for a 33-year interval. Regression is performed separately for the zonal balance (solid curve) and the meridional balance(dashed curve). Units are in 10^{-5} sec^{-1}.

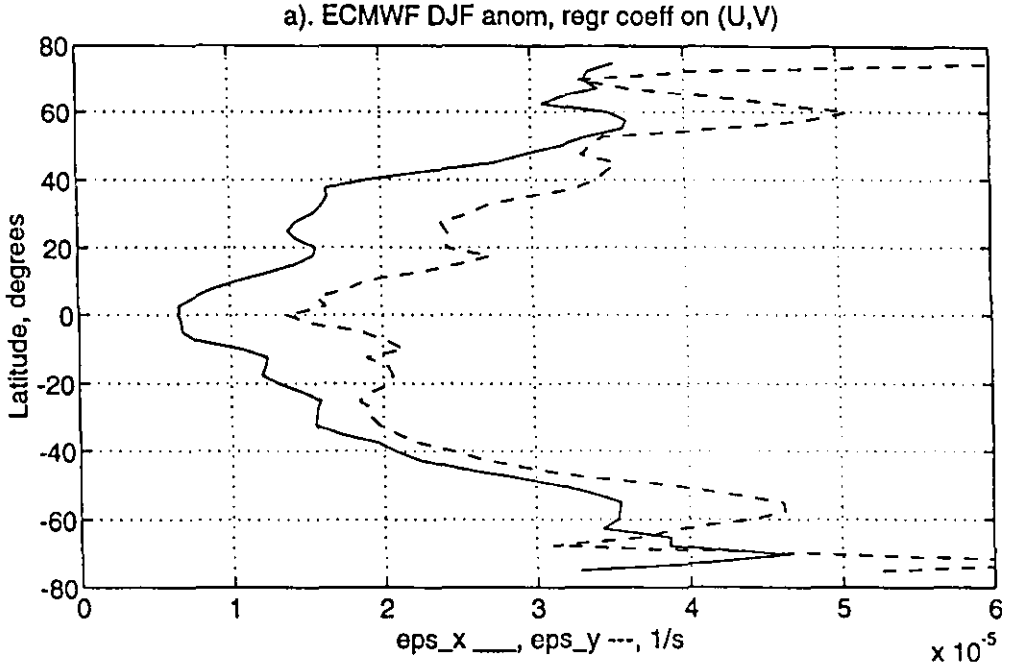

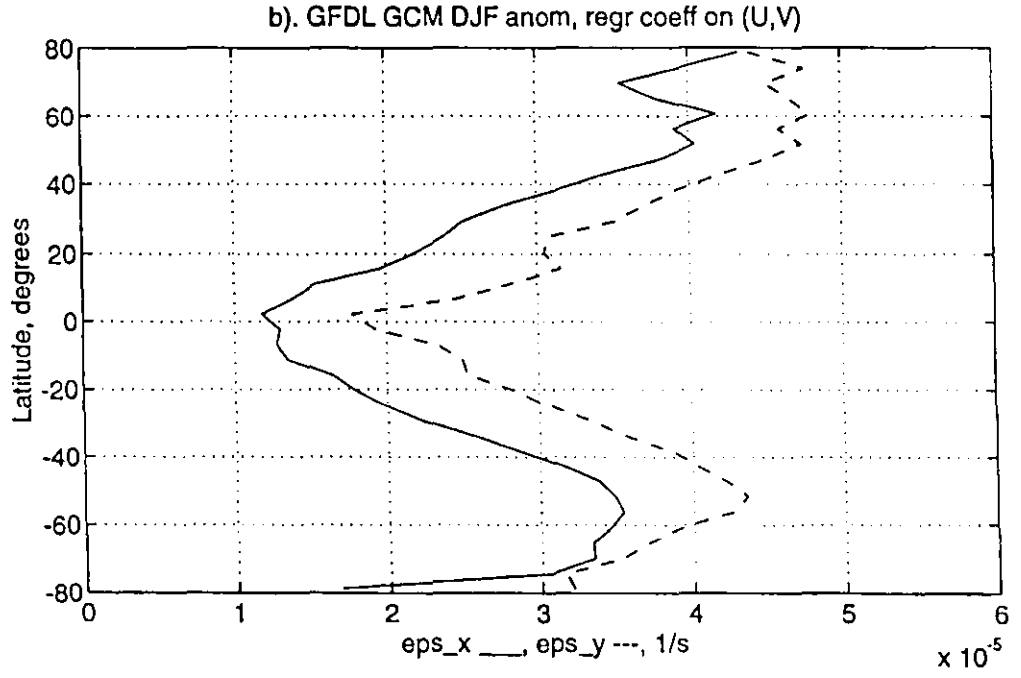

Figure 2: The result of a regression calculation meant to determine the x- and y-direction coefficients ε_1 and ε_2 (see equation (7) in text) using GFDL GCM data. Solid and dashed lines are for ε_1 in the x- and y-direction respectively. Dash-dotted line and dotted line are ε_2 in the x- and y-direction respectively. Units are in 10^{-5} sec^{-1}.

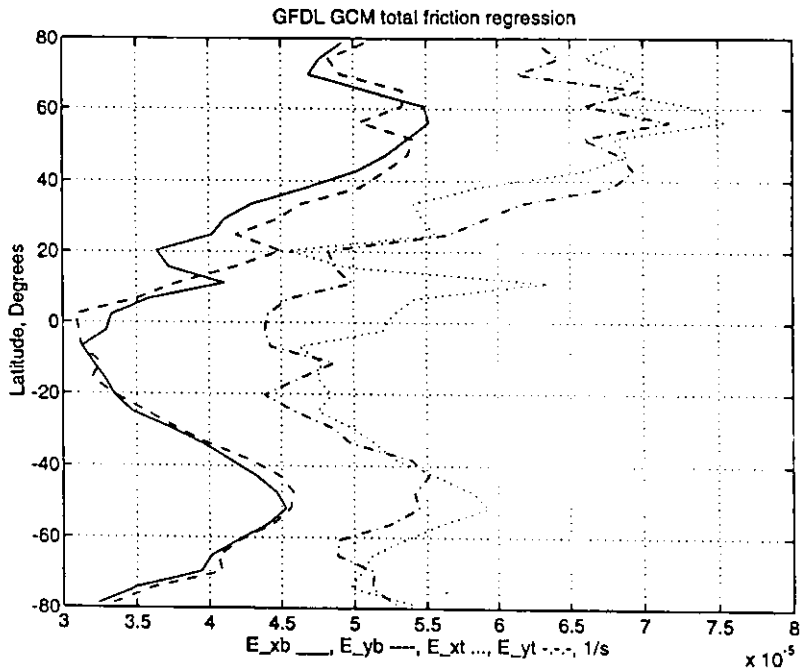

Figure 3: Results of a regression analysis to determine the coefficient α in equation (9) using ECMWF wind and 1000 mb height anomalies as well as the corresponding climatological wind speed for December-February. Solid line is for the x-direction coefficient and dashed line for the y-direction coefficient. Units are in 10^{-6} sec^{-1}.

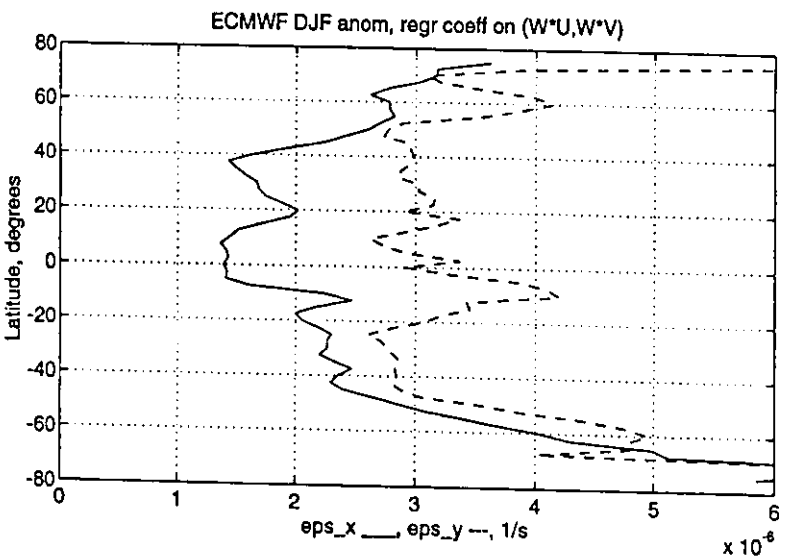

Figure 4: Absolute rms error in the linear frictional balance for anomalous ECMWF wind and 1000 mb height values, and directionally and latitudinally-dependent Rayleigh coefficients. Units are in 10^{-5} sec^{-2}.

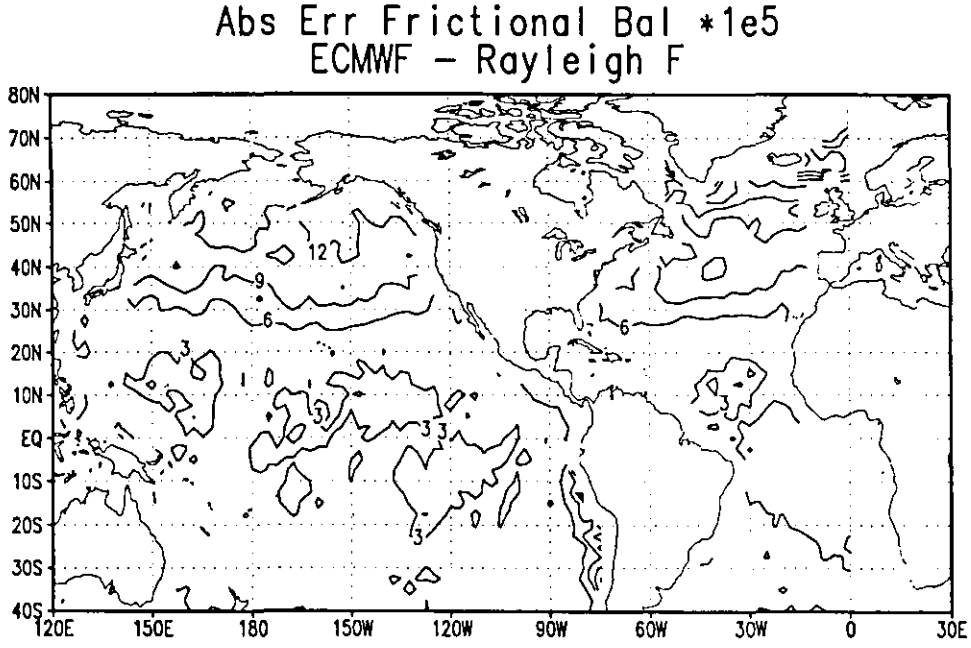

Figure 5: Ratio between error in the linear frictional balance and the geostrophic balance for anomalous ECMWF wind and 1000 mb height values using a) directionally and latitudinally dependent Rayleight coefficients. b) globally constant but directionally dependent "drag" coefficients. Regions where values are larger than 0.8 are shaded

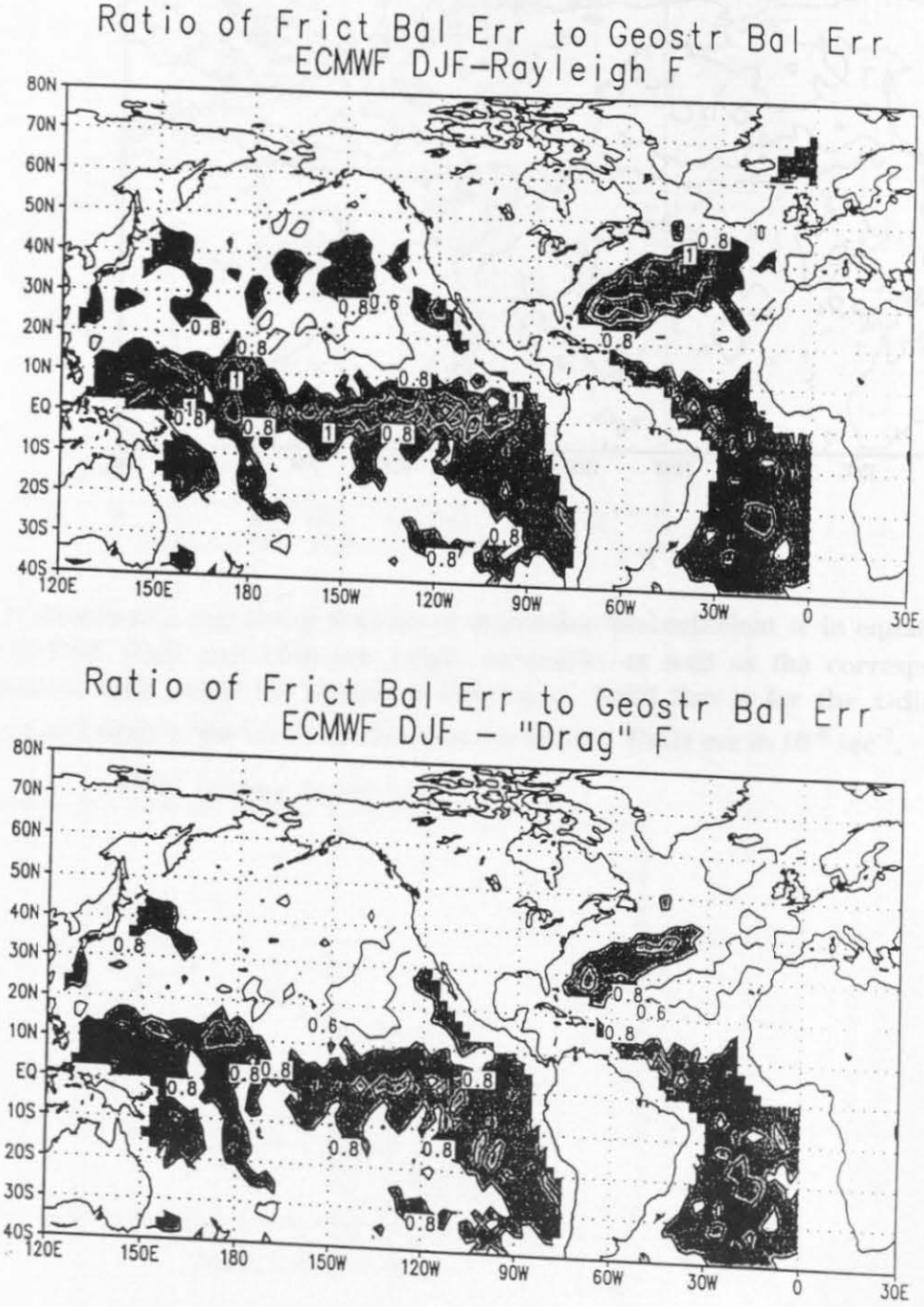

Figure 6: As in 5a but for the GFDL GCM data at the 990 mb level.

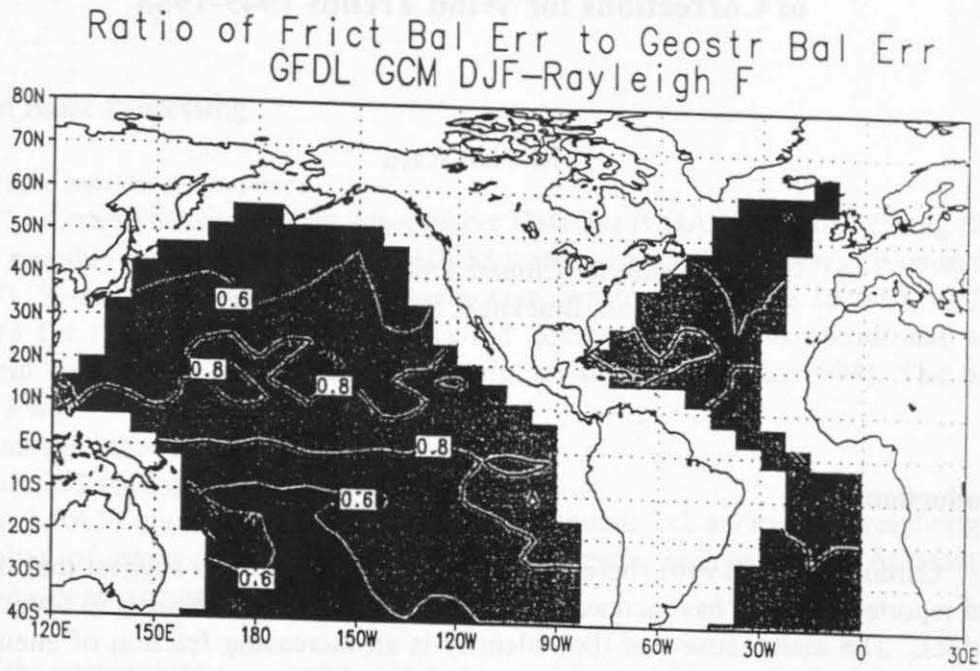

Near-Surface Wind, SLP and SST: Some Inter-relationships and a Set of Corrections for Wind Trends 1949-1988

M. Neil Ward

Hadley center for Climate Prediction and Research
London Road, Bracknell, Berkshire RG12 2SY

Introduction

Cardone et al. (1990) (hereafter, CGC, 1990) and others suggest that the wind speed reported by ships has increased in recent decades due to changes in observational practices. The main cause that they identify is an increasing fraction of anemometer readings, typically now made at a mean height of 20m, relative to Beaufort force estimates, which are converted to 10m winds (using a biased conversion scale) before insertion into computerized datasets like COADS.

This paper aims to contribute to the debate on the reliability of the wind data, and on how to maximize its utility for climate studies. The first section below describes the data and basic processing methods, followed by a discussion of some theoretical relationships that are expected to exist between near-surface wind and sea-level pressure (SLP), and a description of the balanced friction flow (BFF) method for deriving near-surface seasonal mean wind from seasonal mean SLP patterns. To gain confidence in the observed wind and SLP data, it is useful to verify the presence of relationships in the data that are expected from theory. The process is two-way, since the data are also verifying the theory. The next two sections consider a dataset of calculated BFF winds for 1949-88, and present a comparison with the reported observed winds; the trends in the observed wind time-series are adjusted to equal the trends in the BFP time-series, thereby calculating a corrected wind dataset. A wind correction method based on this approach assumes that there is no substantial time varying bias in the estimated pressure gradients, and that the distance between derived wind trend and observed wind trend can be used to isolate time varying bias in wind observation. The derived wind is a function of pressure difference, so will largely be independent of any time-varying bias that may exist in ship pressure data, though other problems such as changes in bias towards reports during fair weather may influence the derived wind trends in some regions. The corrections reported here follow on from those reported in Ward (1992). Finally, two applications of the corrected wind data are reported. Firstly, we illustrate the impact of the corrections on estimated wind patterns associated with multi-decadal rainfall fluctuations in sub-Saharan Africa. Secondly, very close agreement is found in the year-to-year variability of near-surface divergence patterns (calculated from the corrected wind) and sea-surface temperature (SST) patterns in the tropical western Pacific. The close agreement illustrates

the excellent value of the ship data for climate studies once it has been processed carefully.

Data and Basic Processing

Near-surface marine atmosphere

The Comprehensive Ocean-Atmosphere Data Set (COADS) 2°lat x 2°long (2x2) trimmed monthly means for the years 1949-88 were used for the analyses (Woodruff et al., 1987). Seasonal mean anomaly datasets were constructed on the 10°lat x 10°long grid-scale for the variables SLP, zonal wind component (u) and meridional wind component (v). Details of the data processing are in Ward (1992, 1994). The basic procedure was:

- Construct smoothed 2x2 climatologies.
- Construct 2x2 seasonal mean anomaly datasets.
- Construct 10x10 anomalies by averaging all constituent 2x2 anomalies, weighting for the number of observations that contributed to each 2x2 anomaly. At least 20 observations were required to form a 10x10 anomaly.

Sea-surface temperature

SST data were taken from the Meteorological Office Historical Sea-surface Temperature dataset version 4 (MOHSST4) (Bottomley et al., 1990). The data were formed into 10°lat x 10°long seasonal anomalies (details in Ward, 1992, 1994).

Deriving Wind from Sea-Level Pressure

The seasonal mean horizontal momentum equation can be simplified by assuming a three-way balance of forces between seasonal mean SLP (P), seasonal mean friction and seasonal mean coriolis force (f). To a first approximation, it has often been assumed that friction direction opposes the motion, and that the force is directly proportional to wind speed through a constant (k) called the coefficient of surface resistance. Then the horizontal momentum equation can be solved for u and v:

$$u = \frac{kP_x + fP_y}{k^2 + f^2}, \qquad v = \frac{kP_y - fP_x}{k^2 + f^2} \tag{1}$$

where:

$$P_x = -\frac{1}{\rho}\frac{\partial P}{\partial x}, \quad P_y = -\frac{1}{\rho}\frac{\partial P}{\partial y}$$

Such a derived wind is often described as "balanced friction flow" (BFF). In deriving Eq. (1), all terms are time and area averages, and all eddy terms are ignored (validity discussed in Ward, 1994). To apply Eq. (1), assumptions have to be made about the value of k. Typical values of k have been estimated in the range 1-3 x $10^{-5}s^{-1}$ (e.g. Gordon and

Taylor, 1975). Note that as well as varying geographically due to varying mean boundary layer characteristics, k will also depend on location within the boundary layer. For example, Brummer et al. (1974) reports an experiment in the North Atlantic trades at 10°N in which they found that the friction force declined by a factor of two between 15m and 500m, such that the implied value of k falls from about 2.3 x$10^{-5}s^{-1}$ to 1.2 x $10^{-5}s^{-1}$.

It follows from Eq. (1) that k and f prescribe the backing angle (β_F) and ratio (R_F) of the BFF vector to the geostrophic vector:

$$\tan\beta_F = \frac{k}{f} \qquad (2a)$$

$$R_F = \sqrt{\left(\frac{f^2}{f^2+k^2}\right)} \qquad (2b)$$

For the studies in this paper, values of k are derived by assuming a backing angle β_F of 10° for the regions polewards of 50°, and 50° for the average of regions equatorwards of 10°. Backing angles are linearly interpolated over the latitude range 10-50°, assuming 50° at 10° latitude and 10° at 50° latitude. The values of k that these backing angles imply are broadly consistent with the results of previous studies (e.g. Gordon and Taylor, 1975).

Comparison of Observed and Derived Winds 1949-88

The BFF equations (Eq. 1) have been applied to every seasonal mean SLP anomaly field 1949-88. (Note that the BFF equations can be solved using anomalies, whereas the inclusion of the advective accelerations would require the use of the total wind since advection of anomalies is being effected by actual winds, not just the anomalies). Where possible, missing SLP anomalies were spatially interpolated using a simple linear system (Ward, 1994).

Figure 1 illustrates time-series of derived BFF and observed wind anomalies for a 10 x 10 box in the tropical North Atlantic (Fig. 1a) and a box in the tropical South Atlantic (Fig. 1b). The impression is gained that interannual variability of the observed and derived winds agree very well. Figures 2a-d show the correlation of derived and observed wind anomalies over 1949-88 for the seasons Dec-Feb (DJF) and Jul-Sep (JAS). There are many regions where the correlation is >0.7, giving good confidence in the reliability of the data and the BFF theory. The poor performance in some equatorial regions is probably because so close to the equator the equations can be less applicable, and SLP needs to be resolved on a finer spatial scale. The improvement over the geostrophic approximation (see Fig. 2e) is, not surprisingly, most apparent in the tropics, where the improvement in the simulation of the v wind component is significantly greater than that of the u wind component.

In Fig. 1, it is also clear that despite good interannual agreement, there is a systematic difference in the trends of the BFF and observed wind. In both instances, the

observed wind shows a trend towards strengthening easterlies, whereas in the BFF wind, the trends are much reduced or absent.

To give a clear picture of global changes in reported and derived wind circulation strength, global mean zonal wind anomaly time-series of the observed, provisionally corrected (from Ward, 1992) and new BFF wind have been calculated as follows (series were calculated for each of the four seasons separately):

(i) Reject all those 10 x 10 boxes with

$$\frac{|\bar{u}|}{\sigma_u} < 1.282 \qquad (3)$$

where $\bar{u}$ is the particular season's 10 x 10 climatological zonal wind (calculated using the period 1969-88) and σ_u is the standard deviation of the zonal seasonal values over 1969-88. Following normal distribution theory, this criterion ensures that series included in the analysis have less than 10% of seasonal values with a wind vector of sign opposite to the mean vector. Those series with a negative mean zonal wind were multiplied by -1 so that the series effectively represent anomalies in the *magnitude* of the zonal wind. While it is tempting to simply analyze trends in the modulus of the zonal wind, this should not be done, because such a quantity is also a function of data reliability, which of course shows a trend through time.

(ii) Standardize each 10 x 10 series over the period 1949-1988.
(iii) Average the standardized anomalies over all ocean regions.

The mean standardized anomaly time-series for each of the four seasons are plotted together in Fig. 3. The reported wind time-series shows a mean increase of about one standard deviation. The provisionally corrected and new derived wind time-series show no significant trend.

Revised Corrections for Ship Reports of Near-Surface Wind 1949-88

In this section, the correction methodology outlined in Ward (1992) is applied, but using the new BFF derived winds in place of the geostrophic wind used in Ward (1992). Also, the analysis here is on the 10 x 10 scale, compared to 2 x 2 in Ward (1992), so data coverage is much better, affording a more complete coverage for the corrections.

The analysis includes only u and v seasonal wind time-series which have a long-term u or v mean that is substantially different from zero (based on Eq. 3; details in Ward, 1994). So trends in these series can be used to approximate trends in the strength of the circulation. The difference in trend over 1949-88 (termed a_1, units are $ms^{-1}yr^{-1}$) between the BFF wind and observed wind is estimated (for u and v separately). Then the linear component of the implied spurious percentage increase S in the observed wind vector over 40 years is

$$S = \left(\frac{a_1 * 40}{\overline{V_a}} \right) * 100 \qquad (4)$$

where $\overline{V_a}$ is the climatological wind in either zonal or meridional direction, depending on whether the u or v wind is being analyzed. For a given box, up to 8 estimates of S were available (u and v in the 4 seasons). The estimates were averaged, weighting each S as in Ward (1992) by its estimated "reliability", calculated as the 1949-88 derived versus observed wind correlation (r, examples in Fig. 2a-d) multiplied by the number of years with data (N). To smooth the field of 10 x 10 values, a zonally directed weighting scheme of 2:4:2, with one unit of weight each to the boxes to the north and south, was superimposed on the "reliability" weight calculated for each box ($N*r$). If a box did not have a value of S, it was given the area average (before application of the smoothing), using the areas defined in Ward (1992). For equatorial boxes (10°N-10°S), one further smoothing was applied by averaging the target box, the box to the north and the box to the south, weighting according to the sum of the weights that had contributed to each of the boxes in the first smoothing pass. The final result is shown in Fig. 4.

The weighted average of all values of S before smoothing is 14.3%, which is very similar to the overall average of 16.1% calculated in Ward (1992). Ive (1987) shows maps of the percentage of wind reports that contained the code for an anemometer reading in the British Met. Office Marine Data Bank in differing periods, the last of which is 1975-1979. Her maps generally support the geographical variations of S in Fig. 4. Regions that still have low ratios of measured to estimated winds (such as North Atlantic) are expected to have the smallest corrections. However, the *negative* corrections in the far North Atlantic (also found in Ward, 1992) remain unexplained.

Corrected wind datasets have been calculated using the method in Ward (1992). For each 10 x 10 vector wind time series, the corrected data are calculated:

$$\tilde{u} = u_t - [u_t * ((S - 100) * (t - t_b) / 40]$$
$$\tilde{v} = v_t - [v_t * ((S - 100) * (t - t_b) / 40] \qquad (5)$$

where $\tilde{u}_t$ and $\tilde{v}_t$, are the corrected u and v seasonal wind vectors for time t, $\tilde{u}_t$ and $\tilde{v}_t$, are the observed COADS seasonal wind vectors for t, and S is the 1949-88 mean spurious percentage change in wind speed for the 10 x 10 box. Note that the mid-point of the season is used for t (e.g. July-September 1949, t=1949.71). t_b is an arbitrarily selected time which acts as the base time for the corrections. For example, if t_b=1949.0, then when t=1949.0, $\tilde{u}$=u and $\tilde{v}$=v ; 40 years later when t=1989.0, the wind vectors are reduced in magnitude by S%, (or increased by S% if S is negative). To correct the data for use in the studies reported here, t_b, was always set to the mid-point of the 1969-1988 normals period.

Applications of the Corrected Wind Data

Circulation associated with extended Sahel drought

It is known that JAS rainfall in the Sahel region of sub-Saharan Africa was dramatically less in the period 1969-88 than in the period 1949-68. Figure 5 shows the composite difference 1969-88 *minus* 1949-68 for (a) the raw observed near-surface wind data and (b) the corrected data. Compared to the raw data, the corrected data suggest some quite different aspects to the tropical circulation changes:

(i) In the tropical Atlantic, the raw data emphasize enhancement of easterly trades near 15°N during the drought period, whereas the corrected data suggest modest enhancement, linking with circulation changes in the equatorial and South Atlantic that correspond to a weakening of cross equatorial flow. The corrected wind pattern suggests a much stronger modulation of the local Hadley circulation, and the corrected wind pattern is likely to have significant consequences for ocean circulation and cross-equatorial heat fluxes in the western equatorial Atlantic.

(ii) In the northern Indian Ocean, the raw data suggest a strengthening of the monsoon circulation in the Sahel drought period, whereas the corrected data indicate little change or a slight weakening in the monsoon circulation, which is more consistent with the slight reduction in Indian monsoon rainfall 1969-88.

(iii) In the tropical Pacific, the raw data suggest strengthened circulation in many regions, whereas the corrected data suggest little change in circulation strength, but some changes in the meridional wind.

The corrections make little difference to the circulation change in the extra tropical North Atlantic, which is dominated by an anomalous anticyclonic circulation centered near the UK during the Sahel drought period.

The relationship between near-surface divergence and SST in the western Pacific.

In the tropics, direct forcing of the near-surface atmosphere by SST will lead to a close association between anomalies of near-surface convergence and SST maxima in the absence of other forcing (Lindzen and Nigam, 1987).

This section studies the relationship between SST and near-surface divergence in the tropical western Pacific. A 10 x 10 dataset of near-surface divergence was calculated using finite differences of the 10 x 10 seasonal mean vector wind anomalies. Where possible, missing SLP anomalies were spatially interpolated using a simple linear system (Ward, 1994). To further reduce noise, the divergence anomalies were zonally smoothed, weighting 1:2:1.

The first JAS SST EOF for 1949-88 (Fig. 6a) in the tropical western Pacific is an east-west dipole pattern. In the west, the largest weights are at 0-10°S. (The pattern for 1904-90 is very similar (Fig. 6b), supporting the stability of the result). The first JAS divergence EOF (Fig. 6c) has a more complicated pattern. Over the equatorial latitudes 10°N-10°S it is also an east-west dipole. Again, largest weights in the west are at 0-10°S. In the west, the pattern is also a north-south dipole, with large positive weights centered at 0-10°S and large negative weights at 10- 20°N. (Also, in the east, the weights at 10-20°N and at 10-20°S have a sign that is opposite to the weights at 10°S-10°N.)

The correlation between the time-coefficients of SST EOF1 and divergence EOF1 is extremely high (Fig. 6d). So we suggest that, in the region of the EOF analysis, the equatorial atmosphere is responding directly to the SST as predicted by Lindzen and Nigam (1987), especially at 0°-10°S in the western Pacific. At 10-20°N, the atmosphere does not appear to be responding so directly to the local SST. One hypothesis is that equatorial regions of enhanced near-surface convergence lead to a zone of diabatic heating anomaly (enhanced penetrative convection leading to enhanced latent heating), which leads to descent and near-surface divergence anomalies about 10° latitude polewards, which is consistent with the meridional overturning found by Gill (1980) in response to a line of heating in the tropical atmosphere.

That an SST and near-surface divergence time-series can be derived with such near-perfect agreement (Fig. 6d) is extremely encouraging for the utility of ship data in climate studies. As illustrated here, the data can be used to test and explore theories on the relationship between SST and atmospheric circulation.

Discussion and Conclusions

Based on comparisons with the derived BFF wind, this paper estimates that the globally averaged spurious percentage rise in reported wind speed over 1949-88 is 14.3%. This is very similar to the estimate of 16.1% made in Ward (1992). Applying the theory of CGC (1990), such estimates suggest an increase from 0% of anemometer readings in 1949 to 60% of anemometer readings in 1988. However, there is considerable uncertainty as to the fraction of ship wind reports that are based on anemometers around the world (Kent and Taylor, 1991; Ive, 1987).

The results of Ive (1987) suggest more anemometer readings than WMO (1990), but considerably less than the 60% needed for the theory of CGC (1990) to explain the mean value of S calculated above. Thus there may be further cause of the spurious rise in wind speeds. For example, it is possible that there has been a gradual change in the way observers translate sea states into Beaufort numbers. This possibility is suggested by the results of Lindau et al. (1990) who performed a SLP-wind comparison for the 10 x 10 box centered 15°S, 35°W in the tropical South Atlantic. They analyzed only those reports that were stated to be estimated, but still found a spurious rise in the reported wind speed. One possibility is that as anemometers have become widely available, so reporters have tended to tune their estimated winds to that which anemometers typically give. Indeed, it is likely that some reports coded as estimated have in fact been influenced by the presence of an anemometer on board.

The corrections reported in this paper vary sufficiently smoothly and are sufficiently complete to enable the regional correction approach in Ward (1992) to be replaced by a field of smooth corrections (Fig 4). So the new corrected wind data do not have sharp discontinuities across regional boundaries and are therefore potentially well suited to estimations of horizontal divergence, or to forcing ocean numerical models. The new corrections are also much more reliable in the tropics because the BFF method used to derive the wind is one that is well suited to the tropical boundary layer on the seasonal time-scale. Indeed, recent analyses (e.g. Neelin, 1989, Philander, 1990) have pointed out the similarity of the BFF equations with equations used elsewhere to understand the tropical atmosphere. The BFF system is similar to the equations used by Gill (1980) to

boundary layer to heating from the SST. Finally, the BFF system is also similar to the atmospheric part of many simple coupled tropical ocean-atmosphere models.

Some analysis of the terms excluded in the BFF equations is given in Ward (1994). For example, on the 10 x 10 spatial scale, acceleration was found to be important only in a small number of boxes, notably the cross equatorial Indian monsoon flow in boreal summer. The potential importance of the transient eddy friction term, the spatial eddy friction term and the spatial eddy coriolis term were all illustrated. Nonetheless, maps have been presented in this paper (Fig. 2) showing generally good correlation (resulting from the non-trend time scale) between winds derived using BFF and the uncorrected observed wind, suggesting good reliability in both data and theory. Once the spurious wind trend is removed, it is suggested that the ship reported SLP and the corrected wind data form an extremely valuable climate research tool. Two examples of applications to climate studies have been given. Firstly, compared to the raw data, the corrected data give a substantially different picture of tropic-wide circulation changes associated with sub-Saharan drought over recent decades. Secondly, the corrected data were used to create a near-surface divergence dataset. Divergence is a notoriously difficult quantity to estimate, but the near-perfect agreement between the time-series of the first SST EOF and first near-surface divergence EOF in the tropical western Pacific over 1949-88 suggests that the data processing employed here has enabled the calculation of a useful divergence dataset.

References

Brummer, B., Augstein, E., and Richl, H., 1974: On the low-level wind structure in the Atlantic trade. *Quart. J. Roy. Meteor. Soc.*, 100, 109-121.

Bottomley, M., Folland, C.K., Hsiung, J., NewelL R.E., and Parker D.E., 1990: Global ocean surface temperature atlas (GOSTA). Joint Meteorological Office/Massachusetts Institute of Technology Project. Project supported by US Dept. of Energy, US National Science Foundation and US Office of Naval Research Publication funded by UK Depts. of Energy and Environment. pp20 and 313 Plates. HMSO, London.

Cardone, VJ., Greenwood, J.G., and Cane, M.A., 1990: On trends in historical marine wind data, *J. Climate*, 3, 113-127.

Gill, A E., 1980: Some simple solutions for heat-induced tropical circulation. *Quart. J. Roy. Meteor. Soc.*, 106, 447-462.

Gordon, A H., and Taylor, RC, 1975: Computations of surface layer air parcel trajectories, and weather, in the oceanic tropics. International Indian Ocean Expedition, Meteorological Monographs, No. 7, Univ. Press of Hawaii Honolulu, 112 pp.

Isemer, H.-J., and Hasse, L, 1991: The scientific Beaufort equivalent scale: Effects on wind statistics and climatological air sea flux estimates in the North Atlantic Ocean. *J. Climate*, 4, 819-836.

Ive, D.S., 1987: A comparison of numbers of visually estimated and instrumentally measured wind data. Marine Tech Note No. 2, pp43. Available from the National Meteorological Library, Meteorological Office, Bracknell, Berkshire, UK.

Kent, EC., and Taylor, P.K, 1991: Ships observing marine climate - A catalogue of the voluntary observing ships participating in the VSOP-NA. Marine meteorology and related oceanographic activities, Report No. 25, WMO/TD-No. 456. pp 123.

Lindau, R., Isemer, H J., and Hasse, L, 1990: Towards time dependent calibration of historical wind observations at sea. *Trop. Ocean-Atmos. Newsletter*, Spring 1990, 7-12.

Lindzen, RS., and Nigam, S., 1987: On the role of sea surface temperature gradients i forcing low-level winds and convergence in the tropics. *J. Atmos. Sci.*, 44, 241 2436.

Neelin, J.D., 1989: On the interpretation of the Gill Model. *J. Atmos. Sci.*, 46, 2466-246

Philander, S.G., 1990: *El Niño, La Niña, and the Southern Oscillation.* Internation Geophysics Series, Vol. 46, Academic Press, San Diego, London, 293 pp.

Ward, M.N., 1992: Provisionally corrected surface wind data, worldwide ocea atmosphere surface fields and Sahelian rainfall variability. *J. Climate*, 5, 454-475.

Ward, M.N., 1994: Tropical North African rainfall and worldwide monthly to multi-decadal climate variations. PhD thesis, Reading University, pp 313.

WMO, 1990: International list of selected, supplementary, and auxiliary ships, (1990 edition -magnetic tape version) WMO-47, World Meteorological Organization, Geneva.

Woodruff, S.D., Slutz, RJ., Jenne, R L, and Steurer, P.M., 1987: A comprehensive ocean-atmosphere data set. *Bull. Amer. Meteor. Soc.*, 68, 1239-1250.

Figure 1: Raw observed (solid) and derived Balanced Friction Flow (dashed) seasonal zonal wind anomaly time-series. The smooth lines are fitted using a filter with 50% amplitude cut-off at about 6 years. The centre of the 10 x 10 box is indicated alongside the panel. Anomalies for each season are plotted.

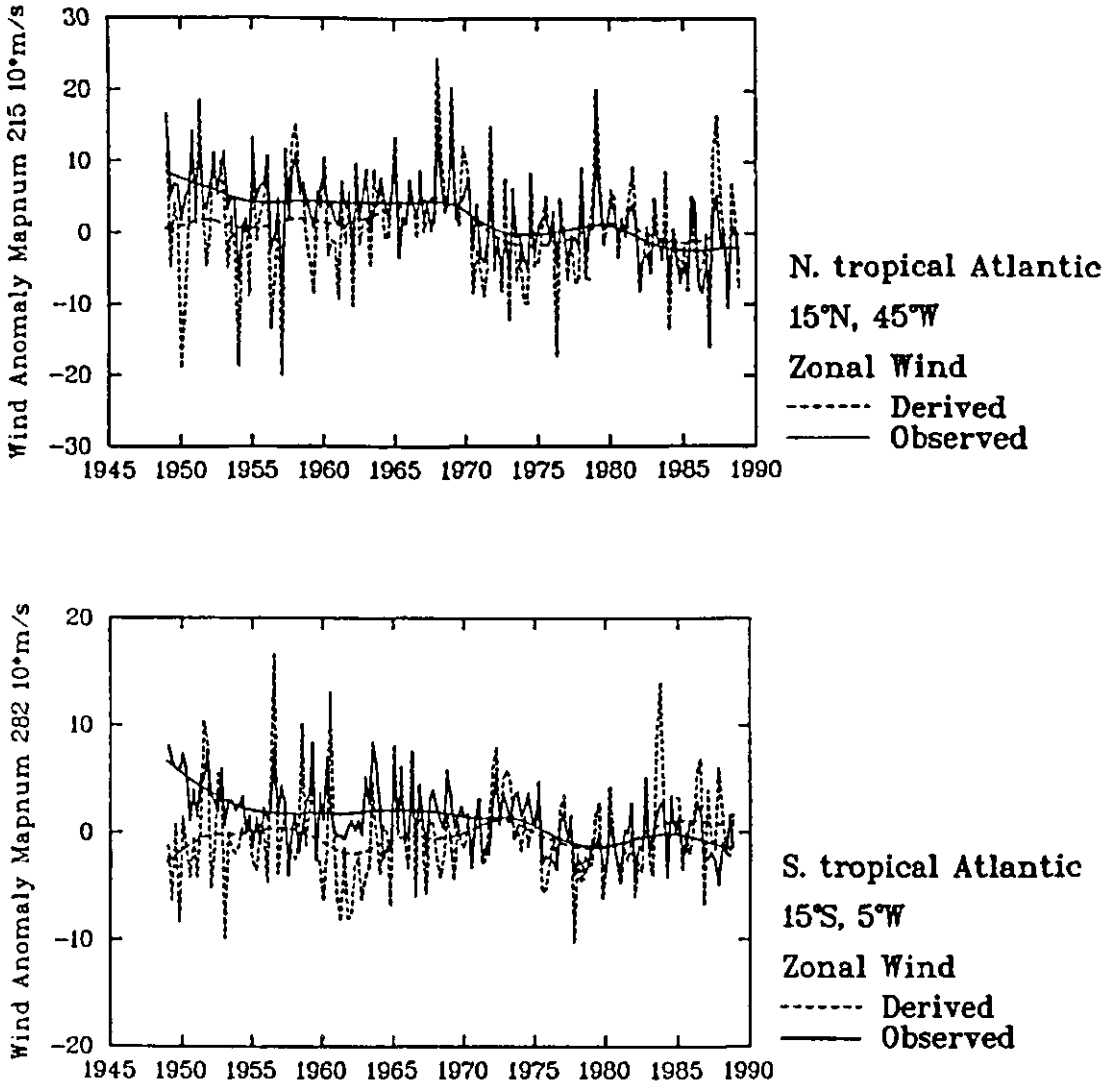

Figure 2a: Correlation (x100) over 1949-88 between time-series of observed wind and time-series of derived balanced friction flow (BFF) wind. Values >0.7 are shaded with dots, values <0.3 are cross-hatched. (a) u-wind in DJF. (b) v-wind in DJF. (c) u-wind in JAS. (d) v-wind in JAS.

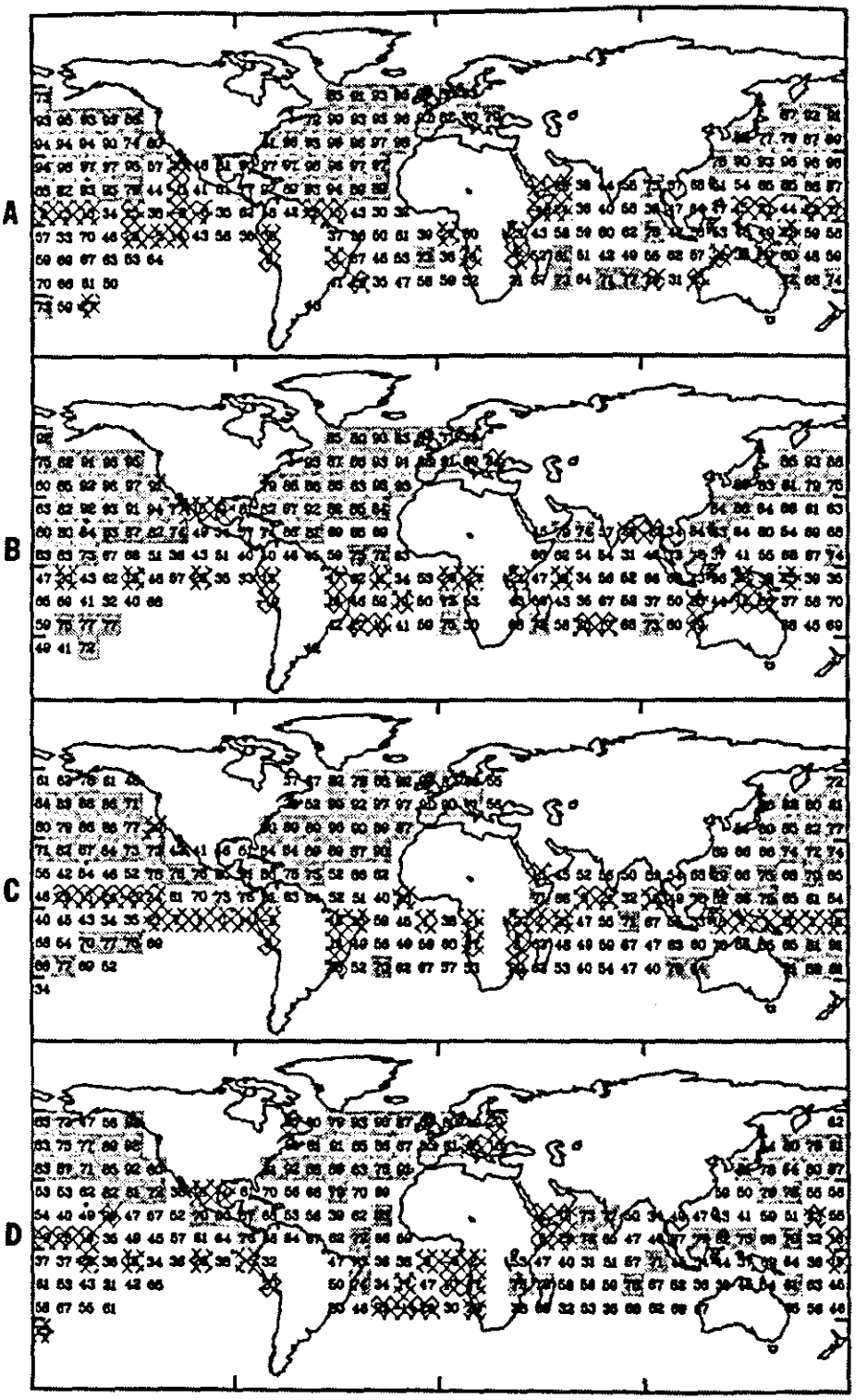

Figure 2b: Mean correlation as a function of latitude for BFF wind versus observed wind (solid) and geostrophic wind versus observed wind (dashed). Bottom panels show the number of correlations that were available for averaging at each latitude

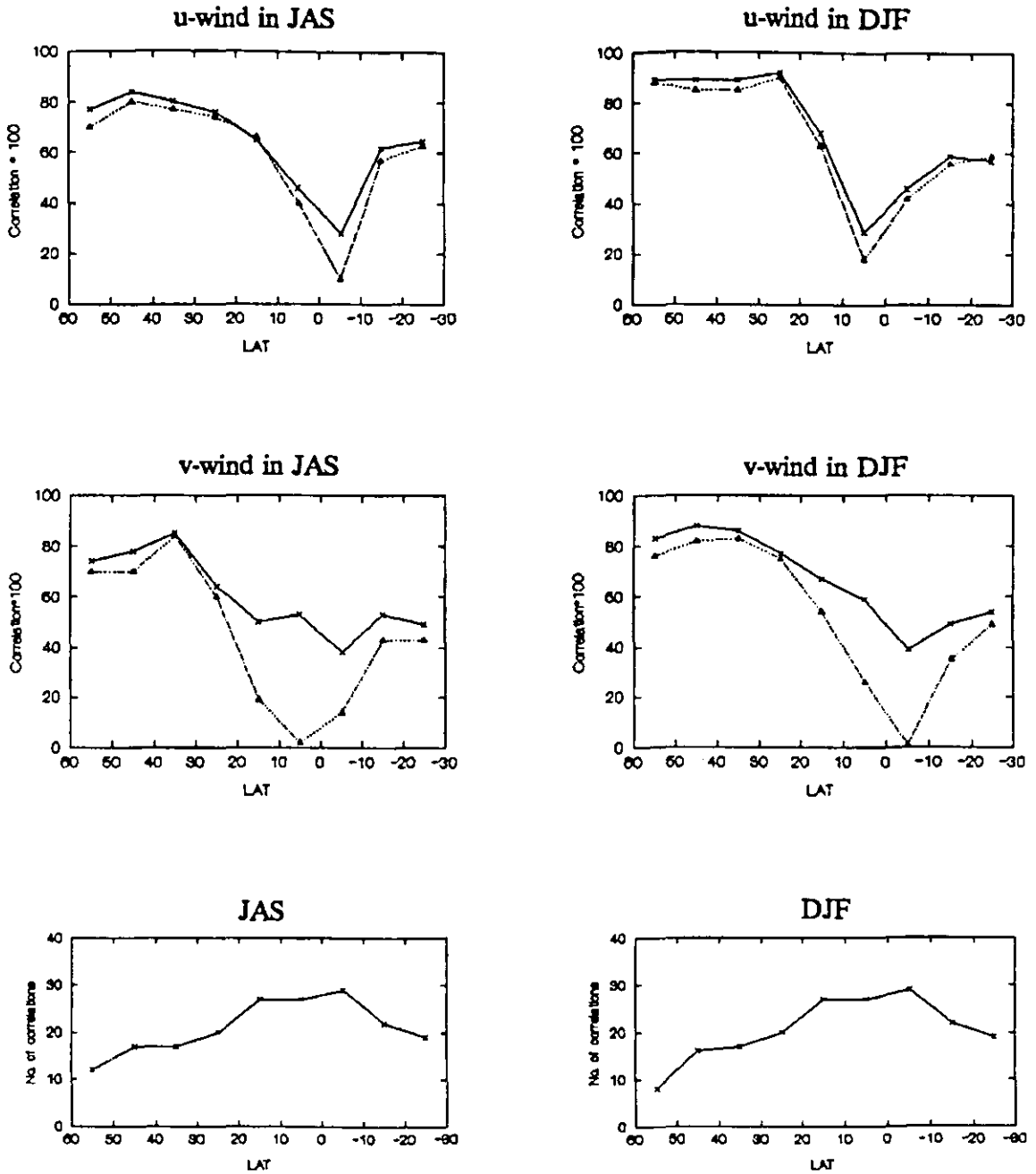

Figure 3: Mean standardised anomaly of zonal wind in each season 1949-88, for (i) reported wind, (ii) provisional corrected wind (version 1, based on Ward, 1992) and (iii) balanced friction flow wind. The value plotted for each season is the average of the standardized anomalies in all available 10 x 10 ocean boxes. The series shown effectively indicates the magnitude of the zonal wind vector, since all the contributing 10 x 10 series with a negative mean were multiplied by -1 prior to analysis, and all time- series with a mean close to zero were rejected (see text for more details).

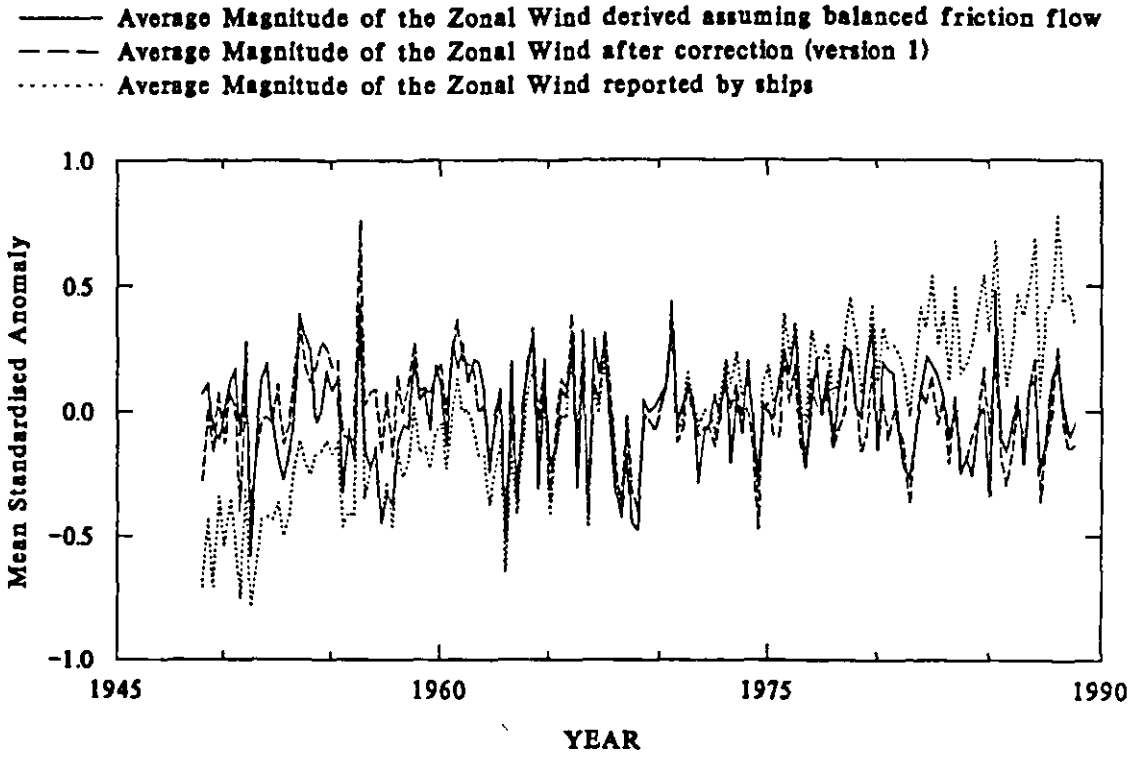

Figure 4: The difference between the increase in the magnitude of the observed wind and the increase in the magnitude of the balanced friction flow wind over 1949-1988, expressed as a percentage of the magnitude of the mean observed wind (the values are referred to as S in the text). Values shown were derived by averaging estimates of S based on u-wind and v-wind series for each of the four seasons. The values were then spatially smoothed.

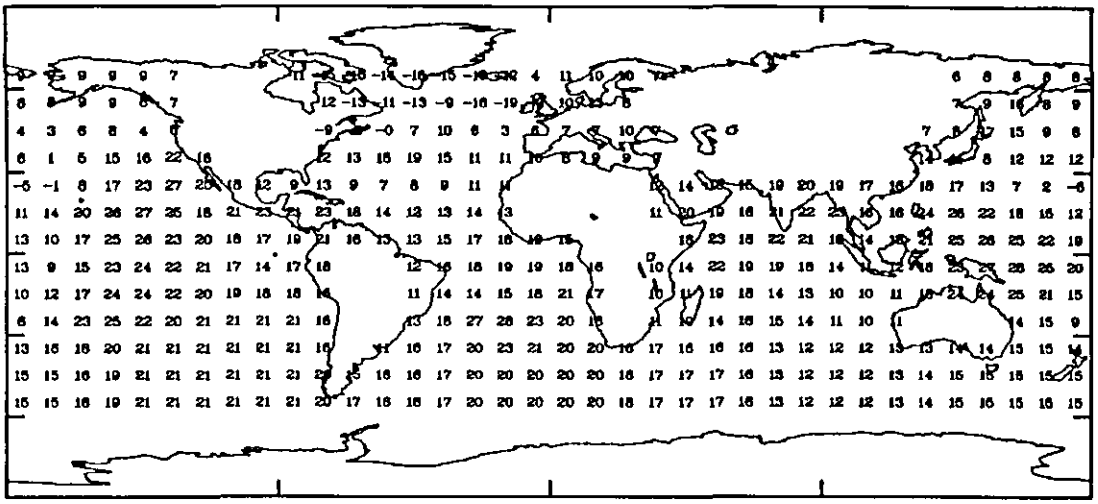

Figure 5a: Composite difference (1969-88 MINUS 1949-68) for July-September of the near-surface raw wind.

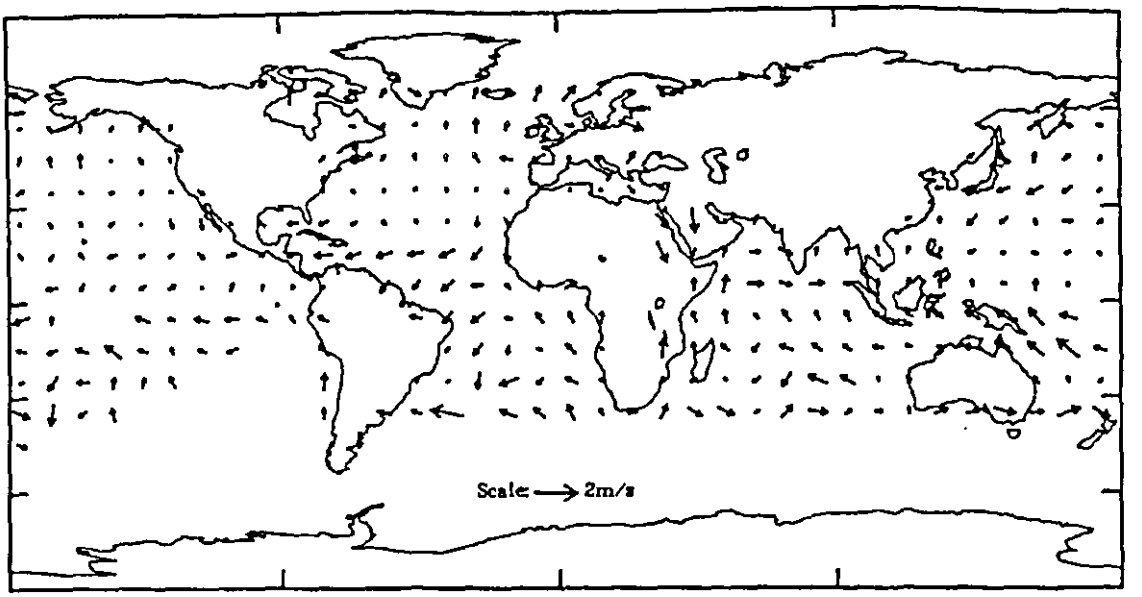

Figure 5b: Composite difference (1969-88 MINUS 1949-68) for July-September of the Corrected wind.

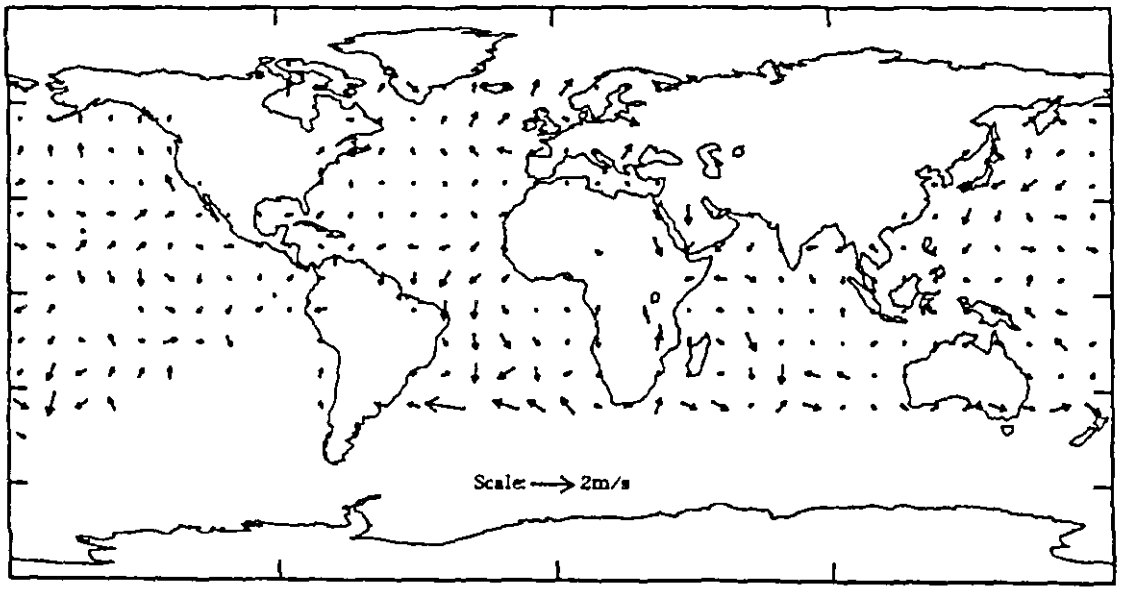

Figure 5c: Composite difference (1969-88 MINUS 1949-68) for July-September of Divergence ($10^{-8}s^{-1}$) of corrected wind.

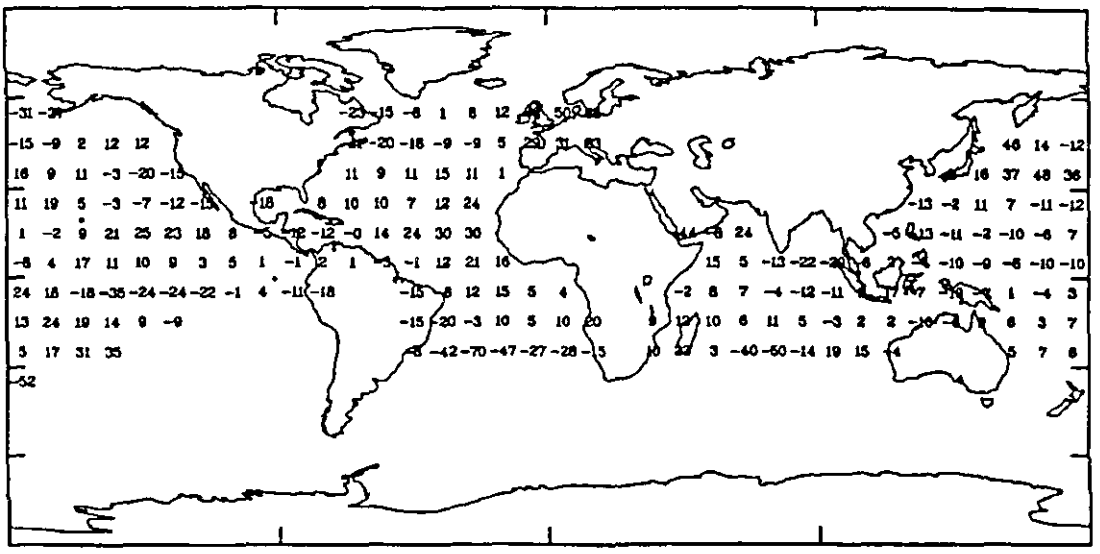

Figure 6a: First correlation EOF 1949-88 for 10 lat x 10 long JAS SST anomalies in the tropical central and western Pacific (28.6% of total variance).

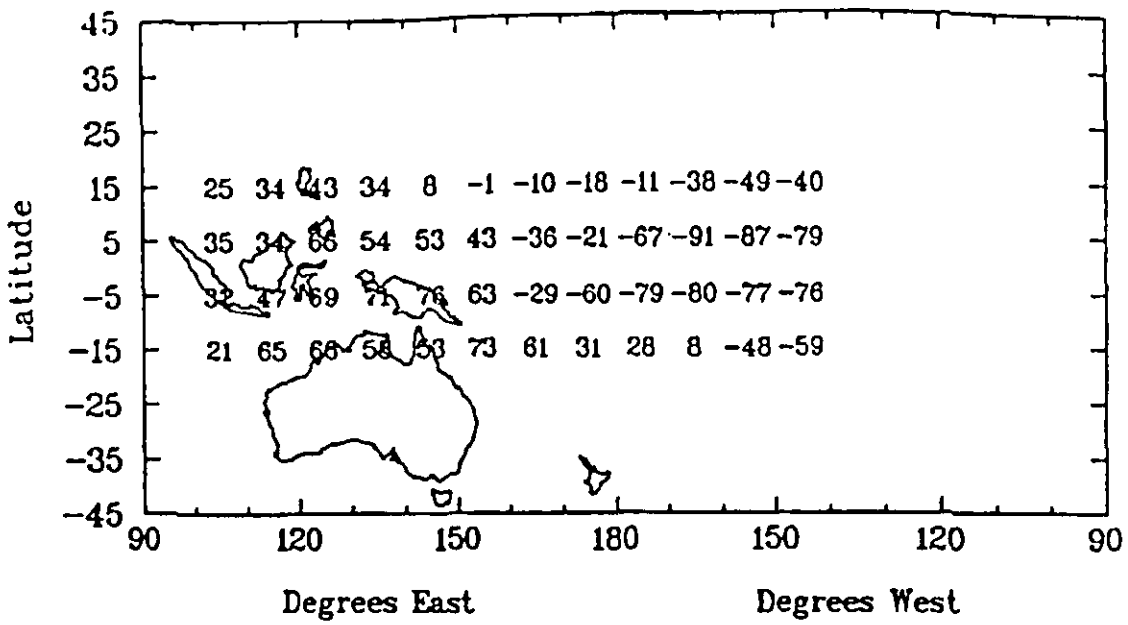

Figure 6b: Same as (a) but for 1904-90 (21.6% of total variance).

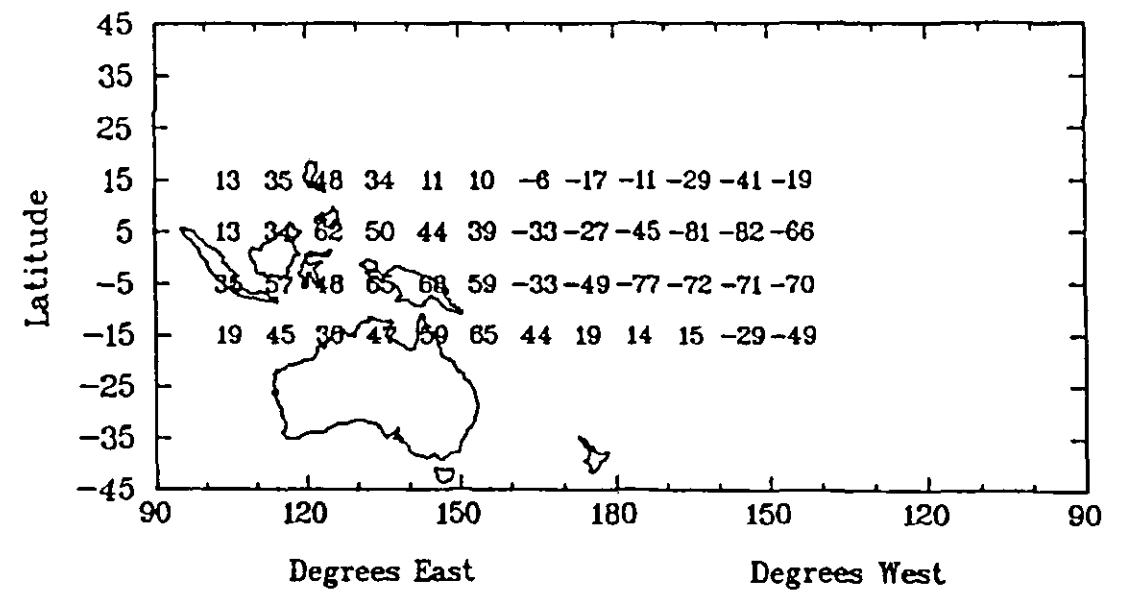

Figure 6c: Same as (a) but for near-surface divergence 1949-88 (35.2% of total variance). All series were high-pass filtered prior to analysis (passing timescales <11.25 years).

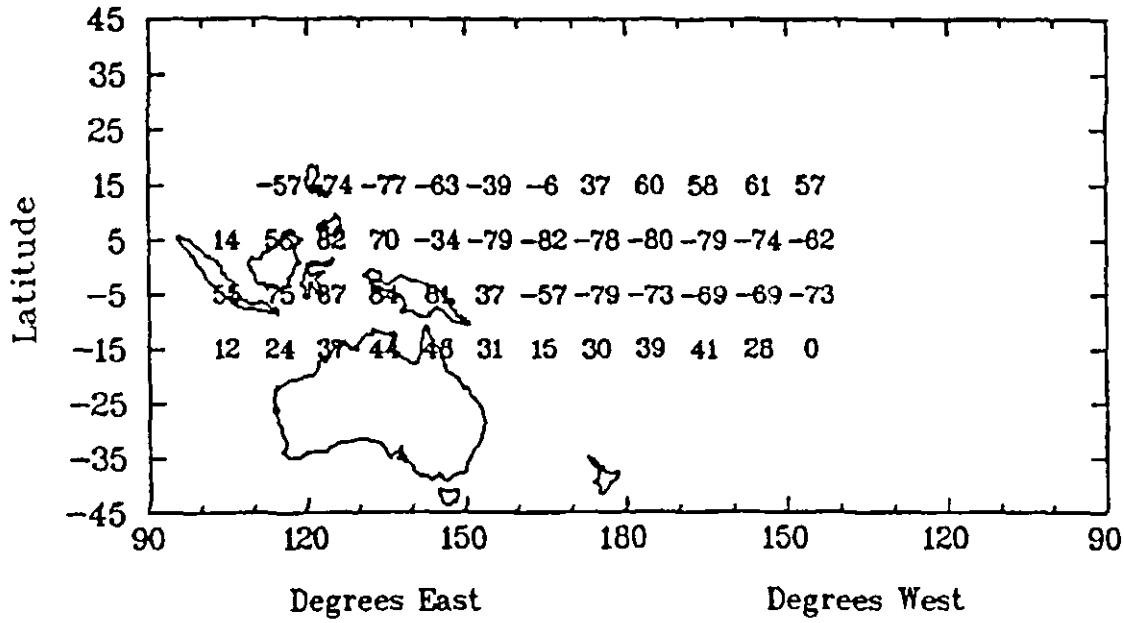

Figure 6d: Observed JAS time coefficients 1949-88 of tropical central and western Pacific SST EOF 1 in Fig. 6a (solid line with crosses) and near-surface divergence EOF 1 in Fig. 6c (dashed line).

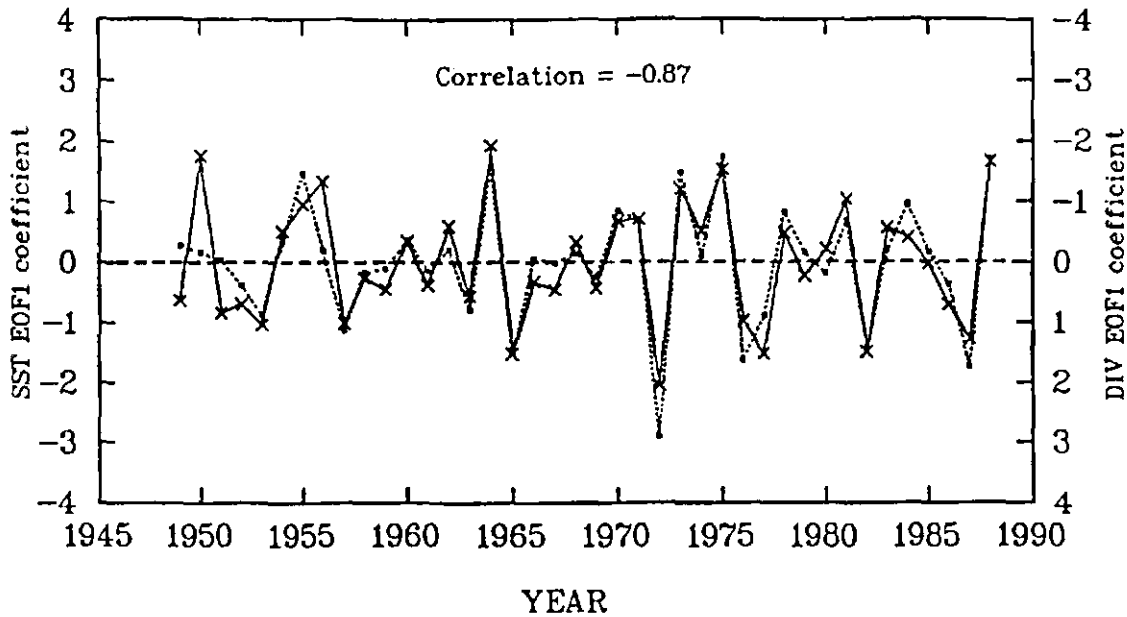

Part III

Accuracy of Wind Measurements

Comparison of COADS winds with SNMC climatology and measurements in the North Atlantic

Sergey R. Gulev

IORAS, Moscow, Russia / IFM, Kiel, Germany

Recent climatological studies often indicate problems with the reliability of COADS winds connected with a number of different and yet poorly understood reasons. During the last years there has been considerable debate about the matter of long-term wind speed trends indicated by COADS (Ramage 1984, Peterson and Hasse 1987, Cardone et al. 1990, Lindau et al. 1990, Isemer and Hasse 1991), ranging from 0.1 to 0.5 m/s per decade with local maximums in tropics and in Norwegian Sea (Isemer and Lindau 1994, Isemer 1993). Reliability of these trends is still a matter of debate due to a number of reasons. As a result, Isemer (1995, this volume) has made a detailed and thorough comparison of COADS winds with measurements at fixed Ocean Weather Stations (OWS) and he has concluded that COADS wind trends in the North Atlantic are in disagreement with those taken at the OWS. These differences may at least be significantly reduced after accurate application of the Beaufort scale and careful consideration of individual sampling statistics. Changes with time of the relative role of anemometer measurements are considered as one of the possible reasons of unrealistically high COADS wind trends. This work discusses the use of additional independent data for the validation of COADS winds.

COADS has been used in the form of Monthly Summary Trimmed Groups (MSTG) taken from COADS Release 1 (Slutz et al. 1985). Monthly means of meteorological variables for 2^{o} x 2^{o} boxes for the North Atlantic Ocean were extracted from original COADS files during the period from 1950 to 1979. We also used COADS Release 1a which covers the period from 1980 to 1992. In order to compare COADS climatology with another one we used a completely different climatological data set, produced on the basis of individual marine reports by another community with the use of slightly different techniques of data processing. This second data set has been prepared during the last several years by the former Soviet National Meteorological Center (hereafter SNMC) on the basis of individual marine reports for the period from 1957 to 1990 (Birman, et al. 1980 Birman et al. 1992). The source of original information appears to be close to those used in COADS. For the period from 1957 to 1969 this data set is based on updated archives of meteorological observations. Since 1970 original reports transmitted by voluntary observing fleet via radio are collected at SNMC. Actually the first release of this data set has been prepared in 1977 for the period from 1957 to 1971 with the extension until 1974 in 1980 (Birman et al. 1980). In 1992 a second data release became available (Birman et al. 1992). When second release has been created all data set was updated in order to use universal technique of data control and averaging. SNMC data

set is organized in the form of monthly means and standard deviation of variables for 5° by 5° boxes over the North Atlantic from the equator to 75° N. Original reports were averaged for every box for the point with so-called "monthly mean coordinates" and then monthly means were re-interpolated to the centers of boxes. This data set contains in contrast with COADS two levels of cloudiness but does not include so-called derive l variables (sea-air temperature and humidity differences and their products with wi d speed) which are available from COADS MSTG. Comparison of the number of repo used in SNMC data set with those for COADS gives in general from 15 to 25 perce smaller values. At the same time, for about 20 percent of 10° x 10° boxes, which a mostly connected with the location of operational activity of former soviet scientif military and fishery fleets, the number of observations in SNMC data set is actual higher than in COADS. These boxes are mostly located around Norway and Greenla seas, North-West Atlantic and Tropical-East Atlantic. Data control procedures and t details of data processing and averaging are described in Birman et al. (1980, 1992). Figu 1 shows differences between zonal climatological seasonal cycle and annual means o scalar wind speed taken from COADS and SNHC data set for the period 1957-197 (overlapping of two data sets). For scalar wind speed we found overestimation o COADS wind in relation to SNMC in the North-West Atlantic and high latitudes and higher SNMC winds in tropics and subtropics. The highest positive differences between SNMC and COADS winds are obtained in subtropical region and ranging from 0.3 to 0.6 m/s. Note that both COADS and SNMC data set used WMO (1970) Beaufort scale. Isemer and Hasse (1985, 1987) using Kaufeld (1981) correction of Beaufort scale obtained 2 m/s increases of climatological means in subtropics on the basis of Bunker's data set. Recently Isemer and Lindau (personal communication) found these values to be too high. Calculations of wind trends from SNHC data set give trends which are approximately 50% lower than those obtained from COADS. Moreover, SNMC data set indicates considerable area in mid latitudes with negative or insignificant trends.

For comparisons with instrumental observations we also used COADS Release la as well as original COADS compressed marine reports (CMR) within some of the 10° x 10° boxes, located in the North-West Atlantic and data from the field experiments, taken for the period 1981-1991 under "SECTIONS" program. These data are taken continuous for the period of 10 years, if only within limited area (Lappo et al., 1989; Gulev et al., 1991, Gulev, 1994). all data were collected by six sister ships by professional meteorological teams. These are the same ships, which operated at OWS C from 1975 to 1990 (Isemer, 1993). Wind data consist exclusively of anemometer measurements. Anemometer level varied within the range from 26.6 meters to 27.6 meters. Temporal resolution is usually 3 hours, but for some cruises 1 hourly sampled data are available. Total number of cruises is 89, total number of reports is 46,800. The most interesting time series were obtained during NEUFOUEX-88 (Lappo et al., 1989) and ATLANTEX-90 (Gulev et al., 1991) experiments. Both of these experiments, as well as the earlier experiment NEWFOUEX-84, were designed to study air-sea interaction processes in the Newfoundland basin during the periods from November 1987 until April 1988 and from December 1989 till May 1990 respectively. Ships, balloons, buoys and moorings were used to measure the atmospheric and oceanic structures and properties. Although the measurement program was designed primarily for the region 40°-48°N, 40°-48°W, voluntary meteorological observations were collected for a larger area. Figure 2 compares

the number of instrumental measurements with the number of reports, indicated in COADS Release 1a for each calendar month. Most of instrumental data were collected during winter and spring, when the number of instrumental observations is from 35 to 55 % of total COADS reports. It is difficult to check precisely how many of these data were included in COADS Release 1a, but approximate estimate is not higher than 20 to 25 %.

In order to compare these data with COADS Release 1a climatology, all wind speed reports were averaged for individual months within 2° x 2° boxes, i.e.. we made the same processing, as has been used to create COADS. Thus wind speed values were obtained for 2° x 2° boxes within the area 36°N - 56°N, 36°W - 56°W. Instrumental measurements indicate generally smaller wind speed within the range from 2 to 10 m/s and slightly higher values for strong winds. Thus, the angle of regression line is always smaller than 45 degrees (Figure 3). In order to adjust instrumental measurements to COADS collection two procedures were followed. First, we can adjust all wind measurements to another anemometer reference level. This procedure changes the angle of the regression line but is not sufficient to adjust the fit to 45 degrees, even for such a small level as 5 meter which is clearly an underestimate of the mean height of anemometers in COADS collection. We also tried to take into account only those 2° x 2° boxes, which contain relatively high number of reports. Note here, that Weare and Strub (1981) found eleven observations to be needed for approximately unbiased intra monthly averaging. This procedure also increases the angle of the regression line, but again, not very much. Results of the use of these two procedures are presented in Figure 4. If we take anemometer reference level of about 10 meters, and minimum monthly number of reports of 24, we obtain a regression of 0.7±0.02. Mean wind speed is from 0.3 to 0.8 m/s higher in COADS compared with instrumental measurements, adjusted to 10 meters anemometer level. Probability density functions, calculated from COADS/CMR collection for the period 1980-1989 for the same area indicate for most of the months a higher percentage of observations with smaller wind speed, and therefore bias of modal value.

For the consideration of seasonal cycle, we chose four 4° x 4° boxes with relatively high number of instrumental observations for every month. These boxes are located within the area 40-48°N, 40-48°W. Figure 5 shows an example of this comparison for 4-degree box number 3 (40-44°N, 40-44°W). If we consider unadjusted measurements, we can point out that COADS wind speed is higher during spring and summer, winter values are very close to each other in both data sets, although instrumental measurements slightly over predict COADS, and during autumn, instrumental measurements give higher values in compare with COADS. After adjustment of 10 meters anemometer reference level, instrumental measurements indicate significantly smaller winds for August, September and October only. During winter and spring COADS wind speed is from 0.7 to 1.3 m/s higher, and differences for November and December under predict the accuracy of sampling and intra-box averaging. Harmonic analyses of the curves in Figure 5 indicate negative phase lag of about 12 days of COADS wind speed compared with research vessels measurements.

We considered also intra monthly high-order statistics from COADS Release 1a and research vessels collection for 1981-1991. Some recent studies (Zorita et al., 1992, von Storch et al., 1993) use such statistics as an important indicator of climate changes.

For this consideration only boxes with the number of reports higher than 24 per month were chosen. COADS standard deviations are higher than those taken from research vessels collected during all months, and for most boxes. Typical difference is about 1 m/s, and appears to be considerable. We can note here, that our collection of instrumental measurements include 1 hourly and 3-hourly sampled data. Typical temporal resolution for voluntary observing ship reports in COADS is 6 hours. Thus instrumental measurements describe also dispersion of subsynoptic scale within the range of several hours. So, we expected even higher standard deviation of instrumental measurements compared with COADS. We repeated calculations of intra-monthly intra-box standard deviation with only those observations of research vessels, which are sampled on 00, 06, 12, and 1800 GMT. Results show a decrease in standard deviation of about 0.2 - 0.4 m/s. So, we can point out, that the higher standard deviation of wind speed from COADS, perhaps has another source, which is different from natural variability, and connected with higher random error of COADS winds.

As has been mentioned earlier, interannual variability of wind speed, and especially its long term changes, is the key question of the reliability of COADS winds. It is rather difficult to use our collection of research vessels measurements for the comparison with interannual variations of COADS winds, due to the fact that even for the area with very high density of observations, not every month is complete with data. Nevertheless, we took some effort to check interannual variations, if only for a number of months, provided with relatively high number of measurements. Again, as before we took the same four 4^{o} x 4^{o} boxes for our comparison. The main problem is that even for those individual months, when research vessels worked in this area, not each 2^{o} x 2^{o} box within every 4^{o} x 4^{o} box has data, or has enough of them to calculate monthly means. So, we first calculated 2^{o} x 2^{o} monthly means for those boxes were it was possible. Then for each of these individual months the procedure of optimal interpolation has been made to obtain monthly means for those 2^{o} x 2^{o} boxes, which are not complete with measurements. Of course, even after this procedure, we couldn't generate values for those months, when there was not one research vessel in the Newfoundland region. Then we removed from COADS Release 1a values for those boxes, which were missing from our collection of instrumental measurements. In this way we obtained another version of COADS for this particular area, which is of the same quality (in terms of data coverage), as research vessels data set. After that for this new version of COADS, the same procedure of optimal interpolation was applied. COADS indicates positive wind speed changes for most of the individual months, and most of the boxes. Upward trends are ranging from 0.3 to 0.9 m/s per decade. This is in agreement with the results of Diaz et al, (1995), this volume. Downward trends are obtained only for August. Re-interpolated version of COADS in 95% of cases supports with confidence these tendencies. On the other hand, data from a selected number of research vessels do not indicate any significant trends for any month, except in December. Figure 6 gives remarkable examples of this disagreement for May. So we can point out that positive wind trends in COADS Release 1a are not supported by the homogeneous data of research vessels. Isemer (1995, this volume) comes to the same conclusion, comparing COADS Release 1a with OWS data.

It is interesting also to make a separate comparison for only those months and 2-degree boxes, which are very complete with data from research vessels. Most of these

data were collected during special boundary layer experiments, carried out mostly during winter and spring of 1984, 1985, 1987, 1988 and 1990. Table 1 shows that the number of reports for certain boxes during these months sometimes is considerably higher in our research vessels collection, than in COADS Release 1a. On the other hand,, we have to note that monthly means in COADS for these months are mostly determined by the contribution from research vessels. So, we shouldn't expect very remarkable differences. Nevertheless, even these 14 cases indicate higher wind speed from COADS in comparison with original sampled data and in comparison with wind, adjusted to a 10 meter level. Standard deviation, taken from COADS release 1a are also higher, although the difference here is not so remarkable, for the whole data set (4.5 m/s and 4.8 m/s respectively for research vessels and COADS).

References

Birman, B.A., E.V. Balashova, D.A. Larin, and T.G. Pozdniakova, 1980: Monthly means of hydrometeorological parameters in the North Atlantic. Vol. 1-5, SMNC/VNIIGMI, Obninsk, 112 pp.

Birman, B.A., and T.G. Pozdniakova, 1985: Climatological parameters for the North Atlantic Ocean. SNMC, Moscow, 84 pp.

Birman, B.A., E.V. Balashova, D.A. Larin, and T.G. Pozdniakova, 1992: Monthly means of hydrometeorological parameters in the North Atlantic 1957-1990. Hydrometeorological Center of Russia, Moscow, 132 pp.

Cardone, J.S., J.G. Greenwood and M.A. Cane. 1990: On trends in historical marine wind data. *J.Climate*, 3, 113-127.

Folland, C.K., T.R. Karl, N. Nicholls, B.S. Nyenzi, D.E. Parker, and R.Y. Viinikov, 1992: Observed climate variability and change. In: Climate Change 1992. Cambridge University Press, 137-170.

Gulev, S.R., 1994: Influence of space-time averaging on the ocean-atmosphere exchange estimates in the North Atlantic mid-latitudes. *J. Phys. Oceanogr.*, in press.

Gulev, S.R., A.Y. Ivanov, A.V. Kolinko, S.S. Lappo and E.G. Morozov, 1991: The ATLANTEX-90 experiment. Meteorology and Hydrology, n.5, 54-70.

Isemer, H.-J., 1993: On the homogeneity of surface wind speed records from Ocean weather stations. Tech. Rep. Institute fur Meereskunde, Kiel, 89 pp.

Isemer, H.-J. and L. Hasse, 1991: The Scientific Beaufort Eauivalent Scale: Effects on Wind Statistics and Climatological Air-Sea Flux Estimates in the North Atlantic.

Isemer, H.-J. and L. Hasse, 1985: The Bunker Climate Atlas of the North Atlantic Ocean. Vol. 1: Observations. Springer Verlag, 218 pp.

Isemer, H.-J. and L. Hasse, 1987: The Bunker Climate Atlas of the North Atlantic Ocean. Vol. 2: Air-sea interactions. Springer Verlag, 252 pp.

Isemer, H.-J. and R. Lindau, 1994: On the homogeneity of surface wind speed records from Ocean Weather Stations. J. Atmos. Ocean. Techn., submitted.

Kaufeld, L., 1981: The development of a new Beaufort equivalent scale. Meteor. Rundsch., 34, 17-23.

Lappo, S.S., R.V. Ozmidov, Y.A. Volkov, S.K. Gulev, A.V. Kolinko, S.P. Malevsky, 1989: the SECTIONS-NEWFOUEX-88 experiment. Meteorology and Hydrology, n.9, 67-77

Lindau, R., H.-J. Isomer and L. Hasse, 1990: Towards time-dependent calibration of historical wind observations at sea. Trop. Ocean-Atmos. Newslett., 54, 7-12.

Peterson, E.W., and L. Hasse, 1987: Did the Beaufort scale or the wind climate change? *J. Phys. Oceanogr.*, 17, 1071-1074.

Ramage, C.S., 1984: Can shipboard measurements reveal secular changes in tropical Air-Sea heat flux? *J. Climate Appl. Met.*, 23, 187-193.

Slutz, R.J., S.J. Lubker, J.D. Hiscox, S.D. Woodruff, R.L. Jenne, D.H. Joseph, P.M. Steurer, and J.D. Elms, 1985: Comprehensive Ocean-Atmosphere Data Set: Release 1. NOAA Envir. Res. Lab., CRP, Boulder, CO, 268 pp.

von Storch, H., J. Guddal, K.A. Iden, T. Jonsson, J. Perlwitz, M. Reistad, J.de Ronde, H. Schmidt, and E. Zorita, 1993: Changing statistics of storms in the North Atlantic. Max-Planck Inst. Met., Rep. No. 116, Hamburg, 19 pp.

Weare, B.C., and P.T. Strub, 1981: The significance of sampling biases on calculated monthly mean oceanic surface heat fluxes. *Tellus*, 33, 211-224

WMO, 1970: Reports on Marine Science Affairs. Rep. No. 3: The Beaufort scale of wind force. 22 pp.

Zorita, E., V. Kharin, and H. von Storch, 1992: The atmospheric circulation and sea surface temperature in the North Atlantic area in winter: Their interaction and relevance for Iberian precipitation., *J. Climate*, 5, 1097-1108

Table 1: Comparison of 2° x 2° monthly mean wind speed from COADS and research vessels measurements for some complete months.

NN	Month /year	number of reports (RV)	number of reports (COADS)	mean V (RV)	mean V_{adj} (RV)	mean V (COADS)	std (RV)	std (COADS)
1	1/84	78	167	11.5	10.0	11.1	3.6	4.2
2	11/85	187	74	12.1	11.0	12.8	4.2	4.4
3	12/85	240	142	12.9	11.8	12.0	5.6	5.5
4	3/86	131	143	12.9	11.6	13.2	5.1	5.4
5	2/87	84	49	10.2	8.9	12.3	4.1	6.0
6	3/87	490	69	12.8	11.6	13.3	5.2	5.1
7	3/88	455	143	11.2	9.8	10.4	4.9	4.9
8	3/88	489	148	12.4	11.2	11.6	5.1	5.4
9	3/88	107	75	9.5	8.6	12.2	4.8	4.0
10	3/88	530	539	12.9	11.6	12.5	5.2	5.7
11	4/90	399	93	8.2	7.0	8.6	4.0	4.4
12	4/90	338	82	10.7	9.6	10.8	4.0	3.9
13	4/90	470	143	8.3	7.5	8.6	3.2	3.8
14	10/90	208	45	11.7	10.7	9.9	4.0	3.8
mean		300	146	11.2	10.1	11.4	4.5	4.8

Figure 1: Comparison of zonal average seasonal cycle and zonal annual mean from COADS and SNMC climatologies.

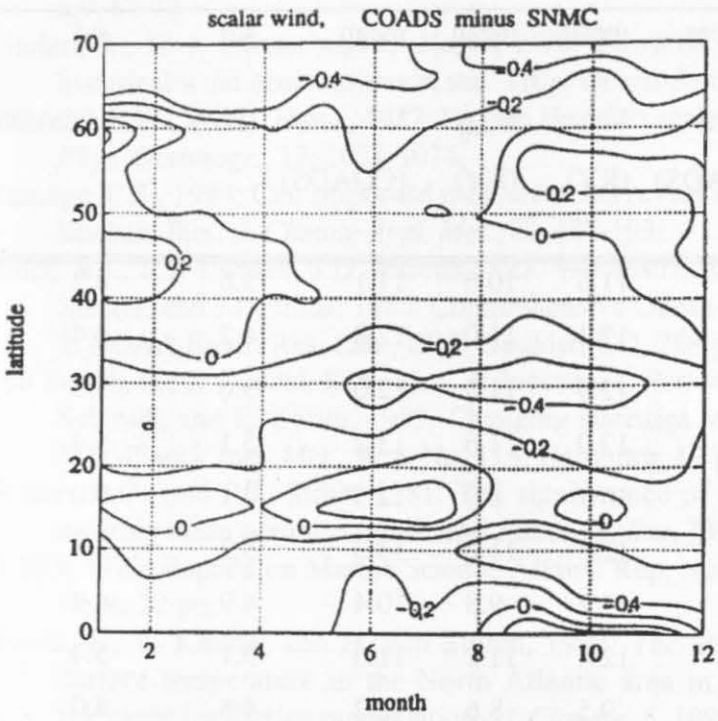

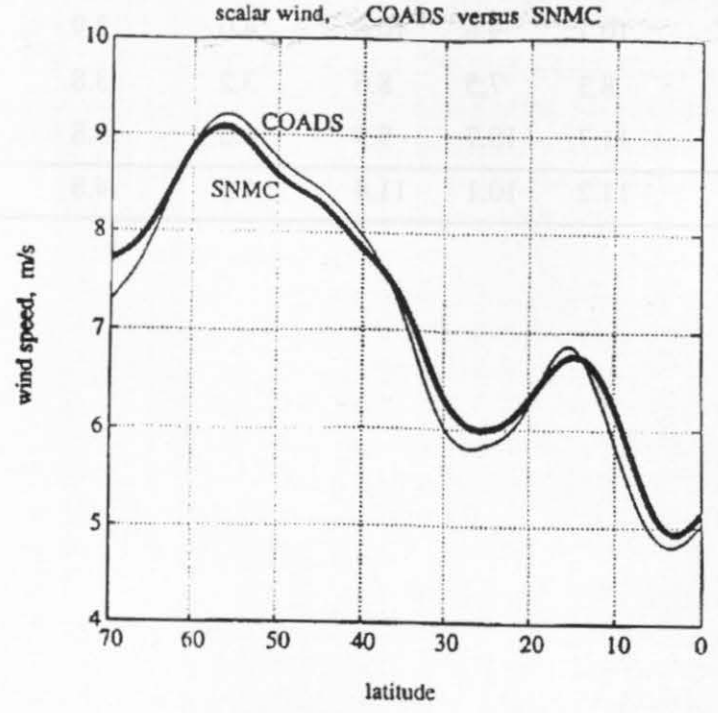

Figure 2: Seasonal distribution of the number of observations in COADS (white area) and in research vessels collection (black area).

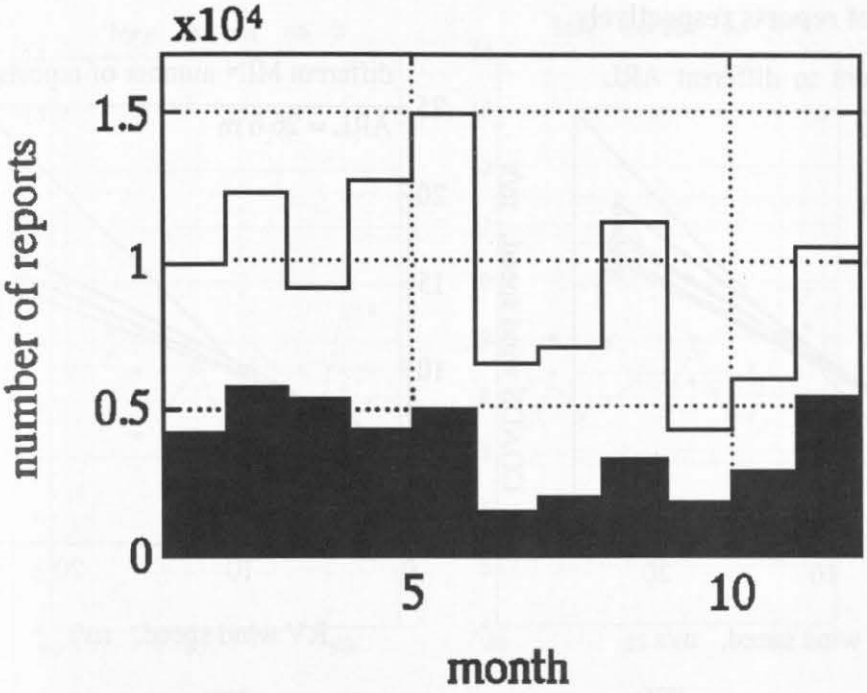

Figure 3: Comparison of COADS monthly mean for 2° by 2° boxes with research vessels monthly means for the period 1981-1991.

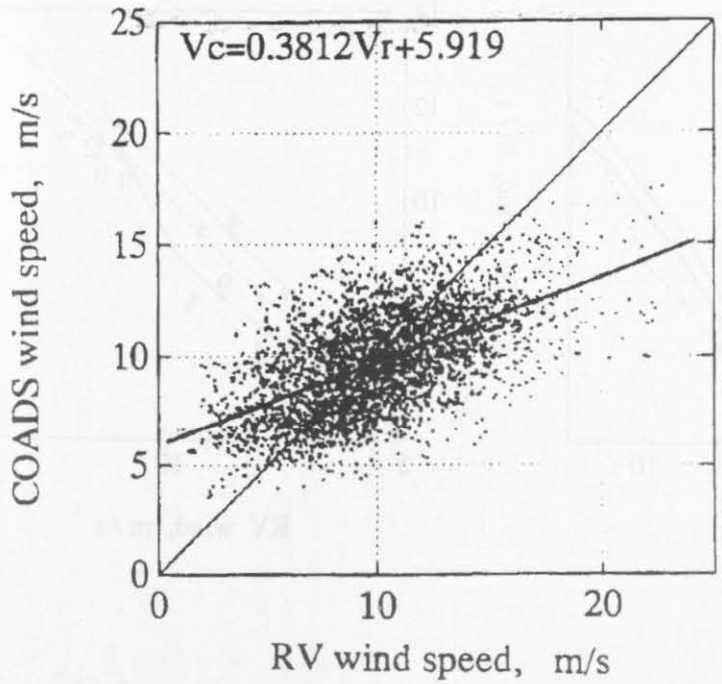

Figure 4: Dependence of regression line between COADS and research vessels wind speed on the anemometer reference level (left panel) and the minimum number of research vessels reports (right panel). Numbers indicate anemometer level and minimum number of reports respectively.

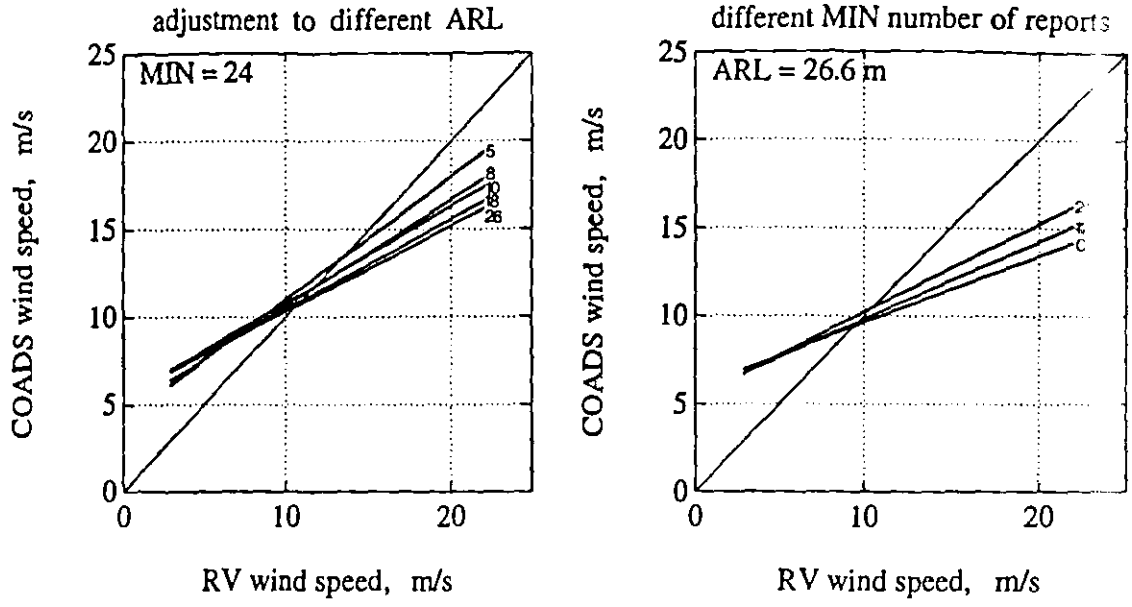

Figure 5: Seasonal march of wind speed, taken from COADS (dashed line) and from research vessels collection before (thin line) and after (bold line) adjustment ot 10 meters anemometer level.

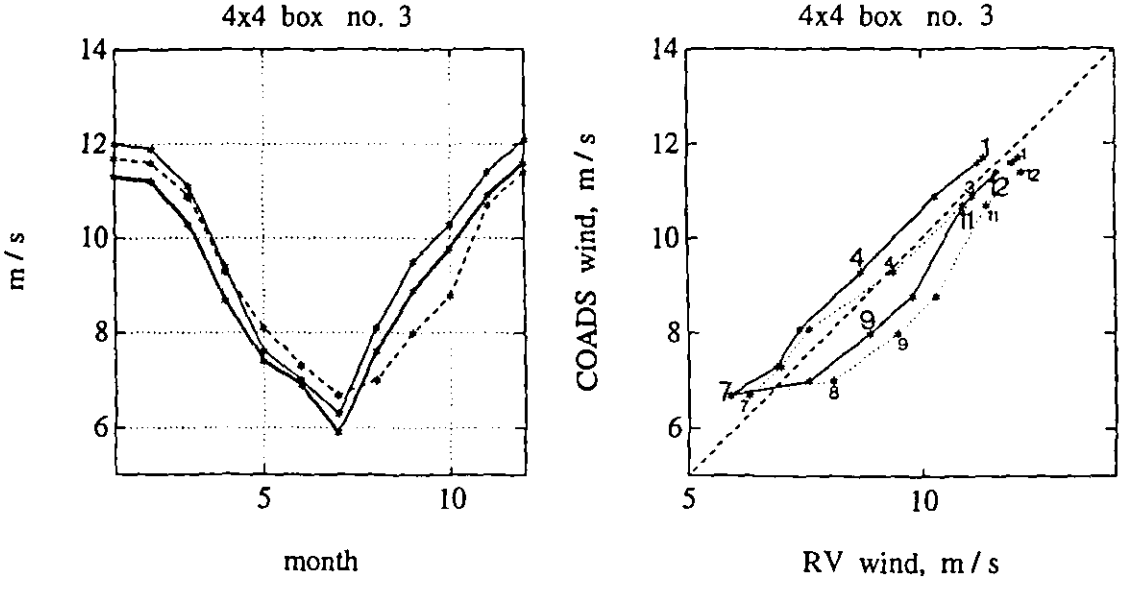

Figure 6: Interannual variability of May values of wind speed, taken from original COADS (dashed line), COADS, adjusted to research vessels data coverage (crosses), and from research vessels collection (black points).

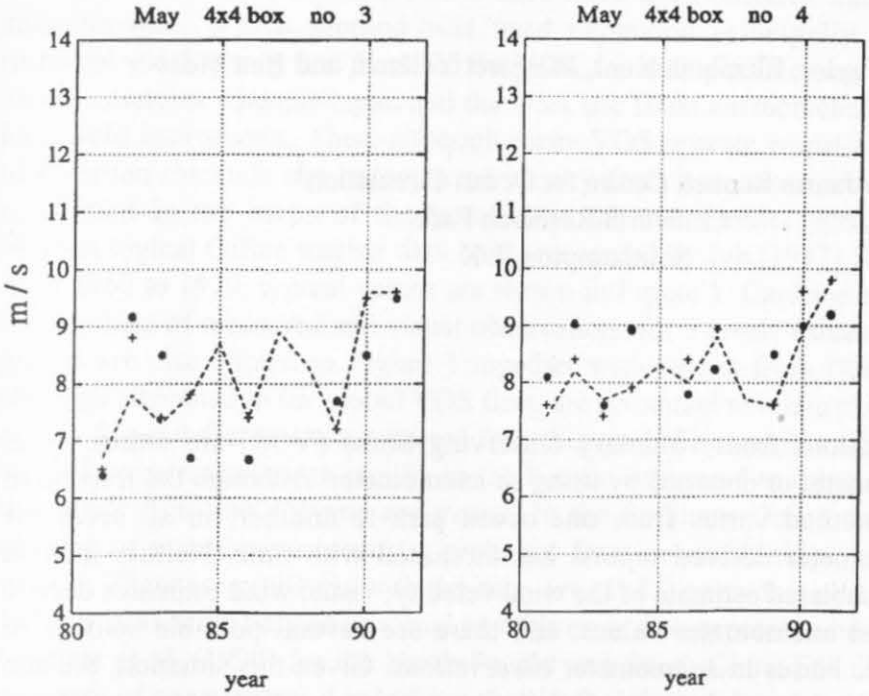

The Accuracy of Wind Observations from Ships

Peter K Taylor, Elizabeth Kent, Margaret Yelland, and Ben Moat

James Rennell Centre for Ocean Circulation[1]
Chilworth Research Park
Southampton, UK

Introduction

Wind observations from voluntary Observing Ships (VOS) are either visual "Beaufort Scale" estimates or obtained by using an anemometer. Although the fraction of reports from each method varies from one ocean area to another, in all areas the percentage of anemometer derived reports has increased with time. Neither method necessarily gives an unbiased estimate of the wind velocity; visual wind estimates depend on calibration against anemometer values, and there are several possible sources of significant, systematic biases in anemometer observations. Given this situation, the aim must be to produce a consistent data set of wind observations in which anemometer and visual derived observations give rise to the same wind speed distributions. Such a data set should eliminate spurious "climatic" trends such as an apparent wind speed increase due to the increased use of anemometers (e.g. Cardone et al. 1990).

In this paper we will present the results of work at the James Rennell Centre on the accuracy of ship winds, occasionally reviewing other work which, having been published in reports, may not be readily available. Considering sampling issues, we shall briefly review evidence on the percentage mix of visual and anemometer winds and comment with regard to the possibility of "fair weather bias" in the VOS wind observations. Since Ocean Weather Ships have frequently been used to verify VOS wind estimates we shall report our results from Ocean Weather Station Lima. Results from the VOS Special Observing Programme - North Atlantic (VSOP-NA) will be used to compare visual winds (corrected to various Beaufort Scales) to observations from ships equipped with anemometers. We will then discuss the accuracy of anemometer wind estimates from ships.

Sampling Issues

Percentage of visual and anemometer winds

---

[1]The James Rennell Centre is a component of the Institute of Oceanographic Sciences Deacon Laboratory

Although it is known to contain inaccuracies, Kent et al. (1993) used the List of Selected Ships (WMO, 1990) to estimate that, at about that time, 70% of the global VOS fleet provided visual estimates, 22% used fixed anemometers, and 8% used hand-held anemometers. Which method was used depended principally on which country's meteorological agency had recruited the VOS, for example Germany and the UK advocate visual estimates whereas Japan and the USA use fixed anemometers and France supplies hand-held instruments. Thus, although many VOS operate world-wide, the mix of wind observation methods can be expected to vary from one ocean area to another. This is confirmed in the maps of the percentage of anemometer wind reports in the UK Meteorological Office marine data bank, presented by Ive (1987) for each 5 year period from 1960 to 1979; typical values are shown in Figure 1. Cardone et al. (1990) also give the numbers of measured and visual observations for 3 areas, values estimated from their graphs are also shown in Figure 1 together with values from (Ramage, 1987) which, although attributed to the global VOS fleet, are presumed to relate to the South China Sea.

Several features are apparent from Figure 1. The number of anemometer derived winds has increased more rapidly in the Pacific compared to other ocean areas. Most of the winds from the Atlantic are visual. In the Southern Ocean there are a significant number of anemometer reports, probably from research ships and Antarctic supply vessels. There are problems with the data. Ive (1987) notes that all USA VOS reports for 1975 to 1981 were flagged as visual and this error also appears to be evident in the data of Cardone et al. (1990) for the North Pacific and South China Sea. The rapid increase in numbers of anemometer winds from the North Atlantic shown by the latter authors also looks suspicious compared to the previous trends.

Figure 1 clearly shows that, unless visual and anemometer winds can be shown to be equivalent, there is the potential for introducing spurious spatial and temporal variations in the calculated wind climate.

Sampling by merchant ships - fair weather bias

The possible existence of fair weather bias must be considered when evaluating visual winds. For example if a Beaufort conversion scale has been derived by comparison of weather ship anemometer and VOS visual wind speed distributions, any fair-weather bias may have been effectively removed from the visual data. Kent and Taylor (1994) noted that the VSOP-NA data set contained fewer observations at high latitudes during the winter months. However this need not have resulted in a bias provided that those observations which were available were randomly distributed with respect to the weather conditions. They tested this possibility by comparing two distributions of wind reports to determine whether the VOS sampled the wind climate at ocean station LIMA (57°N 20°W) in the same way as the weather ship CUMULUS which occupies that station. The first distribution was the full set of wind speeds reported by the OWS CUMULUS. The second distribution was the subset of OWS CUMULUS wind speed reports corresponding to times at which there was a VOS meteorological observation from the 5° by 5° area surrounding LIMA. If more than one VOS report had been received at the same time, the CUMULUS report was included in the distribution the appropriate number of

times. Figure 2 shows the resulting distributions of wind speed occurrences. Using a χ^2-test the data sets were found to be the same to within 97.5% confidence limits.

Kent and Taylor (1994) therefore concluded that there did not appear to be a significant re-routing of ships during periods of high wind speed in the area around LIMA. Presumably those VSOP-NA ships which traveled further south in winter did so because it was winter rather than because it was rough at the time of their voyage; those that traveled north did so whatever the weather.

Accuracy of Ocean Weather Ship Wind Reports

Background

Wind reports from Ocean Weather Ships have been used for comparison with VOS wind reports by Quayle (1980), Graham (1982) and others, and data from the OWS Cumulus will be used in evaluating the VSOP-NA results (Section 4, below). However the weather ship meteorological observations are generally made to the standard required for weather forecasting rather than climate research. In this section we will therefore report the results of Taylor et al. (1994) which compare research quality wind measurements from the Cumulus with the standard weather ship observations. Both sets of observations were derived from anemometers and may therefore contain some of the errors which will be discussed in more detail in section 5.

The Data

The research quality wind data were obtained during the period April, 1992 to January, 1994, from a sonic anemometer mounted on the port side of the foremast platform. Ten minute averaged "horizontal" wind components and a vector averaged total wind vector were available 4 times per hour. There was negligible difference between these two estimates of the relative wind. The ships motion was recorded from a GPS navigation system, and the ship's head from a flux gate compass, at 2 minute intervals. These data were used to calculate true wind values.

The standard hourly WMO wind observations are obtained by a meteorological officer reading an analog dial. There are two cup-anemometer and wind vanes mounted to either side of the aft mast platform; the windward one is read. The ship speed is obtained from the ship's officer on the bridge, the ship's head from a compass repeater. The true wind is calculated using a hand calculator.

Ship operating characteristics

Figure 3 illustrates the recorded behavior of the OWS Cumulus in response to the wind speed climate at Lima. The most likely wind speed is about 10 m/s. For winds up to about 15 m/s the ship usually drifts (sideways with the wind about 10 degrees forward of the port beam) until the edge of the operating area is reached, whereupon the ship steams back to the upwind side of the area. If the wind or sea state is too high (normally above

15 m/s wind speed), the ship heads bow into the wind at slow speed ("hove to"). Note that, while the UK Met. Office anemometers are well exposed when the ship is drifting, they are situated some distance downwind of the ship's bow when steaming or hove to. The anemometers are, however, at a high level compared to the ships superstructure.

The ship's speed when drifting or hove to is shown in Figure 4. As the wind increases the ship drifts downwind faster. When hove-to the engines are kept at a constant setting; as the wind increases the forward motion decreases.

Comparison of wind estimates

Wind estimates were compared for relative wind directions from 60° to starboard to 100° to port; this included most of the observations, and ensured that the sonic anemometer had reasonable exposure. Figure 5(a) shows the averaged wind speed difference (Sonic - WMO) as a function of the true wind speed determined from the sonic data. The sonic and WMO difference was variable but not significantly different from zero when the ship was steaming. The sonic read relatively high when the ship was drifting, and relatively low when the ship was hove-to, compared to the WMO values. This behaviour would be qualitatively explained if the ship's speed were neglected in reporting the true wind. This appears to be confirmed by Figure 5(b) which shows that, when the ship is hove to, the difference between sonic and WMO values corresponds well with the ship speed. When drifting, the difference corresponds to the ship speed plus 0.4 m/s.

Correction for Cumulus WMO wind observations

Assuming that the sonic anemometer values are correct, Figure 6 shows the correction to be added to the reported winds from Cumulus. Below 10 m/s the reports must be increased by about 0.8 m/s. Above 15 m/s, a decrease of about 0.8 m/s is required. Correcting the data in this way will introduce error into the relatively small number of observations obtained when the ship is steaming.

Accuracy of Voluntary Observing Ship Visual Winds - the VSOP-NA Project

Background

Previous studies have compared weather ship data with nearby visual winds (Quayle, 1980, Kaufeld, 1981 and Graham, 1982), compared visual and measured winds from the same ship (Cardone, 1969), or compared wind speed distributions (Quayle, 1980). In analyzing the data from the VOS Special Observing Programme - North Atlantic, Kent et al. (1991, 1993) adopted a different method. Each observation from the 46 ships participating in the two year project was matched with the output from a weather forecast model. By using the model as a comparison standard it was not necessary to restrict comparisons to geographically close pairs of observations. Thus it

was possible to use all the reports in the VSOP-NA data. The method of wind estimation for each VSOP-NA ship was known, including the position and exposure of any anemometer carried (Kent and Taylor, 1991), and the VSOP-NA ships reported both relative and true wind values.

Summary of VSOP results

Kent et al. (1993) noted that, for the VSOP-NA ships which used anemometers, the difference of the reported wind from the model value was greater for ships on which the anemometer was situated at a greater height (Figure 7). Having corrected the anemometer winds to 10m, their analysis suggested that the Cumulus winds were biased low at lower wind speeds and also that the model being used as a comparison standard probably underestimated the wind speed by about 1 to 2 m/s (Figure 8). They suggested that visual winds adjusted to the CMM scale are more compatible with anemometer winds than the original estimates based on the Code 1100 scale.

Kent et al., (1991) showed that visual wind observations above 8 m/s were under estimated at night (compared to daytime observations) unless the ship also carried a fixed anemometer. This suggests that the best Beaufort conversion scale would have different values for day and night. However, where a fixed anemometer was carried but visual winds reported, both day and night time values showed similar characteristics to the day time visual winds from ships which did not carry an anemometer. It appeared that the ships officers were not relying solely on the anemometer at night, but rather using it to ensure consistency in their visual wind estimates. The differences (Figure 9) are of the same order as the difference between the Code 1100 and CMM wind scales.

Re-analysis of the VSOP-NA results

For this paper the VSOP-NA results have been re-analyzed with all wind estimates (anemometer and visual) corrected to the equivalent 10m neutral wind. Height correction was based on the Smith (1988) roughness lengths with the standard Businger-Dyer stability corrections using the observed values of sea surface temperature, air temperature and dew point. For visual winds the Code 1100 estimates represent the 10m wind, the CMM and Kaufeld scales have been corrected from 18m and 25m to 10m respectively. In addition the OWS Cumulus wind estimates have been corrected for the ship motion as discussed in Section 3. Figure 10 shows that the effect of correcting the anemometer wind values was to bring them into closer agreement with the reported Cumulus wind observations. Applying the correction to the Cumulus winds results in close agreement up to about 10 m/s, but increases the difference above about 15 m/s.

The different wind conversion scales are compared to the anemometer wind values in Figure 11a and to the corrected Cumulus reports in Figure 11b. In each case the value is calculated by:

(Average visual wind - model) - (Average anemometer wind - model)

and plotted against model wind speed. In each case the results confirm that, at most wind speeds, the CMM values are to be preferred to the Code 1100 values. For winds below 10 m/s, the CMM scale appears to give better agreement with the anemometer winds than the Kaufeld scale. At higher wind values there is little significant difference between the two scales. Note however that a different conclusion might result if only the night time observations were compared.

Errors for Anemometer Wind Measurements on Ships

Background

The previous section has shown that, on average, the use of the CMM scale gives better agreement with anemometer wind observations than the use of the Code 1100 scale. However this does not necessarily imply that the CMM scale represents more closely the actual wind speed since anemometer winds may be affected by systematic errors. There are several possible sources of error for anemometer winds measurements. It is not known how well the increasing number of anemometers being deployed have been calibrated or what, if any, measures are taken to ensure that the instruments remain within calibration. In use, the anemometer is exposed to a turbulent flow which fluctuates as the ship rolls and pitches and the anemometer may not be "vertical" with respect to the mean flow. The reported wind is an estimate of the average reading of a fluctuating analog dial made by the ship's officer. It is not based on 2 minutes, and certainly not on 10 minutes, of observation; 5 seconds seems more likely. Errors are then made in converting to true wind velocity. The following sections will first summarize results from the VSOP-NA experiment concerning anemometer winds, and then consider the errors likely from ship motion and the airflow disturbance by the ship. A method of establishing an absolute wind speed calibration will then be suggested.

Results from VSOP-NA -- Instrument exposure and calibration

The most likely height of an anemometer on a VSOP-NA ship (Figure 12) was about 30m, considerably more than that shown in WMO (1990) for the VOS fleet as a whole. This may be because the VSOP-NA ships carrying anemometers tended to be large container ships. For each ship the anemometer exposure was estimated on a scale from 0 (poorly exposed) to 9 (well exposed) for winds on the bow, beam, and stem. The most likely ship speed at the time of observation was 16 to 18 knots, similar to the most likely wind speed. As a result the relative wind for 73% of observations was from $\pm 45°$ of the bow and for 97% it was within $\pm 135°$ from the bow. Thus an anemometer mounted forward of a mast structure would have been shielded for less than 3% of the observations, and 63% of observations achieved the top exposure rating. This does not mean that the anemometer was situated in an undisturbed air flow, for example Figure 13 shows the situation of the anemometer on one of the larger VSOP-NA ships.

It will be shown below that possible mean errors from airflow disturbance by the ship may well be of order 10% or more. In analyzing the VSOP-NA results it was not possible to separate these instrument exposure errors from anemometer calibration errors,

and the absolute accuracy was difficult to determine. Perhaps the best comparison standard were the OWS Cumulus winds from station Lima. Unfortunately Lima is north of most of the ship routes and it was necessary to assume that the UK Met. Office model was effective in providing a good comparison standard for observations from different areas[2] . With that proviso, and using the wind observations as reported, Kent et al. (1991) found that the VSOP-NA ship reports were about 1 m/s higher than the Cumulus values. Correcting the VSOP-NA ship winds for the height of the anemometer, the observations were on average about 0.8 m/s higher than the reported Cumulus winds (see Figure 10 and discussion above). Correcting the Cumulus reports for the ship's motion resulted in agreement with the anemometer winds up to about 10 m/s; at higher winds the corrected Cumulus values were lower by something under 10%. Thus even with all corrections applied, the VSOP-NA ships appeared to overestimate the winds compared to the Cumulus.

The VSOP-NA results showed that wind speed estimates obtained using hand-held anemometers were different in character to those from fixed instruments. Below about 7 m/s, wind speeds from hand-held anemometers gave similar results to the visual wind observations based on the Code 1100 scale. At higher wind speeds few observations were obtained, and these showed large scatter.

Concerning wind direction, the mean differences from the model values were within ±5° for most ships with no obvious bias. Mean difference for ships using wind vanes were similar to and sometimes larger than the values for ships using visual estimates.

Calculation of true wind

The VSOP-NA results showed that a significant and unnecessary error was introduced because officers on ships using anemometers must perform the vector subtraction of the ships velocity from the measured relative wind. Since the most frequently occurring wind speed values were similar to or less than the ships' speeds, large errors could result if this calculation was not performed correctly. The VSOP-NA ships had been requested to report ships speed and head, and the relative wind speed and direction, in addition to the true wind values. Thus, this calculation could be tested for about 2500 anemometer based reports. The method used was to calculate the value of the relative wind implied by the true wind report together with the ship's speed and head at the time of observation. This was compared to the relative wind reported. Only about 50% of the reported winds corresponded to calculated relative winds within ±1 m/s of the observed value. A large fraction of the reports (about 25%) were more than ±2.5 m/s different. For wind direction only 70% were within ±10°, and 13% were outside ±50°.

Errors sources for anemometer winds -- Errors due to ship roll and pitch

---

[2] This may have not been the case since the OWS Cumulus wind observations would have been given greater weight when assimilated into the model; however tests suggested this was not a significant factor.

Ramstorf (1988) assessed the likely anemometer errors due to ships roll because of (i) "anemometer pumping" (ii) the tilt of the anemometer, and (iii) the variation of height in the near surface wind gradient, and demonstrated that only the first of these has the potential to contribute an error significantly above 1%. The wind error due to anemometer pumping is a function of:

$$\frac{\text{(anemometer height above roll axis) x (roll angle)}}{\text{(roll period)}}$$

Thus Figure 15 shows the percentage wind speed error for three cases for which possible combinations of anemometer height, roll angle, and roll period are shown in Table 1. The errors are largest for case (c) which might represent a research vessel with a cup anemometer at 20m rolling through 10° with 5 second period. VOS are perhaps more likely to be represented by cases (a) or (b), for example an anemometer at 40 m on a ship with a 20 second roll through 5°. In these cases the errors remain small under most conditions and negligible compared to probable air-flow disturbance effects.

Errors due to airflow disturbance

Attempts to determine the wind error at anemometer sites on research ships due to the airflow disturbance due to the ship were summarized by Taylor (1985). Based on comparisons with meteorological buoys (Augstein et al., 1974; Large and Pond, 1982), or with bow boom anemometers (Ching, 1976; Kidwell and Seguin, 1978), he concluded that for relative winds within ±45° of the bow, ±5% was a reasonable accuracy estimate. For winds from other directions significantly different errors might occur. More recently, wind tunnel studies have been reported by Blanc (1986; 1987) for two naval ships, and Surry et al. (1989) and Thiebaux (1990) for Canadian research ships.

Although referring to a guided missile cruiser, the study of Blanc (1987) is perhaps closest in terms of ship shape and size to a VOS. The errors in speed at the anemometer (Figure 16) show the effects of the main mast which is directly downwind of the anemometer for a relative wind direction of about 100°, and the wake of a smaller obstruction at 90° relative wind. However these effects appear to be super-imposed on an overall wind increase of about 9% which presumably represents the combined effects of the ship's superstructure and of a large radar antenna near the anemometer location. For comparison Figure 17 shows wind errors calculated using the model of Wucknitz (1977). The wind tunnel results for three Canadian survey ships (Thiebaux, 1990) also show an increased wind speed at the main mast site of typically 5 to 10% for most relative wind directions.

Increased wind speeds of this magnitude at typical anemometer heights above the ships accommodation block have also been predicted by numerical modelling. Kahma and Lepparanta (1981) used a potential flow model to predict errors of about 15% at the mast anemometer site on a small research vessel, the R/V Aranda. Dupuis (1994) has used a two-dimensional turbulent flow model to predict a wind speed increase of about 20% at the main mast anemometer site on the research ship le Suroit. The use of three-dimensional computational fluid dynamics (CFD) to model the airflow over a ship is being evaluated at the James Rennell Center. Initially the aim is to simulate the wind

tunnel results of Thiebaux (1990) (and field results of Anderson, 1993) for the survey ship CSS Dawson. The preliminary results (Ricardo, 1994), Figure 18, have been calculated for winds on the bow and have reproduced the wind tunnel results for two anemometer sites to within about 2%.

In summary, for research ships and similar vessels, most studies show that an anemometer positioned on a mast above the accommodation is likely to over-read to order 10% or so. This applies for all wind directions except where the anemometer is in the wake of the mast. The only studies showing a significant underestimate are comparisons with a bow boom by Ching (1976), and comparisons with a buoy (Augstein et al., 1974), in both cases when the wind was on the beam. The Ching (1976) result could be due to errors in the bow boom data. The Augstein et al. (1974) results seem harder to explain; for the same ship Ramstorf (1988) found an over-estimate of order 10% for beam winds. Whether an anemometer on a VOS (see for example, Figure 13), would under-read or over-read is not known. Numerical simulations of typical VOS shapes would give some indication but we know of no such studies in progress or planned. The evidence presented in section 4.3 (Figure 10) suggests that, after correction for the instrument height, VOS anemometers may read high compared to the OWS Cumulus, at least for wind speeds above 10 m/s.

Toward an absolute wind calibration

Given the difficulty of obtaining accurate wind measurements even from an ocean weather ship or research ship, an alternative standard for wind speed measurements must be sought. Meteorological buoys do not present the air-flow disturbance seen on ships. However it is difficult to ensure that the anemometer remains well calibrated over an extended period of time, and care is necessary in allowing for buoy motion and in the correction for the very low instrument height. If we assume that the quantity that is really required is the wind stress, then an alternative calibration method is suggested by the results of Yelland et al. (1994). By comparing different anemometers mounted on the foremast of a research ship, they concluded that, whereas wind stress could be estimated to a consistency of about 5% using the inertial dissipation method, stress estimates based on the mean wind and the bulk aerodynamic formula are likely to have errors of order 20 to 30%. By equipping a subset of VOS with instrumentation to make inertial dissipation estimates of the wind stress, a wind velocity climatology could be produced using a specified drag coefficient formulation. Wind observations which were adjusted to be consistent with this climatology would then automatically produce the correct wind stress value. Suitable automatic instrumentation is available for wind stress estimation but the cost of the fast response anemometers and processing systems needed would be large compared to the cost of standard VOS instrumentation.

Summary

The percentage of anemometer derived wind reports has increased with time to a varying extent in different ocean areas. To prevent spurious temporal or spatial variations in the marine wind climate it is important that anemometer and visually

estimated winds are compatible. Ocean weather ships might be expected to provide an accurate wind velocity estimate with which to calibrate VOS winds. However, by operating a sonic anemometer and GPS navigation system on the OWS Cumulus we have detected systematic errors in the wind reports of order 1 m/s. These appear to be caused by the neglect of the correction for the, relatively small, ship speed when drifting or hove to. Using the Cumulus wind observations and the sampling frequency achieved by the VOS, we can detect no fair weather bias in the wind reports from the area around ocean station Lima.

The accuracy of VOS wind reports was examined in the VSOP-NA project. All the visual wind scales examined (Code 1100, CMM IV, and Kaufeld) showed wind difference trends when compared with both OWS CUMULUS data and with VOS anemometer data. Code 1100 gives significantly larger wind values at higher wind speeds. The closest agreement between VOS visual wind estimates, and VOS or Ocean Weather Ship anemometer derived winds, was obtained using the CMM IV scale. Visual winds at night underestimated the higher wind speed ranges; this should be investigated further.

For anemometer derived winds from the VSOP-NA ships, significant errors were introduced during the calculation of the true wind speed from the observed relative wind. Correcting for the height of the anemometers improved the consistency of the data set. Having applied all corrections, the VOS anemometer derived winds agreed with the OWS Cumulus winds at wind speeds below about 10 m/s; at higher wind speeds the VOS winds appeared to be stronger. The anemometers on the VSOP-NA ships were generally well exposed and it is unlikely that the roll and pitch of the ship resulted in significant error. However field calibrations, wind tunnel studies, and numerical models suggest that, for research ships, an anemometer situated on the main mast is likely to be in error by order 10%. Usually the wind speed is overestimated. The magnitude and sign of this airflow disturbance error for a typical VOS ship is not known. It could be estimated using computer modelling techniques of the sort we are developing for research ships.

At present we have no absolute calibration for marine winds. Estimates of the wind stress using the inertial dissipation method could be used to calibrate marine winds. However the cost of the instrumentation systems would be significant.

References

Anderson, R. J., 1993: A study of wind stress and heat flux over the open ocean by the inertial dissipation method. *J Phys Oceanogr.* , 23(10), 2153 - 2161.

Augstein, E., H. Hoeber and L. Kruegermeyer, 1974: Fehler bei Temperatur-, Feuchte- und Windmessungen auf Schiffen in tropischen Breiten. *Meteor Forschungsergebnisse* B9, 1 - 10.

Blanc, T.V., 1986: Superstructure flow distortion corrections for wind speed and direction measurements made from Tarwa Class (LHA1-LHA5) ships. NRL Report 9005, Naval Research Laboratory, Washington, D.C., 20 pp.

Blanc, T. V.,1987: Superstructure flow distortion corrections for wind speed and direction measurements made from Virginia Class (CGN38-CGN41) ships. Report 9026, Naval Research Laboratory, Washington, D.C., 24 pp.

Cardone, V. J.,1969: Specification of the wind distribution in the marine boundary layer for wave forecasting., New York University.

Cardone, V. J., J. G. Greenwood and M. A. Cane, 1990: On trends in historical marine wind data. *J. Climate*, 3, 113 - 127.

Ching, J. K. S., 1976: Ship's influence on wind measurements determined from BOMEX mast and boom data. *J. Appl Meteorol*, 15(l), 102 - 106.

Dupuis, H., 1994: Wind speed errors for the research ship le Suroit. (personal communication).

Graham, A. E., 1982: Winds estimated by the Voluntary Observing Fleet compared with instrumental measurements at fixed positions. *Meteorol. Mag.*, 111, 312-327.

Ive, D. S., 1987: A comparison of numbers of visually estimated and instrumentally measured wind data, Marine Technical Note No. 2, Revised February 1987, UK Meteorological Office, Bracknell, 43pp.

Kahma, K. K. and M. Lepparanta, 1981: On errors in wind speed observations on M/V Aranda. *Geophysica*, 17(1-2), 155-165.

Kaufeld, L., 1981: The development of a new Beaufort equivalent scale. *Meteorol. Rundsch.*, 34, 17-23.

Kent, E.C. and P.K. Taylor, 1991: Ships observing marine climate: a catalogue of the Voluntary Observing Ships Participating in the VSOP-NA. Marine Meteorology and Relate Oceanographic Activities 25, World Meteorological Organization, Geneva, 123 pp.

Kent, E. C. and P. K. Taylor, 1994: A comparison of heat flux estimates for the North Atlantic Ocean. *J. Phys. Oceanogr.*, (submitted).

Kent, E. C., P. K. Taylor, B. S. Truscott and J. A. Hopkins, 1993: The accuracy of Voluntary Observing Ship's Meteorological Observations. *J. Atmos. & Oceanic Tech.*, 10(4), S91 - 608.

Kent, E. C. , B. S. Truscott, J. S. Hopkins and P. K. Taylor, 1991: The accuracy of ship's meteorological observation - results of the VSOP-NA. Marine Meteorology and Related Oceanographic Activities 26, World Meteorological Organization, Geneva, 86 pp.

Kidwell, K. B. and W. R. Seguin, 1978: Comparison of mast and boom wind speed and direction measurements on US GATE B-Scale Ships. NOAA Tech. Rep. EDS 28, CEDDA, Washington, D.C.

Large, W. G. and S. Pond, 1982: Sensible and Latent Heat Flux Measurements over the Ocean. *J. Phys. Oceanogr.*, 12, 464-482.

Quayle, R. G., 1980: Climatic Comparisons of Estimated and Measured Winds from Ships. *J. Appl. Meteorol.*, 19, 142-156.

Ramnstorf, S., 1988: Wind observations from RV/Rapuhia. Physics Section report (Internal Report 88/2), Division of Marine & Freshwater Science, DSIR, Wellington, New Zealand, 12 pp.

Ricardo, 1994: CFD analysis of airflow over the CSS Dawson. (unpublished report), Ricardo Consulting Engineers Ltd., Shoreham, U.K .

Smith, S. D., 1988: Coefficients for Sea Surface Wind Stress, Heat Flux and Wind Profiles as a Function of Wind Speed and Temperature. *J. Geophys. Res.*, 93, 15467-15474.

Surry, D., R. T. Edey and I. S. Murley, 1989: Speed and direction correction factors for ship borne anemometers. Engineering Science Research Report BLWT-SS9-89, Univ. of Western Ontario, London, Ontario, 83 pp.

Taylor, P. K., 1985: TOGA surface fluxes of sensible and latent heat by in situ measurement and microwave radiometry. Third session of the JSC/CCCO TOGA Scientific Steering Group, Scripps Institution of Oceanography, La Jolla, Ca., WMO, Geneva, 30pp. & figs.

Taylor, P.K., Kent, E.C. and Yelland, M.J. 1994: The accuracy of meteorological measurements from an ocean weather ship (in preparation)

Thiebaux, M. L.,1990: Wind tunnel experiments to determine correction functions for ship borne anemometers. Canadian Contractor Report of Hydrography and Ocean sciences 36, Bedford Inst. Oceanography, Dartmouth, Nova Scotia, 57 pp.

WMO , 1990: International list of selected, supplementary and auxiliary ships., World Meteorological Organization, Geneva.

Wucknitz, J., 1977: Flow distortion by supporting structures.: Air sea interaction: Instruments and methods, F. Dobson, L. Hasse and R. Davis, Ed., Plenum Press, 605 - 626.

Yelland, M. J., P. K. Taylor, I. E. Consterdine and M. H. Smith, 1994: The use of the inertial dissipation technique for shipboard wind stress determination. (accepted by *J. Atmospheric Ocean Technology*)

Table 1: Possible combinations of anemometer height above roll axis (m), roll amplitude (degrees) and roll period (seconds) for the three cases shown in Figure 15.

Anemo Ht	Case (a)		Case (b)		Case (c)	
(m)	Roll (°)	Period (sec)	Roll (°)	Period (sec)	Roll (°)	Period (sec)
10	5	5	10	5	16	4
20	5	10	10	10	10	4
30	5	20	10	20	10	10

Figure 1: Percentage of anemometer wind reports for different ocean areas for year periods from 1960 to 1985. The values have been roughly estimated from [C] Cardone et al., (1990), [I] Ive, (1987), [R] Ramage, (1987). The areas shown are (a) North Atlantic, (b) Indian and southern hemisphere oceans, (c) North Pacific regions.

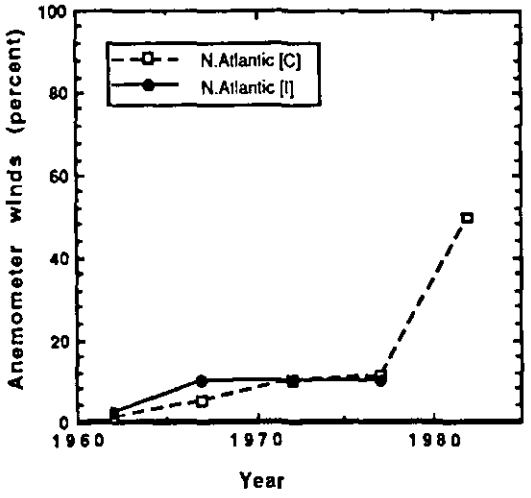

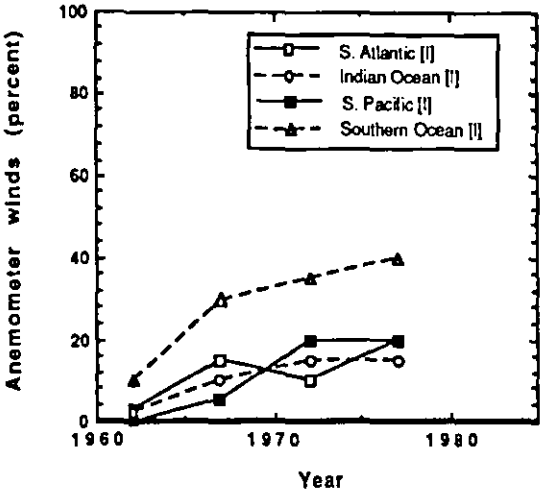

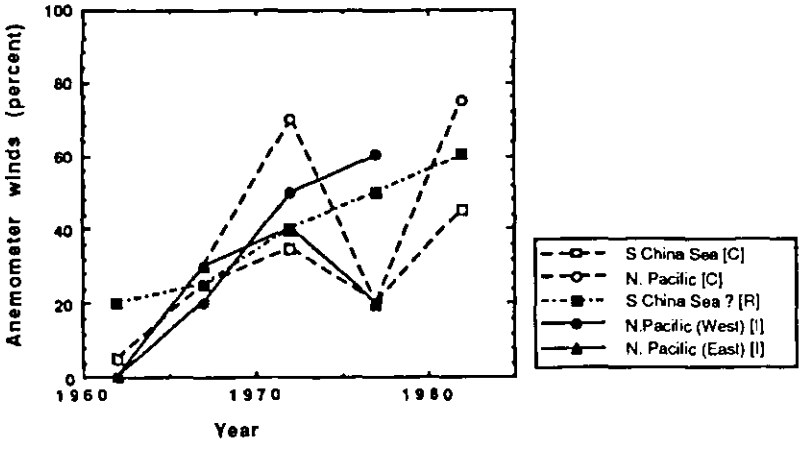

Figure 2: Cumulative percentage distributiojn of OWs Cumulus wind data and vos wind data as a function of OWS Cumulus wind speed (m/s) at the time of the VOS observation.

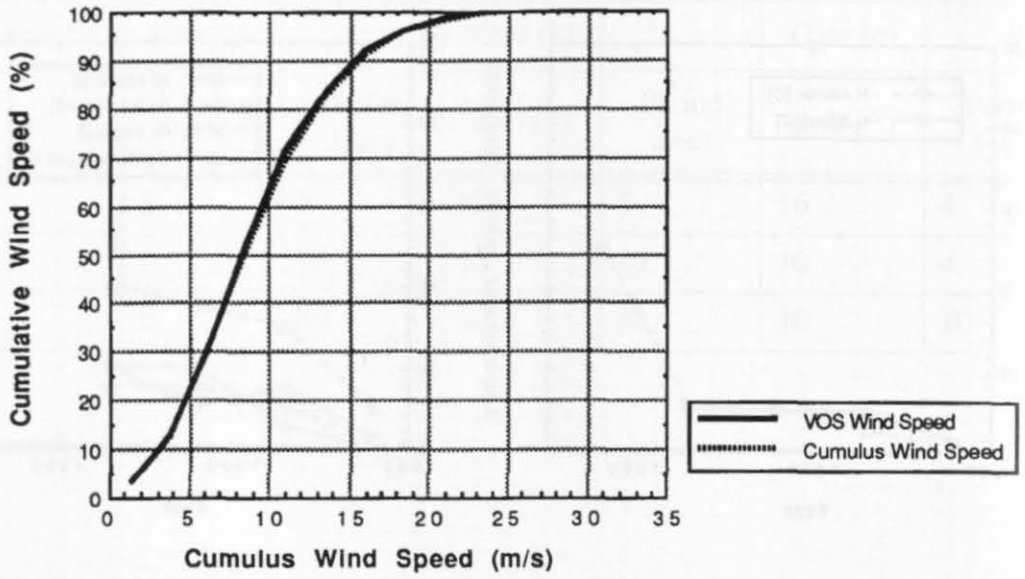

Figure 3: Area plot of wind speed occurrences from the sonic anemometer data from OWS Cumulus. The number of ccurrences is shown for each 2 m/s interval. The shaded area represents the contribution to the total number of cases obtained at each wind speed when the ship was drifting, steaming, or hove to.

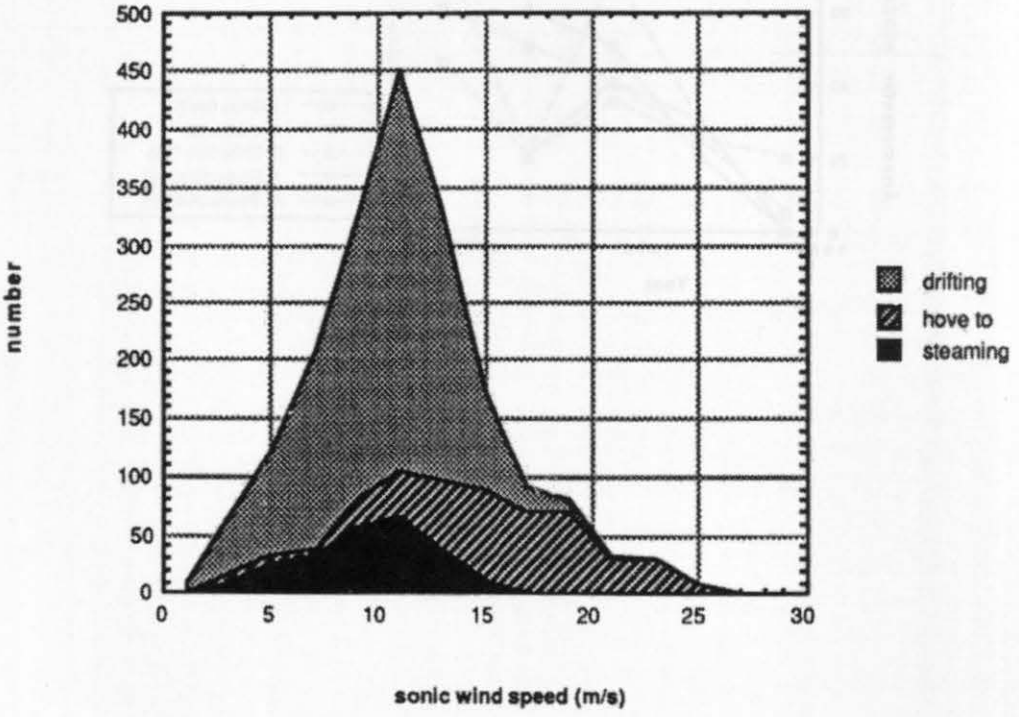

Figure 4: Mean ship speed (m/s) when drifting or hove-to plotted against the true wind speed derived from the sonic anemometer and GPS data.

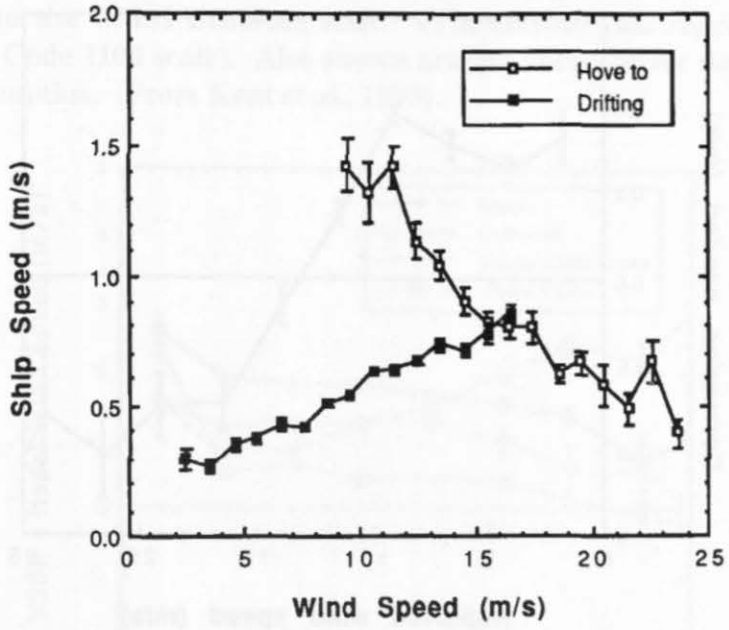

Figure 5: (a) Averaged difference between the wind speed reports, (Sonic - WMO), plotted against the true wind speed derived from the sonic anemometer and GPS data. (b) Averaged difference between the wind speed reports, (Sonic - WMO) when ship is hove-to or drifting plotted against the ship speed.

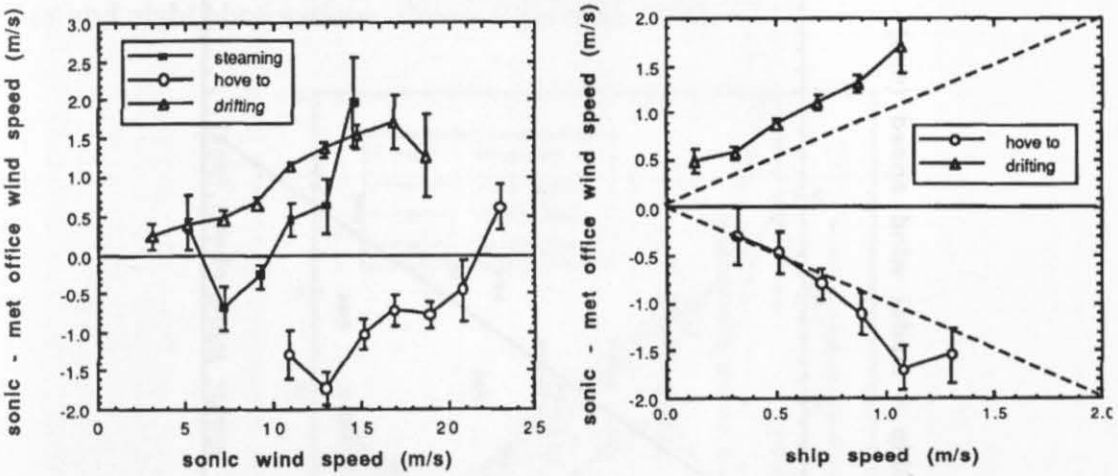

Figure 6: Correction to be added to Cumulus WMO wind observations calculated as a function of the uncorrected WMO observation.

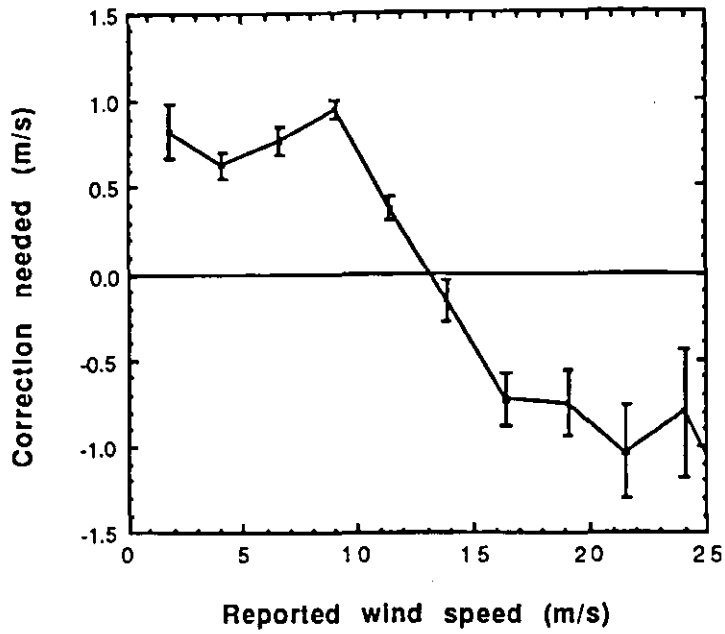

Figure 7: Average difference between the reported wind and the mode value for VSOP-NA ships which used fixed anemometers plotted against the height of the anemometer (adapted from Kent et al., 1993)

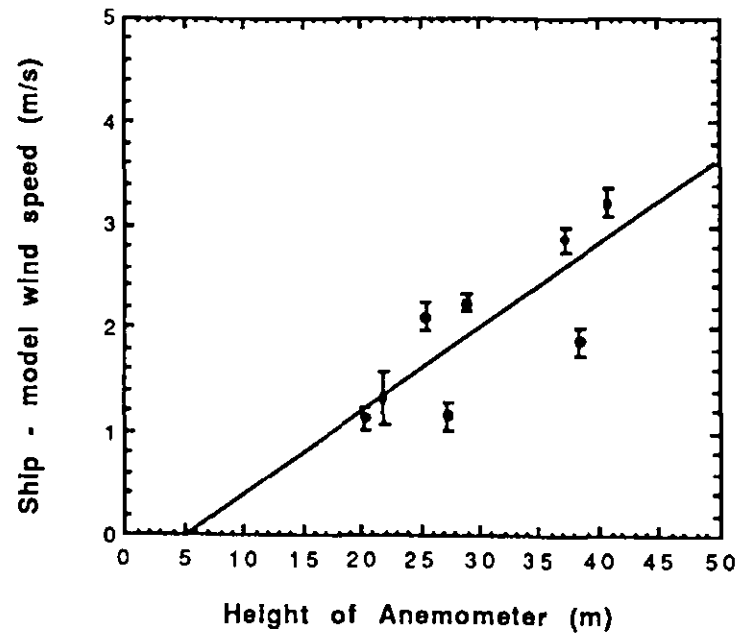

Figure 8: The mean difference in wind speed measurements (VSOP-NA ship minus model value, m/s) plotted against the model wind speed value. The results from fixed anemometers have been corrected for the anemometer height. The visual estimates have been corrected to the CMM Beaufort scale. (The dashed line represents the visual values using the Code 1100 scale). Also shown are the anemometer data for the Ocean Weather Ship Cumulus. (From Kent et al., 1993)

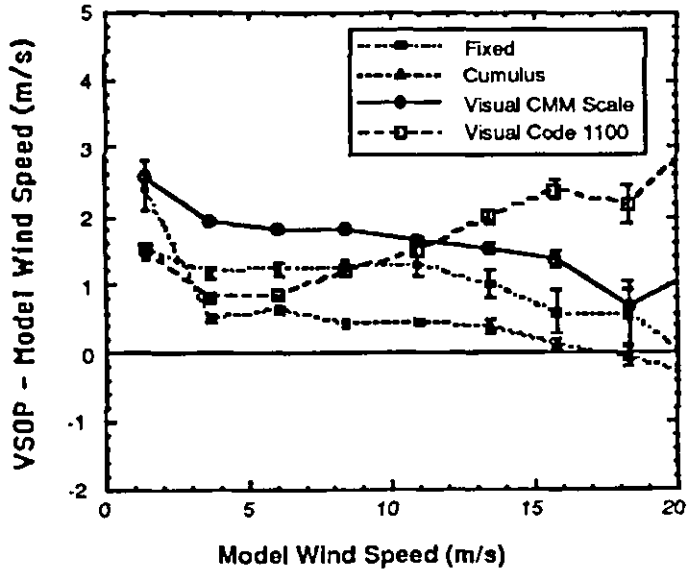

Figure 9: VSOP measured wind speed (m/s) binned on model wind speed (m/s) separately for visual winds reported on ships with and without fixed anemometers and for day and night observations. (From Kent et al., 1993)

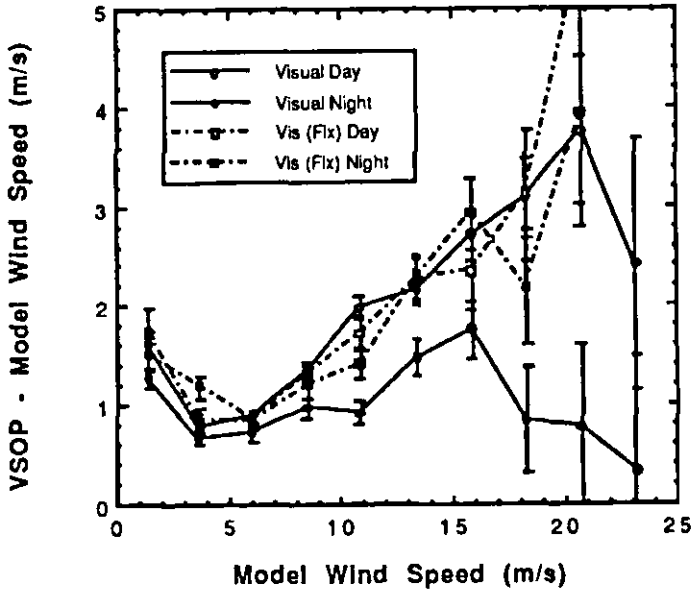

Figure 10: Average difference between the reported wind and the model value for VSOP-NA ships which used anemometers both before and after correcting to the 10m neutral wind values. also shown are the difference for the Cumulus, corrected to 10m height, both before and after correction for ship motion. Uncorrected values are joined by broken lines, corrected values by full lines.

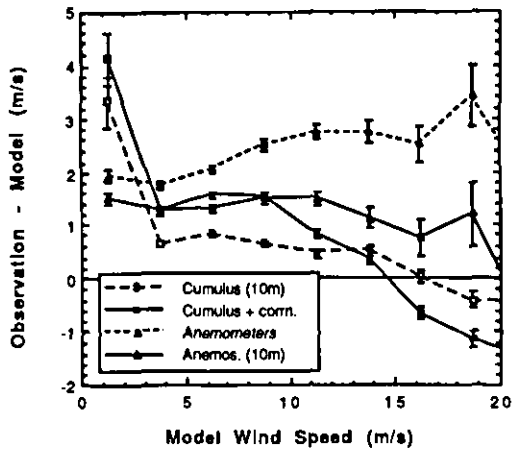

Figure 11: Average difference between 10m neutral values for visual winds corrected to different conversion scales and anemometer derived values. (a) Anemometer values from the VSOP-NA ships. (b) Anemometer wind estimates from the OWS Cumulus (corrected for ship motion.)

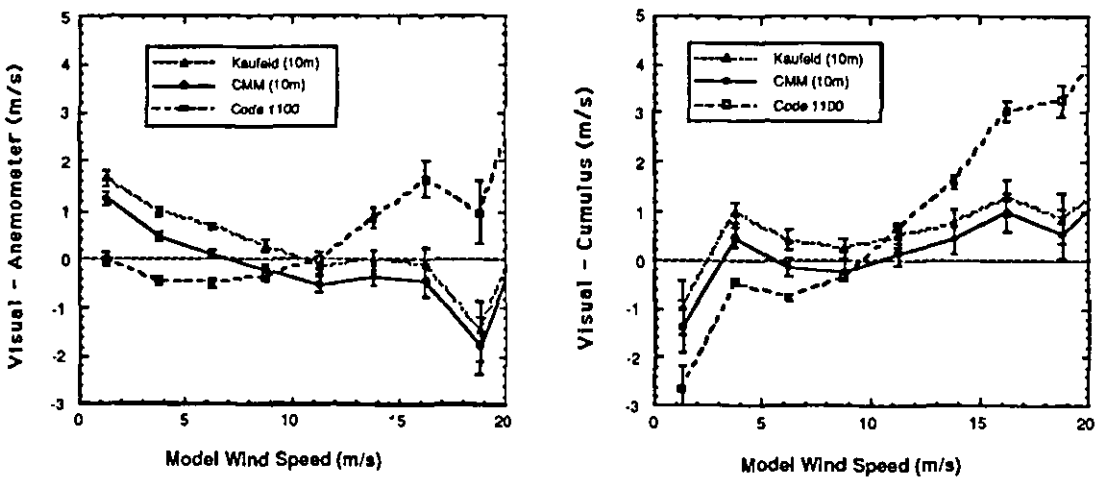

Figure 12: Anemometer heights for the VSOP-NA ships and for the whole VOS fleet. (from Kent and Taylor, 1991)

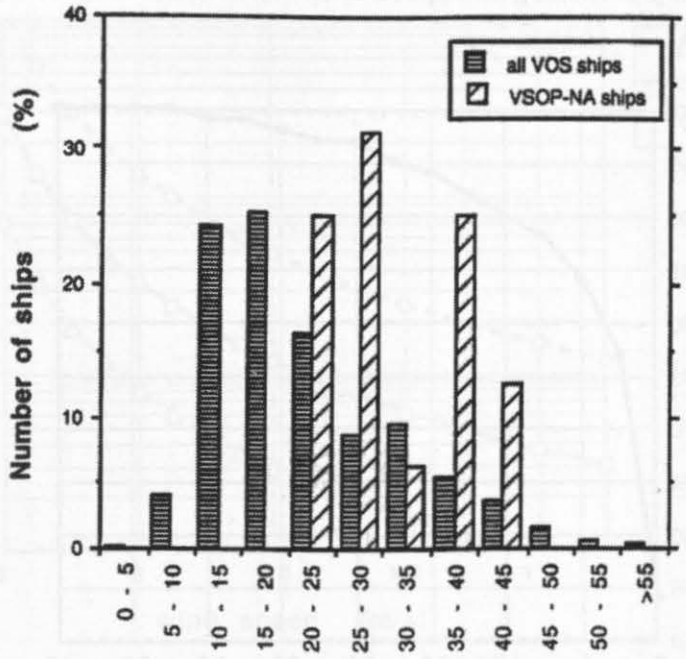

Figure 13: Situation of anemometer on one of the VSOP-NA ships, the Atlantic Cartier. The anemometer was about 40m above sea level

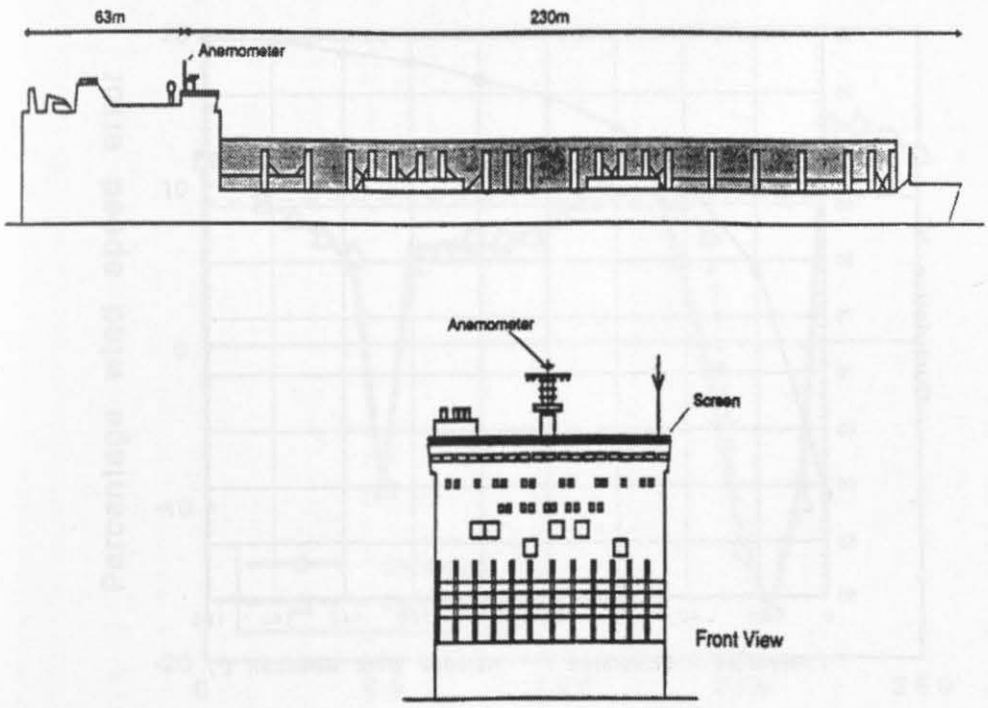

Figure 14: Cumulative percentage plot of the difference in the relative wind reported by the VSOP-NA ship and the relative wind calculated from the reported true wind velocity together with the ship's heading and speed at the time of the observation. (a) wind speed; (b) wind direction.

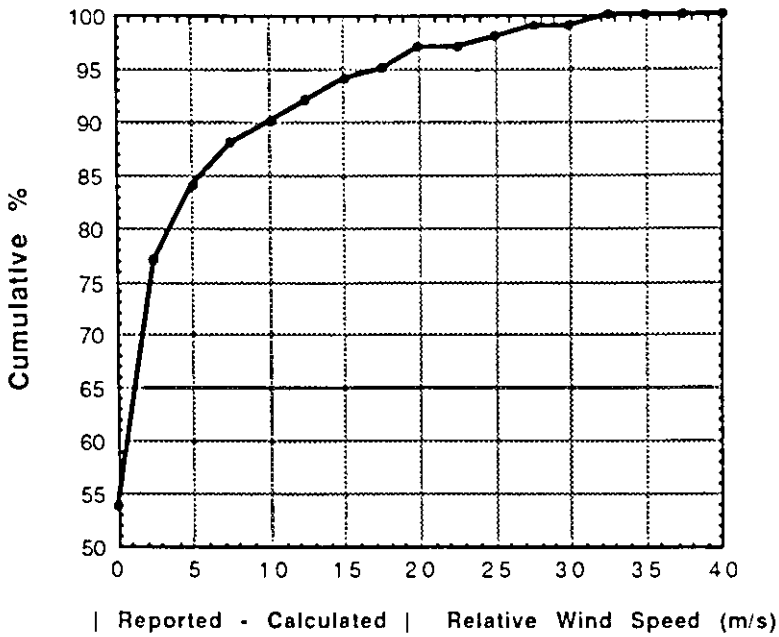

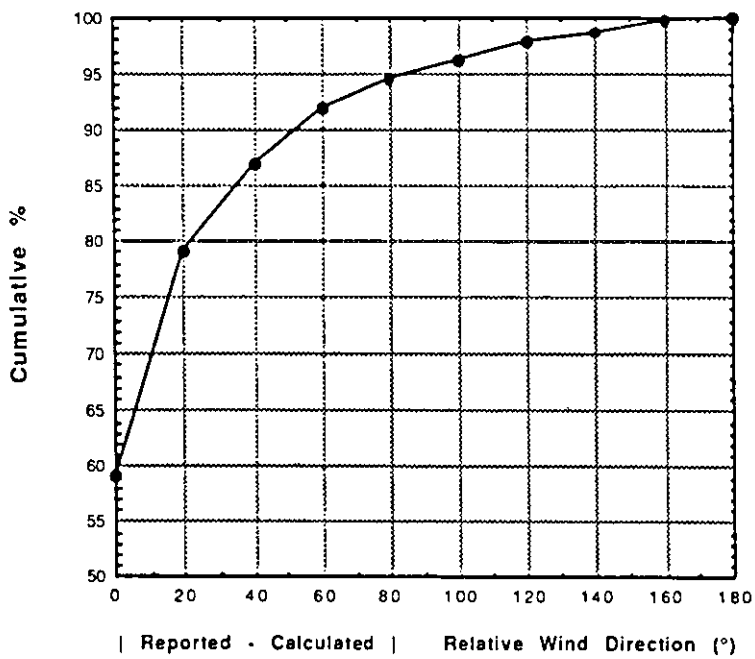

Figure 15: Percentage wind speed error due to anemometer pumping by the ship's roll for three cases (see text)

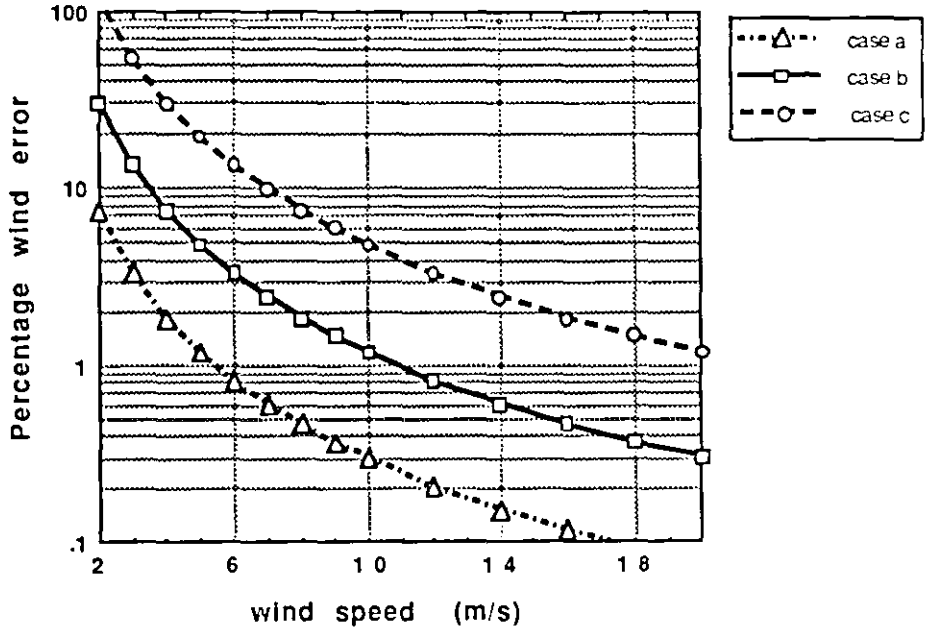

Figure 16: Percentage wind error from the wind tunnel study of Blanc (1987). The data from the port anemometer has been plotted as if the anemometer were situated in the starboard anemometer position.

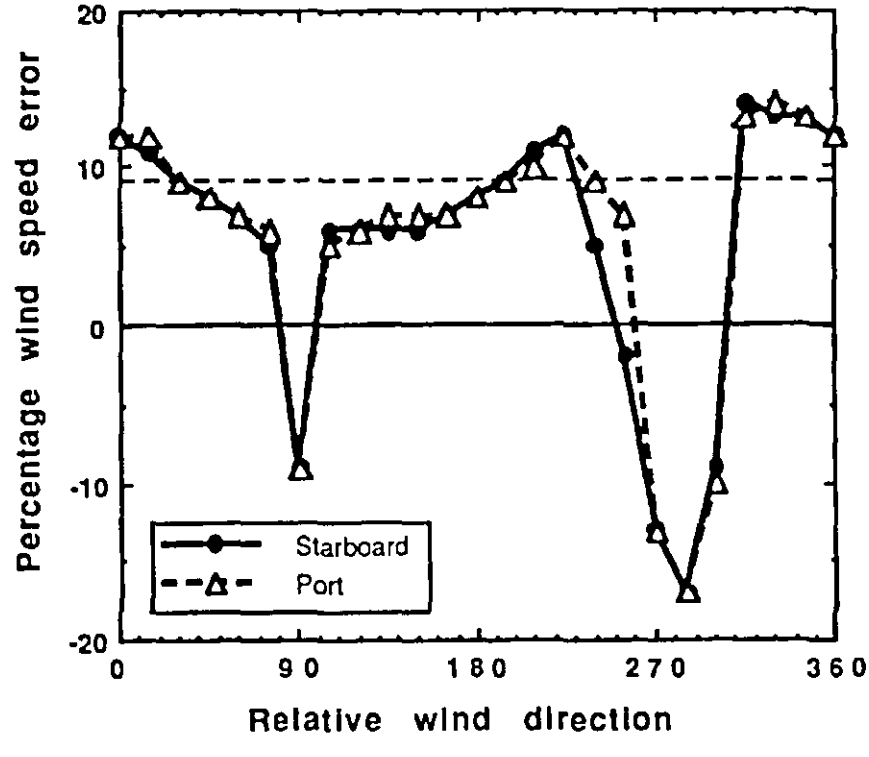

Figure 17: Errors in (a) wind speed (%) and (b) wind direction (degrees) at positions 1.5, 2.5, 5, and 10 mast diameters away from a circular mast, calculated using model of Wucknitz, (1977)

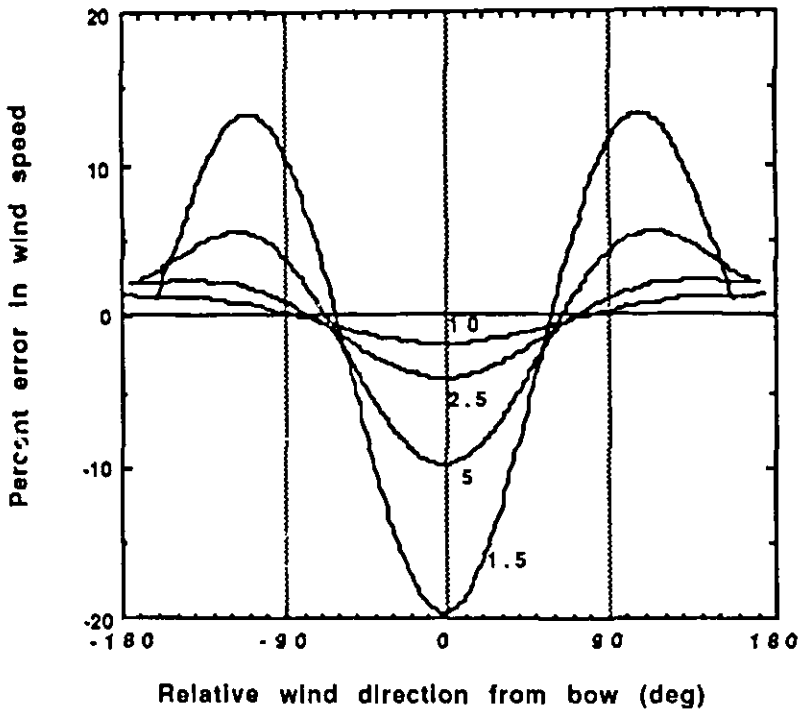

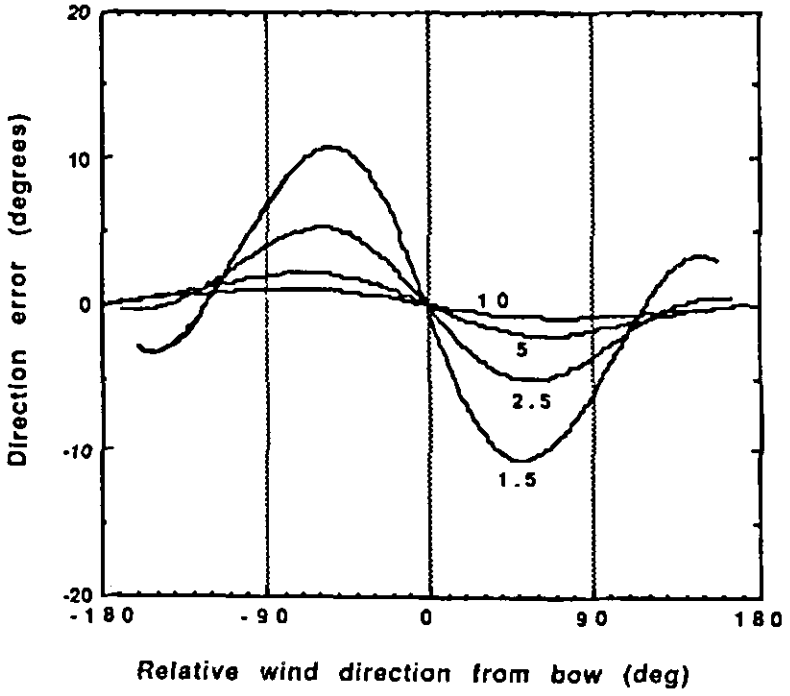

Figure 18: Flow over the CSS Dawson determined by CFD modelling (Ricardo, 1994). Regions of positive and negative wind speed error are marked.

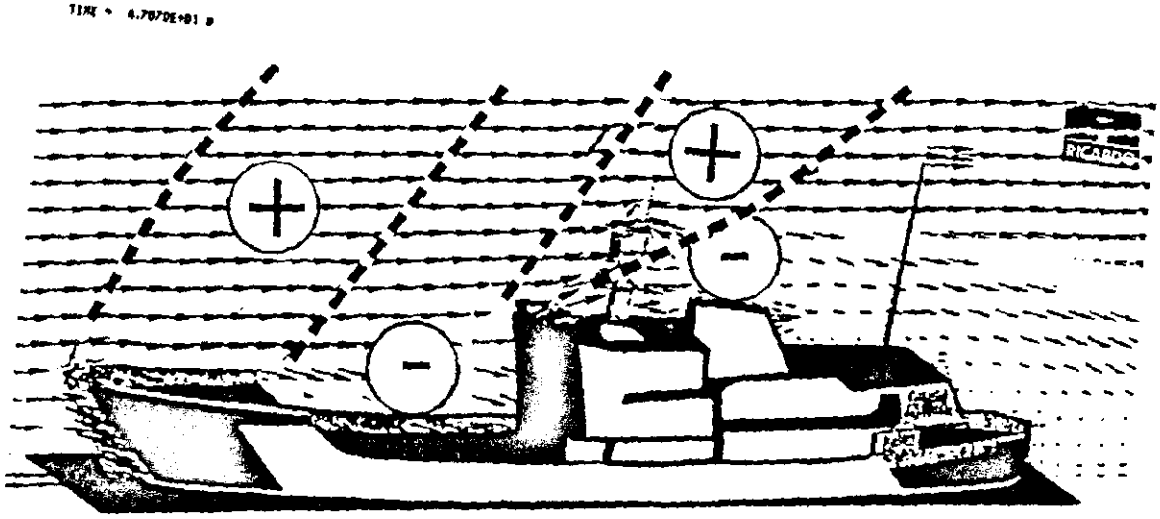

On problems using archived marine wind data: The relation between Beaufort estimations, encoded wind speeds, and real wind speeds

Heiner Schmidt

Deutscher Wetterdienst-Seewetteramt
Postfach 30 11 90
D-20304 Hamburg, Germany

Introduction

A few years ago the author had the task to determine the wind power potential in coastal sea areas along the coasts of the European Community. This had to be performed using marine (voluntary ships') wind observations only. The data base was the marine-meteorological archive of Deutscher Wetterdienst, Seewetteramt (Marine Meteorological Office) in Hamburg which presently consists of some 60 million of marine data records, about 1.5 million of those are along European Community coasts.

Of the latter all those wind observations marked as "measured" (about 15%) were discarded. The reason for this was that the measuring height was unknown, a possible flow distortion by the ships' bodies, and the possibility of an inadequate reduction of ship's speed and course in the wind.

The rest of the marine wind values (85%) are marked as "estimations." The data sets in our archive contain both a Beaufort value and a speed in knots. For technical applications the wind can only be used as speeds in metric units. As a first approach we therefore tried to use the Beaufort forces and then transform them to speeds by the "Beaufort equivalent scale" developed by Kaufeld (1981), as the equivalent scale of WMO was known to be biased. Kaufeld derived his scale by comparing the Beaufort estimations of voluntary ships to the measurements of the former Ocean Weather Ships (OWS), using a very sophisticated comparison method in space and time.

The author re-analyzed the Kaufeld scale especially at low speeds (Beaufort 1-3), and corrected it for an assumed speed reduction of the anemometers due to friction at low speeds (see differences in Table 1, column (1), Kaufeld, and (2), Schmidt). We then immediately learned, that the Beaufort values of our archive are NOT the original wind observations, but the speeds recorded in knots. The Beaufort values in our archive have been SET, according to the WMO Beaufort scale. As far as we know, this is true in all the archives, at least for marine observations after World War II.

For Kaufeld's investigation this was no big problem. At that time our archive more or less only consisted of German observations, and the German observers up to then closely followed the WMO scale, encoding only the "equivalent speeds" of the estimated Beaufort force. So the author could combine columns (4) and (2) of Table 1 and develop a

continuous non-linear transformation from "WMO encoded speeds' into "real speeds at 25 m height" above sea level (see also fig. 1).

Analysis

When we nowadays take a close look at the contents of the wind information in our archive, we find, that the observers in many countries (and also our observers) did or do not follow the strict WMO procedure but set all possible wind speed values between the "Beaufort equivalents". Analyzing the frequency distribution of encoded wind speeds in steps of one knot, we find a lot of different encoding routines (Table 2). This results in a dense, but very inhomogeneous frequency filling of the distribution of "knots".

Since no one is able to estimate wind speeds just by "feeling", the author assumed, that all observers implicitly or explicitly use the wind estimation method recommended by WMO (1949): That is, to look at the sea surface, determine the sea state, and according to that a Beaufort wind value, and finally to look up a table defining an equivalent wind speed and write it down. We further assumed, that these "equivalent wind speed" tables in all countries either are the one proposed by WMO or were derived from it.

When we use the above mentioned transformation (called "transform 1"), and apply it to a well covered wind speed distribution (fig. 2, example for the North Sea with about 500000 observations, showing frequencies of exceedance versus wind speeds), a step function results due to the inhomogeneous probability density. This has an unfavorable effect on curve fitting routines, especially when they are done automatically in limited intervals (in our case we fitted a Weibull distribution in the speed range 3-20 m/s for the calculation of wind energy).

We therefore went one step further, and developed a second transformation (transform 2 in fig. 2), by shifting the speed values of the step function horizontally (i.e. on the speed axis) towards a Weibull distribution, which was carefully fitted piece wise over entire periods of the steps in the distribution (fig. 2 is only the enlarged middle part). The resulting transformation is listed in Table 3, which is further subdivided in German and a mixture of other observation sources. The tables are used in the following way: Given you have a wind speed distribution in knots "encoded", then the lower boundary of the class, e.g. "25 knots" is (as a real speed at 25 m height) 13.7 m/s for German and 12.9 m/s for a typical mixture of "foreign" observations. The resulting frequency distributions are rather smooth and can easily be treated with curve fitting routines.

Admittedly, the method described above is "brute force", but (looking at the results, e.g. fig. 3) it seems to work.

Table 1: Beaufort-Scales

(lower boundaries of Beaufort classes in meters/second)

		Re-analyzed		
	Kaufeld	Schmidt		
Bft	1981	1991	CMM-IV	WMO
	(1)	(2)	(3)	(4)
0	0.0	0.0	0.0	0.0
1	0.8	1.7	1.3	0.3
2	2.8	3.2	2.8	1.8
3	5.4	5.3	4.4	3.3
4	7.5	7.6	6.4	5.4
5	10.0	9.9	8.5	8.0 (8.5)
6	12.1	12.1	11.1	11.1
7	14.7	14.4	13.6	14.1
8	17.2	17.1	16.2	17.2
9	20.3	20.4	19.3	20.8
10	23.4	23.5	22.4	24.4
11	27.0	26.9	26.0	28.6
12	30.6	30.5	29.6	32.7

Scales (1) and (2) are valid for 25 m above sea level, scales (3) and (4) are probably for 10 m above sea level.

The general problem is now, that in most of the modern marine meteorological archives (after 1950), the original values for estimated wind speeds are not the Beaufort forces, but encoded speeds in "knots" or "m/s"

Table 2: Setting of "Knots" due to different encoding procedures

Bft	Kts	A	B	C	D	E	F	G	Sum
0	0	X	X	X	X	X	X	-	6
	1	-	-	-	-	-	-	-	-
1	2	X	X	X	-	X	X	-	5
	3	-	-	-	-	-	-	-	-
	4	-	X	X	-	X	-	-	3
2	5	X	-	-	X	-	X	-	3
	6	-	-	X	-	-	-	-	1
	7	-	-	-	-	-	-	-	-
	8	-	X	X	-	X	-	-	3
3	9	X	-	-	-	-	X	-	2
	10	-	-	X	X	-	-	-	2
	11	-	-	-	-	-	-	-	-
	12	-	X	X	-	-	-	-	2
4	13	X	-	-	-	-	X	-	2
	14	-	-	X	-	X	-	-	2
	15	-	-	-	X	-	-	X	2
	16	-	-	X	-	-	-	-	1
	17	-	X	X	-	X	-	-	3
5	18	X	-	-	-	-	-	-	1
	19	-	-	X	-	-	X	-	2
	20	-	-	-	X	-	-	-	1
	21	-	-	X	-	-	-	X	2
	22	-	-	-	-	-	-	-	-
	23	-	X	X	-	X	-	-	3
6	24	X	-	-	-	-	-	-	1
	25	-	-	X	X	-	X	-	3
	26	-	-	-	-	-	-	-	-
	27	-	-	X	-	-	-	X	2
	28	-	-	-	-	-	-	-	-
	29	-	X	X	-	-	-	-	2
7	30	X	-	-	X	-	-	-	2
	31	-	-	X	-	X	X	-	3
	32	-	-	-	-	-	-	-	-
	33	-	-	X	-	-	-	X	2
	34	-	-	-	-	-	-	-	-
	35	-	X	X	X	-	-	-	3
	36	-	-	-	-	-	-	-	-

Table 2: (Cont) Setting of "knots" due to different encoding procedures

Bft	Kts	A	B	C	D	E	F	G	Sum
8	37	X	-	X	-	X	X	-	4
	38	-	-	-	-	-	-	-	-
	39	-	-	X	-	-	-	-	1
	40	-	-	-	X	-	-	X	2
	41	-	-	X	-	-	-	-	1

A: Beaufort Equivalent in knots	NLD,FRG,UK,ISL
B: Beaufort Equivalent in whole m/s	USA
C: Contin. scale in m/s	USA, USSR, former GDR
D: Contin. scale in 5 knot increments	CAN, UK, NLD, FRA, POL, and others
E: Beaufort equivalent in m/s, (differs from B)	former GDR
F: Beaufort equivalent in knots (differs from A)	YUG
G: Additional "half Bft steps in knots (.. 15 21 27 33 etc.)	FRG and others

further: (all observers)

Preference of even numbers, preference of end digits 0 and 5
Preference of end digits 0 2 5 8 (Israel)

Distribution of observations
total: 537637

NL	7%
USA	27%
UK	27%
F	5%
CAN	0.5%
FRG	17%
ISR	5%
USSR	1%
YUG	2%
POL	3%
GDR	2%

Table 3: Conversion of speeds in knots (encoded according to WMO Beaufort scale, resulting from estimations), into "real speeds" (m/s) at 25m height above sea level. The "real speeds" are lower boundary values for the original knot classes.

Conversion Table - German Wind Observations

Knots	0	1	2	3	4	5	6	7	8	9
00	0.0	1.6	1.7	3.1	3.2	3.3	5.2	5.3	5.4	5.5
10	7.4	7.5	7.7	7.8	9.4	9.5	9.7	9.8	9.8	11.5
20	11.6	11.7	11.8	11.9	12.0	13.7	13.8	13.9	14.2	14.2
30	14.3	16.4	16.5	16.6	16.9	17.0	17.1	17.2	19.8	20.0
40	20.1	20.5	20.6	20.7	20.8	23.3	23.4	23.6	23.7	24.1
50	24.2	24.3	25.0	27.0	27.1	27.2	27.3	27.7	27.8	28.2
60	28.8	31.0	31.1	31.5	31.6	33.3	33.4	33.5	33.6	34.8

Conversion Table - Typical mix of foreign observations

Knots	0	1	2	3	4	5	6	7	8	9
00	0.0	1.8	1.9	2.7	2.8	3.4	4.1	4.5	4.7	5.2
10	6.1	6.6	6.7	7.2	8.0	8.4	8.6	9.1	9.5	10.2
20	10.7	11.0	11.3	11.6	11.9	12.9	13.2	13.4	13.8	14.1
30	14.5	15.8	16.0	16.2	16.5	16.8	17.2	17.4	18.9	19.1
40	19.5	20.2	20.5	20.8	21.1	22.3	23.0	23.2	23.7	24.1
50	24.4	25.0	25.4	26.6	26.7	27.1	27.5	28.1	28.2	28.8
60	28.9	31.0	31.1	31.7	32.1	32.5	33.0	34.2	34.4	35.2

Figure 1:

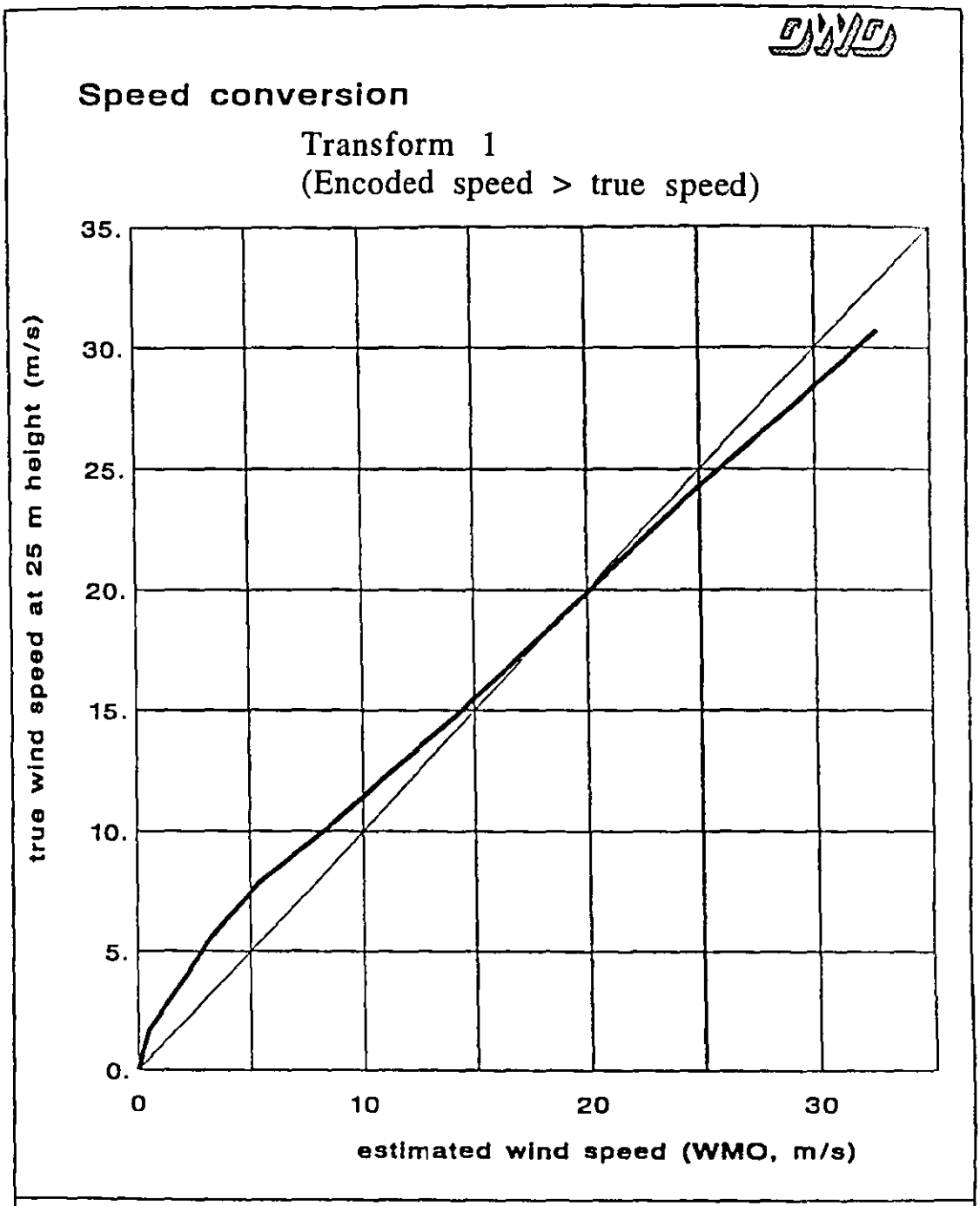

True wind speeds at 25 m height above sea level after KAUFELD (modified) versus estimated wind speeds (Beaufort estimates encoded to m/s according to the WMO scale)

Figure 2:

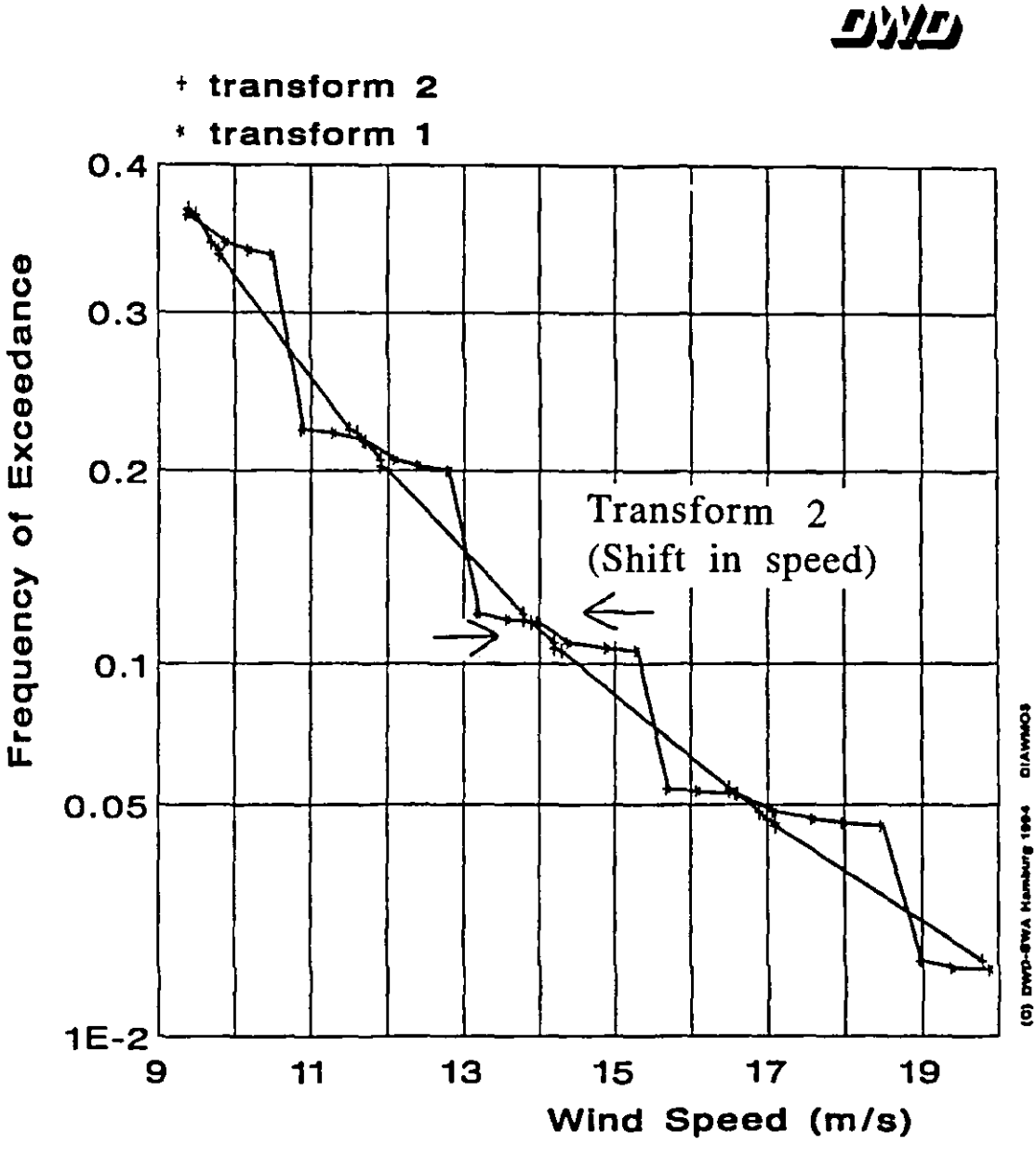

Frequency Distribution of Wind Speed in the North Sea

(only middle part, enlarged)

Figure 3:

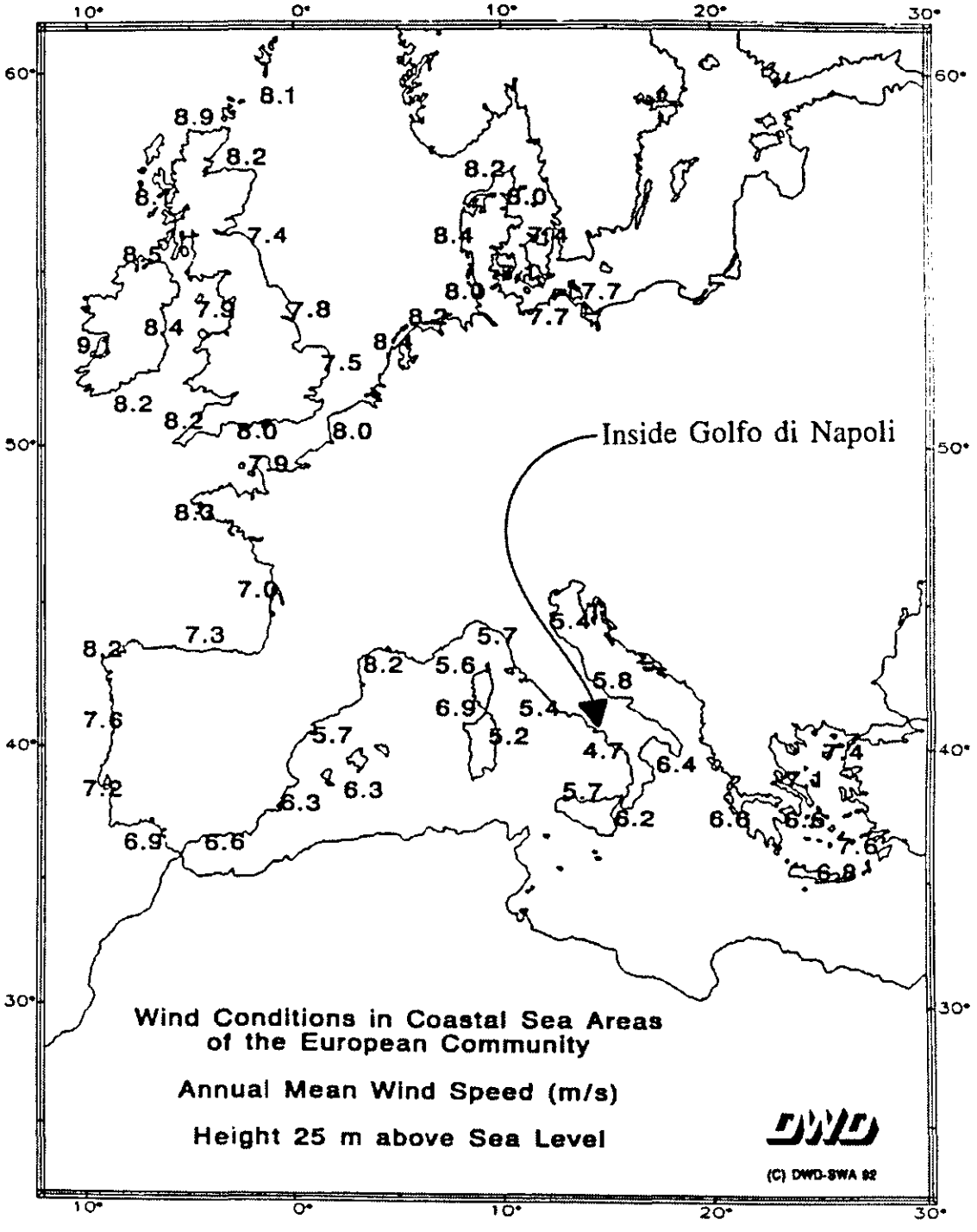
Inside Golfo di Napoli
Wind Conditions in Coastal Sea Areas
of the European Community
Annual Mean Wind Speed (m/s)
Height 25 m above Sea Level
DWD
(C) DWD-SWA 92

Standard Error Estimation of COADS Monthly Mean Winds

Mark L. Morrissey
Oklahoma Climatological Survey
University of Oklahoma
Norman, Oklahoma 73019

Jose A. Maliekal
Dept. of the Earth Sciences
SUNY Brockport
Brockport, New York 14420

Introduction

The Comprehensive Ocean-Atmosphere Data Set (COADS) contains ship observations from 1854 to 1990. Several versions of this data set are available including one containing individual ship reports of various meteorological and oceanographic measurements. The extremely large data volume of this version necessitated another version containing spatially and temporally averaged reports representing monthly averages over 2° x 2° areas (i.e. boxes). The highly variable distribution of ships, especially in tropical regions, produces considerable uncertainty in these box averages. One measure of the random error associated with the monthly averages is the standard error of the mean. Unfortunately, the small sample sizes and the difficulties of incorporating changing ship locations has hindered an early development of a robust standard error equation for COADS box averages.

By defining a grid system based upon the minimum spatial resolution of COADS individual ship reports (i.e. 0.1° x 0.1° latitude-longitude), a practical standard error relationship is presented which can be applied to the monthly averages. By developing the equation using the long-term mean, sample statistics, such as the point variance and the lagged correlation, are relatively unbiased making the standard error equation quite robust. The equation was initially developed for two dimensional fields by Morrissey et al. (1994), but is easily applied to three dimensional box averages.

Equation Development

A grid system is used whereby each 0.1° x 0.1° grid location is numbered systematically from 1 to 400 (i.e. 20 x 20) for hour 1 in the month, from 401 to 800 for hour 2 and so on. The sample time-space average for month m can be defined by,

$$\overline{X}_m = \frac{\sum_{i=1}^{N} x(i)\delta(i)}{n}$$

where $x(i)$ is an individual ship report (e.g. the u component) located at grid i, N is the total number of grid points and n is the number of ship reports in the box. An indicator variable, δ(i) is one if a ship is present at grid i and is zero otherwise. This variable is used to incorporate the ship locations into the equation. Also, the overall mean of the ship reports is removed from each $x(i)$ value. The field mean for month m is defined by

$$\mu_m = \frac{\sum_{i=1}^{N} x(i)}{N}$$

Morrissey et al. (1994) derived a practical form of the standard error equation by substituting these two expressions into

$$\sigma_{\bar{x}}^2 = E[\overline{X}_M - \mu_m]^2$$

and expanding to arrive at

$$\sigma_{\bar{x}} = \sigma\left[\frac{1}{n} + \frac{2}{n^2}\sum_{L=1}^{N-1}\rho(L)w(L) - \frac{2}{N^2}\sum_{L=1}^{N-1}(N-L)\rho(L)\right]^{\frac{1}{2}}$$

where σ = *point variance*

$$w(L) = \sum_{iu=1}^{N-L}\delta(i)\delta(i+L)$$

ρ(L) = *lagged auto correlation*

where $w(L)$ is a weight factor which is a function of the network configuration. The quantity in the large brackets is the variance factor which accounts for the sample size and the dependence among the reports in both time and space. The second term in the variance factor accounts for the variance of the sample mean about the long-term mean and the third term accounts for the variance of the population monthly field about the long-term mean. The second term is an estimate of the average correlation within the time-space volume. A clustered network will generally provide overestimates of the average correlation since $w(L)$ will be large when the correlation is large (i.e. L is small). Thus, the difference between terms 2 and 3 should be rather large for a clustered network.

Examining the Standard Error Equation

By assuming a two dimensional anisotropic exponential spatial correlation function (figure 1), the behavior of the standard error given specific grid configurations can be observed. Four grid configurations are shown in figure 2, a random, a clustered, a uniform and a linear network (i.e. linear network #1). A fifth network (not shown) is a simple 90 degree rotation of the linear network #1 (i.e. linear network #2). By multiplying the denominator in the exponent of the correlation function by a constant, the e-folding distance along the major axis can be varied. It can be observed (figure 3) for different e-folding distances, the variance factor, and hence the standard error, generally decreases with increasing correlation. This results from the increased areal representation of a given ship report (i.e. increased dependence among ship reports). Also, linear network #2, which is aligned along the major axis of the spatial correlation function provides higher variance factor values per e-folding distance than does linear network #1. This is due to a larger amount of redundant information measured by linear network #2 (i.e. w(L) is large when the correlation is high). It can also be observed that for all of the networks except the random and uniform networks, the variance factor initially increases with increasing enfolding distances. This results from the increasing difference between terms two and three in the variance factor with these networks. This behavior is dependent upon, not only the network configuration, but the correlation function as well.

Relevance to COADS

The use of the long-term mean in the sample statistics means that the sample statistics should be relatively unbiased. Thus, the standard error equation is fairly robust. By estimating a representative time-space correlation function for different oceanic regions, the standard error of monthly box averaged wind components can be found given different COADS ship distributions. Thus, standard error estimates can now be produced for COADS 2° x 2° monthly averages.

References

Morrissey, M.L., J.A. Maliekal, J.S. Greene, and J. Wang, 1994: The uncertainty of simple spatial averages: The standard error equation, submitted to the *J. Climate*.

Figure 1: The two dimensional exponential correlation function used to test the standard error equation.

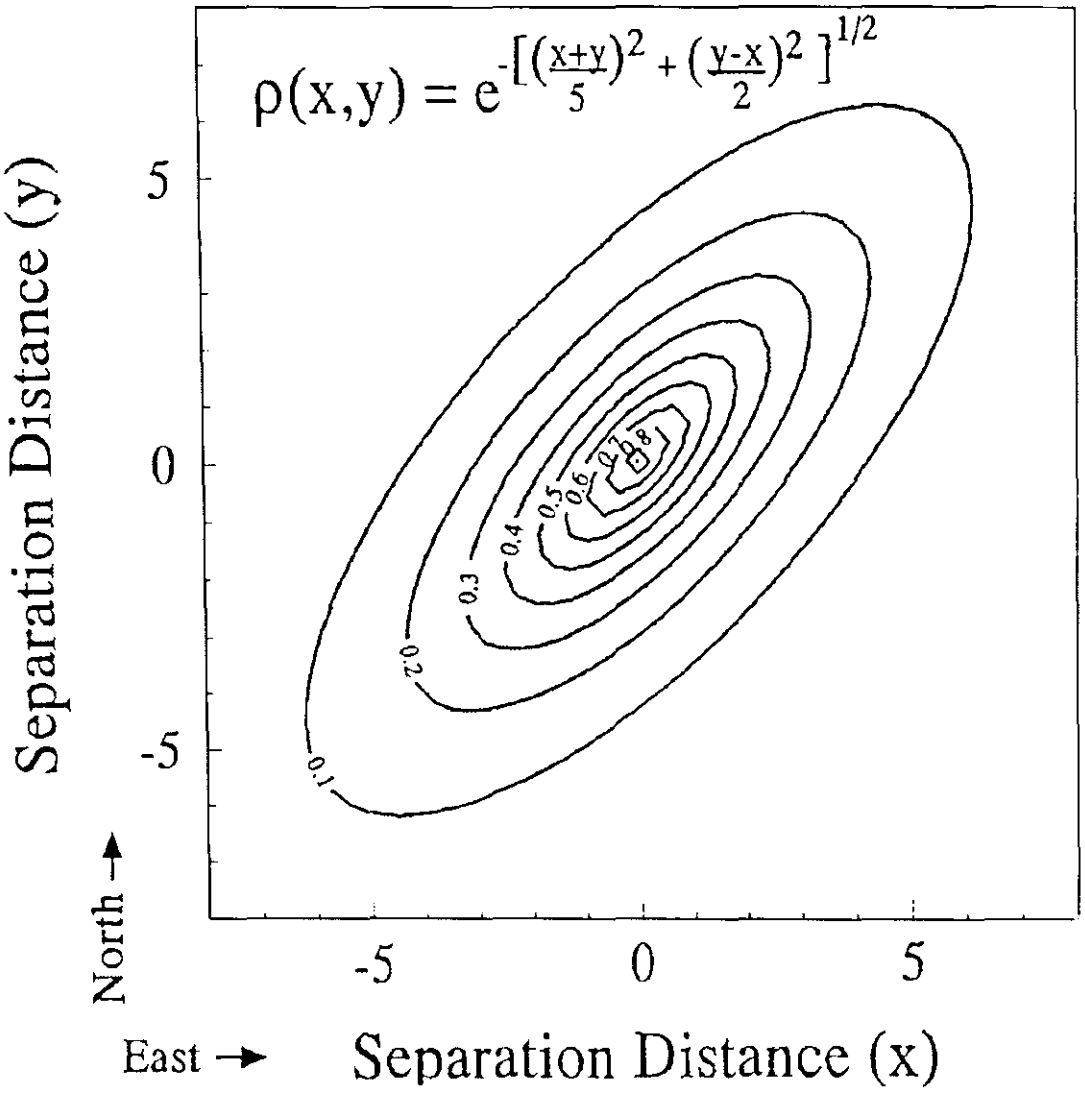

Figure 2: Four sample network configurations overlaid on a 100 x 100 grid.

Random Network

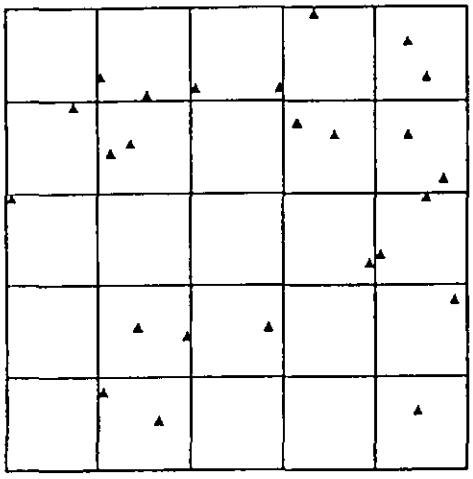

Clustered Network

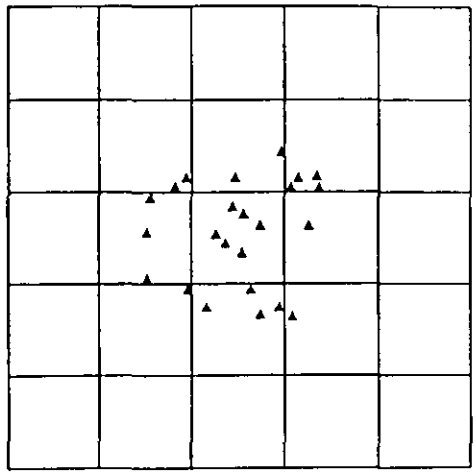

Linear Network #1

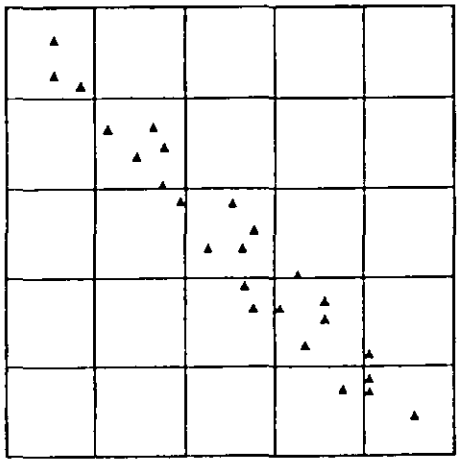

Uniform Network

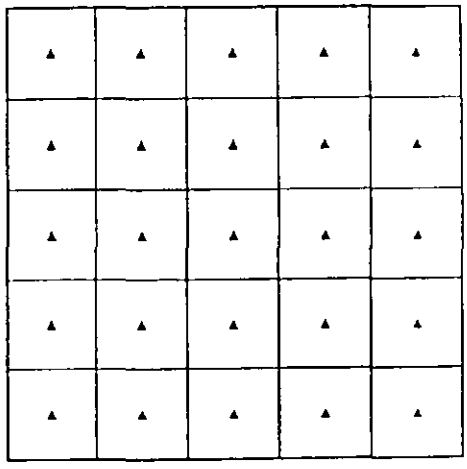

Figure 3: The variation of the variance factor defined in the text as a function of the e-folding distance using the anisotropic spatial correlation function shown in figure 1.

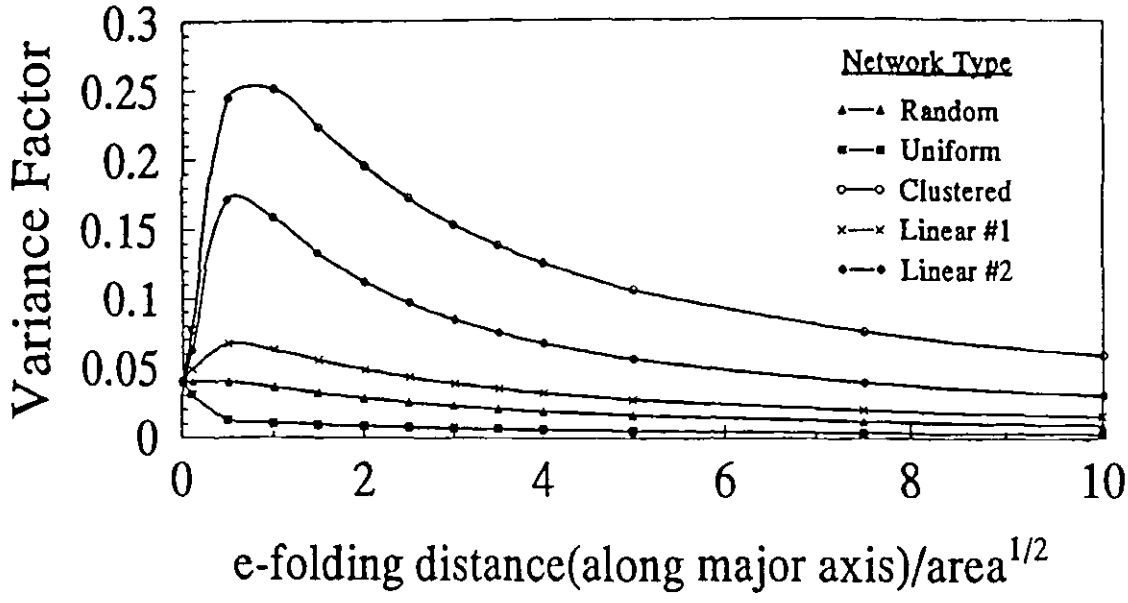

Effects of Different Wind Stress Climatologies on the North Atlantic Circulation: Model results

Claus W. Böning

IfM Kiel, Germany

Can we use ocean circulation models to test wind stress fields? Even in the case of a perfect model, several issues need to be considered if we want to learn something from comparing simulated volume transports with observations. Obviously, we have to identify circulation regimes where the oceanic transports are (predominantly) driven by the wind stress, so that changes in the winds have significant effects on the resulting circulation. In addition, we have to focus on those areas in the ocean where the transport is well-known from observations. In this report, I shall discuss these issues for the case of the North Atlantic. The model being used is that developed by Bryan and Holland (1989) as a "Community Modeling Effort" (CME) under the World Ocean Circulation Experiment (WOCE). The model spans the Atlantic Ocean between 15° S and 65° N. In recent years, a suite of model experiments has been conducted by the CME groups at NCAR and at IfM Kiel, differing in a number of model factors, including horizontal resolution, frictional parameterization, wind and thermohaline forcing. For model descriptions, list of experiments, and detailed accounts of the mean circulation in different parts of the basin, the reader is referred to Bryan et al. (1994) and Böning et al. (1994). Model results discussed in this report are all from a model version with a grid resolution of 1/3 deg. in latitude, 2/5 deg. in longitude, and 30 levels in the vertical.

Large-scale ocean circulation is forced by the momentum, heat and freshwater fluxes at the surface. The thermohaline forcing in the Atlantic Ocean is associated with deep water renewal in subarctic regions, driving an overturning motion with a northward flow of warm water in the upper 1000 or 1200 m, and southward flow of cold, North Atlantic Deep Water between 1000 m and 4000 - 4500 m. The deep flow has a strong impact on the vorticity balance of the horizontal circulation in the subpolar North Atlantic. Both the CME-results (Bryan et al. 1994) and diagnostic modeling by Greatbatch et al. (1991) suggest that the structure and strength of the subpolar gyre is governed by the thermohaline-driven flow and its interaction with bottom topography, and to a much lesser degree by the wind stress. (This does not hold, however, for the seasonal variability which, in good approximation, can be understood in terms of a linear response to the variation in the wind stress curl. Lack of data would presently not allow to use this behavior for a test of different wind stress fields in the subpolar North Atlantic.) A model evaluation in terms of a wind-driven transport has to be restricted to the upper-layer circulation in the tropics and subtropics, south of the Gulf Stream recirculation regime.

The second requirement noted above, knowledge of volume transports from observations in the ocean, readily lead to further restrictions. As recently discussed in the review of Schmitz and McCartney (1993), there is very little quantitative information on

oceanic transports; the singular exception for the North Atlantic is the transport through the Straits of Florida which had been studied over many years with different methods. The mean northward transport is 30 - 31 Sv, with little interannual variability, and a well-defined seasonal cycle. Both the mean and the seasonal variation of the Florida Straits transport had been studied with the CME model, using two different wind stress climatologies (i.e., HR and IH, respectively; see below) (Böning et al. 1991a). As it turns out, however, focusing on the Florida Straits transport alone is of limited value for a test of the wind driven circulation in the subpolar gyre. The seasonal variation of the Florida Current is largely due to the variation of the meridional wind stress along the coast (Böning et al. 1991a). The mean transport, on the other hand, only partly represents the northward return flow of the wind-driven, southward flow over the interior of the basins; about 40% is considered to be part of the meridional overturning (Schmitz and Richardson 1991). Some fraction of the wind-driven gyre flow does not enter the Caribbean Sea to feed the Florida Current, but flows northward in a western boundary current to the east of the Bahamas (in what is sometimes called the Antilles Current, though it does not represent a continuous flow along the Antillean Archipelago). In the context of model validation, this leads to at least two problems. First, even after several years of current meter measurements, there is considerable uncertainty about the mean transport due to a strong variability on monthly time scales, associated with a meandering of the current axis (Lee et al. 1990); recent estimates seem to converge at 5 - 10 Sv (at 26.5° N). Second, in model simulations the fraction of the flow entering the Caribbean through the narrow island passages must be sensitive to details of the topography, friction, etc. The situation for the 1/3-degree CME model is illustrated in Fig. 1, showing the mean flow in the western subtropical North Atlantic at 232 m and 2125 m, and Fig. 2, showing a zonal section of the mean meridional velocity at 26° N.

According to the situation described above a quantitative model-data comparison concerning the wind-driven transport in the subpolar gyre cannot focus on the Florida Current; it has to be based on the total northward transport in the western boundary currents (WBC) to the west and east of the Bahamas. Present estimates for this are 35 - 40 Sv (and one can expect the uncertainties to decrease over the next several years due to ongoing measurement programs east of the Bahamas). In addition we need information about the fraction of the total WBC transport associated with the thermohaline overturning. (Model results indicate that at this latitude, because of the confinement of the deep flow to the western boundary, the total northward transport may in good approximation be considered as a linear superposition of a thermohaline and a wind-driven part.) From zonal, transatlantic hydrographic sections along 25° N the overturning is estimated to be about 15 Sv, leaving 20 - 25 Sv for the net contribution of the wind-driven gyre to the northward, upper-layer flow at the western boundary. The transport budget at this latitude is schematically illustrated in Fig. 3.

CME experiments have been carried out with four different, monthly mean wind stress climatologies: the stresses based on historical marine observations given by:

(i) Hellerman and Rosenstein (1983); in the following denoted HR;

(ii) Isemer and Hasse (1987), denoted IH;

(iii) the model stresses given by Trenberth et al. (1990) based on their analysis of the 1000 mb winds of the ECMWF for the period 1980 - 1986, denoted ECMWF; and

(iv) monthly mean stresses from a 10 yr. control integration of NCAR's Climate Community Model 2; denoted CCM2.

A more detailed discussion of the mean circulation in these experiments may be found in Bryan et al. (1994). The wind stress climatologies in (i) and (ii) are compared in Böning et al. (1991b). The interesting question in the present context is to which extent these climatologies lead to differences in the transport of the subpolar gyre in the North Atlantic. As outlined above, this may be boiled down to a single number: the southward transport in the upper layer (top 1000 m) at 25° N, between the coast of Africa and the eastern edge of the WBC east of the Bahamas. The results are

24 Sv for HR
31 Sv for IH
25 Sv for ECMWF
19 Sv for CCM2.

These numbers represent averages over several years of integration. (For a discussion of the interannual variability see Bryan et al., 1994.) Comparison with the observed wind-driven transport indicates IH to be too strong, HR and ECMWF about right, and CCM2 somewhat too weak at this latitude.

In summary, it is important to stress the singularity of the situation at 25° N: it represents the only latitude in the North Atlantic where we both have fairly good information on the total volume transport and can, to a good approximation separate the relative contributions from the thermohaline and wind-driven flows. It is important to stress also, that for a model-data comparison a circulation model with sufficiently fine grid spacing to resolve the WBC system is required; and that a comparison can not be based on the well-measured Florida Current alone, but has to take into account the significant, but less-known transport to the east of the Bahamas.

References

Böning, C.W., R. Doscher, and R.G. Budich, 1991: Seasonal transport variation in the western subtropical North Atlantic: Experiments with an eddy-resolving model. *J. Phys. Oceanogr.*, 21, 1271-1289.

Böning, C.W., R. Doscher, and H.-J. Isemer, 1991b: Monthly mean wind stress and Sverdrup transports in the North Atlantic: A comparison of the Hellerman-Rosenstein and Isemer-Hasse climatologies. *J. Phys. Oceanogr.*, 21, 221-235.

Böning, C.W., F.O. Bryan, W.R. Holland, and R. Doscher, 1994: Thermohaline circulation and poleward heat transport in a high-resolution model of the North Atlantic. Submitted to *J. Phys. Oceanogr.*

Bryan, F.O. and W.R. Holland, 1989: A high-resolution simulation of the wind and thermohaline-driven circulation in the North Atlantic Ocean. In: parameterization of small-scale processes. Proceedings "aha huliko'a", Hawaiian Winter Workshop, University of Hawaii, 99-115.

Bryan, F.O., O.W. Boning, and W.R. Holland, 1994: On the mid-latitude circulation in a high-resolution model of the North Atlantic. Submitted to J. Phys. Oceanogr.

Greatbatch, R.J., A.F. Fanning, A.D. Goulding, and S. Levitus, 1991: A diagnosis of interpentadal circulation changes in the North Atlantic. *J. Geophys. Res.*, 96, 22009-22023.

Hellerman, S. and M. Rosenstein, 1983: Normal monthly wind stress over the world ocean with error estimates. *J. Phys. Oceanogr.*, 13, 1093-1104.

Isemer, H.-J. and L.Hasse, 1987: The BUNKER Climate Atlas of the North Atlantic Ocean. Vol. 2: Air-Sea Interactions. Springer Verlag, 256 pp.

Lee, T.N., W. Johns, F. Schott, and R. Zantopp, 1990: Western boundary current structure and variability ast of Abaco, Bahamas, at 26.5 N. *J. Phys. Oceanogr.*, 20, 446-466.

Schmitz, W.J., Jr. and W.S. Richardson, 1991: On the sources of the Florida Current. *Deep-Sea Res.*, 38, 379-409.

Schmitz, W.J., Jr. and M.S. McCartney, 1993: On the North Atlantic circulation. *Rev. Geophys.*, 31, 29-49.

Trenberth, K.E., W.G. Large, and J.G. Olson, 1990: The mean annual cycle in global wind stress. *J. Phys. Oceanogr.*, 20, 1742-1760.

Figure 1a: CME model estimate of mean flow in the western subtropical North Atlantic, at 232 m depth.

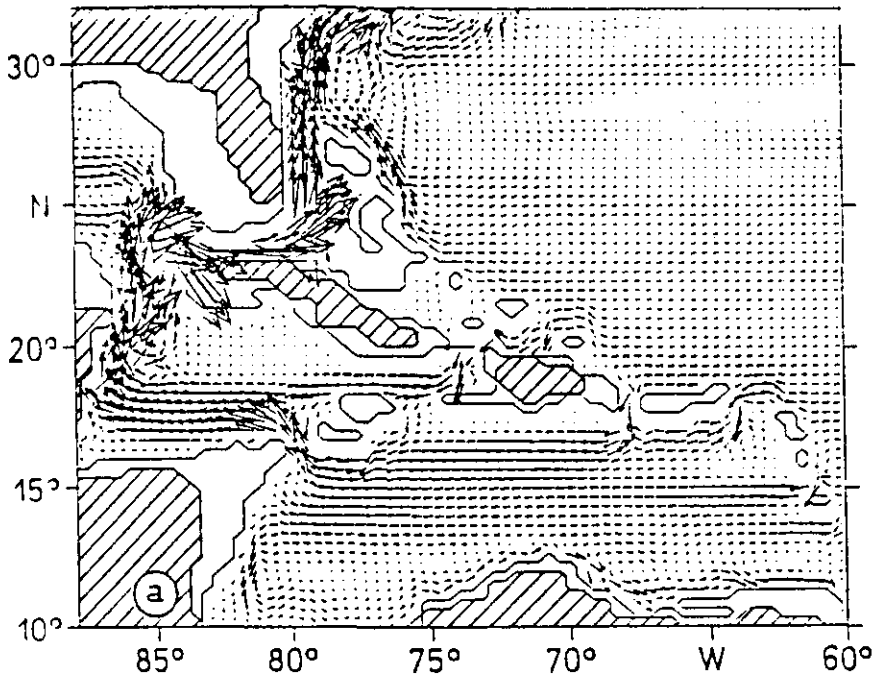

Figure 1b: CME model estimate of mean flow in the western subtropical North Atlantic, at 2125 m depth.

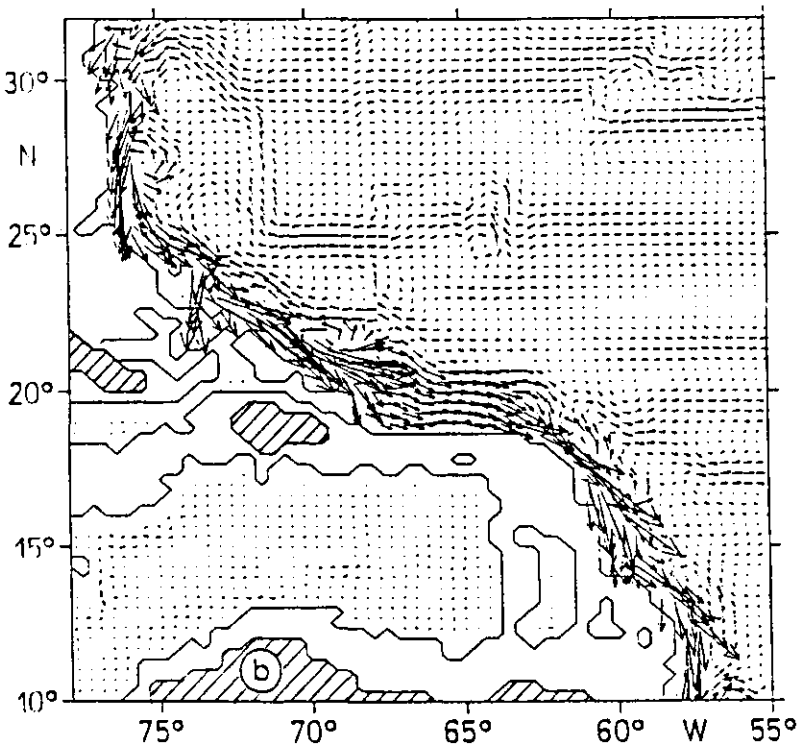

Figure 2: Zonal cross-section of mean meridional velocity near 26 N.

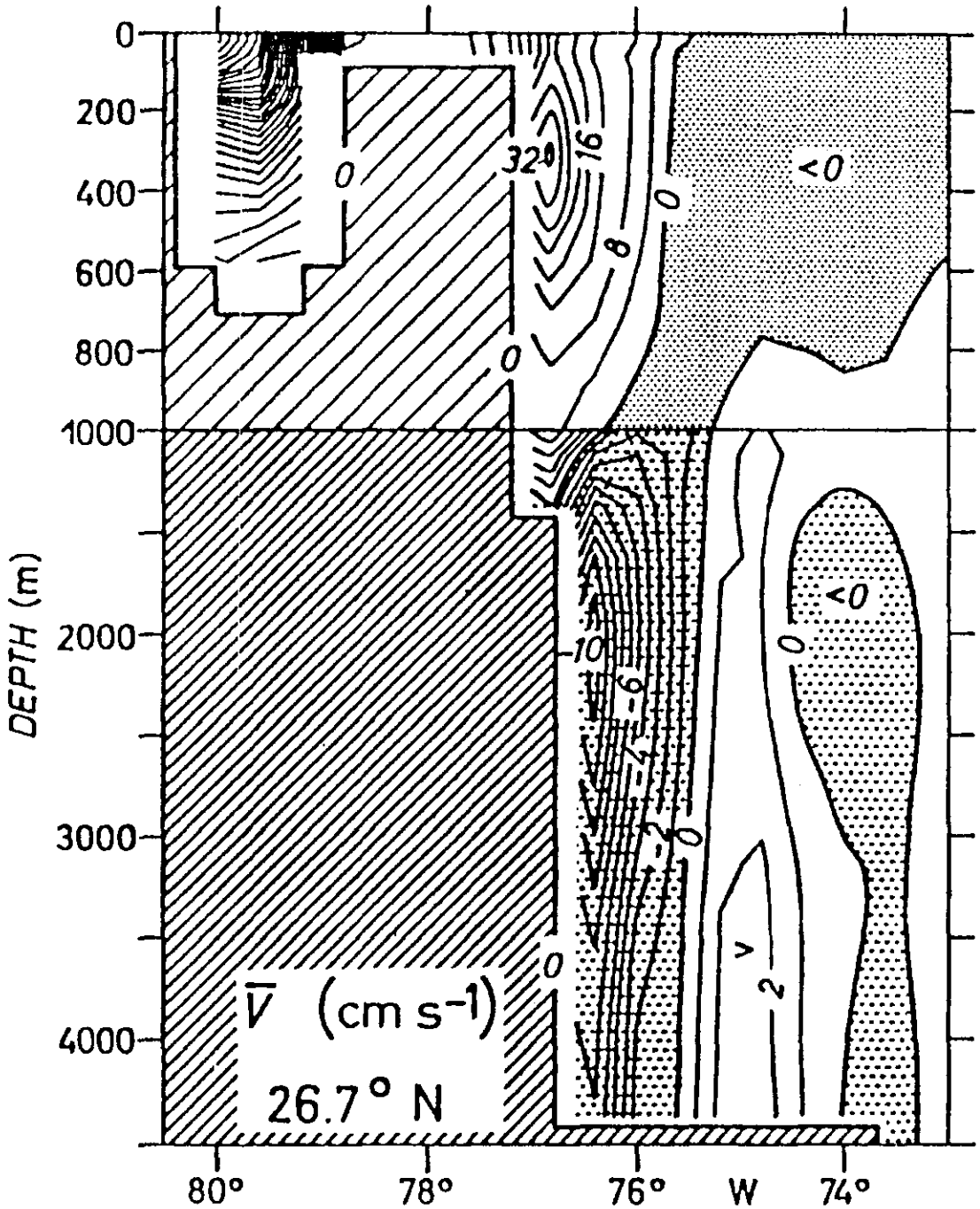

Figure 3: Oceanic transport budget at 26 N. Values is Sv.

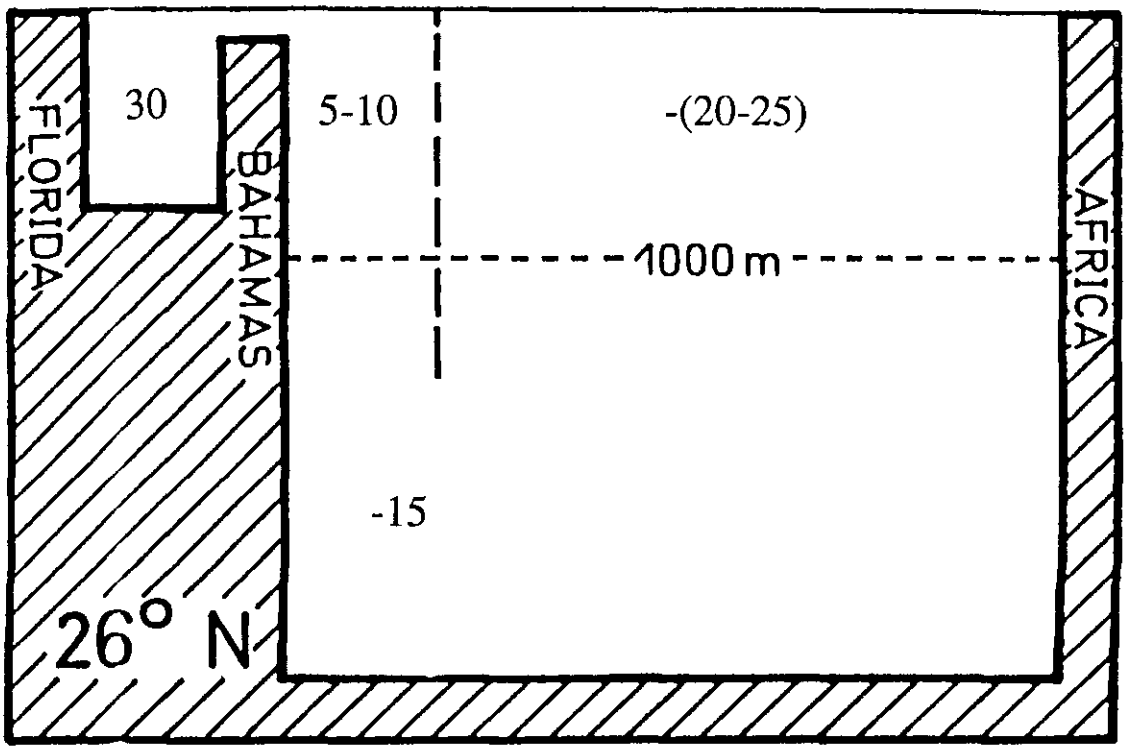

Part IV

Applications and Data Improvements

Use of COADS Wind Data in Wave Hindcasting and Statistical Analysis

V. R. Swail

Climate Research Branch, Environment Canada
Downsview, Ontario

Introduction

Wind observations from the Comprehensive Ocean Atmosphere Data Set (COADS) are used for two primary applications by Environment Canada: (1) the production of various wind statistics for design and operational planning, and (2) hindcasting of ocean waves, particularly in severe storms.

For wind statistics, the wind data are used directly in the Marine Statistics (MAST) interactive statistical analysis suite of programs (Swail et al., 1983), which produce both point statistics and contour analyses for marine climate atlases. Although problems relating to consistency in shipboard wind observations have been well documented (Dobson, 1981; Pierson, 1990), no modification is made to the wind observations in COADS for these analysis. It is generally considered that for these purposes that differences in measurement or observation methods are unimportant (e.g. Ramage, 1987). However, when these wind observations are used as input to wave hindcasting (or forecasting), or for other applications such as flux calculations, or for climate change detection, errors in wind observations become very important.

Wave Hindcasting using COADS Winds

It is well-documented that wind field errors are the single largest source of error in spectral wave modeling. Winds produced directly from numerical weather prediction models do not provide the same degree of accuracy for wave modeling as winds produced by kinematic analysis of wind fields from surface wind observations from ships and buoys (e.g. Khandekar et al., 1994). However, since the wave models are very sensitive to the wind input, it is very important to remove as many of the sources of error as possible from the data.

Wind observations from COADS may be either anemometer measurements or estimated by an observer, either from the state of the sea, or from the effect of the wind upon the ship (or the observer). There is no way to determine which method of estimation was used for a report. In order to carry out an accurate wave hindcast the surface winds must be adjusted to provide a consistent set of values. The following paragraphs briefly describe the corrections applied to both measurements and estimates

to arrive at a consistent wind field. The method is described in detail by Cardone et al. (1990).

Wind speed reports based on Beaufort estimates are adjusted to 20 m using the Beaufort equivalent scale developed by Cardone (1969). This scale was derived from paired estimates from British and Canadian weather ships in the open ocean, and related the Beaufort number to a 20 m level. The official WMO (1946) scale relates to 10 m level winds, while Kaufeld's (1981) scale presumably relates to the 25 m level, the average height of the shipboard anemometers in his study; no reference level is specified for the WMO (1970) scientific scale. Cardone's and Kaufeld's scales diverge at Beaufort 12, likely due to the limited sample in Cardone's study at that wind speed class (9 occurrences). Otherwise, for neutral stability, the differences between Cardone's and Kaufeld's estimates due to reference level is about 3%. The Cardone scale (and the other newer scales) show that the operational WMO scale under light winds and over estimates strong winds. To correct, the reported wind speed, presumably derived from the operational scale, is related to the Beaufort force number. This is converted to a 20 m wind speed using Cardone's scale. No further correction is made for stratification, since the Beaufort estimates already incorporate this effect. The Cardone conversions fit the form:

$$U_{20} = 2.16 U_r^{7/9}$$

where U_r is the reported wind speed in knots. The method assumes that the estimate is made from the state of-the-sea rather than the apparent wind, which may or may not be true.

Dobson (1981) suggests that measured wind speeds from ships not be adjusted for height differences unless corrections are made at the same time for flow distortion effects. Since it is virtually impossible in practice to know even the sign of the flow distortion, let alone the magnitude, such a correction is never carried out except in limited experimental studies using calibrated ships. Nevertheless, the most commonly used techniques for adjustment of measured winds do incorporate some form of height adjustment. In this application, all wind measurements are adjusted for height and stability to the so called "effective neutral wind" at 20 m elevation, defined by Cardone (1969) as:

$$U_e(Z) = (U_* / k) \log[Z / Z_0(U_*)] \qquad (1)$$

where U_* is the friction velocity, k is the von Karman constant, and Z_0 is a roughness parameter. If the marine surface layer is neutrally stratified, the effective and actual 20 m wind speeds are the same. For non-neutral stratification, U_e is related to the actual wind through U_*. U_* is first calculated from the measured wind speed and air-sea temperature difference; then U_e, is calculated from (1), using anemometer heights determined from the WMO ship list where possible. However, many observations do not contain the call sign, or the anemometer height is not available for the reported call sign. In those cases

the anemometer height is assumed to be 20 m, close to the 19.3 m average height found by Cardone et al. (1990) based on nearly 3000 ships. In recent years the average anemometer height on Canadian cooperating vessels has risen to nearly 30 m, while buoys and drilling vessels provide measurements at about 5 m and 100 m respectively. Considerable efforts are made to identify data from such sources which depart significantly from the mean anemometer height. One further adjustment is made to Canadian buoy data, to account for the fact that those measurements are 10-min. vector averages, while all other measurements are scalar values. The effect may be as much as 7-12% for higher wind speeds. The approach is based on a linear analysis of the 8-sec gust speed reported by the buoy to the 10-min mean wind speed.

Figures 1(a-d) show the results of Cardone et al. (1990) in applying these techniques for the South China Sea. The measured winds as observed are significantly higher than the uncorrected estimated winds for speeds up to 15m/s. This tendency became more pronounced when the measured winds alone were corrected; when the estimated winds alone were corrected using Cardone's revised scale, there was an overcompensation, and the estimated winds were higher. Only when both the estimated and measured winds were corrected as described above did the wind speeds match reasonably well.

It can be seen from Figures 2 and 3 that, when wave hindcasts are run with winds adjusted according to the procedures described above, the results are very accurate, implying that the wind fields are temporally and spatially consistent. Figure 4 shows that when these wind adjustments are applied (Run 4), the results are considerably improved for all wave height classes than when observed winds are assimilated uncorrected into NWP model runs. It should be recognized however that many problems may still exist with individual wind observations, including observer errors, instrument calibration, flow distortion effects, improper averaging intervals, uncertainties in atmospheric stability, unknown true anemometer height. Cardone et al. (1990) point out that such sources are apt to introduce random errors which are likely to average out if sufficient data are available. However, the Beaufort equivalency scale introduces systematic errors. Because it is biased low at low wind speeds and high at high winds speeds it alters patterns as well as overall amplitudes.

Correlation Analyses

The blending of wind observations into an analysis field requires information on the shape of the spatial auto correlation function for each data source, and the intrinsic noise level of each data source. The slope of the decay of wind speed correlation with distance provides information on the structure of the wind field and the quality of the data - the magnitude of the correlation coefficient in minimum separation classes gives an indication of the noise in the observation method. By itself, spatial correlation cannot distinguish "true" noise (i.e. from sensors, flow distortion, etc.) from small-scale wind variability, and it yields no information about the accuracy of a wind observation technique. When applied to a number of different observing techniques, spatial correlation analysis provides useful information without the problem of which method should be considered the independent variable. Brown and Swail (1988) applied spatial

correlation analysis techniques to investigate the structure and noise levels of marine wind observations off the east coast of Canada for measured and estimated ship winds, as well as winds from drilling platforms winds, satellite and buoys. In the analysis, pairs were constructed of all possible combinations of wind speeds observations at the same report time, randomly reversed to ensure no geographic bias, and the great circle distance between them calculated. Separation classes for both coarse scale (100 km) and fine scale (10 km) were considered.

The correlation results are shown in Table 1. For most distance classes, measured ships have higher correlation's than estimated ships. The drilling platform winds show much higher correlation's than the measured ship winds. There are several likely explanations for this: (1) 8-10 platforms accounted for most of the drilling platform comparisons; (2) the platforms are mostly structurally similar, i.e. semi-submersibles with anemometers mounted on top of the derricks, (3) the range in anemometer heights is not large, (4) since the platforms are not moving, no errors are introduced in computing the true wind from the relative wind. As would be expected, correlation's of wind data from satellite scatterometer were very high. Microwave radiometer coefficients were significantly less than the scatterometer values; this is likely attributable to data problems with the SMMR instrument. Decreases in correlation of estimated winds at night (0.52) were consistent with similar decreases found by Laing (1985) for waves; measured winds were not greatly affected at night, except for increased variability.

References

Brown, R.D., and V.R. Swail, 1988: Spatial correlation of marine wind speed observations. *Atmosphere-Ocean* 26: 524-540.

Cardone, V.J., 1969: Specification of the wind distribution in the marine boundary layer for wave forecasting. Report TR69-1, New York University, New York, N.Y., I31 pp. [NTIS AD 702 490].

Cardone, V.J., J.G. Greenwood and M.A. Cane, 1990: On trends in historical marine wind data. *J. Climate*, 3: 113-127.

Cardone, V.J., and V.R Swail, 1994: On surface wind and ocean wave coupling in severe marine extratropical cyclones. Proc. Symposium on the Life Cycle of Extratropical Cyclones, Bergen, Norway, June 25-July 1, 1994. American Meteorological Society, Boston, MA.

Dobson, F.W., 1981: Review of reference height for and averaging time of surface wind measurements at sea. Report No. 3, Marine Meteorology and Related Oceanographic Activities. World Meteorological Organization, Geneva, Switzerland, 56 p.

Kaufeld, L. 1981: The development of a new Beaufort equivalent scale. *Meteor. Rundsch.*, 34, 17-23.

Khandekar, M.L., R. Lalbeharry and V.J. Cardone, 1994: The performance of the Canadian spectral ocean wave model (CSOWM) during the Grand Banks ERS-1 SAR wave spectra validation experiment. *Atmosphere-Ocean* 32: 31-60.

Laing, A.K., 1985: An assessment of wave observations from ships in southern oceans. *J. Clim. Appl. Meteor.* 24: 481-494.

Pierson, W.J., 1990: Examples of, reasons for, and consequences of the poor quality of wind data from ships for the marine boundary layer: implications for remote sensing. J. Geophys. Res. 95: 13,313-13,340.

Ramage, C.S., 1987: Secular change in reported surface wind speeds over the ocean. *J. Clim. Appl. Meteor.*, 26: 525-528.

Swail, V.R., A. Saulesleja and T. Mathews, 1983: A climatological analysis system for decision makers, Proceedings 8th Conference on Probability and Statistics in the Atmospheric Sciences, Hot Springs, Arkansas, p. 105-110.

Table 1: Summary of Minimum separation class values for r_s,, as a function of observing method.

Method	r_s(0-10 km)	r_s(0-100 km)
SEASAT-A Scatterometer	-	0.93
Bouy	0.90*	0.81‡
Drilling Platforms	0.84	0.85
NIMBUS-7 RADIOMETER (SSMR)	-	0.79
Ship (measured)	0.65	0.69
Ship (estimated)	0.66	0.64
Ship wind-wave (Laing, 1985)	-	0.43†

* refers to separation of 40 km; ‡ refers to separation of 110 km; † refers to separation class 0-74 km.

Figure 1: Comparison of monthly mean wind from (a) estimated and ship winds as reported, (b) adjusted estimated winds and reported measured winds, (c) reported estimated winds and adjusted measured winds, (d) both estimated and measured winds adjusted. Mean difference and ratio of points below the line to total points are given. (after Cardone et al., 1990)

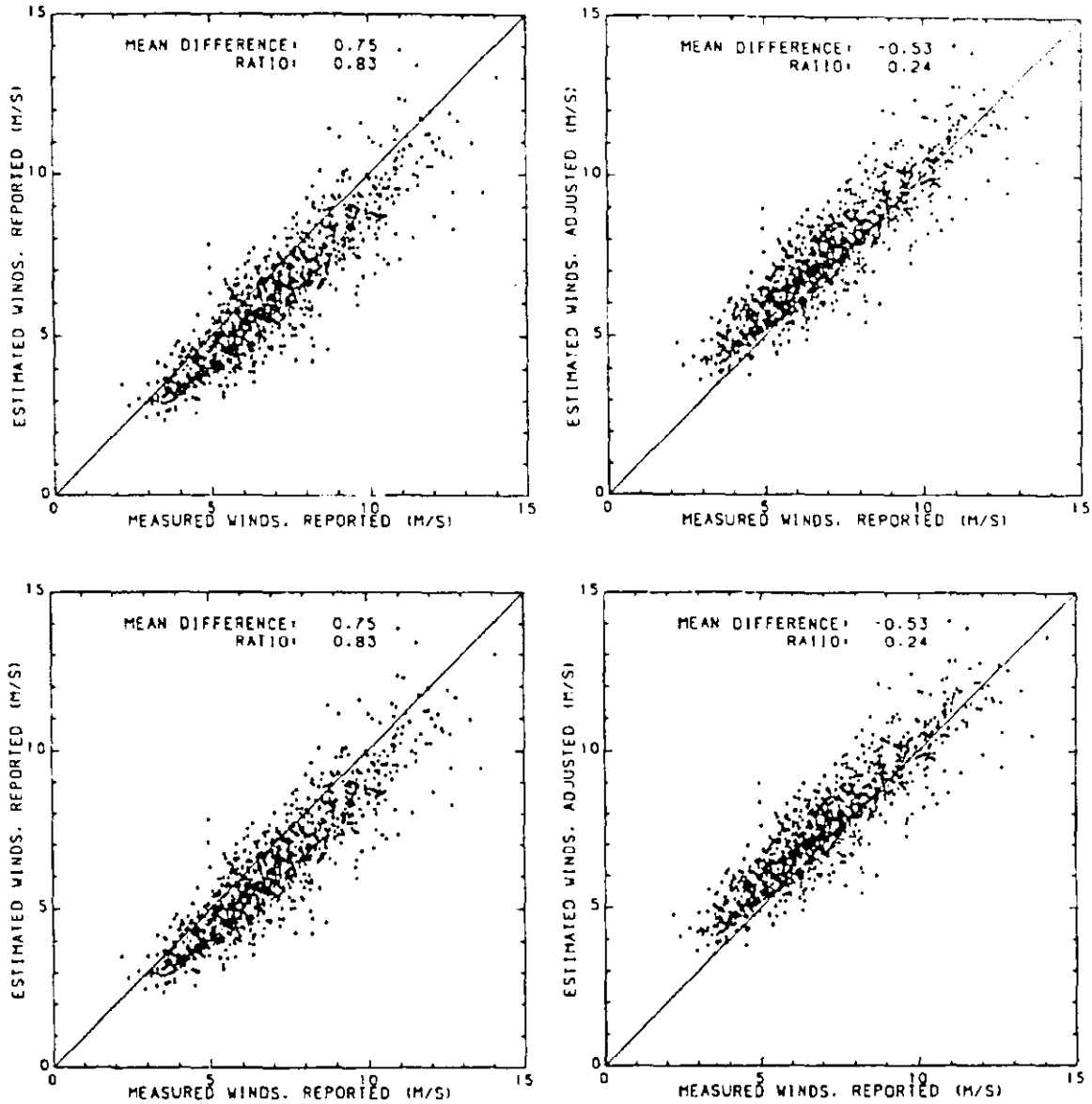

Figure 2: 3-G hindcast from kinematic winds, and measured HS at buoys north (a) and south (b) of the cyclone track in SWADE IOP-1. (after Cardone and Swail, 1994)

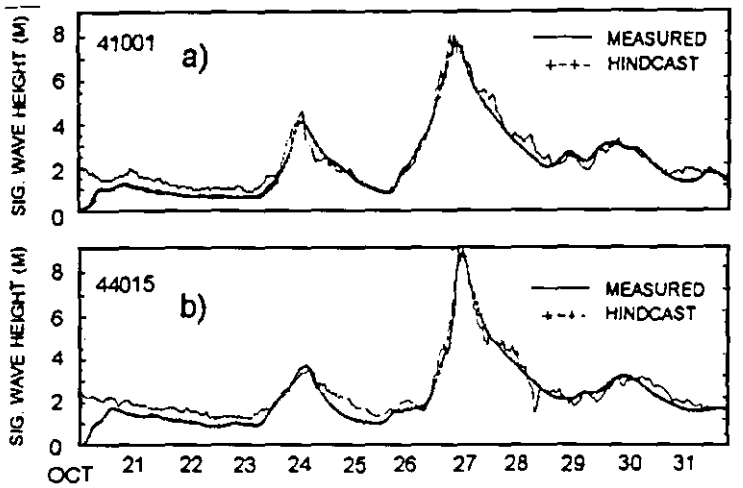

Figure 3: Wave Hindcast at buoy 41002 using adjusted wind fields in the Storm of the Century, March 11-18, 1993

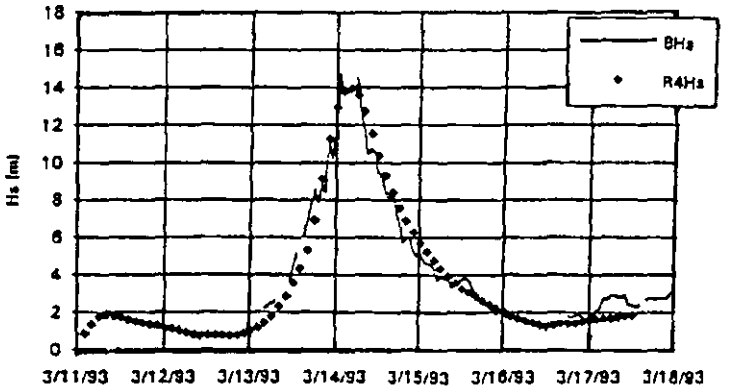

Figure 4: Wave height error statistics by percentile for adjusted wind speeds (solid line) versus model winds (dashed lines) compared to buoy observations in the northwest Atlantic ocean.

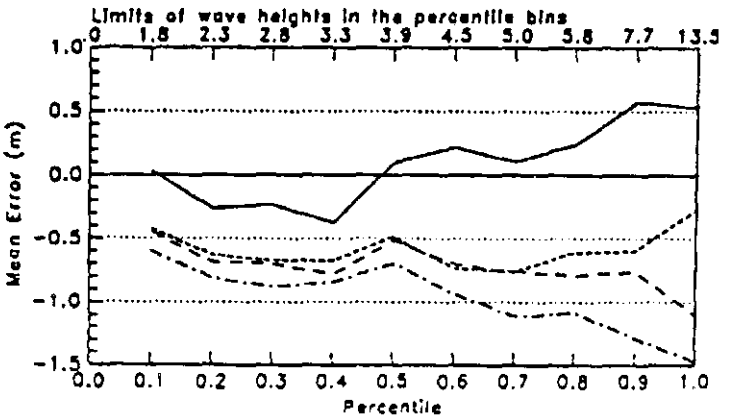

Scales of Coastal Wind Variability Addressed by COADS Wind Summaries in 2° Square Areas

Fredric A. Godshall[1], Henry A. Walker[2] and Stephanie C. Cayula[1]

[1]Science Applications International Corp.
[2]U.S. Environmental Protection Agency

U.S. EPA Environmental Research Laboratory
Tarzwell Dr., Narragansett, RI 02882

Abstract

Randomly selected periods of COADS archive wind data in U.S. Mid-Atlantic 2° square summary areas are a basis for estimates of wind variability between decades of wind summary periods. Similar treatment of coastal observations provide estimates of decades variability which is compared with the COADS summaries variability. The variability is expressed in terms of speed and direction components of the wind as vector parameters. Spatial variability is also examined to determine the representativeness of 2° COADS spatial summaries in coastal gradients of wind variation. The representativeness of decade COADS summaries, to define intra-regional scales of climate variability, is tested by comparing observed change with change expected from theoretical boundary layer processes. Periods of northern hemisphere air temperature variation are used as indicators of climate variability and these periods are used to evaluate the resolution of such variability with COADS wind data. Wind constancy computed from COADS wind summaries is used to evaluate possible long period changes of wind over the North Atlantic.

Introduction

The coastal zones are known to be areas with large spatial changes because of physical differences between land and water surfaces that affect the atmosphere boundary layer. The temporal changes are related, in the short term, to boundary layer adjustment from contrasting land and water surfaces and, over longer periods, to responses of the coastal zone to influences of air-sea interaction and meteorological regimes. These regimes might include wind direction or speed changes and atmospheric circulation with different meteorology.

Wind forces are important parameters of environmental change in the coastal zone where marine circulation in shallow water may be controlled by wind effects. Wind forced circulation influences coastal navigation, fisheries productivity, and water quality of coastal embayments.. Therefore understanding wind variation along coastal regions and trends which may obscure optimum coastal resource management are topics to be served by data archives. This paper will evaluate how 2° square area summaries of wind data in COADS serves coastal analyses in the mid-Atlantic region of the United States (Figure 1). The evaluation is offered as an example of COADS use to define climate related change in any coastal region.

Wind change and comparison of wind records is based on the treatment of wind as vector quantities. Wind vector comparisons between locations (spatial changes) and between decade and long-term means (temporal changes) are quantified by their direction and speed differences through a least-squares procedure (Godshall et al., 1976; Figure 2). The comparison results are estimates of direction and speed adjustments which could be applied to one of data sets to make the wind similar to the basis of comparison, i e. the long-tern mean or the basic station, Boston, MA. When these direction (phi) and speed (nu) adjustment factors are mapped they provide a measure of the spatial variability of the wind and when these factors are compressed between different decades, temporal variations are quantified. These factors from the vector comparisons are computed as if no correlation between changes of speed and direction exist. Any climate variation with feed-back effects on wind is assumed to envelope the whole study area but physical differences in each 2 study area are assumed to produce a local orientation to any wind regime over the area.

The temporal variability in each COADS 2° square are based on decade summaries of wind data compared to long-term monthly averaged data from the period 1900 to 1989. Although the use of decade summary periods for wind circulation analysis is empirical, decade summaries by Budyko(1977) have shown wind circulation and Godshall et al. (1991) have defined change in U.S. coastal regions from decade summaries. In this paper, the statistical significance of temporal change from decade wind summary is based on comparison of summary results with wind variations from ten-year data groups of randomly selected dates.

Spatial changes of decade summarized COADS 2 winds are quantified by change relative to Boston, MA an observation station located northwestward and up-wind of the study area. Observed spatial changes are related to expected changes in the atmospheric boundary layer from ocean surface temperature variations and surface-drag characteristics. The significance of these changes is based on geographic distribution of wind summaries characteristics relative to the geographic distribution of surface changes.

Spatial Changes

COADS 2° square wind summaries for each month were computed from derived U (east/west) and V (north/south) wind components (NOAA, 1985). We mapped long-term means from these resultant wind data over the period 1900 to 1992 and these resultant U and V components are the basis for winter (average of COADS data from January, February and March) wind direction and speed (Figures 3a, b). The distribution

of winter wind is produced from the broad-scale pressure distribution over the western Atlantic. The area of the subtropical anticyclone (the Bermuda High) and the area of low pressure over the north Atlantic (the Iceland Low) are the primary features of the pressure distribution. These wind maps also show the average wind speed and direction of winter season wind at Boston, MA, Providence, RI New York, NY, Baltimore, MD, and Norfolk, VA. Visual comparison of the wind from these on-land stations with the wind characteristics offshore from COADS indicates the wind characteristics are similar over the whole mid-Atlantic region. Therefore, spatial changes of wind within the region are interpreted to be caused by local influences.

Over the mid Atlantic region, the COADS winter wind data are compared with Boston winter winds within decade periods. Figures 4a, b, c, and d show the regional-scale spatial change of wind, measured by the phi and nu factors, during the decades from 1950 through 1990. All these decade summaries of COADS winds show the same general spatial distribution of change which we attribute to atmospheric boundary layer changes. The mean position of the winter season Gulf Stream (NOAA, 1975-1992) is within the area of negative or low positive magnitude phi factors. The relationship between Gulf Stream and these phi values is interpreted to indicate areas where the atmospheric boundary layer vertical mixing is forced by surface heating. Vertical mixing brings the influence of upper-level winds to the surface which is expected to cause cyclonic (counter-clockwise) turning of surface wind fields in the mid-Atlantic region (U.S. Navy, 1958). Nu factors increase in these same areas with relatively low phi factors which indicate the winter winds increase relative to wind in areas westward and north of Gulf Stream influence. The local increases in wind speed are expected from the vertical exchange of momentum in air from aloft with the air near the surface. These effects from relatively warm surface water temperatures which are shown over decades are also shown by Figures 3a, b the long-term mean directions and speed

Temporal Changes

Temporal variability of decade averaged-wind at each station or COADS summary area is the basis used for climate variability description. The temporal variation is measured by the relative change of each decade from the long-term mean conditions at that same station or area Estimates of significance of these changes are based on expectation that multiple data samples, such as numerous decades, will have statistical quantities, means and standard deviations, which will vary from data set to data set. For each station and COADS summary area we produced multiple ten-year data sets by randomly selecting the data years to be included in each set. The frequency distributions of 30 ten-year periods wind factors from Boston, from a 2° summary area centered at 39°N, 71°W are shown in Table 1. Table 2 lists the nu and phi factors computed from the decades of data (1950-1959, 1960-1969, etc.). The significance of the decade nu and phi are judged relative to the distribution of these factors frequency distributions. For example, the Boston winter change in wind direction relative to the long-term mean, given as phi, is 6.7883° in the decade 1960-1969. From Table 1 we see that a phi of this magnitude is expected from less than 5.0 percent of ten-year periods. Therefore, the change in this decade averaged wind at Boston is significant at a confidence level better than 95 percent.

The phi factors from the COADS 2° square area decades 1920-29 and 1970-79 and the nu from the decades 1900-09 and 1920-29 are significantly different from expected factors at the 95 percent confidence level. However, the lack of association of these wind changes with another changing parameter of climate, such as air temperatures (Figure 5), reduces the physical significance of these COADS indicated changes.

The decade summary for wind analysis was tested by computing nu and phi factors from the multiple data sets (set sizes 5, 10, 15, 20, 25, 30, 35 and 40) of randomly chosen dates from the Boston data record 1949-1992 (NOAA, 1949-1992) and from the data records 1900-1992 from the COADS summary area centered at 39°N, 71°W. The standard deviation of nu and phi factors from these data sets are graphed with data sets sizes in Figures 6a, b. As expected, these examples show the magnitude of standard deviation of nu and phi changes little when large sets are increased by the magnitude of standard deviation changes significantly when small data sets are increased. We recognize the convergence of standard deviations to constant value as the random set size approaches the data record size but we hope the principle expectation for a consistent statistic from large data sets is demonstrated. We fit an empirical function with power of data-set-size as independent variable and factor standard-deviation the dependent variable. The magnitude is decreasing through the decade size data set. Therefore, the decade size data set is not quite large enough to provide a stable statistic but relatively consistent statistical measure is expected from data sets of about 20-30 years. The data records are not very long from on-land observation stations and data sets larger than decade would prevent interpretation of temporal change. However since the decade summaries are known to be effective for analysis of climate, we have elected to use these summaries also even though variation from one period to another may be increased by this choice.

Climate is a condition resulting from many environmental variables but, considering climate change to be a change in any of the variables, changes of air temperature are indicators of climate change. The periods of temperature changes at New Haven, CT (Figure 5) are used here to indicate periods of change in the mid-Atlantic region. Decade summaries of wind data from island stations (Table 3) indicate a northward wind shift, relative to long-period average wind conditions during the period of cool air temperatures, roughly 1945 to 1970. However, none of the COADS 2° square decade summaries show these same periodic changes in wind.

The COADS Summaries

The COADS wind data summaries for each summary area were produced with quality control which prevented data values of a magnitude greater than 3.5 standard deviations(3.5 sigma) from entering the summaries (NOAA, 1993). Review of these "standard" summaries revealed the possibility of storm-wind exclusion from the summaries and, during the period 1980-1992, "enhanced" wind data summaries were produced that allowed 4.5 sigma wind magnitudes into the summaries. Quantitative comparison of the "standard" and the "enhanced" winter summaries in the 2° square areas in the mid-Atlantic region (Table 4) indicate little difference between these summaries results from the different quality controls. However, the Nu factors less than 1.0 indicate

the enhanced summaries generally have lower speeds than the standard summaries. This suggests the summarization processes allowed low speed winds into the enhanced summaries, however all the COADS standard and the enhanced sets were positively skewed relative to normal distribution.

Wind Constancy

In Figure 5b the long-term mean COADS wind speeds generally decrease northward of 50°N, , these northward Atlantic regions are known to be regions of frequent storms and high wind speeds. The relatively low wind speeds on this map are probably the effect of resultant wind computation in regions were the wind constancy is low (Figure 7). A map of wind factors for speed (nu values) computed from COADS 2° square area wind comparisons with Boston, MA (Figure 8) suggests the spatial distribution of nu values is similar to constancy. These winter wind speed factors and the wind constancy percentages are compared in Figure 9. The functional relationship between the factors and constancy in the trade wind zone is evidently different in the westerly wind regime that encompasses Boston. The mapped distribution of phi factors extend the geographic regions shown on Figures 4a-d is extended across the Atlantic in Figure 10. This map of factors simply illustrates the changes of wind regimes across the Atlantic.

We discovered no significant change in wind constancy from decade to decade based on the 2° square winter months COADS summaries (Figure 11).

Summary and Conclusions

The vector wind comparison computations from COADS produced estimates of differences between decade summaries of wind and long-term means. In an attempt to assess the utility of COADS 2° area wind summaries in climate analysis of coastal regions we defined periods of climate variation in the mid-Atlantic regions from air temperature changes. Comparison of the wind variation from island stations and the COADS summaries with these periods of temperature change indicates that singly, COADS 2° area summaries are poor sources of data to evaluate climate variability from decade to decade. However, changes over groups of 2° areas provide information about climate.

The relatively low mean wind speeds mapped in 2° square areas north of 50° are suspected to be a product of summarization processes. These latitudes are associated with stormy conditions and high wind speeds but these conditions are not well defined by computation of resultant wind vectors. Wind comparison factors computed from Boston appear to be closely related to wind constancy.

The comparison factors from Boston depict regional scales of change in air-sea interaction and the factors from the mid-Atlantic region appear to be part of the broad-scale distribution of factors of the North Atlantic.

Computation of enhanced COADS summaries probably does not provide unbiased summaries which include storm wind because of the inclusion of very low wind

speeds in the summaries. Perhaps special summaries which only contain the infrequent but important high wind data are necessary.

References

Budyko, M.I., 1977: Climate Changes American Geophysical Union, Washington, DC, 72-97.

Godshall, F.A., 1976: GATE Convection Subprogram Data Center: Analysis of Ship Surface Meteorological Data Obtained During GATE Inter comparison Periods, NOAA Tech. Rpt. EDS 17, 62-65.

Godshall, F.A., H.A. Walker, and G.R Mapp, 1991: Assessment of Responses to Climate Variation in the Marine Environment of Coastal regions of the United States, Global Change Research Project EPA-Narragansett, RI unpublished.

Hansen, J.. and S. Lebedeff, 1987: Global Trends of Surface Air Temperature, *Journal of Geophysical Research* 92, 13345-13372.

Ingham, M.C., 1982: Weather Conditions and Trends in the Maine-Virginia Coastal and Offshore Areas During 1970-79, Northwest Atlantic Fisheries Organization Scientific Council Studies, Number 5, 33-37.

National Oceanic and Atmospheric Administration (NOAA), 1985: COADS, Comprehensive Ocean Atmosphere Data Set, Release 1, Boulder, CO, Al- A18.

National Oceanic and Atmospheric Administration (NOAA), 1949-1992: Local Climatological Data Summaries, Asheville, NC

National Oceanic and Atmospheric Administration (NOAA), 1975-1992: The Gulf Stream, Washington, DC.

National Oceanic and Atmospheric Administration(NOAA), 1993: Comprehensive Ocean-Atmosphere Data Set (COADS) Release la: 1980-1982, *Earth System Monitor* (4) No. 1, 1-8.

U.S. Navy, 1958: Marine Climatic Atlas of the World, NAVAER50-lC-528, Washington, DC.

Table 1: Distribution of Nu and Phi Factors from Multiple (n=30) Decade Data Sets of Random Dates

		Nu	Phi
Boston MA			
	1st Quarter	0.964	-6.035°
	median	1.000	-2.623°
	3rd Quarter	1.018	0.605°
	95 percent	1.037	4.350°
COADS 2° area centered 39° N, 71° W		Nu	Phi
	1st Quarter	0.920	-2.457°
	median	0.970	0.631°
	3rd Quarter	1.074	7.119°
	95 percent	1.172	12.204°

Table 2: Nu and Phi Wind Factors for Decades of Wind Data

		Nu	Phi
Boaston, MA			
	(1950-59)	1.0433	5.429°
	(1960-69)	1.0545	6.788°
	(1970-79)	1.0026	-7.790°
	(1980-89)	0.9437	0.604°
COADS 2° area centered 39° N, 71° W			
	(1900-1909)	1.1961	1.0260°
	(1910-1919)	0.8066	2.2772°
	(1920-1929)	0.6965	-7.6314°
	(1930-1939)	0.8968	10.7698°
	(1940-1949)	1.1378	7.0156°
	(1950-1959)	1.0178	-0.5424°
	(1960-1969)	0.9848	-1.3274°
	(1970-1979)	1.0700	-10.7744°
	(1980-1989)	1.0253	8.7477°

Table 3: Decade summaries of wind data from Islands in the Mid-Atlantic compared to long-period average wind.

		Nu	Phi
Nantucket Island			
	(1900-1909)	1.51	-4.41°
	(1910-1919)	1.40	-13.17°
	(1920-1929)	1.65	-20.45°
	(1930-1939)	1.29	-18.55°
	(1940-1949)	1.08	-2.03°
	(1950-1959)	0.52	19.18°
	(1960-1969)	0.61	14.60°
	(1970-1979)	0.61	9.05°
	(1980-1989)	0.59	35.26°
Block Island			
	(1900-1909)	1.27	-5.28°
	(1910-1919)	1.15	-6.36°
	(1920-1929)	1.32	-15.48°
	(1930-1939)	1.11	-20.24°
	(1940-1949)	1.15	1.38°
	(1950-1959)	0.91	12.62°

Table 4: Comparison of Standard and Enhanced COADS Wind Summaries for Winter

Location of 2° Summaries	Nu[1]	Phi
37° N, 73° W	0.998	0.791°
37° N, 71° W	1.000	0.378°
37° N, 69° W	0.981	0.221°
39° N, 73° W	1.004	0.803°
39° N, 71° W	0.962	-1.527°
39° N, 69° W	1.004	1.811°
41° N, 73° W	0.969	1.248°
41° N, 71° W	1.006	0.531°
41° N, 69° W	0.908	0.531°
[1]Wind comparison factors are applied to Standard summaries.		

Figure 1: Geography of middle Atlantic 35-43N and 68-78W.

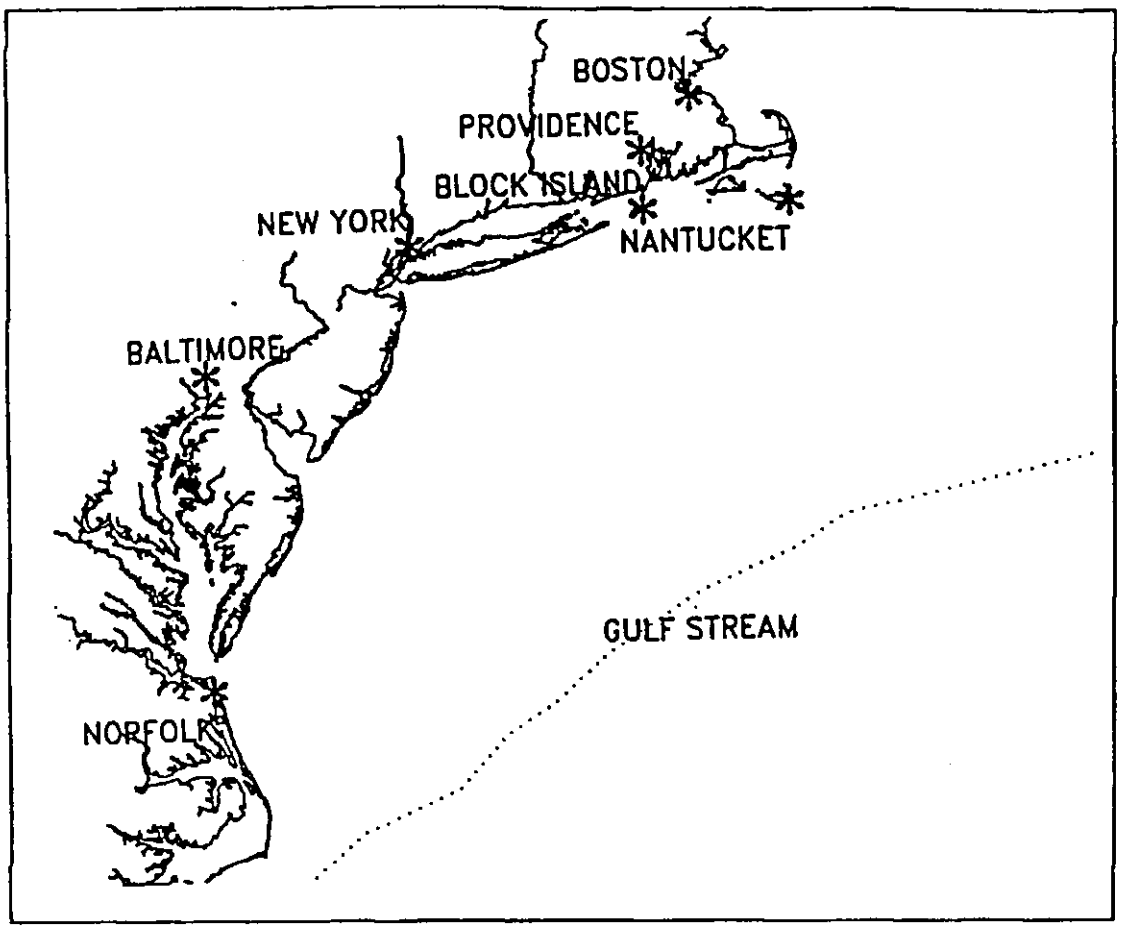

Figure 2: Wind Vector Differences and Ratio

$$R_k = \rho_k e^{i\theta_k}$$

$$D_j = \rho_{1j} e^{i\theta_{1j}} - \eta \rho_{2j} e^{i(\theta_{2j}+\phi)}$$

$$S = \sum_{j=1}^{N} |D_j|^2 = \sum_{j=1}^{N} D_j \overline{D_j} = \sum_{j=1}^{N} \left[(\rho_{1j} e^{i\theta_{1j}} - \eta \rho_{2j} e^{i(\theta_{2i}+\phi)})(\rho_{1j} e^{-i\theta_{1j}} - \eta \rho_{2e} e^{i(\theta_{2i}+\phi)} 0 \right]$$

$$S = \sum_{j=1}^{N} |D_j|^2 = \sum_{j=1}^{N} \left[\rho_{1j}^2 + \eta^2 \rho_{2j}^2 - 2\eta(\rho_{1j}\rho_{2j})\cos(\theta_{1j} - \theta_{2j} - \phi) \right]$$

$$\frac{\partial S}{\partial \eta} = \sum_{j=1}^{N} \left[2\eta \rho_{2j}^2 - 2(\rho_{1j}\rho_{2j})\cos(\theta_{1j} - \theta_{2j} - \phi) \right]$$

$$\frac{\partial S}{\partial \phi} = -2\eta \sum_{j=1}^{N} \left[(\rho_{1j}\rho_{2j})\sin(\theta_{1j} - \theta_{2j} - \phi) \right]$$

$$\eta = \frac{\sum_{j=1}^{N} (\rho_{1j}\rho_{2j})\cos(\theta_{1j} - \theta_{2j} - \phi)}{\sum_{j=1}^{N} \rho_{2j}^2}$$

$$\phi = \tan^{-1}\left[\frac{\sum_{j=1}^{N} \rho_{1j}\rho_{2j}\sin(\theta_{1j} - \theta_{2j})}{\sum_{j=1}^{N} \rho_{1j}\rho_{2j}\cos(\theta_{1j} - \theta_{2j})} \right]$$

Figure 3a: Winter Wind Direction from COADS 2° Summaries (1900-1992).

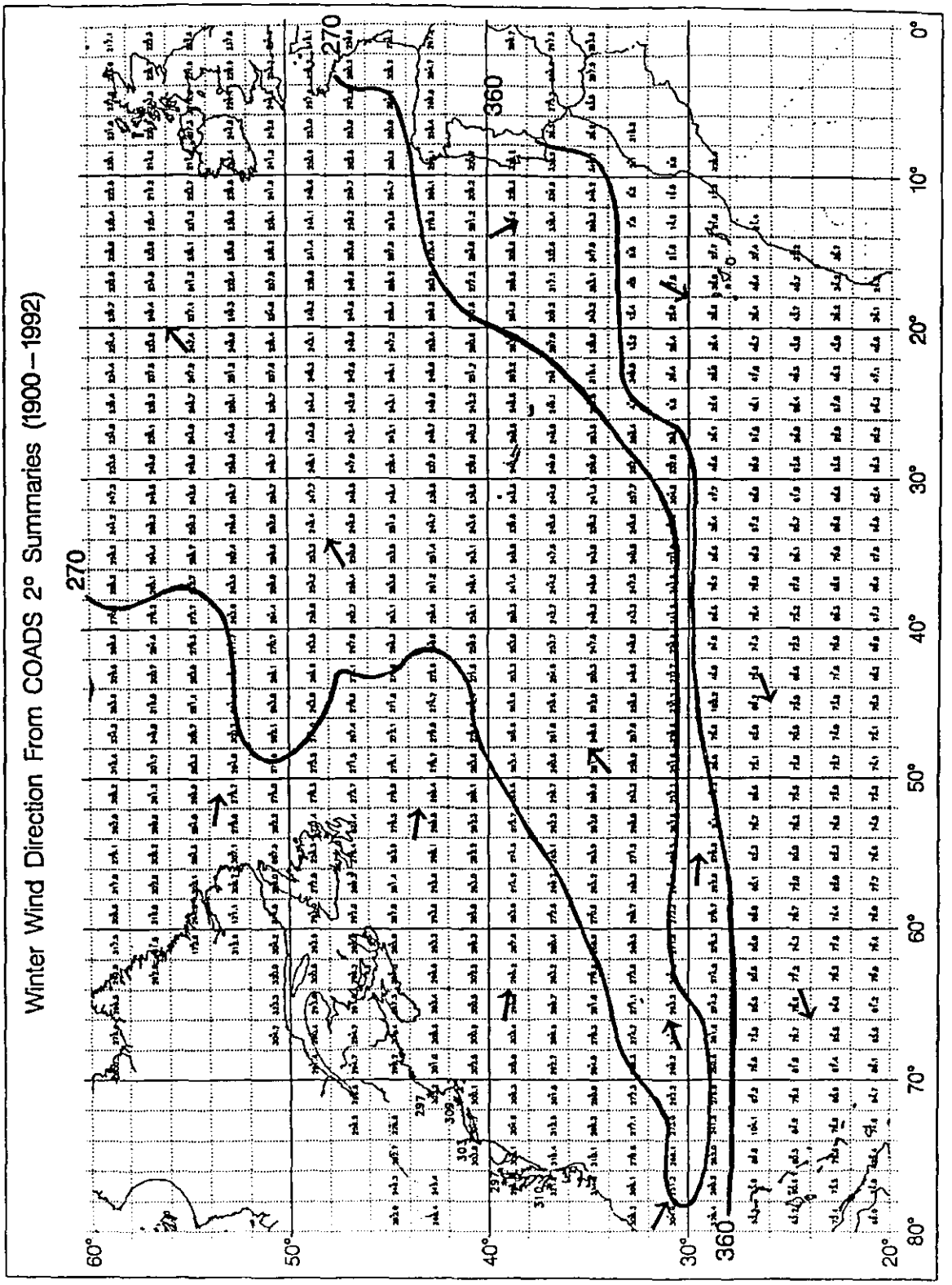

Figure 3b: Winter Wind Speed from COADS 2° Summaries (1900-1992).

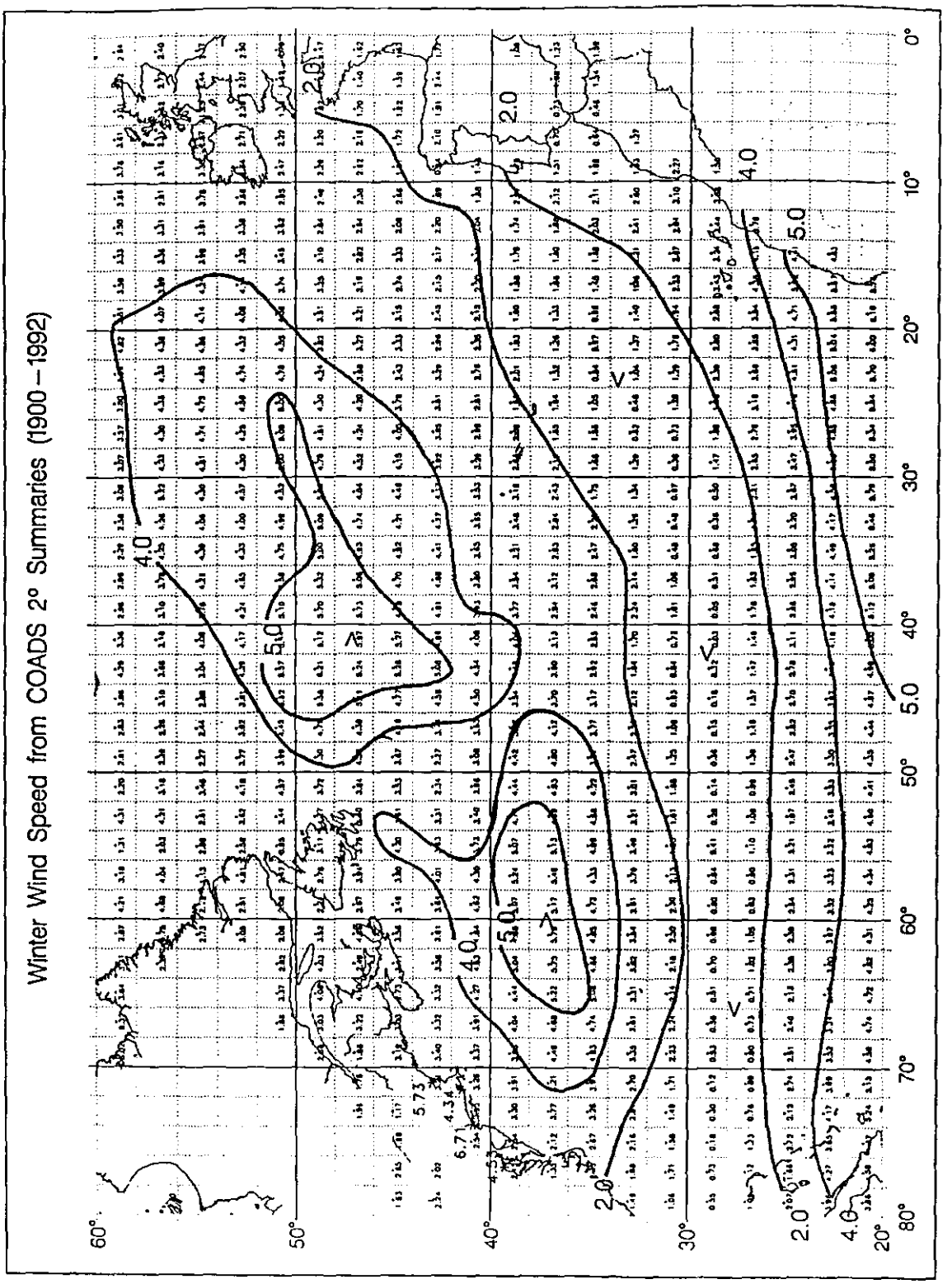

Figure 4a: Comparison of phi and nu between selected 2° square and Boston, MA (1950-59).

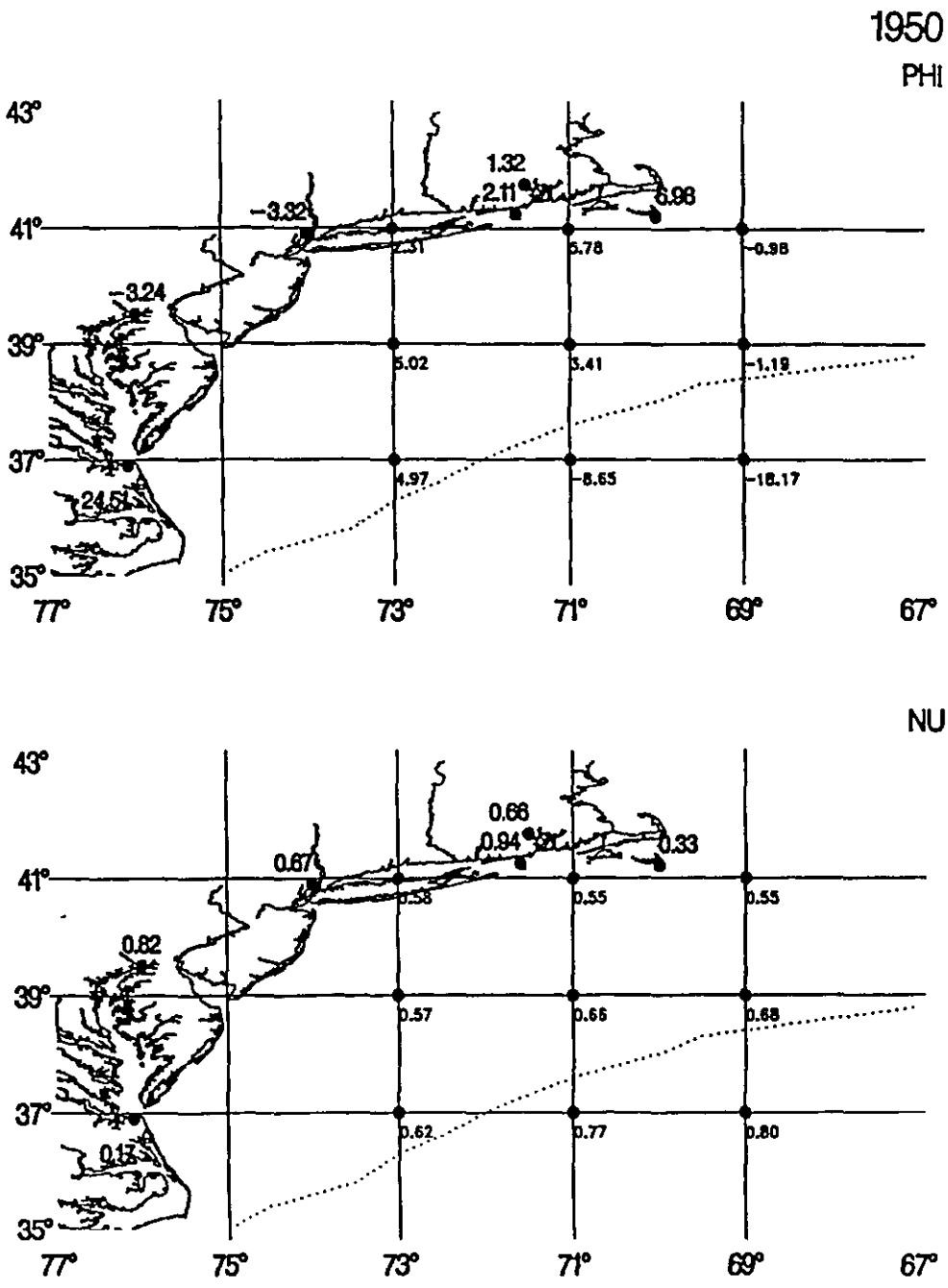

Figure 4b: Comparison of phi and nu between selected 2° square and Boston, MA (1960-69).

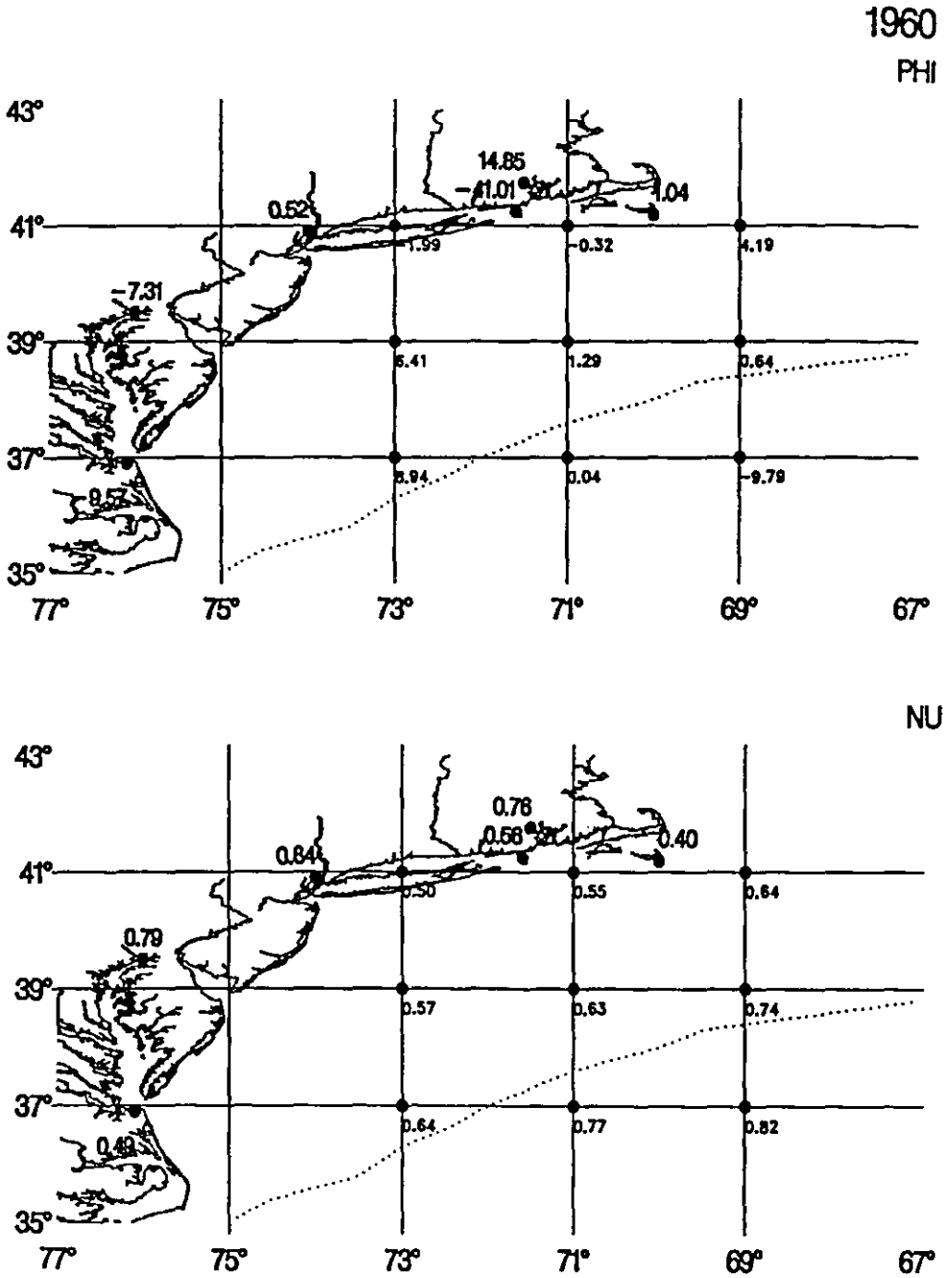

Figure 4c: Comparison of phi and nu between selected 2° square and Boston, MA (1970-79).

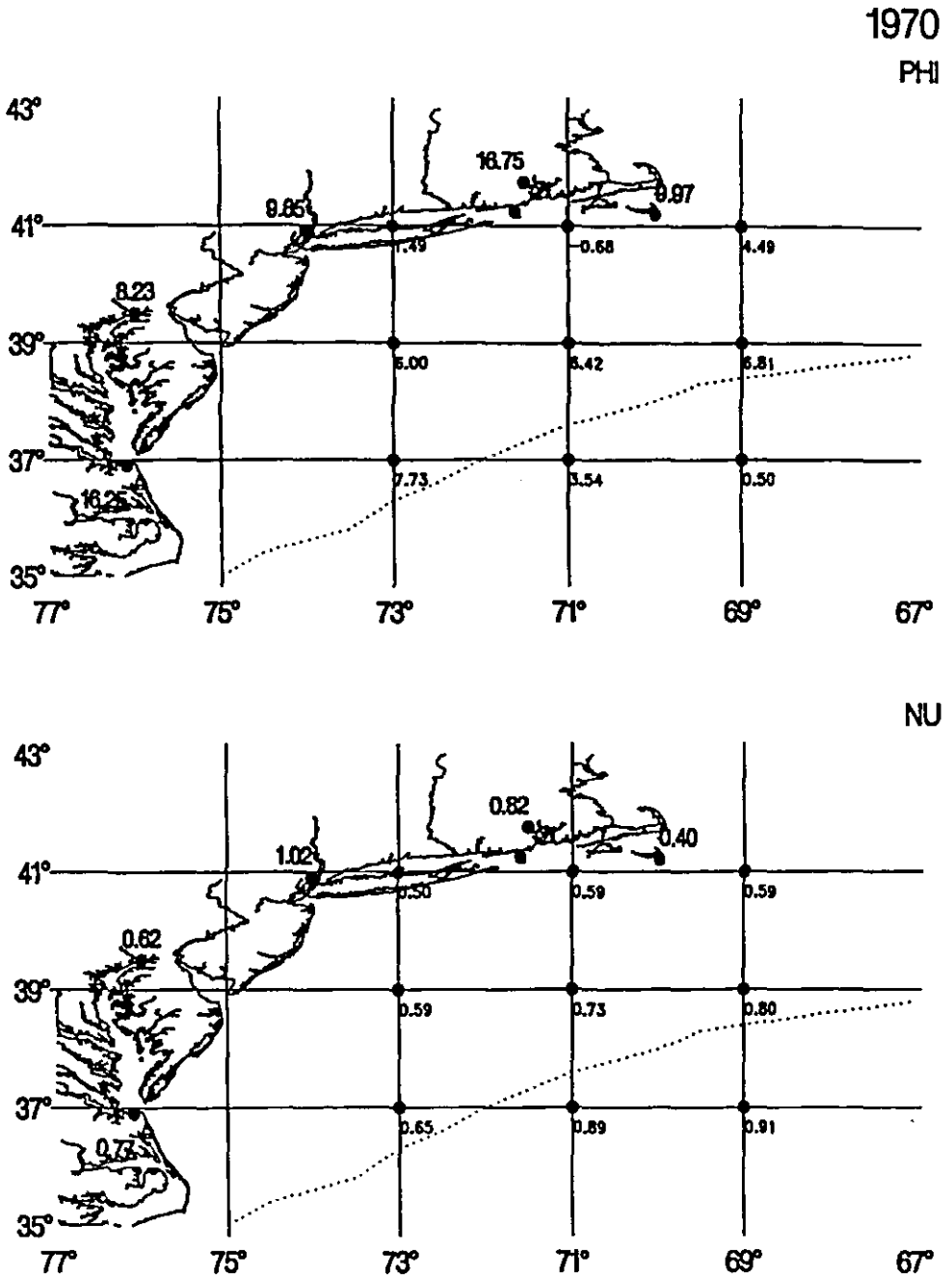

Figure 4d: Comparison of phi and nu between selected 2° square and Boston, MA (1980-89).

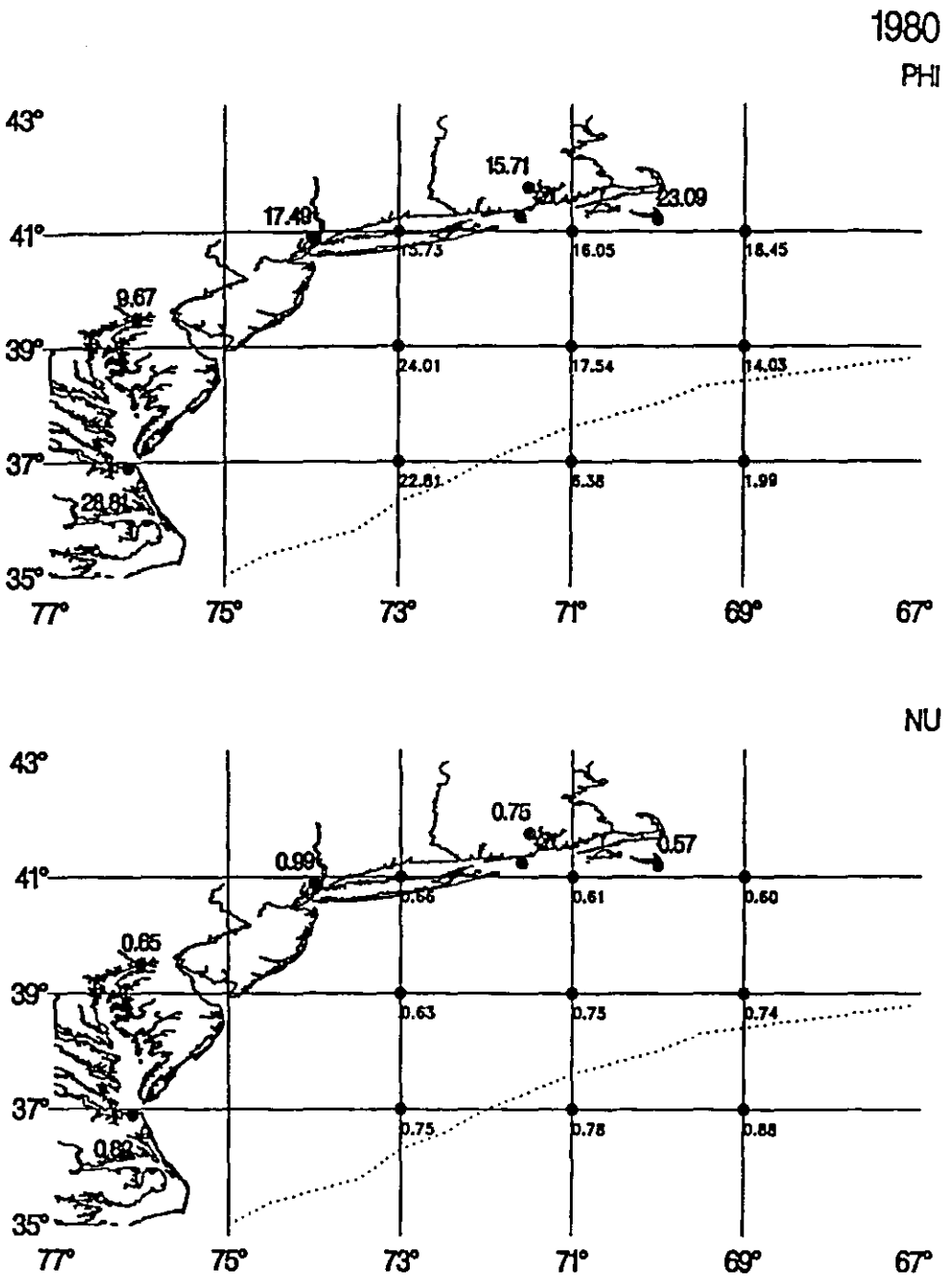

Figure 5: Air temperature at New Haven, CT with longitudinal average air temperature anomaly from the latitude band of the mic-Atlantic rregion (from Ingham, 1982, and Hansen and Lebedeff, 1987).

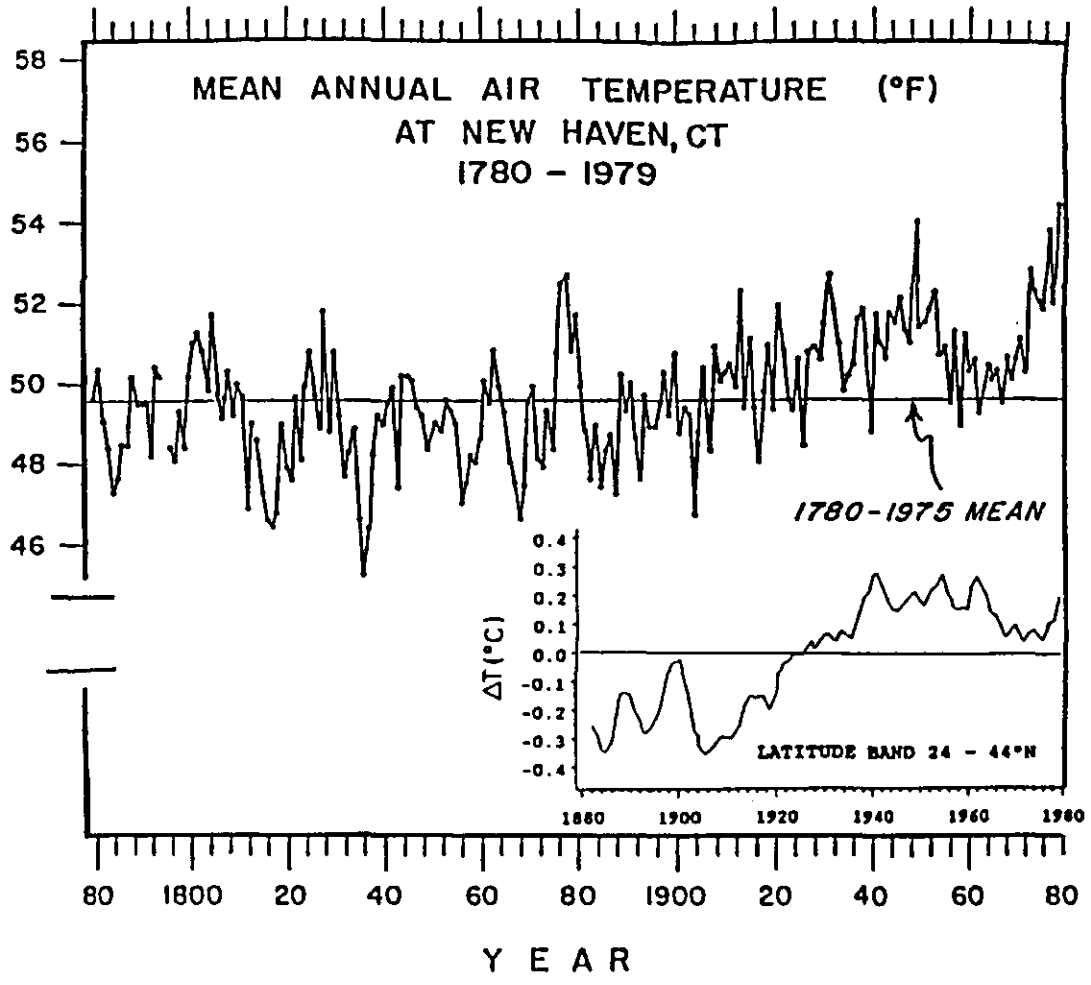

Figure 6a Standard deviation of winter nu and phi factors from multiple (n=20) data sets from randomly selected dates.

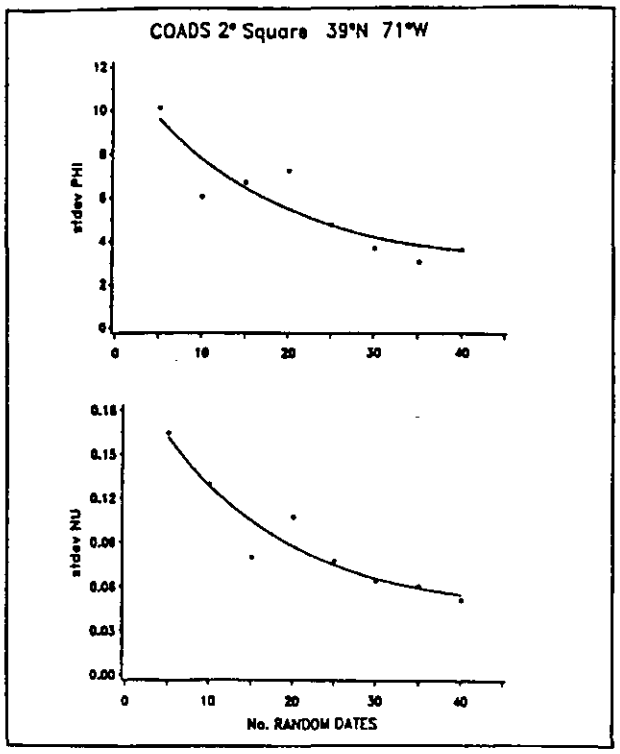

Figure 6b Standard deviation of winter nu and phi factors from multiple (n=30) data sets from randomly selected dates.

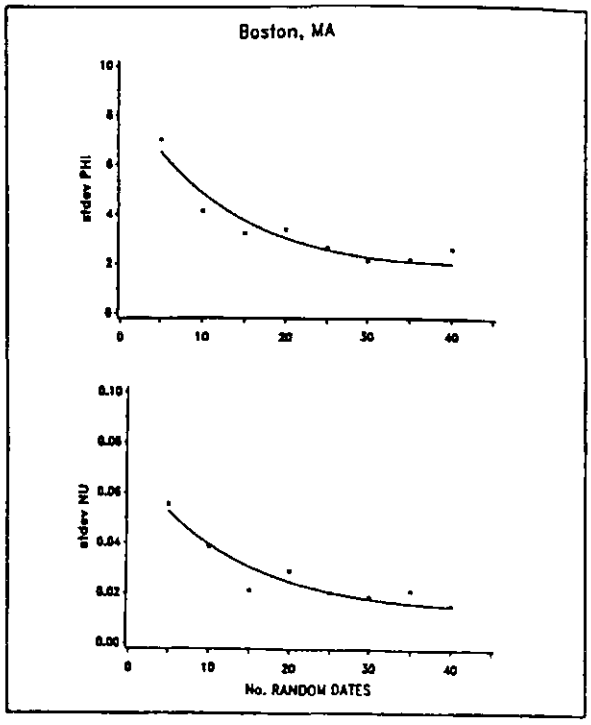

Figure 7: Wind Constancy.

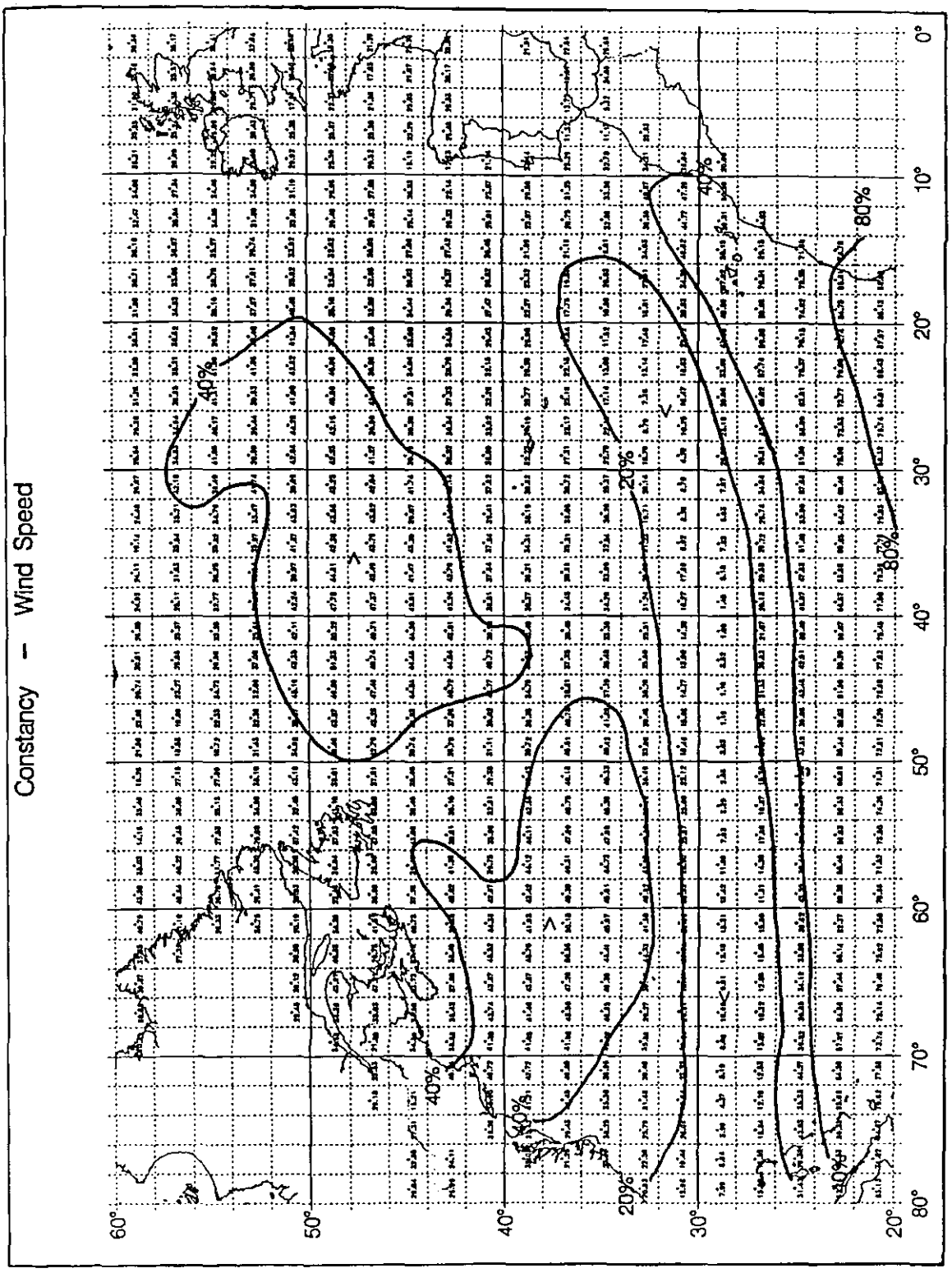

Figure 8: Comparison of Wind Direction between the Atlantic 2° squares and Boston, MA.

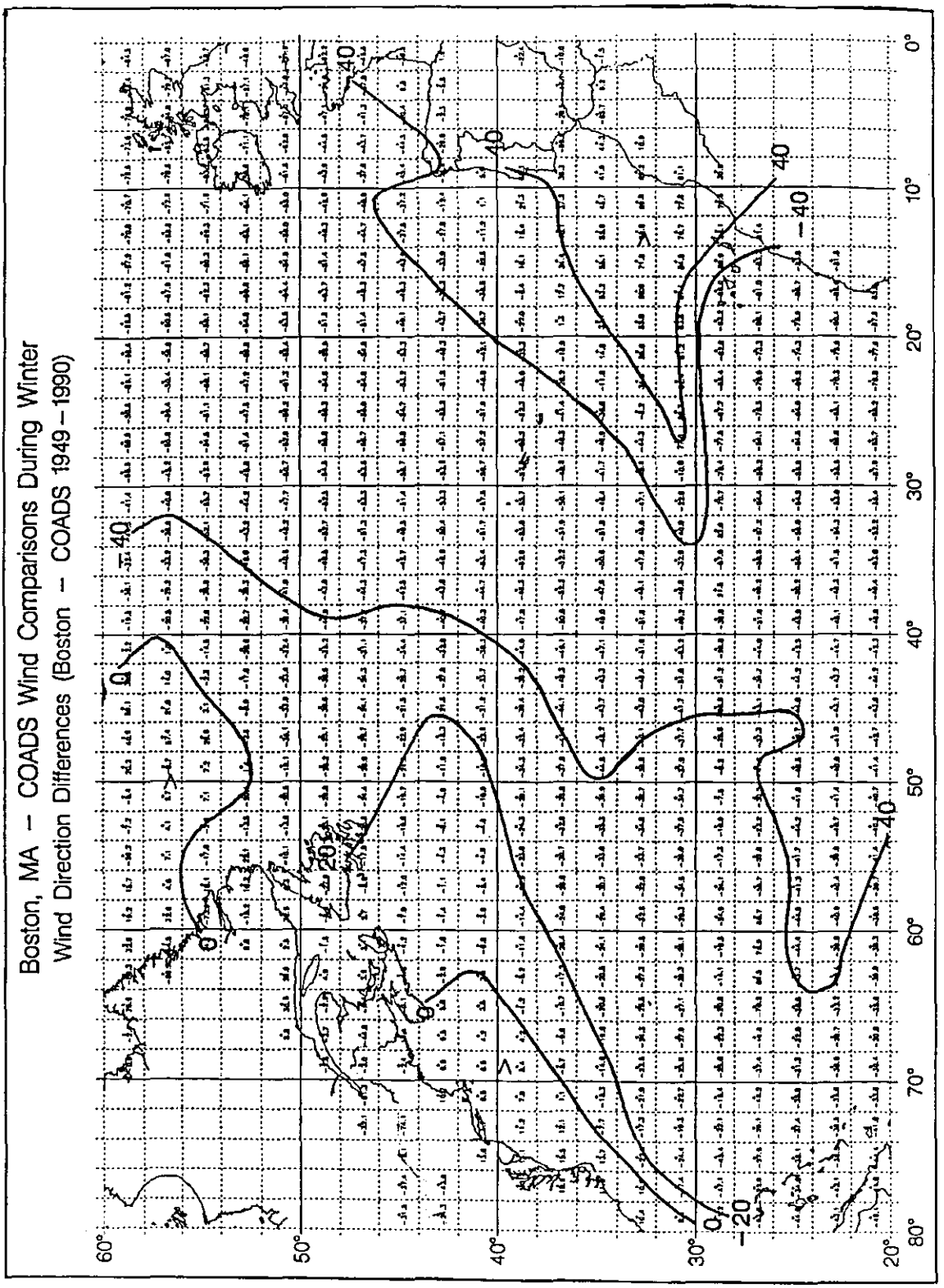

Figure 9: Wind constancy and wind factors from winter COADS summaries in the North Atlantic.

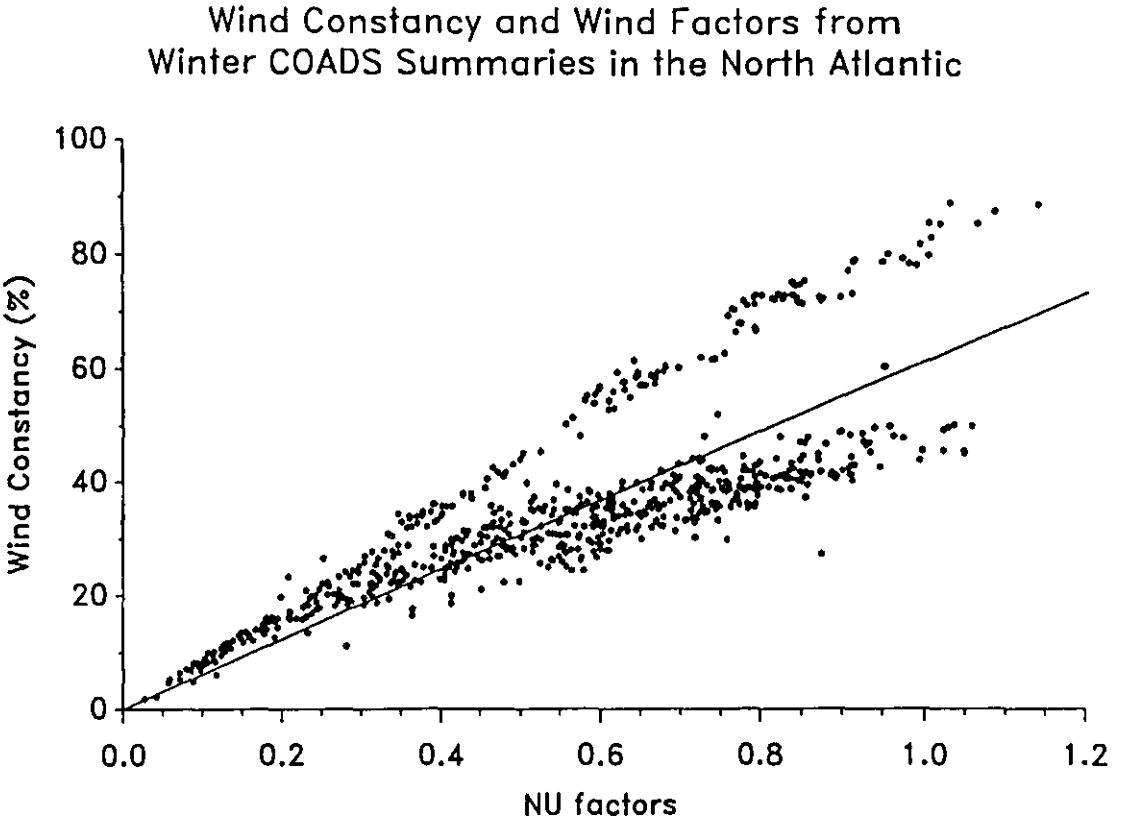

Figure 10: Comparison of wind speed between the Atlantic 2° squares and Boston, MA.

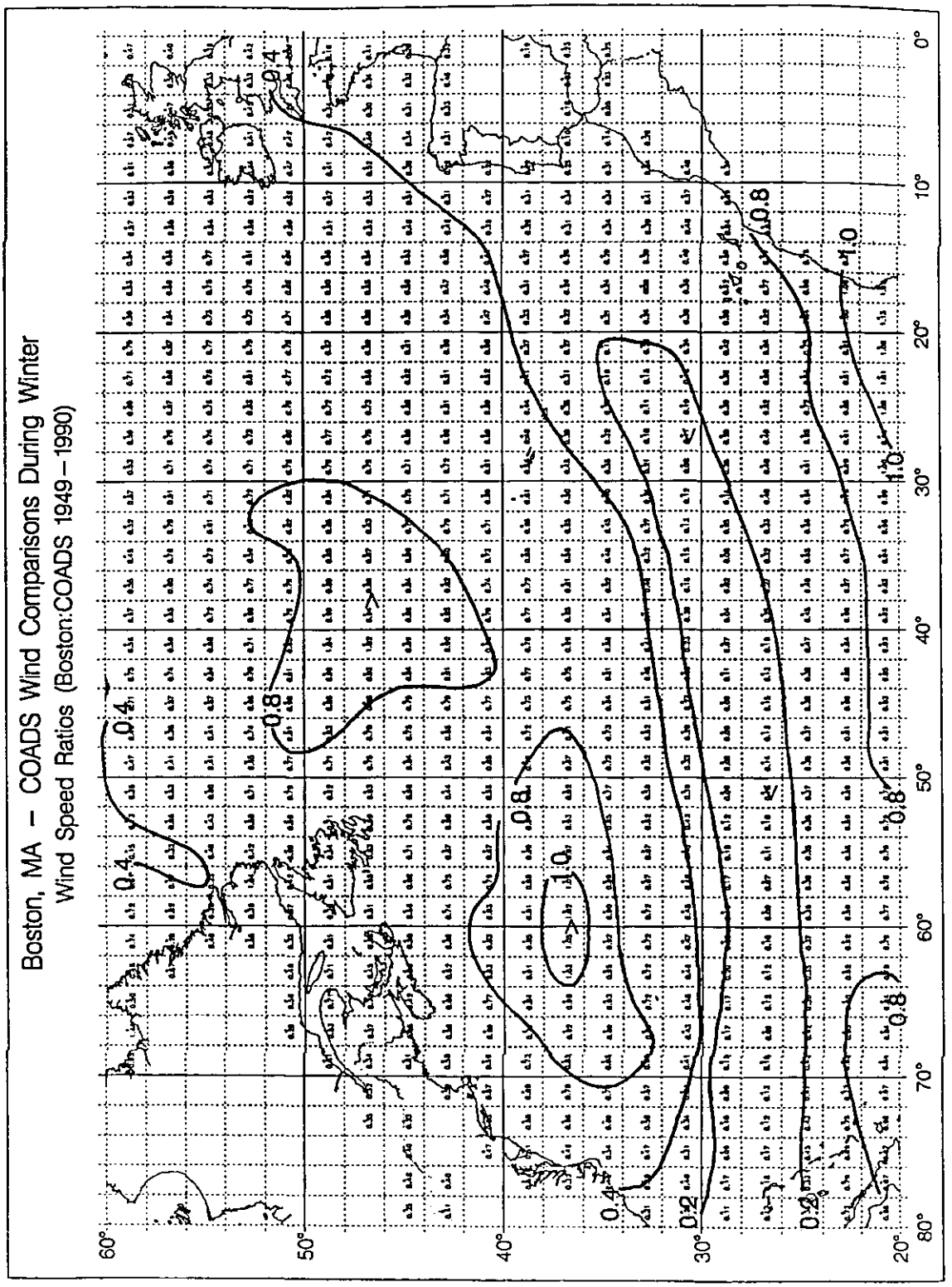

Figure 11: Winter wind constancy in the North Atlantic by decade.

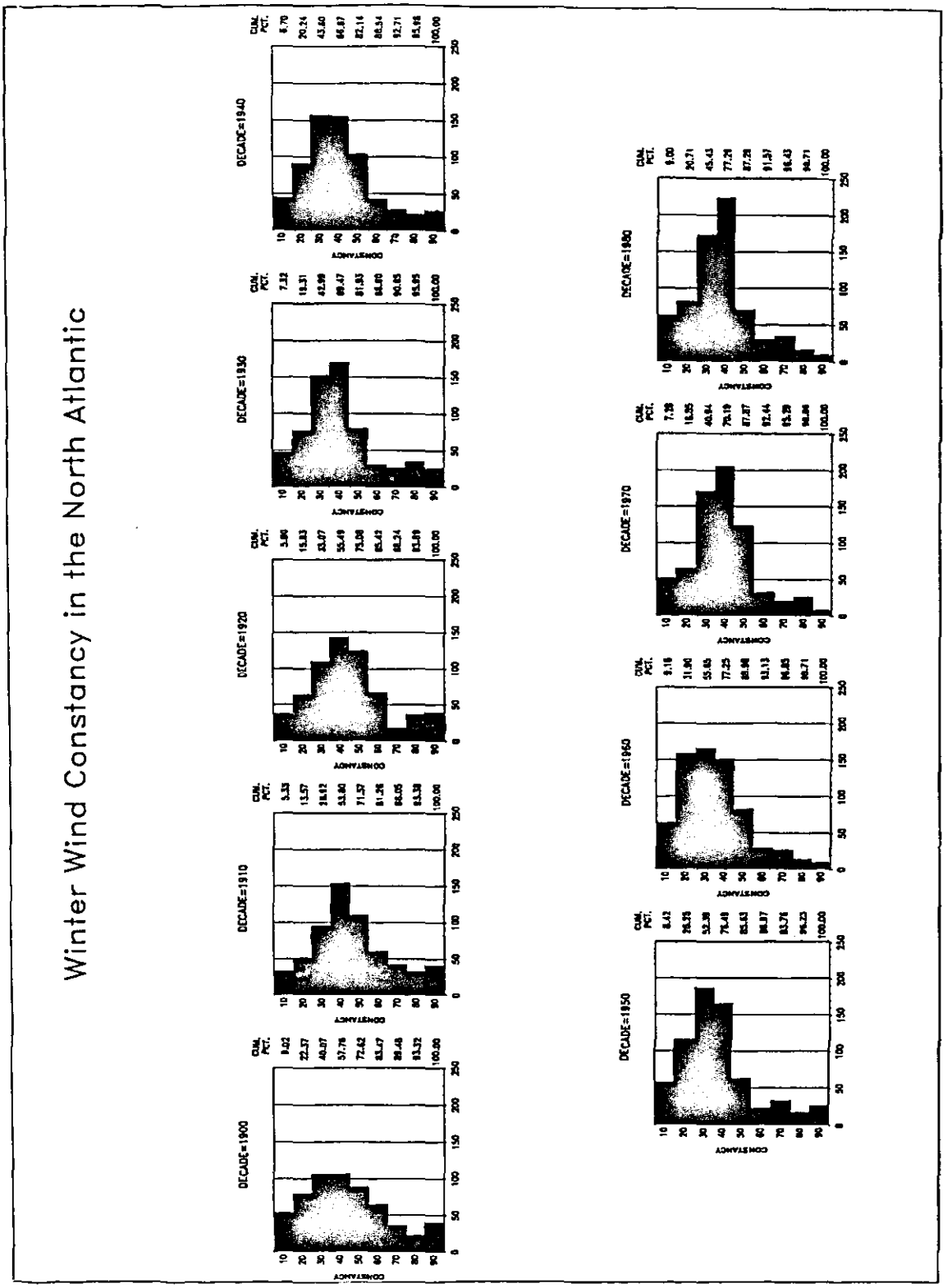

Wind Speed Discontinuity Related to Beaufort Wind Observations and Its Influences on Latent Heat Flux

Zhongxiang Wu
Department of Earth, Atmosphere, and Planetary Sciences
Massachusetts Institute of Technology

Kerang Li
Institute of Geography
Chinese Academy of Sciences

Introduction

The global oceans are the main energy source for our climate system. The oceans can absorb 65PW of direct solar radiation and 108PW of downward thermal radiation, two times more than the total absorbed by the atmosphere and land surfaces (Wood, 1984). The oceans redistribute the received energy through oceanic currents, and finally hand it over to the atmosphere in the forms of latent heat and sensible heat. The global oceans are more important than the continents in the hydrological cycle in the climate system. The oceans contribute 87% to the total world water budget which is about 577,000 km^3/yr, while the continents only 13% (Korzoun et al., 1977). Proper estimates of the energy fluxes and water vapor entering the atmosphere from the oceans are essential for modeling the climate and its variations. Great efforts have been made for quite a long time to achieve such estimates (e.g., Budyko, 1963; Esbensen and Kushnir, 1981; Hsiung, 1986), but the problems still exist. One example is given in Figure 1 which is the time series of latent heat anomalies calculated using the COADS (Woodruff et al., 1987) for four tropical regions for the period of 1949-1990. The statistics and the significance test are given in table 1. The positive trends obtained using the least square method are indicated by the dashed lines in the figure, and range from 17 Wm^{-2} in the eastern tropical Pacific (ETP) to 31 in Wm^{-2} the western tropical Pacific (WTP) during the 42-year period, all above the 95% significance level. Are these trends a real signal of climate change? The following discussion about the inhomogeneous wind observations and their influence on the latent heat flux may give us some clue to the answer.

Discontinuity of the Wind Observation

Some Japanese whaling ship data, which covered some data-sparse areas close to Antarctic region in COADS, were processed recently. The wind speed was recorded in Beaufort scale, providing therefore a relative uniform data set from one country using one method. The whaling ships usually passed the Australian coast and went to the area

south of 50°S in the South Pacific before 1961, but afterward went through South China sea and entered the southern Indian Ocean during 1962-66. An example of ship track is shown in Figure 2a. The wind measured by whaling ship from 1949 to 1961 in the region 50°—80°S, 120°E—80°W is plotted in Figure 2b; the COADS wind is shown in Figure 2c for the same region. During this period the whaling ships went to South Pacific. It is also during this period that the COADS winds all over the global oceans showed large positive trends (Wu and Newell, 1992). The dashed lines in figure 2b are the trends obtained by least square method. It is obvious that the wind trend in the whaling ship data is much smaller (0.16 ms^{-1}/13yrs) than that in COADS (2-26 ms^{-1}/13yrs).

The wind trend in COADS has been noticed by many researchers (e.g., Ramage, 1987; Cardone et al., 1990; Isemer and Hasse, 1991). Two factors were suggested to be the main contributors to the trend. One is the transfer of Beaufort wind observation to anemometer measurement, and the other the change of the ship size. Correcting the spurious trend needs much more work than locating its sources. Quantitative correction is needed, but is extremely difficult to get. It is almost unrealistic to correct the wind speed based on individual ships. It is not easy to find ships which conducted both scale wind observations and anemometer measurements to get hard numbers for the correction. The ship observations were usually not made in the same time and environment as that on nearby islands or buoys, which makes their intercomparison difficult considering the fact that the wind is the most variable component in the climate system.

Some land station data, however, may provide useful information for such correction. Most Chinese weather stations recorded the wind speed in Beaufort scale based on an instrument called wind-pressure plate, or on the states of smoke, dust, flag, trees etc., when wind-pressure plate was not available before late 1960s; and early 1970s. The instrument was very similar to the wind-force indicator in Hook's instruments, which was invented by Wild in about 1861 and used first by the British Royal Society (Khrgian, 1959). The Beaufort scale number on the wind-pressure plate was calibrated in wind tunnel according to WMO code 1100. The instrument was replaced by the standard cup anemometer around 1970. Most Chinese stations were established in early 1950s. There are 15-20 years of Beaufort wind observations and 20-25 years of anemometer measurements, which could be very useful to derive the quantitative correction needed in the COADS wind data. The cup anemometer was mounted at the same place as for the wind-pressure plate. The environment and observation schedule were also same as before. The systematic differences of the wind speed before and after were not likely caused by the natural variations. The way to get Beaufort scale number on the ship is different from that at Chinese land station, but both methods were calibrated by the WMO code 1100. They should reflect each other.

Parallel comparison of the wind speed measured by standard cup anemometer with that from wind-pressure plate has been done in many Chinese stations in the process of transfer. Unfortunately the data were not well collected and not too many survived. Table 2 is such comparison at 7 stations conducted at the time of the instrument changes. The wind-pressure plate was replaced by anemometer around the end of 1971. Column 2 is the wind speed converted using WMO 1100 from Beaufort scale obtained by wind-pressure plate, and column 3 the wind speed measured by cup anemometer simultaneously. The wind speed in these stations ranged from 4 to 12 ms^{-1}, corresponding to the Beaufort scale 4 to 6. The anemometer wind speed exceeded Beaufort wind speed

at all stations, 17% on average. At Tomaho station, the anemometer wind speed was 27% higher than the Beaufort wind speed, but only 1% at Zanjan station. The ratio increased with the height of station.

The annual mean wind speed also showed similar changes. Table 3 gives the yearly averaged wind speed for 10 stations. The times of replacement of wind-pressure plate are shown by the underlined numbers. The wind speed increased at 8 stations after the replacement. The first five stations were located at high altitude, and all showed higher wind speed after the replacement. The other five stations were at low altitude near coast; three of them with weak wind speed showed 7 - 17% increase, but the two with relative strong wind speed showed 3 - 9% decrease. The t-test showed that the increases at four stations are above 95% significance level.

At high wind speed, however, the relationship is reversed. Table 4 is also the parallel comparison at 3 stations, but for strong wind (wind speed > 16ms^{-1}). The anemometer wind speed was much lower than Beaufort wind speed. The difference increased with the increasing of wind speed. It reached 10 ms^{-1} or more at Beaufort wind speed 34 ms^{-1}. The drop of the number of strong-wind days (wind speed > 16ms^{-1}) also reflected such tendency (Table 5). After the change from Beaufort wind observation to anemometer measurement, the number of strong-wind days were 16 - 90% less than before except at station Tia which showed only 1% decrease. At station Ron, the average of strong wind days was 27 days during the 7-year period before, but dropped to 3 days during the 11-year period after 1968 when the Beaufort wind observation was abandoned. Statistics showed that the changes at 4 stations are above 95% significance level.

Being consistent with the results of the Commission for Maritime Meteorology WM0 in 1960 (CMM-IV, WM0, 1970), the above land observation data also show the feature that the Beaufort wind observations underestimate wind speed in low wind cases and overestimate wind speed in the strong wind cases. However, there are two points which deserve attention: one is that the difference between the Beaufort wind observation and the anemometer measurement increased with height, and the other is that the underestimate of strong wind was much larger than what CMM-IV showed.

The first point is related to the air density. Beaufort wind observation is based on the wind force F exerted on some object, which equals to

$$F = c\rho s v^2 \qquad (1)$$

where ρ is the density of air, s the area of the subject perpendicular to the wind direction, v the wind speed and c the proportional coefficient. Density ρ is a function of temperature, pressure and water vapor, and could be 15% higher over the oceans in high latitudes than that over the tropical warm ocean areas, corresponding to a wind difference of 7% with higher wind speed in tropical regions. The Beaufort scale equivalent wind of WM0 1100 was originally determined by the observations on the British island of St. Mary's (Scilly) which is located near 50°N. This equivalent wind scale would underestimate the wind speed in the warm, moist regions and overestimate in the cold, dry regions. Lin and Le (1975) deduced a correction coefficient, r,

$$r = 1.622\sqrt{T/(P - 0.378e)} \qquad (2)$$

where T, P and e are temperature, pressure and water vapor pressure respectively, to determine the anemometer wind speed corresponding to the Beaufort wind speed based on WM0 1100 in various conditions. This coefficient is listed along with the observed ratio between two wind speeds in the column 5 and 4 in table 2. They fit each other closely.

As to the second point, it is probably related the observation error of gusty wind. This is schematically shown in Figure 3. Strong wind is always gusty, but the calibration of wind pressure plate is conducted in steady flow. The wind force F_2 exerts a torque on plate to balance the torque caused by F_1 which is related to the gravity force mg. The torque of wind is

$$\tau = 0.5c\rho v^2 \ell^2 \cos^2 \alpha \tag{3}$$

where ρ, ℓ, and α are the line-density, the length and the angle of the plate. Assuming that the plate would be in position A at steady wind v_o, say 20 ms^{-1}, and that the wind is gusty and suddenly increases to this speed from v', say 17 ms^{-1}, when the plate is at position B with angle $\beta(< \alpha)$, the wind force and its torque exerted on the plate would be larger than that needed for the plate to stay at position A, and the plate would reach the position higher than A. The excess of the gusty wind torque is inversely proportional to the initial wind speed v', and could be expressed in the form

$$\Delta\tau = \cos^2 \beta / \cos^2 \alpha_\circ \tag{4}$$

where $\alpha_\circ$ is the calibrated angle for wind speed $V_\circ$. β can be determined by v' using

$$\sin\beta = \{-\lambda / v'^2 + \sqrt{(\lambda / v'^2)^2 + 4}\} / 2 \tag{5}$$

$$\lambda = v_\circ^2 \cos^2 \alpha_\circ / \sin\alpha_\circ. \tag{6}$$

Table 6 listed a sample calculation for $v_\circ = 20 ms^{-1}$ and $\alpha_\circ = 45°$. It shows that a 20 to 30% overestimate of torque in gusty winds is quite possible by Beaufort wind observation.

This principle should work to the surface wind waves in the ocean. The wind energy transmitted to the surface wind wave can be expressed in the form (Titov, 1969)

$$N_w = Ah(w-c)^2 \tag{7}$$

where A is a constant, h the wave height, w the wind speed and c the wind wave speed. This form is similar to (1). The gusty wind could give the observer an impression of higher Beaufort scale. But the magnitude of the overestimate would be much smaller because of the large inertia of the surface wave. This could be one of the reasons for the overestimate of wind speed at high Beaufort scales.

Influence of the wind trend on the latent heat flux

Wind is the major factor controlling the evaporation at ocean surface. The wind trend was shown globally (Wu and Newell, 1992), and needed to be considered in the calculations of latent heat flux. The wind speed obtained by Beaufort wind observation was transferred back to its Beaufort scale using WMO 1100, then transferred to CMM-IV equivalence, a better code than WMO 1100 (WMO,1970). Since most ships were higher than 10 meters, the height required by bulk equation, the anemometer wind speed was subjected evaporation to the height adjustment using the equations (Smith, 1980; Wu, 1980)

$$\frac{U_z}{u_*} = \frac{1}{\kappa} \ln \frac{z}{z_o} \tag{8}$$

$$\frac{\frac{z_o}{u_*^2}}{g} = a \tag{9}$$

Where U_z is the wind speed in height z, u_* the friction velocity, κ the von Karman constant and z_o the roughness length. The a in (9) is a constant and equals 0.00185. The ship height has assumed to be 20 meters (Cardone et al., 1990). The Newton iterative method was used along with the measured wind to find z_o, then calculate the wind speed at 10 meters. The ratio of Beaufort wind observations to anemometer measurements from Ramage (1987).

The latent heat flux was calculated using bulk equation except in the light wind condition over warm ocean surface where the Stelling formula was used (Brutsaert, 1982). the transfer coefficient from Large and Pond (1982) was used form neutral conditions, and adjusted for other conditions following the ratios of Isemer and Hasse (1991).

The evaporation in light wind over warm pool region needs to be considered with extra caution. The bulk equation is base on the formula of evaporation

$$E_z = -\rho k_z \frac{\partial q}{\partial z} \tag{10}$$

where E_z is the water vapor flux in the z-direction and $\partial q/\partial z$ the vertical gradient of the specific humidity. k_z is the eddy diffusivity for water vapor, and is determined by the vertical wind profile on the proposition that the eddy diffusivity for the water vapor is the same as that for momentum. Assuming the vertical wind profile near the surface follows the logarithmic distribution, the above formula can be expressed in the form

$$E_z = -\rho c_e (u_2 - u_1)(q_2 - q_1) \tag{11}$$

$$c_e = \frac{\kappa_2}{\ln \frac{z_2 + z_0}{z_1 + z_0}} \qquad (12)$$

where κ is the von Karman's constant. The bulk equation is the specific case of this form when u_1 equals zero. The vertical transport of water vapor related to buoyancy is not included in the bulk equation, and therefore there would be no evaporation if there is no wind. In the warm pool region, where the wind speed is the lowest and the surface temperature the highest over the global ocean, the buoyancy effect should not be neglected.

The latent heat fluxes measured in the tropical west Pacific at zero wind speed is 25 Wm^{-2} (Bradley et al., 1991). Newell et al. (1978) and Newell (1979, 1986) proposed that net heat flux should be close to zero when the SST reaches its limit of 30°C because of the buffering of the evaporation. Using the experiment data measured from the ship R/V Franklin, Godfrey and Ländstrom (1989) have shown that the net heat flux is near zero at the sea surface near New Guinea. The ocean mixing and advection processes in the western equatorial Pacific are too weak to carry away heat flux more than 10 Wm^{-2}. The current results are from 20 to 100 Wm^{-2} (Esbensen and Kushnir, 1981; Reed, 1985). A fine adjustment of latent heat in low wind speed over the tropical ocean surface does matter to the ECMWF model forecast (Miller et al., 1992). A new parameterization of evaporation, which raises the latent heat flux from zero to about 25 Wm^{-2} at calm weather condition, can greatly improve the model simulation, including the rainfall distribution, monsoon circulation et al.

Stelling first formulated an equation in 1882 to include the zero wind evaporation (Brutsaert, 1982)

$$E = A_s + B_s u(e_s^* - e_a). \qquad (13)$$

where A_s = 0.0702 and B_s = 0.00319. E is the evaporation in mm/(2 hrs), u the wind speed in km/hr at 7.5 m above the surface, and e the water vapor pressure in mm Hg. This formula is still widely used in engineering with various coefficients of A_s and B_s.

Stelling formula was used to calculate the latent heat flux in the light wind ($u < 3ms^{-1}$) and warm SST ($\geq$ 28.5°C) conditions. But the coefficients need to be determined since the original ones were only suitable for the continent region at high latitude. The averaged values of $q_s - q_a$, and $T_s - T_a$, in the light wind and warm SST circumstances are 6.75 g/kg and 2.23°C according to the COADS. Assuming that the bulk equation is valid for the wind speed of 3 ms^{-1} and above, and that the latent heat flux is 25Wm^{-2} at zero wind speed, the Stelling equation would be

$$Q_L = (3.70 + 3.952u)(q_s - q_a) \qquad (14)$$

where Q_L is latent heat flux in Wm^{-2}, u and q are in ms^{-1} and g/kg, respectively.

The time series of latent heat flux and their trends for the same regions in Figure 1 are shown in Figure 4, and their statistics included in Table 1. The trends are greatly reduced, very close to zero in the ETP and tropical Atlantic. They are about 10 Wm^{-2} in the WTP and the western tropical Indian ocean, but the estimated errors of the coefficient b for trends are overlapped with zero at 95% significance level and therefore the remained trends may not be real.

The effect of wind adjustment on the climatology of latent heat flux is shown in Figure 5, which is the differences between latent heat fluxes calculated with and without wind adjustment for January, July and yearly mean. The adjustment raises the latent heat fluxes about 5 - 10 Wm^{-2} over the tropical and subtropical oceans, but lowers the fluxes about 5 Wm^{-2} over the oceans in the middle and high latitudes. Comparing with the wind climatology, it is found that the zero line corresponds to the wind speed of 8 ms^{-1}, below which the latent heat correction is positive and vice versa. Generally speaking, however, the adjustment does not change the pattern of the latent heat flux.

It seems impossible to justify the individual wind correction in COADS, but there are some constraints which could be used to test the validity of adjustment as a whole. One constraint is the water balance. The difference of the evaporation and the precipitation (E-P) over the global oceans should be balanced by the river runoff. It was calculated using the Q_L and Jaeger's predication (Jaeger, 1976). The results are listed in Table 7. The total water deficit of oceans is 47.2 x 10^3 km^3 yr^{-1}. The UNESCO (1978) river flow into three oceans is 41.7 x 10^3 km^3yr^{-1} and underground flow 2.2 x $10^3km^3yr^{-1}$. The water deficit obtained with unadjusted wind is 29.9 x 10^3 km^3yr^{-1}. The latent heat flux calculated using adjusted wind ends up with a better water balance coinciding the fact that the values of E—P south of 40°S are not all included because of missing data and that the precipitation there is usually larger than the evaporation.

Another constraint is the total net heat flux entering the oceans. Latent heat flux affects not only the water balance but also the energy balance of the oceans. The global mean net heat flux of the oceans should be very close to zero since the oceanic temperature is quite stable on the time scale of several decades. The global averaged net heat flux of Esbensen and Kushnir (1981) is 5 Wm^{-2} and the lowest among others, which would warm the global oceans 0.1°C per decade, and Hsiung's and Weare's numbers would result in more warming (Reynolds, 1988). The net heat flux of Reed in the tropical Pacific is about 80 Wm^{-2} more than Esbensen and Kushnir's number and would lead to tremendous warming of the ocean. The global mean of net heat flux after taking account of wind correction is given in Table 8. The long term annual mean is 1 Wm^{-2}, close to zero, but the amplitude of seasonal variation could reach 30 Wm^{-2}. The oceans lose more heat in northern winter, which is the results of the strong latent heat and sensible heat losses in the Gulf Stream and Kuroshio regions.

The energy balance in the warm pool region is also a constraint. The net heat fluxes in this region should be close to zero (Newell et al., 1978; Newell, 1979, 1986; Godfrey and Ländstrom, 1989). The time series of the net heat fluxes in WTP and ETP regions are given in Figure 6. The 12 - months running mean (dash line) is close to zero in the WEP region, but 40 - 50 Wm^{-2} in the ETP region except during the strong El Niño in

1982 - 83 period when the SSTs there were close to sea surface temperature limit (Newell, 1986).

Summary

Beaufort-only wind data from Japanese whaling ship did not show positive trend for the period of 1949 - 61 while the wind speed from COADS increased 2.26 ms^{-1} during this period. A homogeneous wind data set may give us a picture about trend closer to the reality than mixed data set. More efforts are needed to search for such data sets in order to verify our knowledge about the climate changes.

Parallel comparison of Beaufort wind observation with anemometer measurements at land stations confirms the fact that Beaufort scale wind could underestimate wind speed at low wind speed and overestimate wind speed at high wind speed. The comparison shows that difference between Beaufort wind and anemometer wind increases when the air density decreases. The bias of Beaufort scale wind would be more in warm and moist region than that in cold and dry region. The overestimate of Beaufort scale at high wind speed is more severe at land stations. The gusty nature of wind is the main source for the overestimate error. The same principle should work for the wind waves at ocean surface.

The wind trend in COADS causes spurious latent heat trend. According to this trend, the latent heat flux received by the atmosphere would be 30 Wm^{-2} more in 1990 than in 1949 in the WTP alone. If the COADS wind is adjusted following the CMM-IV code, and then used in the latent heat calculation, the latent heat trend is reduced significantly, failing to pass the statistic test in most regions. The global water balance, the energy balances of the global oceans and of the warm pool region support the wind adjustment, which leads to more reasonable results.

Acknowledgments

Z. Wu was supported by the National Science Foundation Climate Dynamics Program under Grant No. ATM 9106902. We thank S.M. Leite, a UROP student at MIT, for the Japanese whaling ship data input.

References

Bradley, E. F., P. A. Coppin and J. S. Godfrey, 1991: Measurements of Sensible and Latent Heat Flux in the Western Equatorial Pacific Ocean. *J. Geophys. Res.*, 96, 3375-3398.

Brutsaert, W., 1982: *Evaporation into the Atmosphere*. D. Reidel Publishing Company, London, 299 pp..

Budyko, M.I., 1963: *Atlas of the Heat Balance of the Earth*. Gidrometeorozdat, Moscow, 69 pp..

Cardone, V.J, J.G. Greenwood and M. Cane, 1990: On Trends in the Historical Marine Wind Data. *J. of Climate*, 3 113-127.

Esbensen, S.K., and Y. Kushnir, 1981: The Heat Budget of the Global Ocean: An Atlas Based on the Estimates from Surface Marine Observation. Rep. 29, 27 pp., Climatic Res. Inst. Oregon State Univ., Corvallis.

Godfrey, J. S. and E. J. Lindstrom, 1989: The Heat Budget of the Equatorial Western Pacific Surface Mixed Layer. *J. Geophys. Res.*, 94, 8007-8017.

Hsiung, J., 1986: Mean Surface Energy Fluxes over the Global Ocean. *J. Geophys. Res.* 91, 10585-10606.

Isemer, H.J. and L. Hasse, 1991: The Scientific Beaufort Equivalent Scale: Effects on the Wind Statistics and Climatological Air-Sea Flux Estimates in the North Atlantic Ocean. *J. of Climate,* 4, 819-836.

Jaeger, L., 1976: Monatskarten des Niederschlags für die ganze Erde. *Ber. Der Deutsche Wetterd.*, 18 No. 139, 38 pp.

Khrgian, A.K., 1959: Meteorology, A Historical Survey. Vol. 1, 387 pp., GIMIZ, Gidrometeorologicheskoe Izdatel'stove, Leningrad.

Korzoun, V.I., A.A. Sokolov, M.I. Budyko, K.P. Voskrensky, G.P. Kalinin, A.A. Konoplyantsev, E.S. Korotkevich and M.I. Lvovich, 1977: *Atlas of World Water Balance.* UNESCO Press, Paris, 34 pp and 65 maps.

Large, W., and S. Pond, 1982: Sensible and latent Heat Flux Measurements over the Ocean. *J. Phys. Oceanogr.*, 12, 464-482.

Lin, G. and Li K., 1975: Problems of Wind Speed Related to the Instrument Changes. Science and Technology in Meteorology (in Chinese), 3, 5-10.

Miller, M. J., A. C. M. Beljaars and T. N. Palmer, 1992: The Sensitivity of the ECMWF Model to the Parameterization of Evaporation from the Tropical Oceans. *J. Climate*, 5, 418-434.

Newell, R. E., A. R. Navato and J. Hsiung, 1978: Long-term Global Sea Surface Temperature Fluctuations and their Possible Influence on the Atmospheric CO_2 Concentrations. *Pure and Appl. Geophys.*, 116: 351-371.

Newell, R. E., 1979: Climate and the Ocean. *American Scientist*, 67: 405-416.

Newell, R. E., 1986: El Niño: An Approach towards Equilibrium Temperature in the Tropical Eastern Pacific. *J. Phys. Oceanogr.*, 16: 1338-1342.

Ramage, C.S., 1987: Secular Change in the Reported Surface Wind Speeds over the Ocean.. *J. Climate and Appl. Meteor.*, 26, 525-528.

Reed, R.K., 1985: An Estimate of the Climatological Heat Fluxes over the Tropical Pacific Ocean. *J. Clim. Appl. Meteor.*, 24, 833-840.

Reynolds, R.W., 1988: Computation of the Global Air-Sea Flux Climatology. Atmospheric Forcing of Ocean Circulation, Tulane University, New Orleans, Louisiana p20-40.

Smith, S.D., 1980: Wind Stress and Flux over the Ocean in the Gale Force Wind. *J. Phys. Oceanogr.*, 10, 709-728.

Woodruff, S.D, R.L. Slutz, R.L. Jenne and P.M. Steurer, 1987: A comprehensive Ocean Atmosphere Data Set. *Bull. Amer. Meteor. Soc.* 68, 1239-1250.

Woods, J.D., 1984: The Upper Ocean and Air-Sea Interaction in Global Climate. 141-181, in *The Global Climate.* J.T. Houghton (Ed.), Cambridge University Press, Cambridge, 233 pp. .

Titov, L.F., 1969: Wind -Driven Waves. p78, translated from Russian, Israel Program for Scientific Translations Ltd., Keter Press, Jerusalem.

UNESCO, 1978: World Water Balance and Water Resources of the Earth. *Unesco Series Studies and Reports in Hydrology*, 25, Leningrad, 663pp.

WMO, 1970: The Beaufort Scale of the Wind Force. Report No. 3, Geneva, Switzerland, pp. 22.

Wu, J., 1980: Wind Stress Coefficients over Sea Surface near Neutral Conditions - a Revisit. *J. Phys. Oceanogr.*, 10, 727-740.

Wu, Z and R.E. Newell, 1992: The Wind Problem in COADS and Its Influence on the Water Balance. In H. F. Diaz, K. Wolter and S. D. Woodruff (eds.) Proceedings of the International COADS Workshop, Boulder, Colorado, pp. 189-200.

Table 1. Trends of the latent heat fluxes in the tropical regions.

Region	Without Adjustment			With Adjustment		
	b	δb	trend(Wm^{-2})	b	δb	trend(Wm^{-2})
Trop W. Pac.	0.536	0.234	30.7(Y)	0.195	0.231	9.5(N)
Trop E. Pac.	0.354	0.214	16.6(Y)	-0.006	0.215	-0.2(N)
Trop. Atl.	0.569	0.139	19.7(Y)	0.050	0.140	1.4(N)
Trop. W. Ind.	0.492	0.238	27.6(Y)	0.208	0.230	10.0(N)

Note: b is the linear coefficient of the trend, and δb its error. Y/N indicates above/below 95% significance level. Coordinates of the regions are:

Trop. W. Pac: 10°S - 10°N, 140°E - 180°;
Trop. E. Pac: 10°S - 0, 120° - 80° W;
Trop. Atl. 5°S - 10°N, 40° - 10°W;
Trop. W. Ind 5°S - 5°N, 40° - 60°E.

Table 2. Parallel comparison of Beaufort wind speed with anemometer wind speed.

stn.	Height(m)	W_b	W_a	W_a/W_b		obs.	month/year
		ms^{-1}	ms^{-1}	(obs)	(cal)		
Tomaho	4700	9.6	12.16	1.27	1.278	35	12/1971
Wudolan	4700	8.29	10.24	1.26	1.27	32	12/1971
Mado	4222	7.58	9.10	1.20	.123	52	12/1971
Goulo	3719	7.56	8.87	1.16	1.21	32	12/1971
Zaka	3086	6.81	8.23	1.21	1.18	22	11/1971
Daton	2567	5.16	5.65	1.10	1.12	20	11/1971
ZanJan	26	4.6	4.66	1.01	1.00	5	1/1972

Note: W_b is the Beaufort wind speed, W_a anemometer wind speed. Month /year is the month and year of the instrument change.

Table 3. Annual mean wind speeds before and after replacement of wind pressure palate at 10 stations.

yr	Chu	Jin	Bal	Ban	Min	Tia	Wen	Don	Chi	Bin
60	-	-	-	-	-	2.9	4.7	7.2	3.9	7.6
61	2.1	2.5	3.6	3.2	1.9	2.8	4.2	7.3	4.2	7.8
62	-	2.6	2.6	2.9	2.2	3.0	4.7	7.0	3.5	7.3
63	2.5	2.4	2.6	2.5	2.2	2.9	4.0	6.4	3.4	6.3
64	2.7	2.4	2.9	3.1	1.8	2.6	3.8	8.0	3.3	7.4
65	2.6	2.2	2.6	2.8	1.6	2.8	4.4	7.4	3.4	6.9
66	2.8	2.3	2.7	3.2	1.8	2.7	4.5	7.1	3.8	6.4
67	2.4	2.2	3.0	3.1	1.4	2.7	3.7	7.4	3.6	6.5
68	2.9†	2.6	2.3	3.1	2.3	2.9	3.8	7.1	3.3	6.1
69	3.6	3.5	2.7	3.5	2.3	3.1	4.0	6.5	3.7	6.2
70	3.5	3.5	3.6	4.9	2.3	3.1	3.9	7.0	3.7	6.2
71	2.9	3.1	4.0	4.4	2.1	3.3	4.1	6.9	3.7	6.1
72	2.8	3.1	2.7	4.5	2.0	3.3	4.2	6.9	4.0	6.0
73	2.7	3.2	3.4	4.6	2.3	3.1	4.1	7.4	4.1	6.4
74	2.3	3.3	3.8	4.8	2.2	3.3	4.2	7.5	4.2	6.6
75	2.3	3.0	3.9	4.7	2.0	3.0	4.1	6.8	4.3	5.8
76	2.6	3.3	-	-	2.0	2.8	4.2	6.9	4.3	6.5
77	2.4	3.2	-	-	1.7	2.5	3.9	6.1	4.1	6.8
78	-	3.2	-	-	1.4	2.5	5.9	6.9	4.1	6.5
79	2.4	3.1	-	-	1.5	2.7	5.8	6.7	4.4	6.0
80	2.3	3.0	-	-	1.5	3.3	5.7	6.8	4.2	5.8
$\bar{v}_1$	2.6	2.4	2.7	3.0	1.87	2.8	4.2	7.1	3.6	6.9
$\bar{v}_2$	2.7	3.2	3.6	4.7	2.0	3.0	4.7	6.9	4.2	6.3
$\Delta v(\%)$	4.0	33.0*	33.0*	57.0*	11.0	7.1	11.9	-2.8	16.7*	-8.7*

†: The corresponding year was the year of replacement of wind-pressure plate.

$\bar{v}_1$, $\bar{v}_2$: The mean annual wind speeds before and after the replacement.

*: above 95% significance level.

Table 4. Parallel comparison of maximum wind speeds from Beaufort scale and anemometer at 3 stations.

Station	W_b*(ms^{-1})	34.0	28.0	24.0	20.0	18.0	17.0
Kanemen	W_a†	22.9	18.9	18.7	16.8	15.3	15.4
	obs.	4	3	28	31	27	13
Sanbo	W_a	24.1	22.0	20.0	18.6	-	-
	obs.	2	4	8	4	-	-
Wanjan	W_a	23.5	21.2	19.2	17.5	16.1	15.1
	obs.	4	9	18	19	24	3
Average	W_a	23.5	21.0	19.1	17.2	15.7	15.4
	obs.	10	16	54	54	51	16

*: Beaufort wind speed; †: anemometer wind speed

Table 5. The changes of number of strong wind days at 6 stations

yr	Ron	Tia	Jia	Don	Chi	Bin
61	-	39	-	132	139	126
62	-	27	-	128	113	106
63	36	38	16	100	105	81
64	34	21	14	165	94	150
65	22	42	22	147	106	108
66	25	47	28	141	128	88
67	15	50	13	140	136	81
68	26	39	28	142	105	51
69	36†	32	30	113	83	60
70	5	32	16	105	58	53
71	4	23	12	95	50	80
72	1	44	17	100	55	53
73	0	32	8	133	84	83
74	1	39	17	125	57	106
75	1	37	14	104	73	58
76	0	34	16	111	76	67
77	0	43	12	82	75	101
78	2	57	17	96	85	94
79	4	43	-	91	107	72
80	14	34	-	122	76	108
$\overline{N}_1$	27.7	37.9	21.4	134.2	101.5	94.6
$\overline{N}_2$	2.7	37.5	14.3	105.8	76.4	79.5
ΔN(%)	-90.3*	-1.1	-33.2*	-21.2*	-24.7*	16.0

†: corresponding year was the year of replacement of wind-pressure plate.

$\overline{N}_1$: averaged strong wind days before replacement.

$\overline{N}_2$: averaged strong wind days after replacement.

*: above 95% significance level.

Table 6. Gusty wind effect on the torque of wind-pressure plate†

Initial wind speed(ms^{-1})	15.0	16.0	17.0	18.0	19.0	20.0
$\tau_{gust} / \tau_{steady}$	1.389	1.304	1.221	1.143	1.069	1.000

†: Assuming the calibrated position of the plate to be 45° at wind speed of $20ms^{-1}$.

Table 7. Water budget in three oceans (unit: 10^3 km^3)

	Pac			ATL			IND			ALL		
	N	S	N+S	N	S	N+S	N	S	N+S	N	S	N+S
P	112.2	115.9	228.1	48.4	31.3	79.9	18.6	62.4	81.0	179.2	209.6	388.8
E	115.1	96.8	211.9	61.8	37.7	99.5	19.5	62.6	81.7	196.3	196.7	393.1
E-P	3.4	2.3	5.7	14.8	12.2	27.0	0.9	13.7	14.6	19.1	28.2	47.2

Table 8. Monthly global mean of net heat flux (unit: W/m^2)

JAN	FEB	MAR	APR	MAY	JUN	JUL	AUG	SEP	OCT	NOV	DEC	YR
-9.3	1.0-	12.4	13.2	7.8	1.78	4.8	4.2	9.4	-0.82	-11.1	-15.2	1.0

Figure 1: The time series of latent heat flux without wind correction (solid lines) in four tropical oceanic areas. The dashed lines are the trends obtained by least square method.

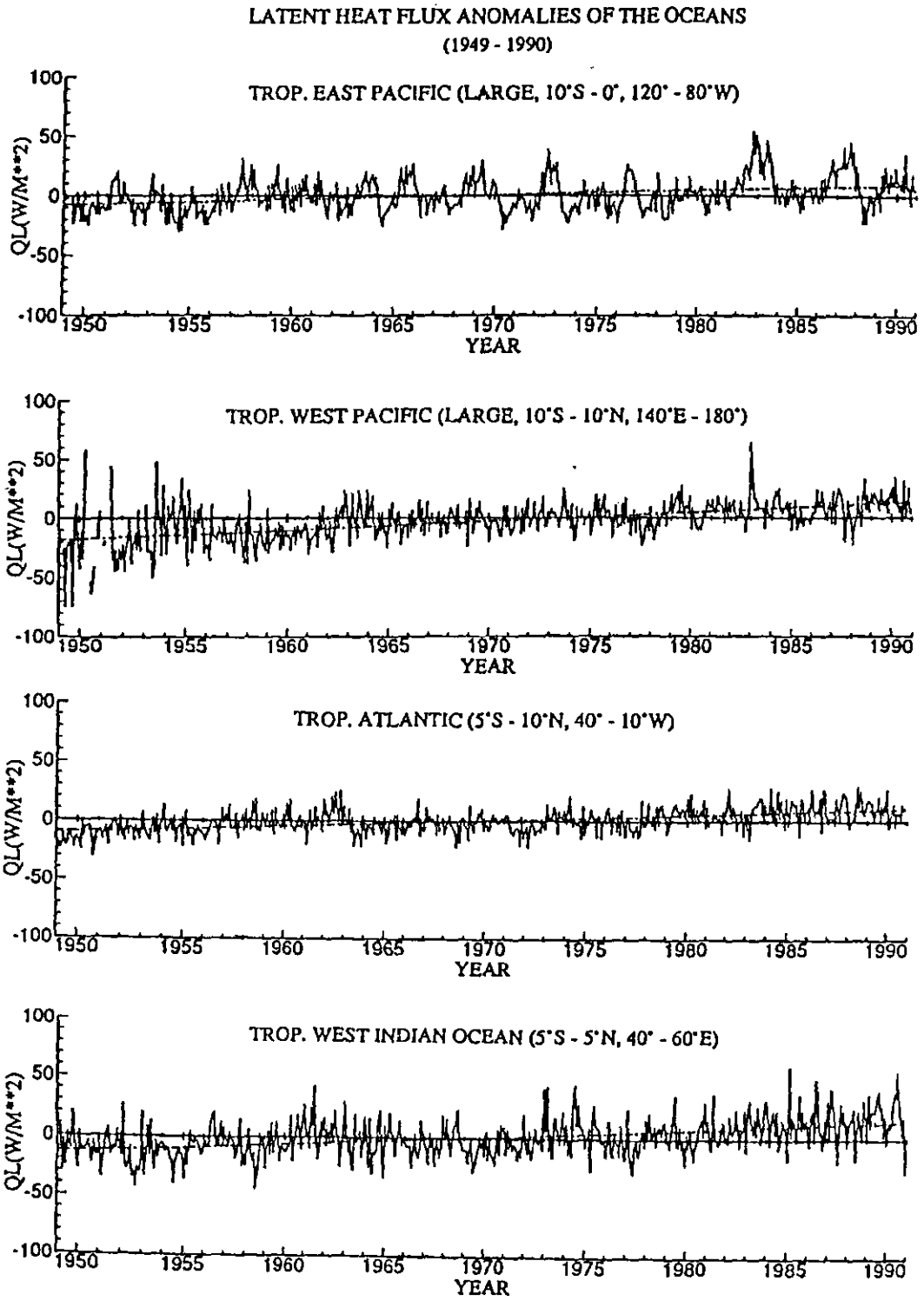

Figure 2: Japanese whaling ship route (top), measured wind (middle) and the COADS wind in the same region.

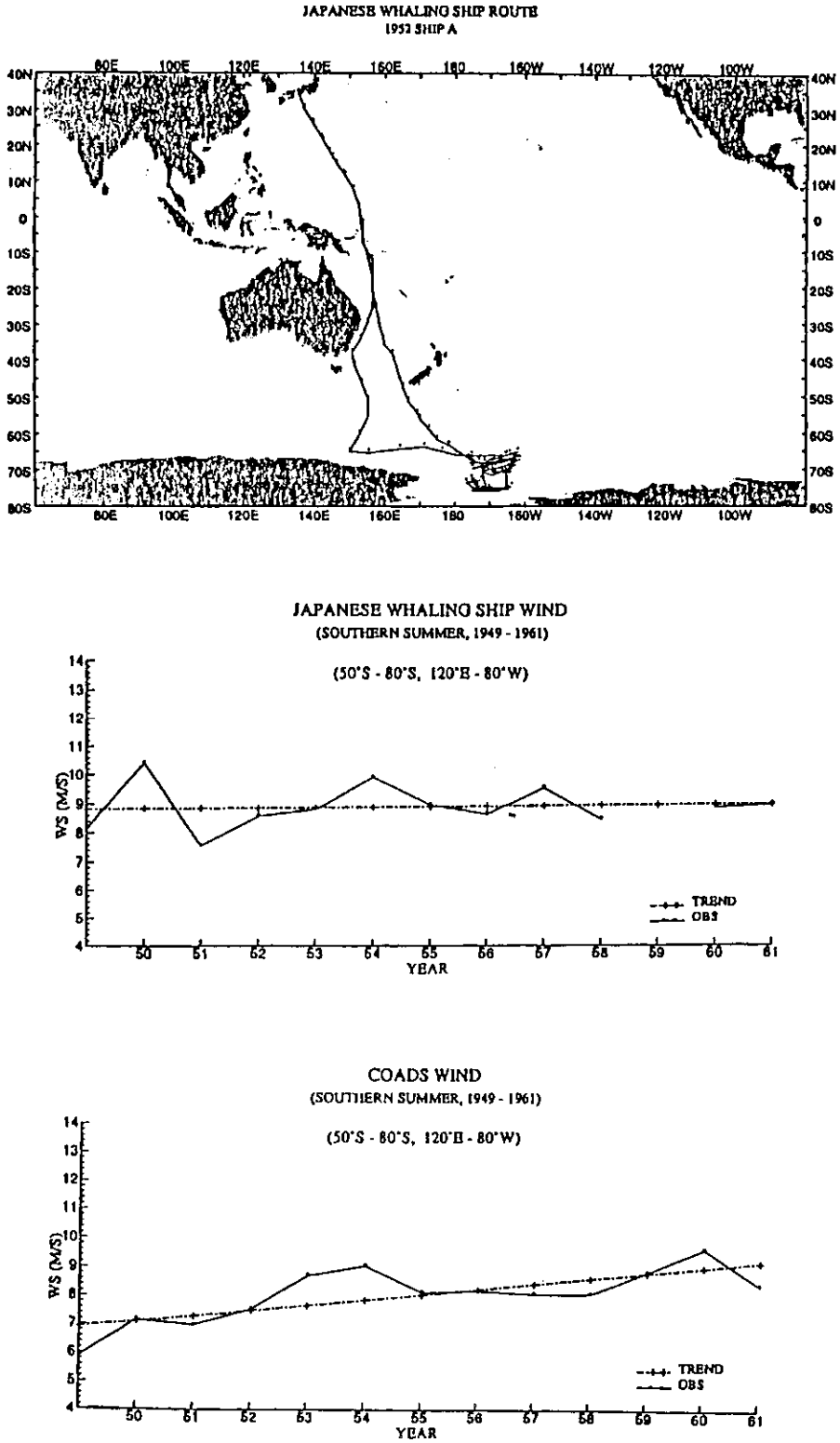

Figure 3: Forces exerted on the wind plate.

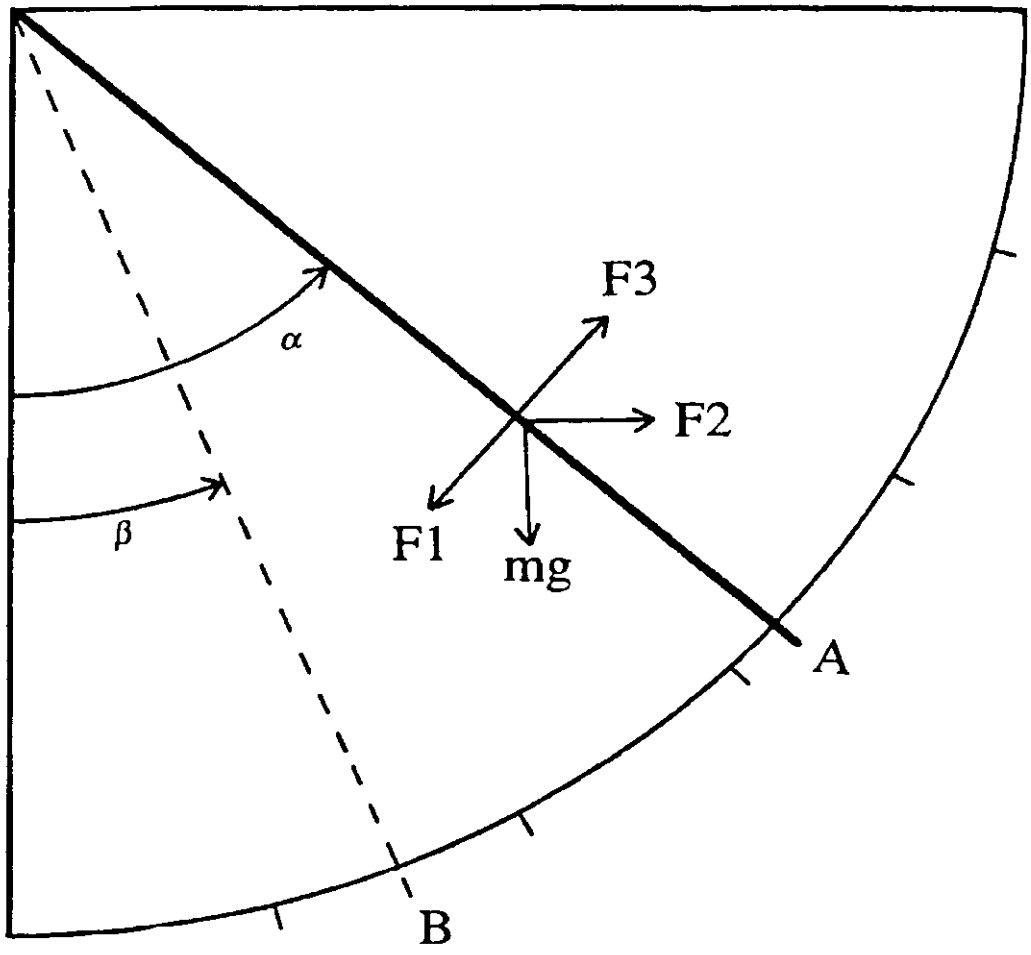

Figure 4: Same as Figure 1 but with wind correction.

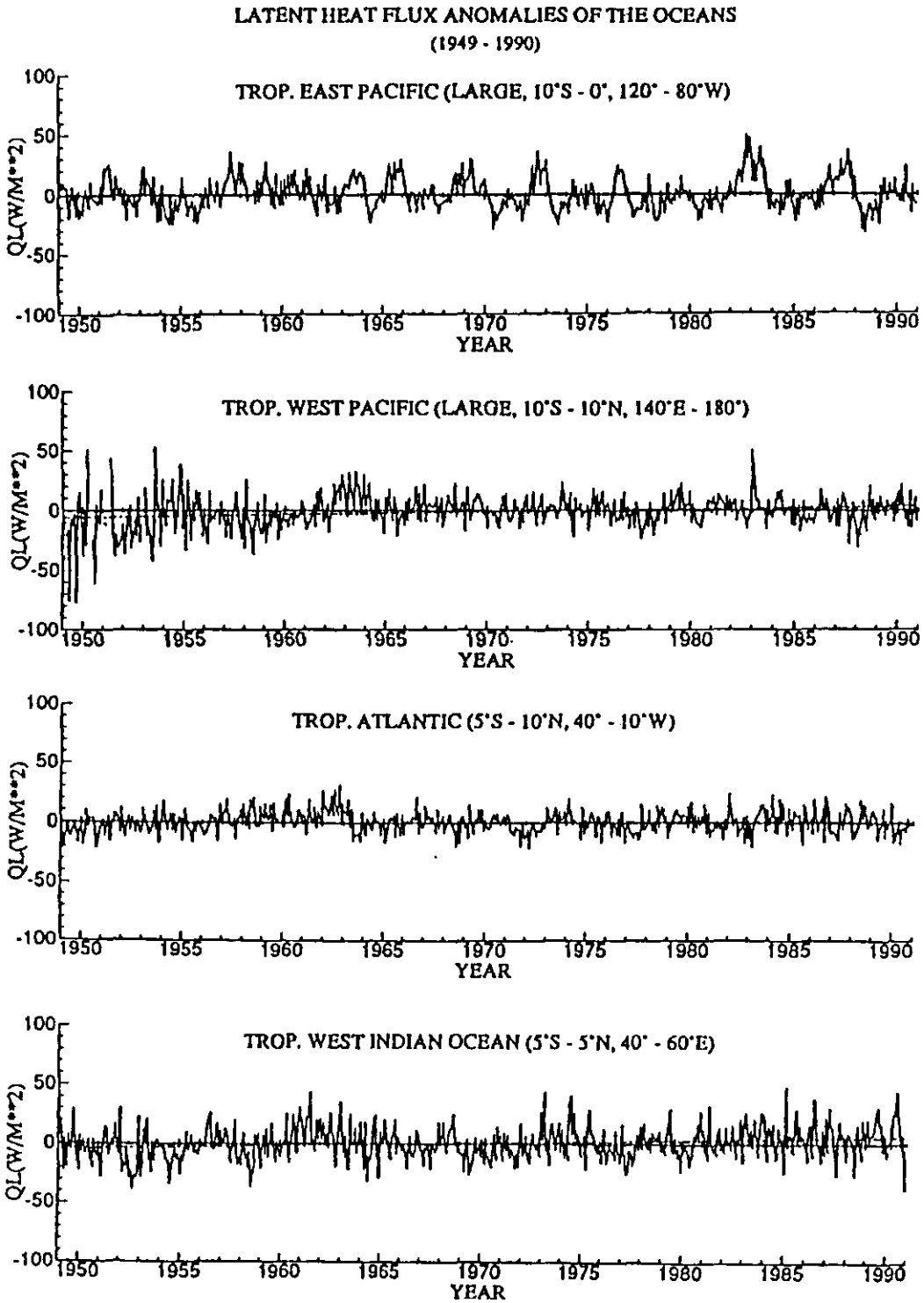

Figure 5: The effects of wind correction on the latent heat flux.

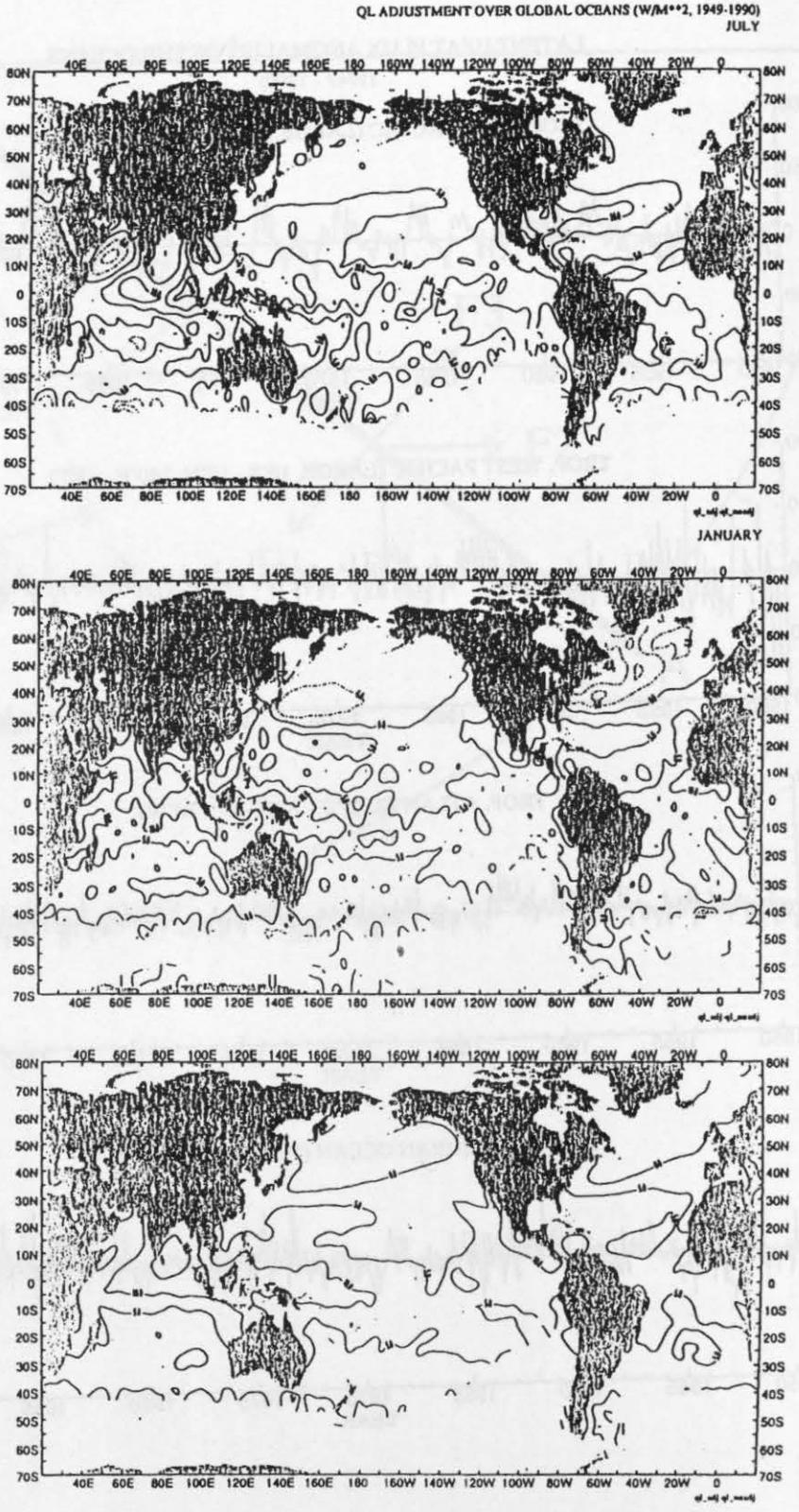

Figure 6: Net heat flux into the ocean in the western and eastern tropical Pacific Oceans.

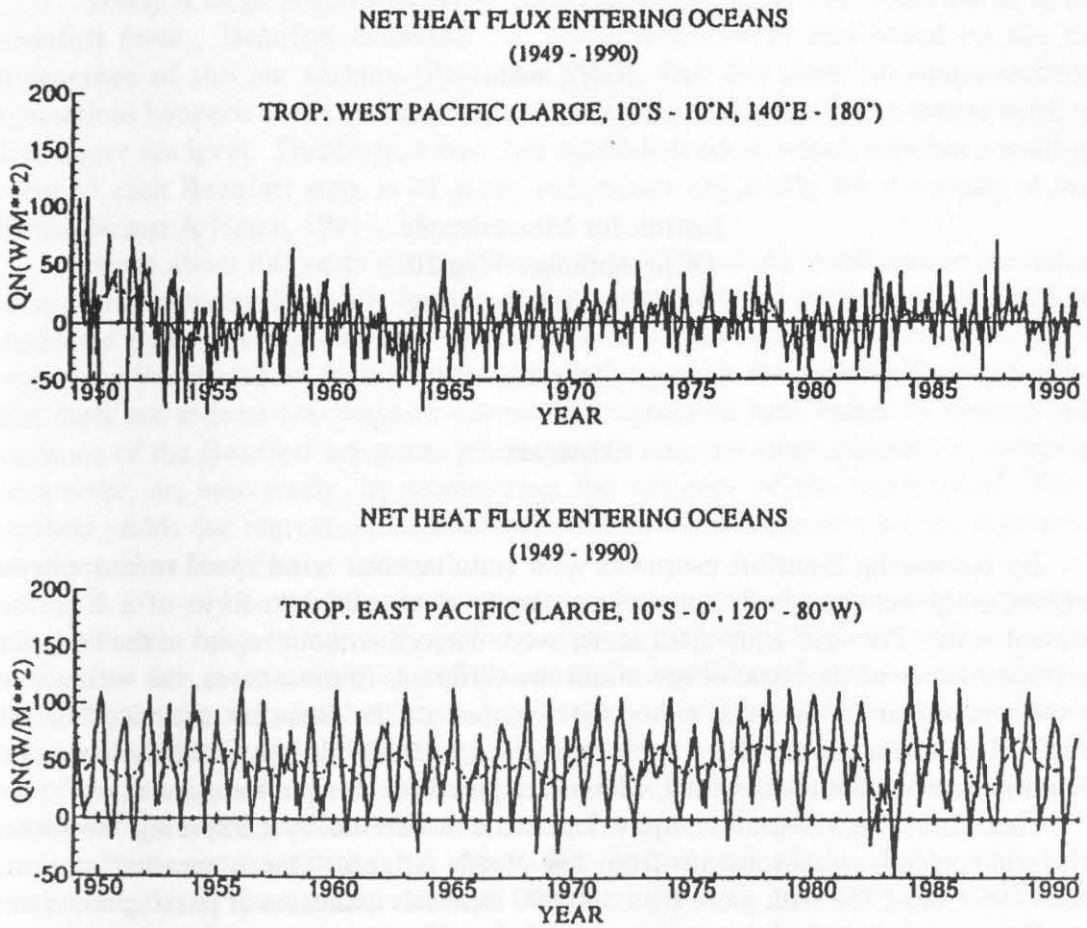

A New Beaufort Equivalent Scale

Ralf Lindau

Institut für Meereskunde
Düsternbrooker Weg 20
D-24105 Kiel, Germany

Abstract

By comparing Beaufort estimates with simultaneous wind speed measurements the relationship between both parameters can be determined in form of a Beaufort equivalent scale. Previous equivalent scales were derived without regard to the fact, that the error variances of the basic observations are different. In most cases, the variance of only one parameter minimized, either the variance of the Beaufort estimated or the variance of wind measurements. Such regression methods do not yield the universal relationship between both parameters, which is required for an equivalent scale.

Therefore a new Beaufort equivalent scale is derived by comparing the three-hourly wind speed measurements from six North Atlantic Ocean weather stations between 1960 and 1971 with more than 300,000 Beaufort estimates of passing merchant ships. But these two raw data sets are not comparable without regard to the different structure of error variances.

Firstly the random observation errors of the estimates and of the measurements are calculated to separate the error variance from natural wind variability in both data sets. In this way it can be shown that, as expected, the measurements from ocean weather stations are much more accurate than wind estimates. The difference in accuracy can be quantified. Secondly, daily means of wind speed from the measurements of the stationary ocean weather ships and spatial means from simultaneous estimates of surrounding merchant ships within an averaging area are computed. The latter comprise more individual observations than the means of ocean weather ships, so that the effects of the different observation accuracies are compensated. The radius of averaging areas are calculated separately for each season and each region, so that the spatial variability within this area is equal to the temporal variability at the ocean weather station within 24 hours. Only such pairs of averaged observations are suitable, because neither random observation errors nor natural variability has a falsifying effect. On these especially generated data pairs the method of cumulative frequencies, which allows one to detect also non-linear relationships, is applied in order to obtain the optimal Beaufort equivalent scale.

Introduction

Today a large portion of wind observations at sea is still reported in terms of Beaufort force. Beaufort estimates are made subjectively and based on the visual appearance of the sea surface (Petersen, 1927). But the usual parameterizations of interactions between ocean and atmosphere need the information of the metric wind speed 10 m above sea level. Therefore, a Beaufort equivalent scale, which attaches a wind speed value to each Beaufort step, is of great importance especially for the study of air-sea fluxes (Isemer & Hasse, 1991).

Since about 100 years many attempts have been made to determine the universal relationship between Beaufort force and wind speed. In any case, equivalent scales are evaluated by comparing Beaufort estimates with neighboring wind measurements. The regression line, based on such pairs of observation, yields the requested equivalent scale. But there are at least two ways to calculate a regression line: either by minimizing the variance of the Beaufort estimates while considering the measurements as independent parameter, or, conversely, by minimizing the variance of the wind speed. The first method yields the regression of Beaufort on wind speed, the second the regression of wind speed on Beaufort

It is well known, that these two one-sided regressions are useful to predict the most probable value of the wind speed for a given individual Beaufort estimate, and vice versa. But this is not, what an equivalent scale should perform. An equivalent scale should give the universal relationship between both parameters. In principle, this relationship is defined by the orthogonal regression, lying exactly between the two one-sided regressions. However, the error variances of both parameters have to be equal, otherwise the best equivalent scale is tilted to the more accurate parameter.

These considerations are rather old. At the end of the last century Köppen proposed, firstly in a publication of Waldo (1888), to consider the wind speed as independent and to average the Beaufort force. Other researchers followed him, and it became customary to use the regression of Beaufort on wind speed as equivalent scale. The most famous example for this kind of evaluation is the Code 1100, originally derived by Simpson (1906). This old WMO scale (Fig. 1) is still in use.

In contrast, since about 1945 most scales have been based on the reverse regression: the wind is averaged for each Beaufort number (Roll, 1951; Verploegh, 1956; Richter, 1956; WMO,1970). Consequently, the regression of wind speed on Beaufort is obtained. The accordance of nearly all modern scales in their relatively low slope does not prove the shortcoming of the old WMO scale. The reason for the difference is simply the use of different regression methods. Neither method is absolutely correct for deriving an equivalent scale. However, the old method, averaging the estimates, is better, if the measurements are more accurate. (Actually they are, which is shown subsequently.) In any case it is impossible to derive a correct equivalent scale without knowledge of the error variance in both parameters.

Data

Individual wind observations from six Ocean Weather Ships (OWS) in the North Atlantic and from neighboring Voluntary Observing Ships (VOS) were taken from COADS (Fig. 2). In order to derive a Beaufort equivalent scale, wind measurements and estimates have to be separated to be able to compare measurements from OWS with estimates from VOS. However, the only information in COADS concerning the kind of observation is a flag, indicating whether the wind is measured or whether the observation method is unknown. Additionally, this flag seems to be not very reliable. (Isemer & Lindau, 1994). For this reason all wind observations from OWS are assumed to be measured without regard to the flag. All VOS reports, flagged as unknown, are assumed to be Beaufort estimates.

In COADS direct information about Beaufort force is only available in some decks. The standard information concerning the wind force is given in knots, even if the wind was originally estimated. Obviously the wind speed was obtained by converting the estimates with the old WMO scale Code 1100. In the following computations these knot-values will be used, because averaging Beaufort numbers is difficult due to the non-linear character of the Beaufort scale.

In this study the period from 1960 to 1971 is considered. The fifties and sixties were the decades with the largest number of OWS in the North Atlantic. The evaluations are restricted to an even more limited period, because there are indications of a time-drift of the scale. Therefore, first an equivalent scale has to be developed for a certain, relatively short period. After that, a calibration with pressure gradients allows to calculate a time dependent scale. The latter was done in another study, also published in this volume.

Error Variances of the Observations

As mentioned above, it is necessary to know the magnitude of the observation errors in both parameters, in measurements and in the estimates, before deriving an equivalent scale.

The random error variance of Beaufort estimates from VOS is calculated in the following way. Pairs of simultaneous observations are formed within the VOS data set. The difference in wind speed between two ships is computed, squared and summed up, separately for 50 different classes from 10 km to 500 km. In this way the mean total variance of the observed wind is obtained as a function of distance Δx (Fig. 3). Two factors contribute to the variance: on the one hand true natural wind variability, in this case pure spatial variability because the observations are simultaneous, and on the other hand random observation errors. Of course the total variance is growing with increasing distance, reflecting the spatial wind variability. At the distance $\Delta x=0$ no natural wind variability remains, so that here the total variance consists exclusively of the error variance σ_o^2. The σ_o^2 cannot be calculated directly, because two ships cannot be in the same place at exactly the same time. However, an estimate of σ_o^2 may be obtained by a linear fit for the total variance and extrapolating to $\Delta x=0$. In this way an error variance

Not only error variances in both parameters must be equal, but also the mean natural variability which is included in the averages. For example, monthly means are not at all comparable to 10-minute means. In this regard a problem appears because of the different structure of OWS and VOF data. Measurements from stationary OWS have to be averaged in time, but merchant ship reports have to be averaged in space. Therefore, corresponding spatial and temporal averaging radii have to be defined.

While OWS measurements were always averaged over 24 hours, the corresponding spatial averaging radius for VOS was computed for each season and each region. Figure 6 shows for example the evaluations at the vicinity of OWS I in autumn. First, the error variance of OWS is computed analogous to the method described in Section 3, but taking time lags instead of spatial distances. This value is subtracted from the total measured variance to obtain the true natural variability within 24 hours. Taking now the VOS data, the error variance is computed too, and the natural variability can be separated. Then the radius is searched, where the pure spatial variability is equal to the pure temporal variability within 24 hours deduced from OWS data. In most cases a radius between 300 and 400 km results.

The New Scale

We are now able to derive an equivalent Beaufort wind scale. Daily means of OWS measurements are compared to spatial means of observations from neighboring merchant ships, within the averaging radius evaluated above. OWS means are always based on 4 individual reports. VOS means are calculated, if at least three simultaneous observations are available. The VOS means are based on about 6 individual reports in average. These averages fulfill two conditions: (1) their mean accuracy is equal and (2) they contain the same natural variability.

The method of cumulative frequencies yields the new Beaufort equivalent scale (Fig. 7 and Table 1). Actually, the old WMO scale Code 1100 is calibrated, because the COADS knot-values, which are based on this scale, are used for the computations. The new scale is valid for a height of 25m, since this is the OWS anemometer level. The general features of the new scale, compared to the Code 1100, are considerable higher values for the most frequent Beaufort numbers. This is not at all surprising, because the new scale is valid for 25m instead of 10m.

An alternative scale is derived using reduced OWS measurements. The wind speed reduction from 25m to 10m was carried out as described previously. Figure 8 shows the resulting 10m-scale. The equivalent values of this new scale are rather similar to the old WMO scale code 1100 for the most frequent Beaufort numbers 2 to 6. Their trifling rise compared to the old WMO scale is compensated by considerable lower values for the stronger and less frequent Beaufort numbers. This result confirms entirely the previous consideration concerning the regression methods: it is true, the Code 1100 curve ascends slightly too strong if equivalent values are plotted against Beaufort number, since measurements are of course not totally accurate. However, the old WMO scale is not at all as insufficient as most of the newer derivations suggest, because the accuracy of measurements, at least at OWS, is much better than the accuracy of Beaufort estimates.

Applications of the Scale

If the new Beaufort scale is well derived, wind speed measurements of OWS should coincide with converted estimates of surrounding merchant ships. In this manner, the new 25m-scale is tested. Individual monthly means within an area of 5° latitude and 7° longitude are evaluated from VOS data by using the new scale. They are compared to monthly means of the OWS, which is situated in the center of the area. This is carried out for the period 1960 to 1971 for the selected area surrounding the six OWS, which are used for the derivation. For such comparisons the orthogonal regression has to be used, because error variances of monthly means, based on several hundred individual reports, are negligibly small. Figure 9 shows the almost optimal agreement of OWS measurement and converted VOS estimates.

This result is not totally trivial. Only a relatively small part of the VOS data was used to derive the new scale, in order to satisfy the requirements with regard to the variances. The test proves, that the restricted sample is representative for the whole data.

Some further remarks are necessary concerning the application of the new scale. In order to compute fields of wind stress the squared wind speed v^2 has to be evaluated. But observation errors affect the results as follows. A wind speed observation V may be divided into the true part v and an observation error Δv according to:

$$V=v+\Delta v$$

Consequently, the mean pseudo stress $[V^2]$, calculated simply from the observations, contains not only the true value $[v^2]$, but also the error variance $[\Delta v^2]$.

$$[V^2]=[v^2]+[\Delta v^2]$$

Thus, as a matter of principle, calculating wind stress is impossible, if the observation error of the wind speed is unknown. This holds true, if the calculations are based on Beaufort estimates. In this case the error variance of the converted estimates has to be ascertained. Since the scale recommended in this study is derived by separating natural variability and error variance, the effect of observation inaccuracy is easy to calculate. It is exactly the error variance which was computed for merchant ship observations in an earlier section.

Universality of the Scale

Further equivalent scales are derived for different meteorological conditions, for example stability-dependent and seasonal scales (Fig. 10). The differences are small, so that the conversion of all wind estimates with only one universal scale is possible without great errors.

Unfortunately, the nations of the merchant ships are not registered in COADS until the year 1970. In order to derive special scales for each nation a data set from

Seewetteramt Hamburg is used. These observations show, that different nations estimate the wind's force very differently.

In average American Beaufort estimates are about 2 knots higher than neighboring German observations! Consequently national equivalent scales are quite different (Fig. 11). For this reason, a multi-national scale which is derived in the North Atlantic cannot be transferred into a region with another nation-mix, like the Pacific ocean. In order to convert Beaufort estimates of COADS, it would be very helpful, if the nationality of the ships were available, so that the different national scales could be applied.

Summary

Evaluations of the error variance for OWS measurements and for VOS estimates show, that wind measurements on board of OWS are much more accurate. Paying attention to the different observation errors and also taking care for comparable natural variability in both data sets, a new equivalent scale results, which is not very different to the old WMO scale Code 1100. The similarity is due to the fact, that the regression method used in former times was very reasonable: In contrast to the present, the more accurate wind speed measurements were considered as an independent parameter.

Strictly speaking, the recommended scale is valid only in the North Atlantic and for the period 1960 to 1971. A transfer in time is attainable by using gradients of air pressure. A transfer in space seems to be possible without problems, because special scales for different meteorological situation are rather similar. However, the obvious differences in estimating wind force between different nation raise some problems, if the scale is transported in regions with other prevailing countries of origin. For a careful conversion of Beaufort estimates different scales should be used for different nations.

References

Cardone, V.J., 1969: Specification of the wind distribution in the marine boundary layer for wave forecasting. Report TR69-1, New York University, New York, N.Y., 131 pp.

Isemer, H.J. & L. Hasse, 1991: The Scientific Beaufort Equivalent Scale: Effects on Wind Statistics and Climatological Air-Sea Flux Estimates in the North Atlantic Ocean. *J. Climate*, 4 , 819-836.

Isemer, H.J., & R. Lindau, 1994: On the Homogeneity of Surface Wind Speed Records from Ocean Weather Stations. Submitted to Journal of Atmospheric and Oceanographic Technology.

Kaufeld, L., 1981: The development of a new Beaufort equivalent scale. *Meteorol. Rundsch.*, 34, 17-23.

Köppen, W., 1916: Beaufortskala und Windgeschwindigkeit. *Meteorol. Zeitschr.*, 33, 88-91.

Köppen, W., 1926: Über geschätzte Windstärken und gemessene Windgeschwindigkeiten. *Annalen d. Hydrographie u. Marit. Met.*, 54, 362-366

Large, W.G. & S. Pond, 1981: Open ocean momentum flux measurements in moderate to strong winds. *J.Phys.Ocean.*, 11, 324-336

Lindau, R., H.-J. Isemer, L. Hasse, 1990: Towards time dependent calibration of historical wind observations at sea. *Trop. Ocean-Atmos. Newslett.*, 54, 7-12.

Petersen, P., 1927: Zur Bestimmung der Windstärke auf See. *Annalen der Hydrographie* 55, 69-72.

Roll, H.U., 1951: Zur Frage der Umrechnung Beaufort - Knoten auf See. *Annalen d. Meteorol.* 4, 408-410

Richter, J., 1956: Geschwindigkeitsäquivalente der Windstärkeschätzungen nach Beobachtungen auf deutschen Feuerschiffen. *Annalen der Meteorologie*, 7, 267-287.

Simpson, C.G., 1906: The Beaufort Scale of Wind-Force Report of the Director of the Meteorological Office, Official No. 180, London

Verploegh, G., 1956: The Equivalent Velocities for the Beaufort Estimates of the Wind Force at Sea. Koninklijk Nederlands Meteorologisch Institut, *Medelingen en Verhandelingen*, 66, 1-38.

Wonnacott, R.J., T.H. Wonnacott, 1981: *Regression: A second course in statistics.* John Wiley & Sons, New York, 556pp.

Waldo, F., 1888: Vergleich von Beauforts Skala und Windgeschwindigkeit. *Meteorol. Zeitschr.*, 5, 239-241.

World Meteorological Organization, 1970: Reports to marine science affairs. Rep. No. 3: The Beaufort scale of wind force. WMO, Geneva, Switzerland, 22pp.

Table 1: New Beaufort equivalent scale, valid for a height of 25m above sea level.

Bft	0	1	2	3	4	5	6	7	8	9	10	11	12
knots	0.0	2.3	5.4	9.5	15.0	20.5	25.5	30.9	36.8	43.2	50.6	58.9	68.8

Table 2: Mean scalar wind speed difference between VOS estimates compared to simultaneous and neighbouring (up to 150 nm) measurements from OWS.

Nation	Former SU	USA	France	United Kingdom	FR Germany	Nether-lands
Δu kn	0.0	-0.3	-1.2	-1.5	-2.0	-2.3

Figure 1: The old WMO scale Code 1100 compared to the scientific Scale of the WMO CCM IV. The old scale is based on the regression of Beaufort on wind speed, the latter on the regression of wind speed on Beaufort.

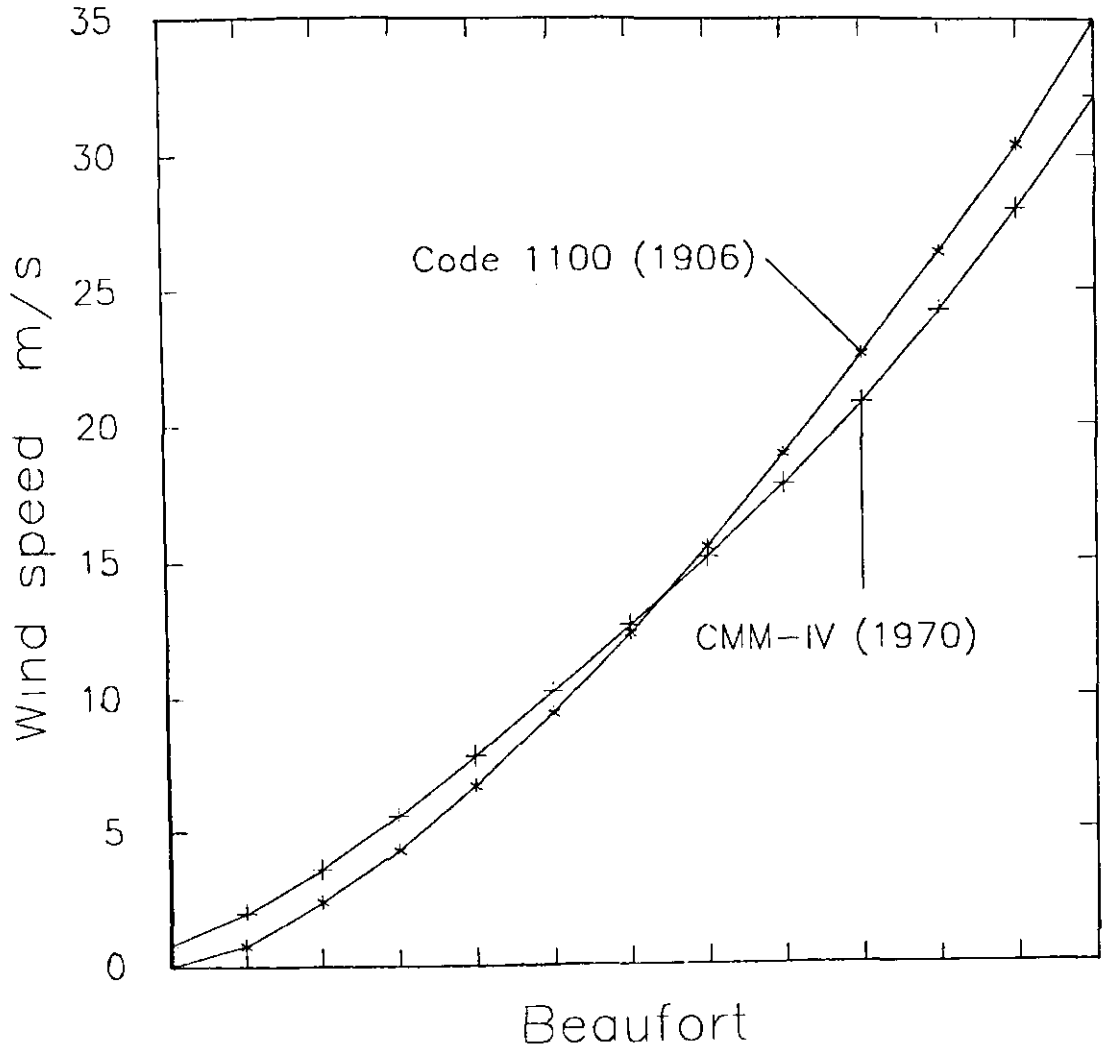

Figure 2: Locations of six North Atlantic ocean weather stations. Their wind speed measurements were used to derive a new Beaufort equivalent scale.

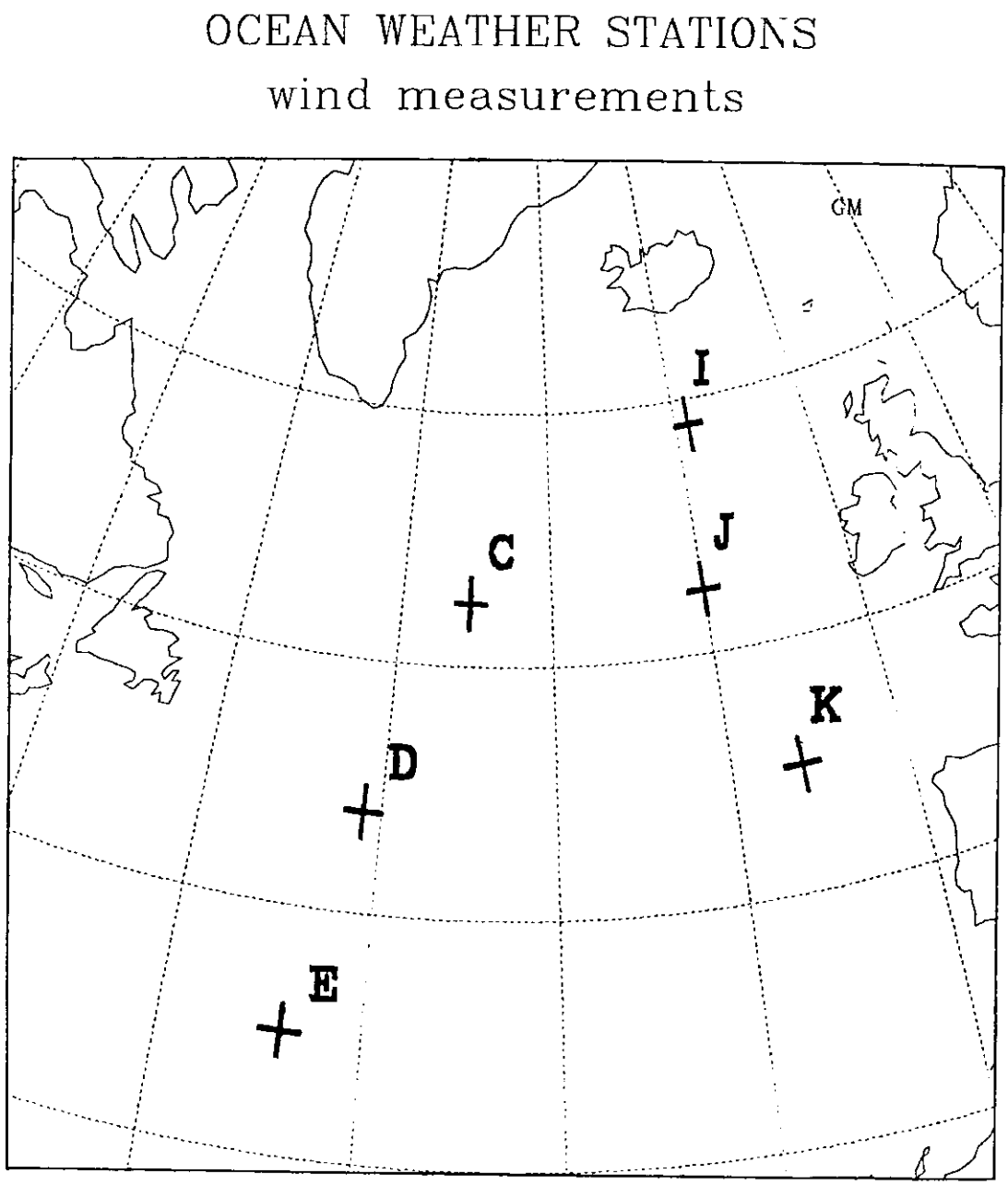

Figure 3: Mean squared difference of wind speed as a function of distance. The results are based on pairs of VOS-VOS estimates.

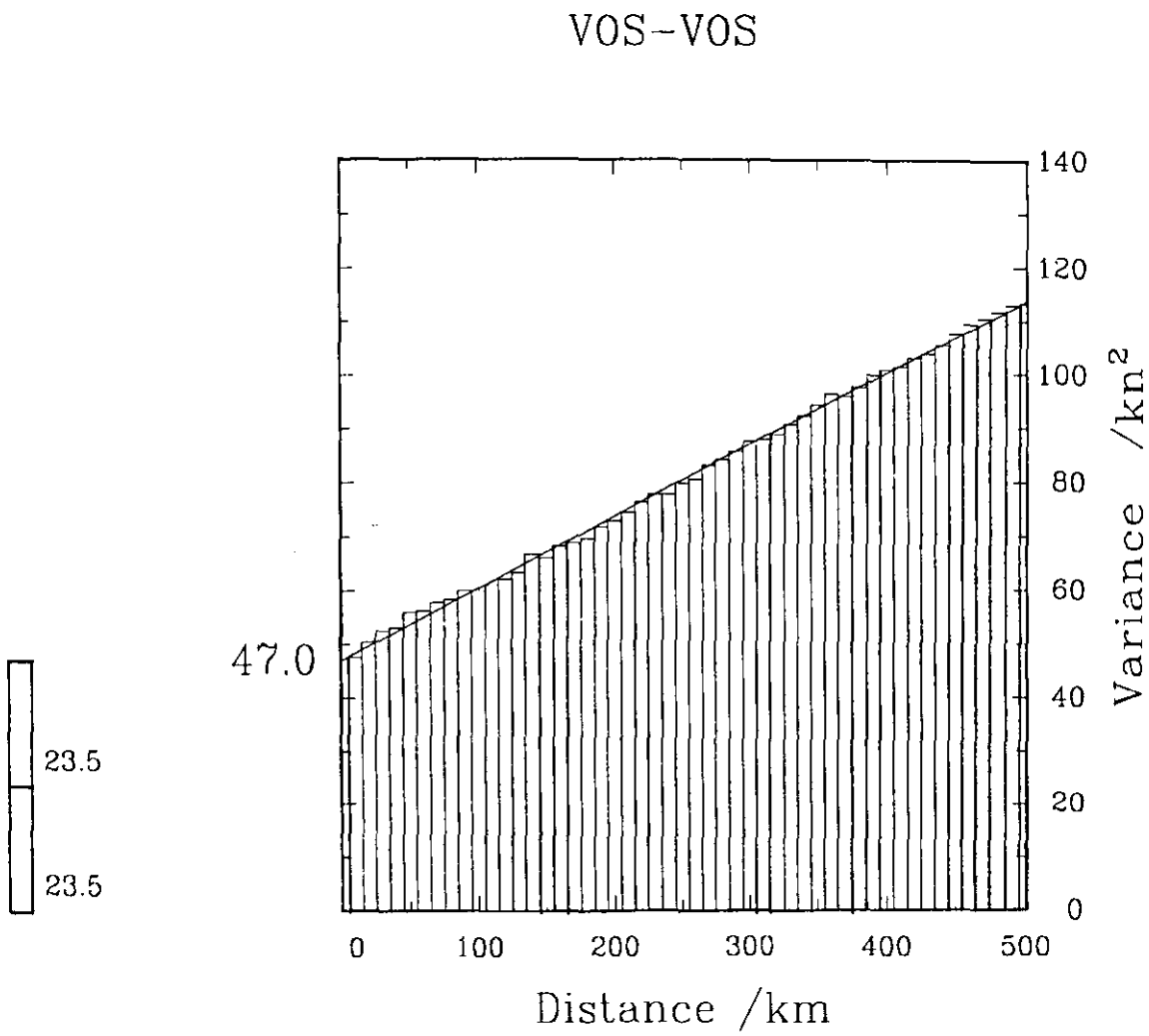

Figure 4: As figure 3, but additionally the results for pairs of OWS-VOS as hached portion of the bars. The measurements of OWS are not reduced.

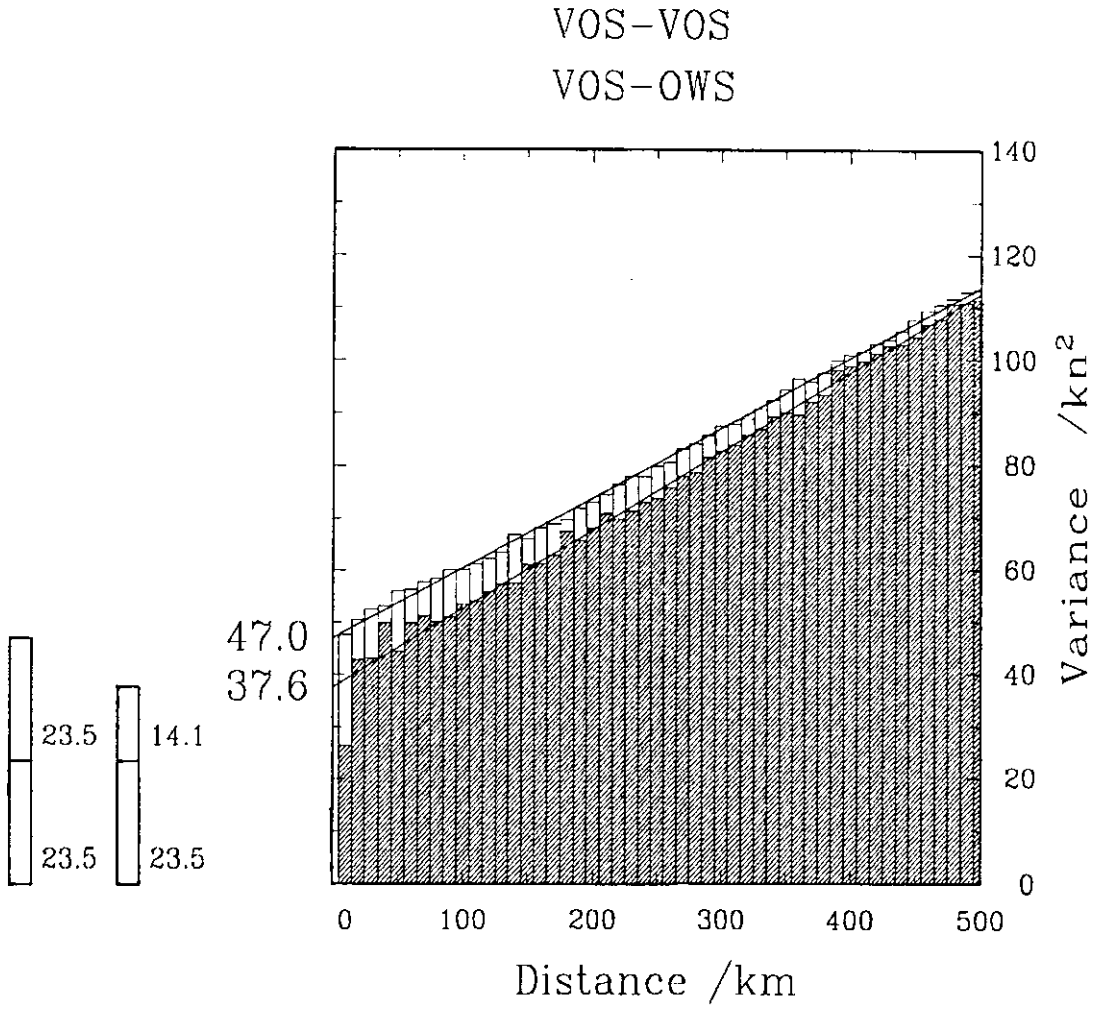

Figure 5: As figure 4, but the measurements of OWS are reduced from 25m to 10m.

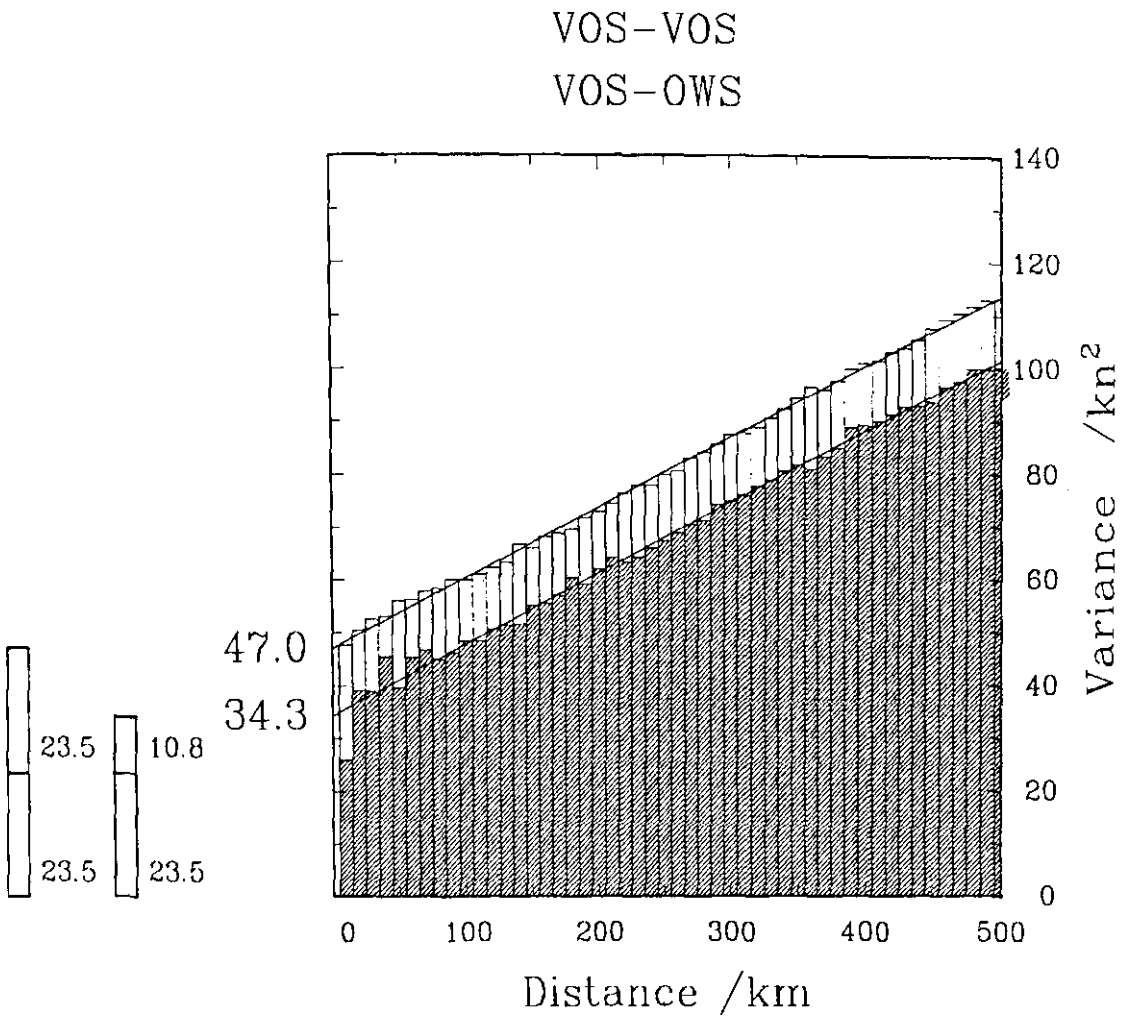

Figure 6: Illustration of computing the averaging radius, examplified by the season autumn in the vicinity of OWS I.

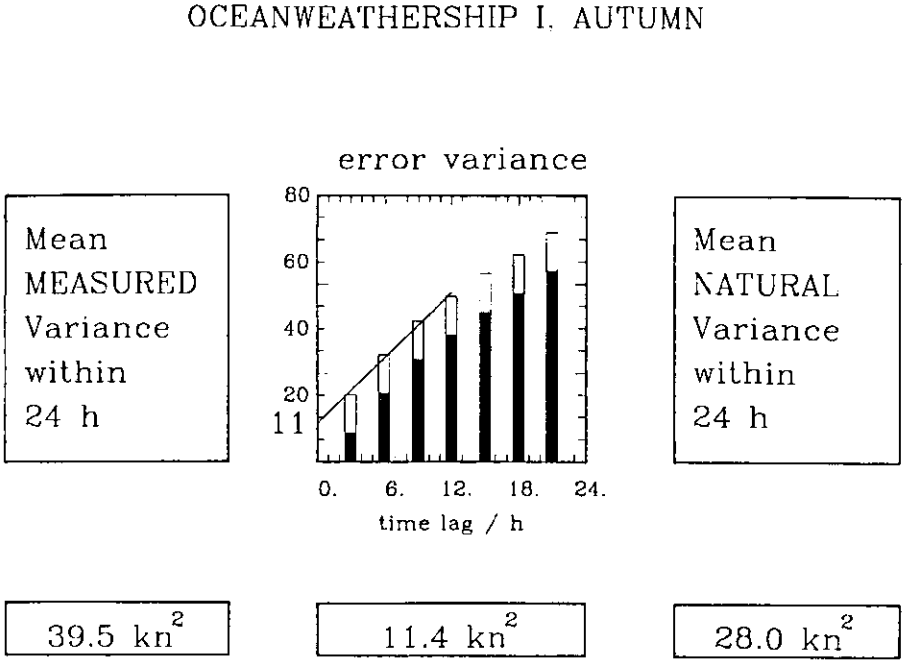

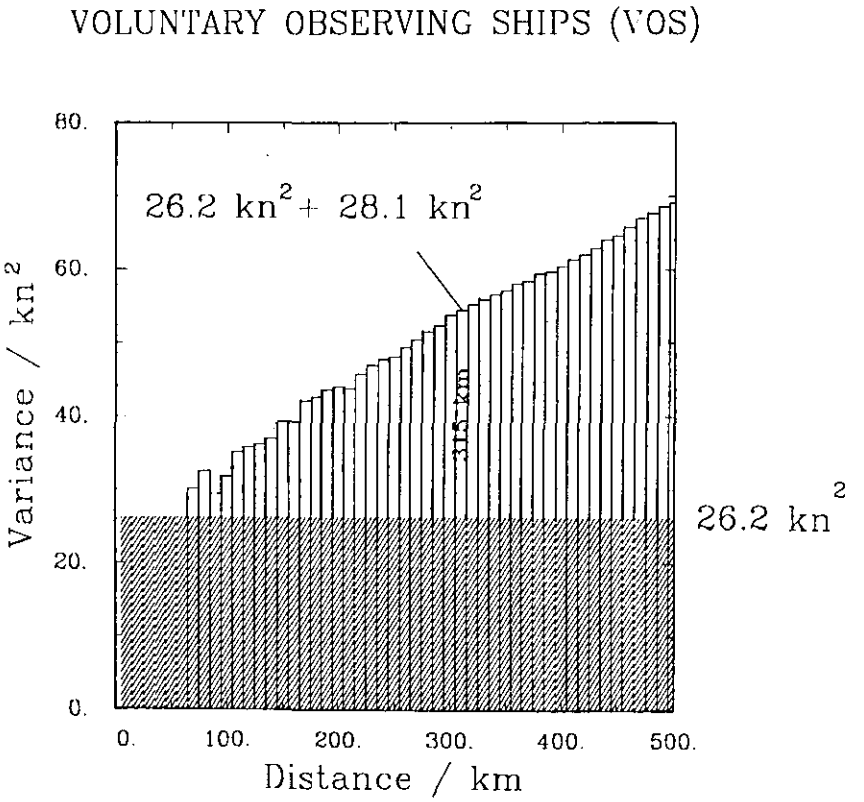

Figure 7: New Beaulort equivalent scale valid for a height of 25m above sea level.

BFT	0	1	2	3	4	5	6	7	8	9	10	11	12
WMO	0.0	1.7	4.7	8.4	13.0	18.3	23.9	30.2	36.8	44.0	51.4	59.4	67.7
NEW	0.0	2.3	5.4	9.5	15.0	20.5	25.5	30.9	36.8	43.2	50.6	58.9	68.8
N	6	378	2287	8441	17197	11598	8870	4655	2068	597	122	15	1

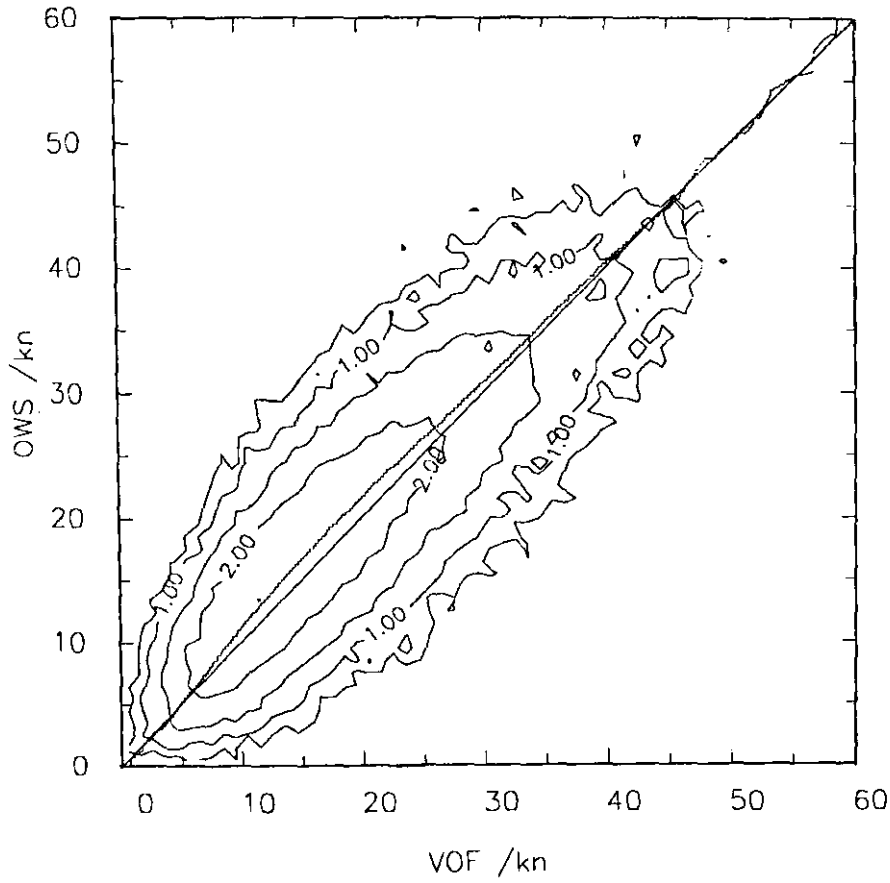

Figure 8: New Beaufort equivalent scale based on reduced OWS measurements, therefore valid for a height of 10m.

BFT	0	1	2	3	4	5	6	7	8	9	10	11	12
WMO	0.0	1.7	4.7	8.4	13.0	18.3	23.9	30.2	36.8	44.0	51.4	59.4	67.7
NEW	0.0	2.3	5.2	8.9	13.9	18.9	23.5	28.3	33.5	39.2	45.5	52.7	61.1
N	6	378	2287	8441	17197	11598	8870	4655	2068	597	122	15	1

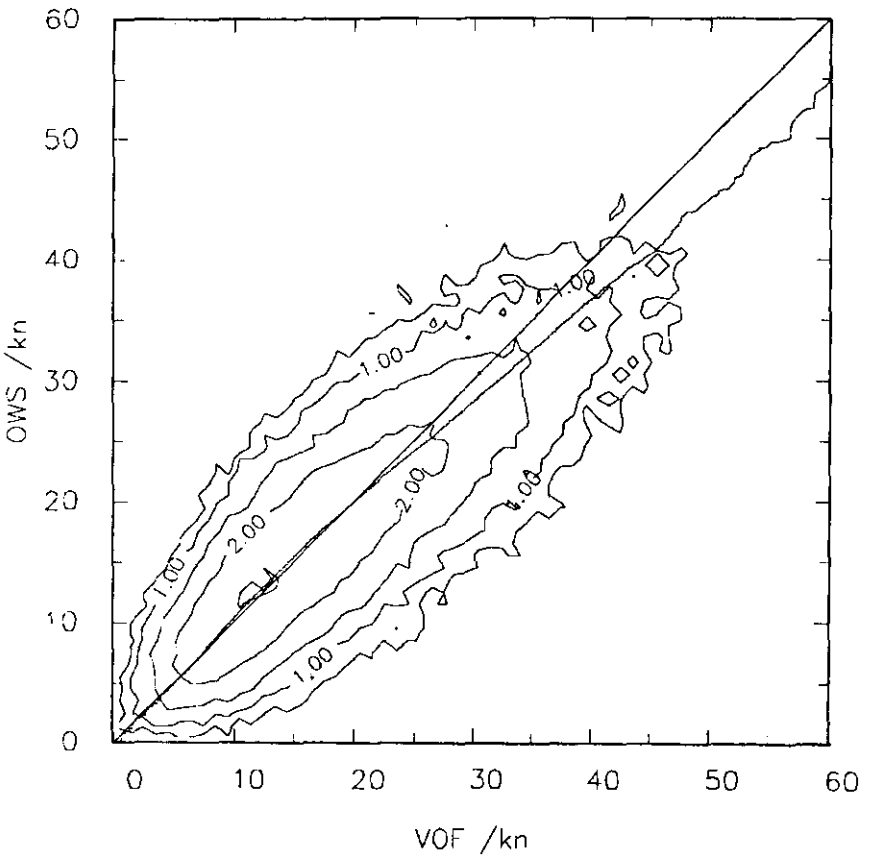

Figure 9: Individual monthly means of the wind speed in the North Atlantic from 1960 to 1972. In order to test the new 25m-scale, converted Beaufort estimates of VOS are compared to OWS measurements. VOS estimates are taken from a 5° x 7° areas surrounding the respective OWS.

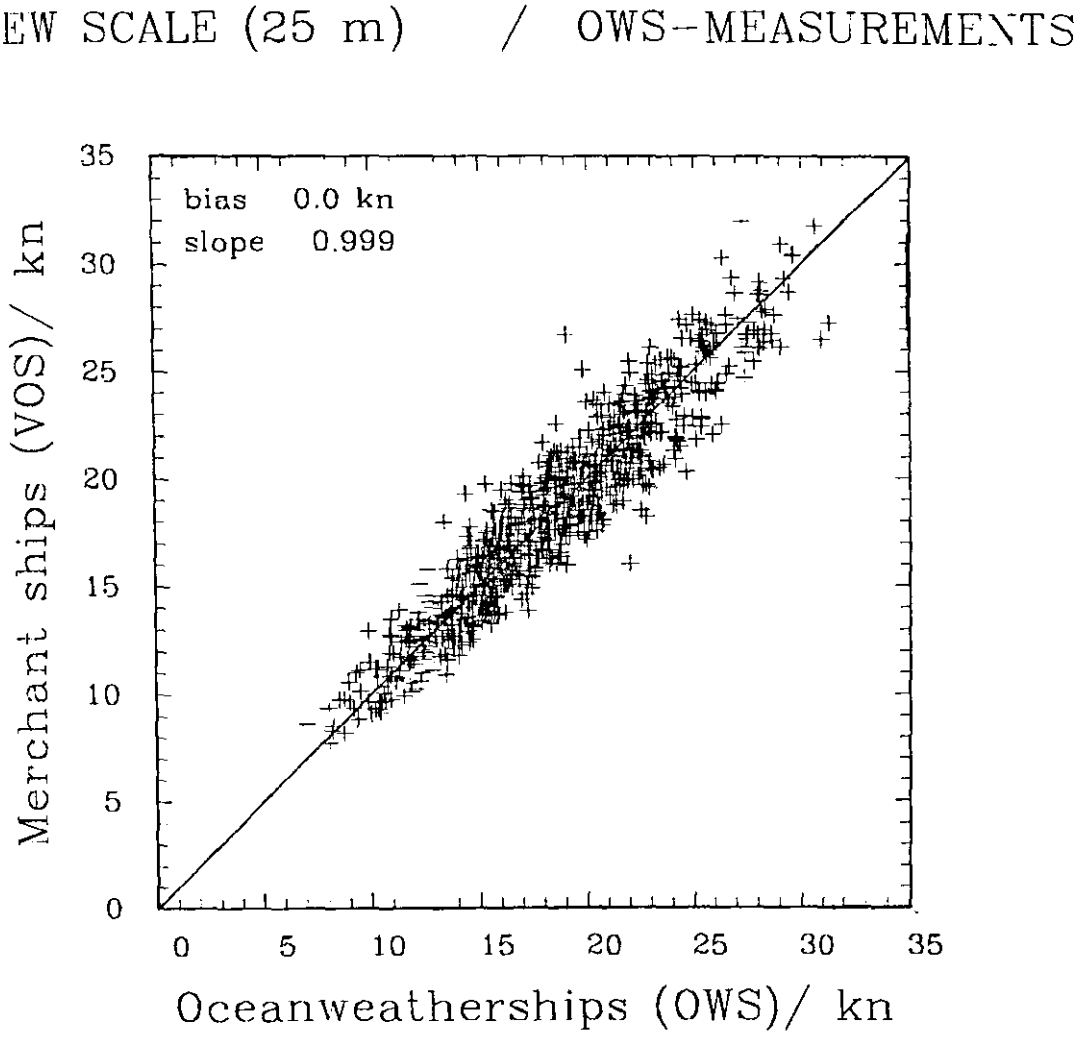

Figure 10a: Beaufort equivalent scales derived separately for each season. Differences to the proposed universal scale are evaluated.

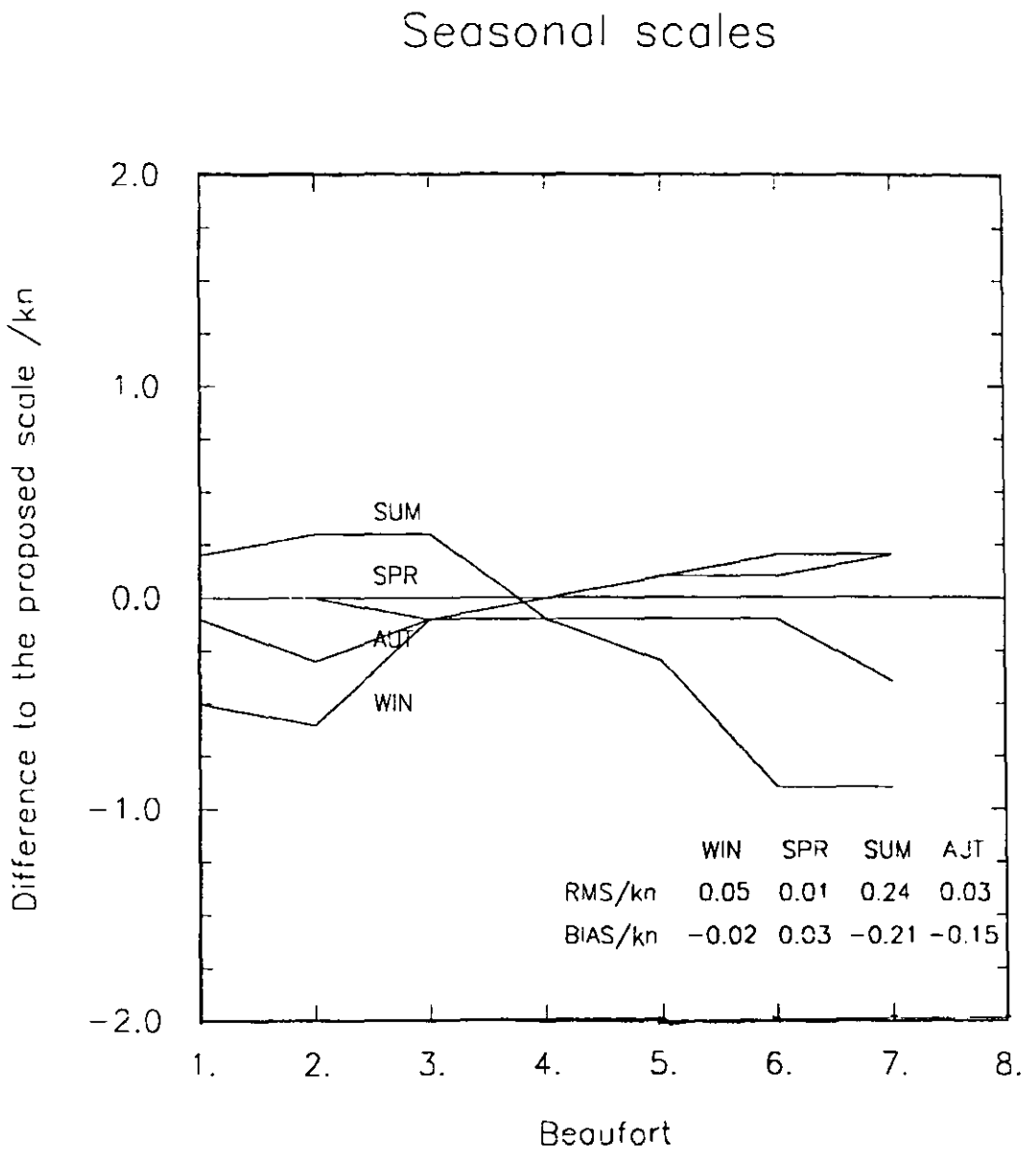

Figure 10b: As Figure l0a, but for (1) instability and (2) stability of near neutral conditions, respectively. The critical value separating both conditions is a temperature difference of -1 K between air and sea.

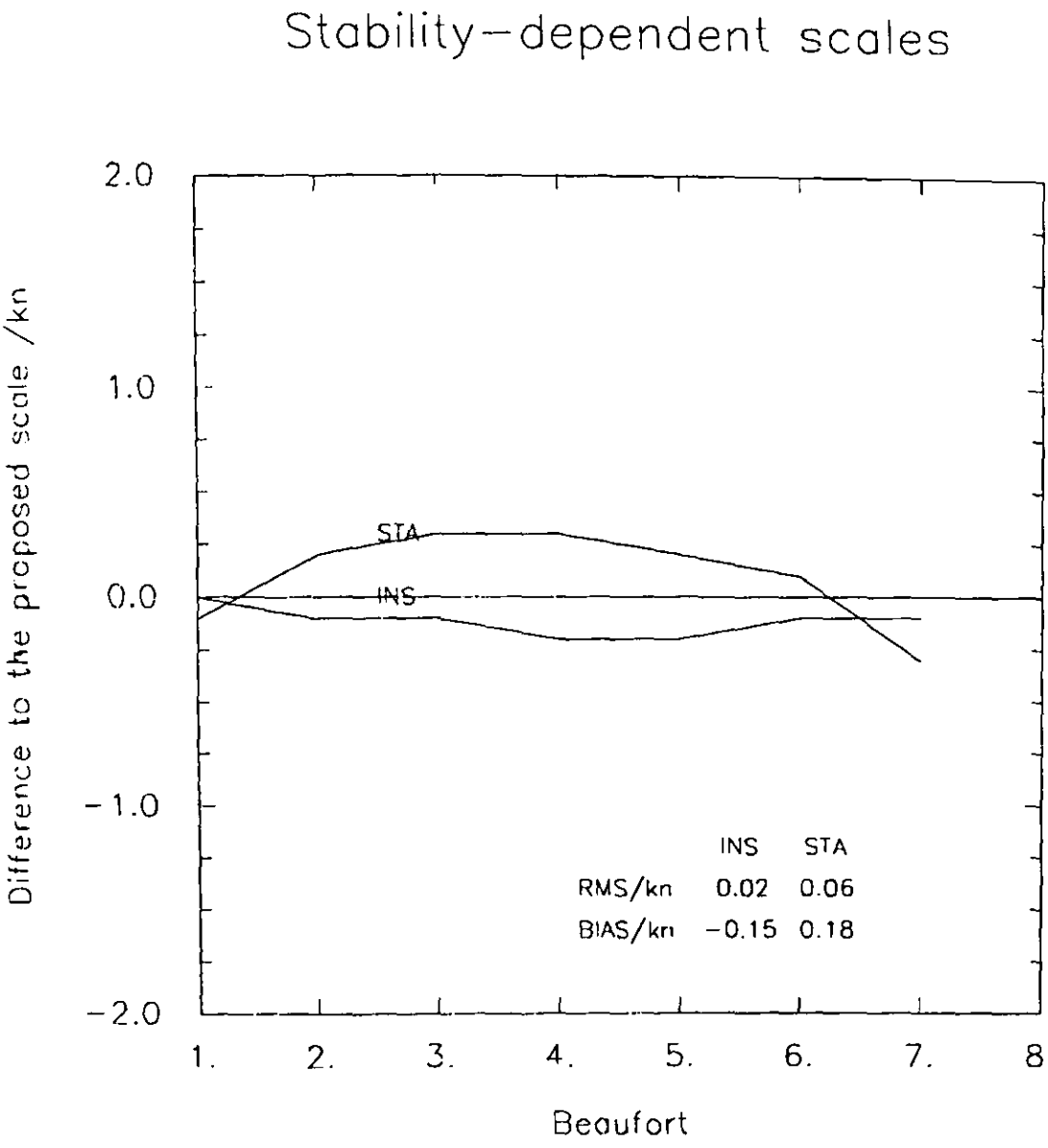

Figure 11: As Figure 10, but for the USA and Germany, respectively.

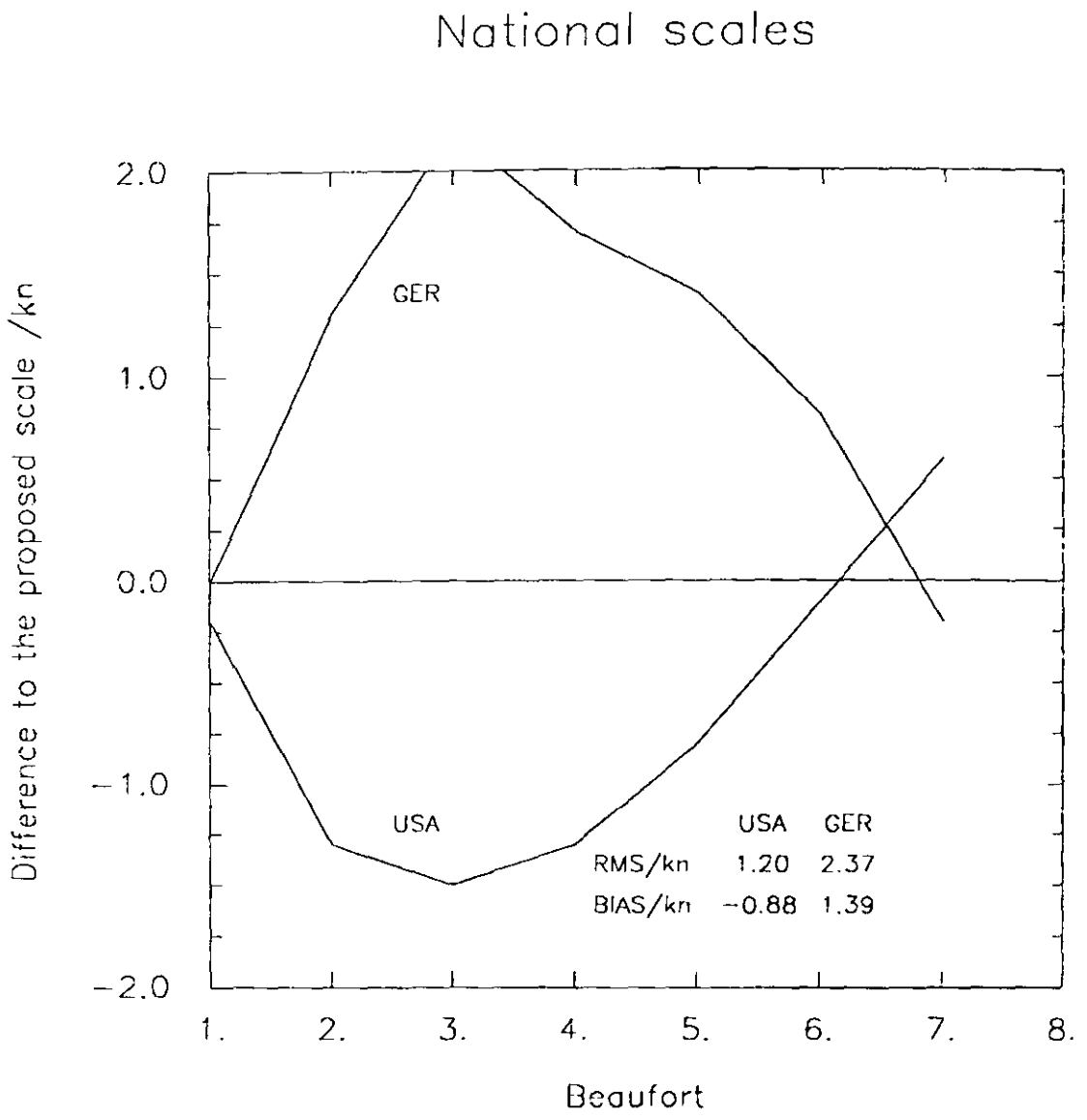

Time Dependent Calibration of Marine Beaufort Estimates Using Individual Pressure Differences

Ralf Lindau

Institut für Meereskunde
Düsternbrooker Weg 20
D-24105 Kiel, Germany

Abstract

COADS contains wind estimates from the last 130 years. They indicate a considerable negative trend until World War II, after that an often discussed increase of the wind force. Whether these trends are a true climate signal is questionable because the observing practices have changed during the last century which probably introduced an artificial interdecadal trend into the wind series.

In order to examine this question, Beaufort estimates from COADS are compared to individual pressure differences between two ships. In this way the geostrophic wind component perpendicular to the function line of the ships is obtained. Assuming a constant geostrophic angle this component depends on the wind direction relative to the function line and a sinusoidal fit over all relative wind directions leads to the geostrophic wind speed, when effects of observation inaccuracies in the wind direction are eliminated.

According to this method mean geostrophic wind speeds are computed for each month of an individual year, separately for the four 10° latitude zones between 20°N and 60°N in the North Atlantic. With an orthogonal regression the relationship between wind force and geostrophic wind is determined for each year, based on the 12 monthly values. It is assumed that this relationship has to be constant through the years and each deviation is referred to a temporal drift of the Beaufort scale. In this way a time-dependent equivalent scale is evaluated, using the scale for the period 1960-1971 (see Lindau: "A New Beaufort Equivalent Scale", this volume).

If Beaufort estimates of COADS are converted with the time dependent equivalent scale the negative trend in the period before 1945 is converted into a positive trend of the same magnitude. The mean historical wind speed is increased and becomes equal to the mean wind speed since the year 1945. In the modern period the positive trend vanishes.

Introduction

Meteorological observations on board Voluntary Observing Ships (VOS) are an important data source for climatological studies. They date back to the middle of the last century. Even today, the wind observations of VOS are based mostly on Beaufort estimates. The reports indicate a significant decrease of the wind speed up to 1945, after this a considerable increase is registered (Peterson & Hasse, 1987). Whether these trends are a true climate signal is questionable because the observing practices have changed during the last century which probably introduces an artificial interdecadal trend into the wind series. In earlier times, when sailing ships were dominant, the Beaufort wind force was defined by the amount of sail a special type of ship were able to carry (Kinsman, 1969). With the introduction of steamships the Beaufort scale had to be redefined and the wind force has been estimated by the sea state (Petersen, 1927). Since the sixties more and more merchant ships have been equipped with anemometers and wind estimates have been partly substituted by measurements.

For this reason the unreliable wind trends deduced from ship reports have to be verified by objective criteria, e.g. by comparing to mean air pressure gradients (Ramage 1987). However, his method requires extremely high directional steadiness of the wind. Consequently, it is applicable in only some regions of the world ocean. Therefore, in this study *individual* pressure differences are used.

A necessary condition of the purposed absolute interdecadal calibration of the Beaufort estimates, is the availability of an equivalent scale valid for a fixed period. This is accomplished by the "New Beaufort" equivalent scale derived in the North Atlantic for the period 1960 to 1971 (Lindau, 1994). Whether this scale is valid also for other decades or whether a time dependent scale is necessary will be examined in the following by a calibration against pressure differences.

Data

Individual wind and pressure reports of the North Atlantic between 20°N and 60°N dating from the period 1890 to 1990 are taken from COADS. Only Beaufort estimates are considered, in order to exclude the well known artificial increase of the wind speed due to measurements (Cardone et al., 1990). Measurements are separated according to a flag given in COADS, indicating whether the wind was measured, or whether the observation practice is unknown. The latter are here considered to be Beaufort estimates.

In COADS direct information about the Beaufort force is available only in some data sets. The standard information concerning the force is given in knots, even if the wind was originally estimated. Obviously, the wind speed was obtained by converting the estimates with the old WMO scale Code 1100. In following computations the original knot-values are first changed into Beaufort (with the old WMO scale) and then re-converted into knots with the *new* equivalent scale (Lindau, 1994) valid for the period 1960 to 1971.

The resulting wind speeds are shown in Figure 1. Anomalies with respect to monthly means of the respective 1° x 1° box indicate a significant negative trend of more

than 1 cm/s/year for the period 1890 to 1945, and even stronger but positive trend of 1.5 cm/s/year since 1946.

Method

Outline

Individual ship reports are used, if they contain the air pressure and the wind strength and direction. Pairs of simultaneously observing ships are formed, provided that the distance between them is larger than 200 km and less than 500 km. Their pressure difference yields the momentum geostrophic wind component perpendicular to the junction line between the two ships. The magnitude of this component depends not only on the wind strength but also on the wind direction relative to the junction line, if a constant but unknown geostrophic angle is assumed (Fig. 2). Therefore, the geostrophic wind component is averaged separately for 36 classes of relative wind direction. A sinusoidal fit over all relative wind directions leads to a function which provides the requested parameters: The amplitude of the resulting sine curve represents the magnitude of geostrophic wind, its phase shift defines the mean geostrophic angle (Fig. 3).

Effects of observation errors

Inaccuracies in estimating the wind direction may falsify the results as follows: The pressure differences may be sorted into wrong classes of relative wind direction, which effects a diminished amplitude of the fitted sine curve. If Δd denotes the mean observation error of the wind direction, the amplitude decreases with the factor $\cos\Delta d$.

The mean error of wind direction is evaluated by computing differences in the reported wind direction $D_1 - D_2$ between two simultaneously observing ships, which are separated by a certain distance. A linear fit for values of $\cos(D_1 - D_2)$ with respect to ships' distance allows to extrapolate to the distance $\Delta x=0$, where only observation errors are responsible for a value less than 1. If the errors are random the mean value of $\cos(D_1 - D_2)$ at the distance $\Delta x=0$ is equal to $\cos^2\Delta d$, representing the squared mean observation error of the wind direction. Figure 4 illustrates the evaluations. At the distance $\Delta x=0$ a value of 0.804 remains for the mean cosine of $D_1 - D_2$, which is equivalent to observation error of 26.3°

Time Dependent Calibration

According to the method introduced above monthly magnitudes of the geostrophic wind are computed firstly for the standard period 1960 to 1971, separately for the four 10°-latitude zones between 20°N and 60°N in the North Atlantic. Figure 3 shows the result for the month of January in the zone between 40°N and 50°N. Based on more than 1 million pairs of observation a mean geostrophic wind of 13.3 m/s is found, together with an geostrophic angle of 17.6°. However, because of the large observation errors in estimating the wind direction (Δd=26.3°, see Fig. 4), the amplitude of the computed sine curve is diminished by the factor $\cos\Delta d$. Hence, the computed raw value has to be

enlarged by the factor $\cos^{-1}\Delta d$, in order to get the true magnitude of the geostrophic wind. A value of 14.8 ms^{-1} results. The magnitude of the simultaneously observed wind speed, according to the New Beaufort scale, amounts to 10.2 ms^{-1} (Fig. 5).

For the standard period 1960 to 1971, the procedure is carried out for each month and each 10° zone, so that 48 pairs of geostrophic wind "G" and observed wind "U" are available. A linear and orthogonal regression provides the relationship between both parameters, according to:

$$G = A_1 U + A_0$$

Figure 6 shows the result, which yields the following values for the constants A_0 and A_1:

$$A_0 = -3.7\ ms^{-1}$$
$$A_1 = 1.81$$

This relationship between G and U is considered to be highly reliable, since it is derived within the standard period, when the New Beaufort scale used is valid. It is further assumed, that this relationship has to be constant through the years. Each deviation is referred to a temporal drift of the Beaufort scale.

Then, relationships between G and U are analogously computed for other periods. The evaluations are carried out for each individual year, if at least 40,000 pairs of observations are available per 10° zone, otherwise observations of surrounding years are included. Figure 7 illustrates the results for some selected years.

In general, the constants a_0 and a_1 defining the relationship between G and U in a certain year differ from the constants A_0 and A_1, which are derived for the standard period. a_0 and a_1 are considered to be falsified, because a non-time-dependent scale has been used.

True relationship (1960-71): $G = A_1 U + A_0$ (1)

Potentially falsified relationship for a certain year: $G = a_1(t)u + a_0(t)$ (2)

In order to obtain the true relationship for each year, the equivalent scale has to be transformed according to: $U = c_1(t)u + c_0(t)$ (3)

$$c_1(t) = a_1(t)/A_1$$
$$c_0(t) = (a_0(t) - A_0)/A_1$$

Hence, the intended calibration of the new equivalent scale is reduced to the two time dependent coefficients $c_1(t)$ and $c_0(t)$. Their application on all years yields the time dependent equivalent scale showed in Fig 8.

Results

If Beaufort estimates of COADS are converted with the time dependent equivalent scale, the negative trend in the period before 1945 is reversed into a positive trend of the same magnitude (Fig. 9). However, the mean historical wind speed is raised and becomes equal to the mean wind speed since the year 1945. In this modern period the positive trend vanishes. The increasing wind speed of the uncorrected COADS is obviously due changing observational practices.

References

Cardone, V.J., 1969: Specification of the wind distribution in the marine boundary layer for wave forecasting. Report TR69-1, New York University, New York, N.Y., 131 pp.

Kinsman, B., 1969: Historical notes of the original Beaufort scale. *Mar. Obs.*, 39, 116-124.

Lindau, R. , 1994: Eine neue Beaufort-Äquivalentskala., Ph.D. thesis, University of Kiel. Berichte aus dem Institut fur Meereskunde No. 249 ,134 pp

Lindau, R., H.-J. Isemer, L. Hasse, 1990: Towards time dependent calibration of historical wind observations at sea. *Trop. Ocean-Atmos. Newslett.*, 54, 7-12.

Petersen, P., 1927: Zur Bestimmung der Windstarke auf See. *Annalen der Hydrographie* 55, 69 -72.

Peterson E.W. & L. Hasse, 1987: Did Beaufort scale or wind climate change? *Journ. Phys. Ocean.*, 17, 1071-1074.

Ramage, C.S., 1987: Secular changes in reported surface wind speeds over the ocean. *J. Climat. Appl. Meteor.*, 26, 525-528.

Figure 1: Wind anomalies for the period 1890 to 1990 in the North Atlantic between 20N and 60N. The values are based on Beaufort estimates converted to the New Beaufort scale. Anomalies are computed against monthly 1° x 1° box averages. One year running means of these anomalies are plotted. A linear regression yields for the period 1890-1945: -1.03 ±0.21 cm/s/year. For the period 1946-1990 results a linear trend of + 1.48 ±0.20 cm/s/year.

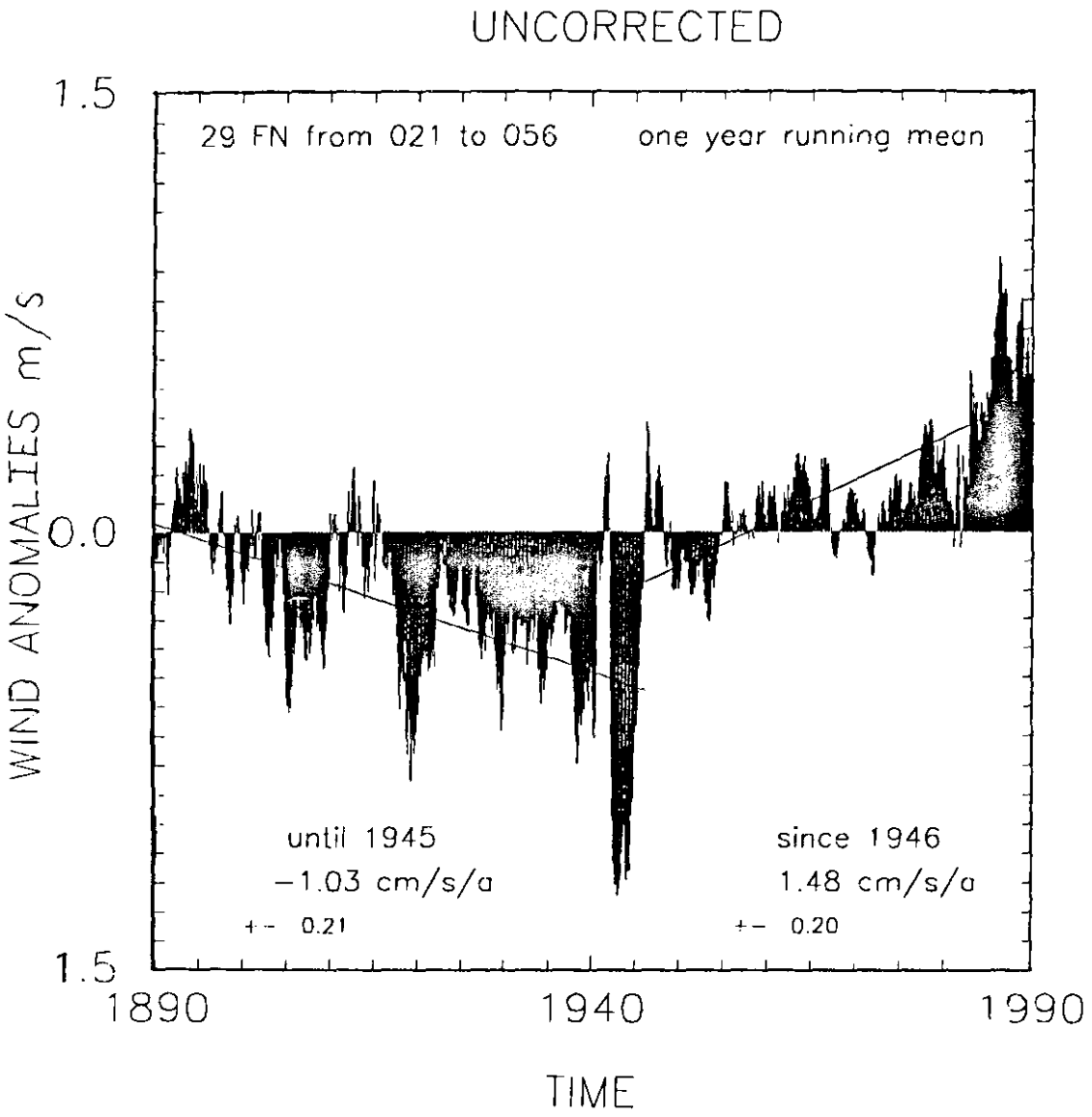

Figure 2: **Wind direction** *Drel* **relative to the junction line between two individual ships. The value is basing on the mean observed wind direction. The figured example shows** *Drel* **= 290 .**

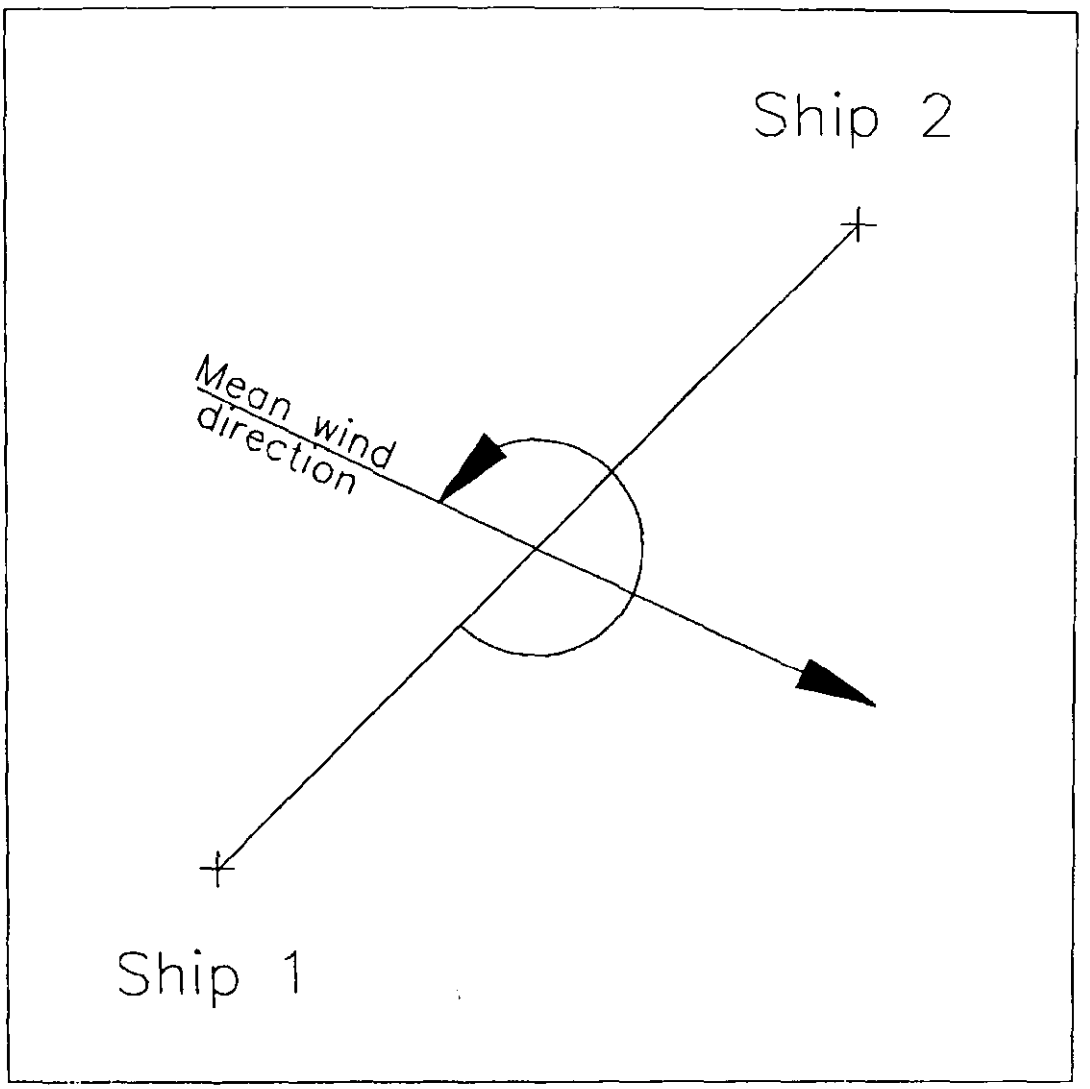

Figure 3: Magnitude of the geostrophic wind for the month of January in the standard period 1960 to 1971 and in the North Atlantic between 40 N and 50 N. The computed sine curve is based on mean geostrophic wind components for 36 classes of relative wind direction. The evaluations yield a geostrophic wind of 13.3 ms^{-1} and an geostrophic angle of 17.6 .

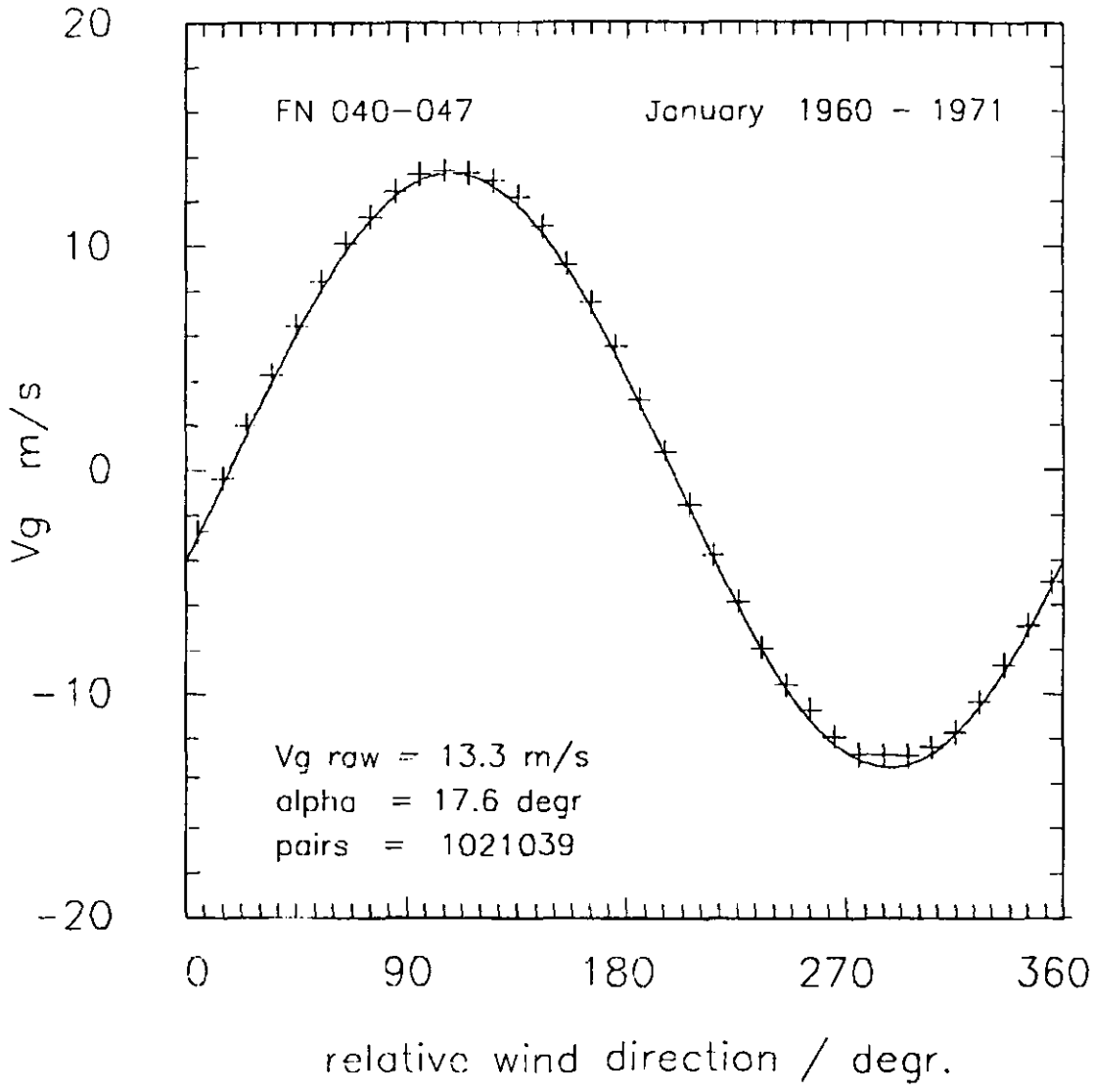

Figure 4: Example for the evaluation of the mean observation error in estimating the VOS wind direction. The mean cosine of the differences between two ship reports are figured as a function of distance. The value at the distance $\Delta=0$ represents the mean observation error. The results are referred to the same region, period and month as in figure 3.

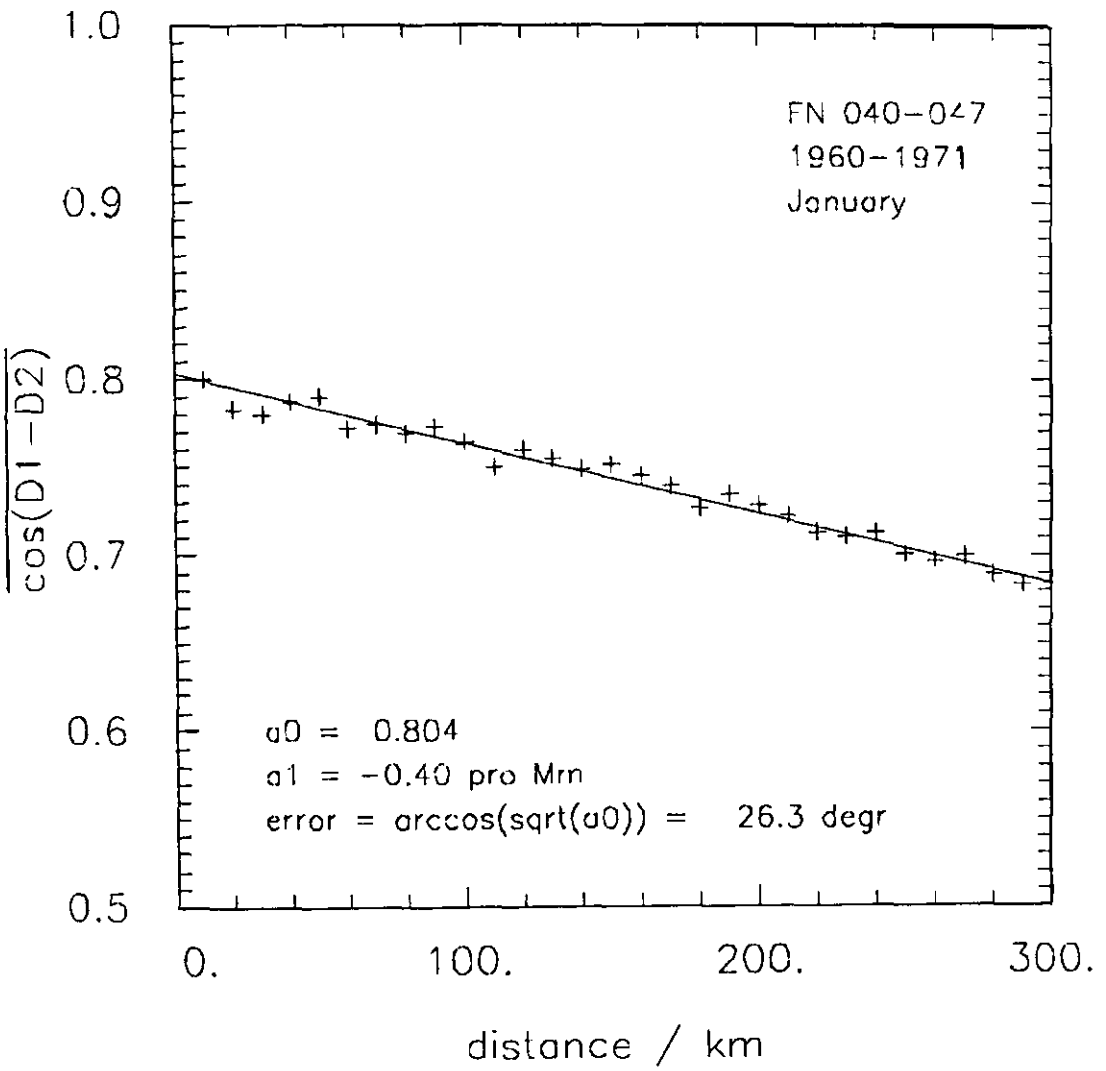

Figure 5: As figure 3, but including the true geostrophic wind figured as dashed line after the correction with $\cos^{-1} \Delta d$. The correction compensates for the effects of observation errors in the wind direction. The resulting geostrophic wind of 14.8 ms^{-1} should be compared to the simultaneously observed wind speed of 10.2 ms^{-1}.

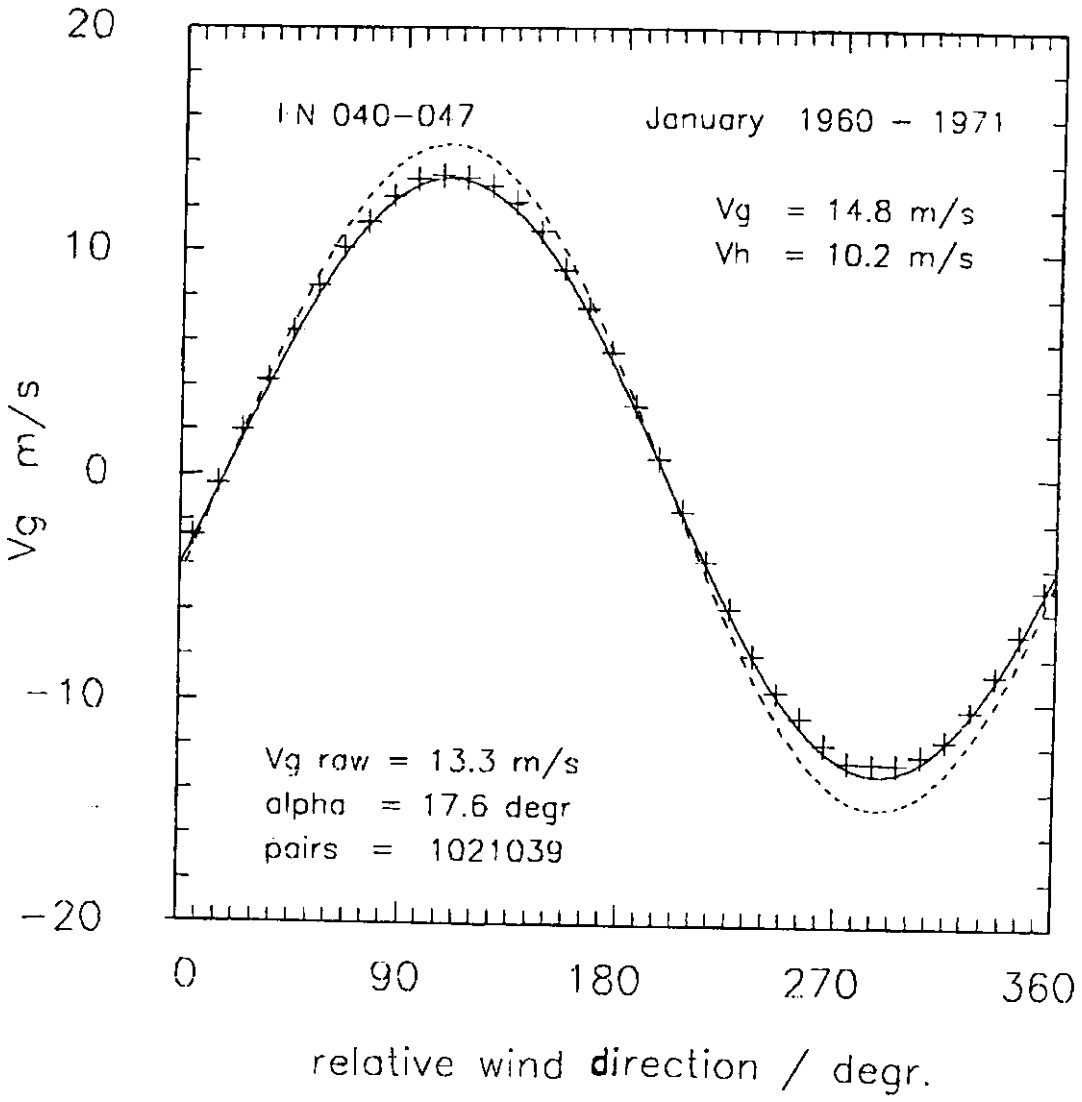

Figure 6: Determination of the relationship between geostrophic wind G and observed wind U for the standard period 1960 to 1971. The evaluations are basing on 48 G vs. U pairs derived for 12 month and four 10° zones. The linear and orthogonal regression yields G = 1.81*U - 3.7 ms^{-1}.

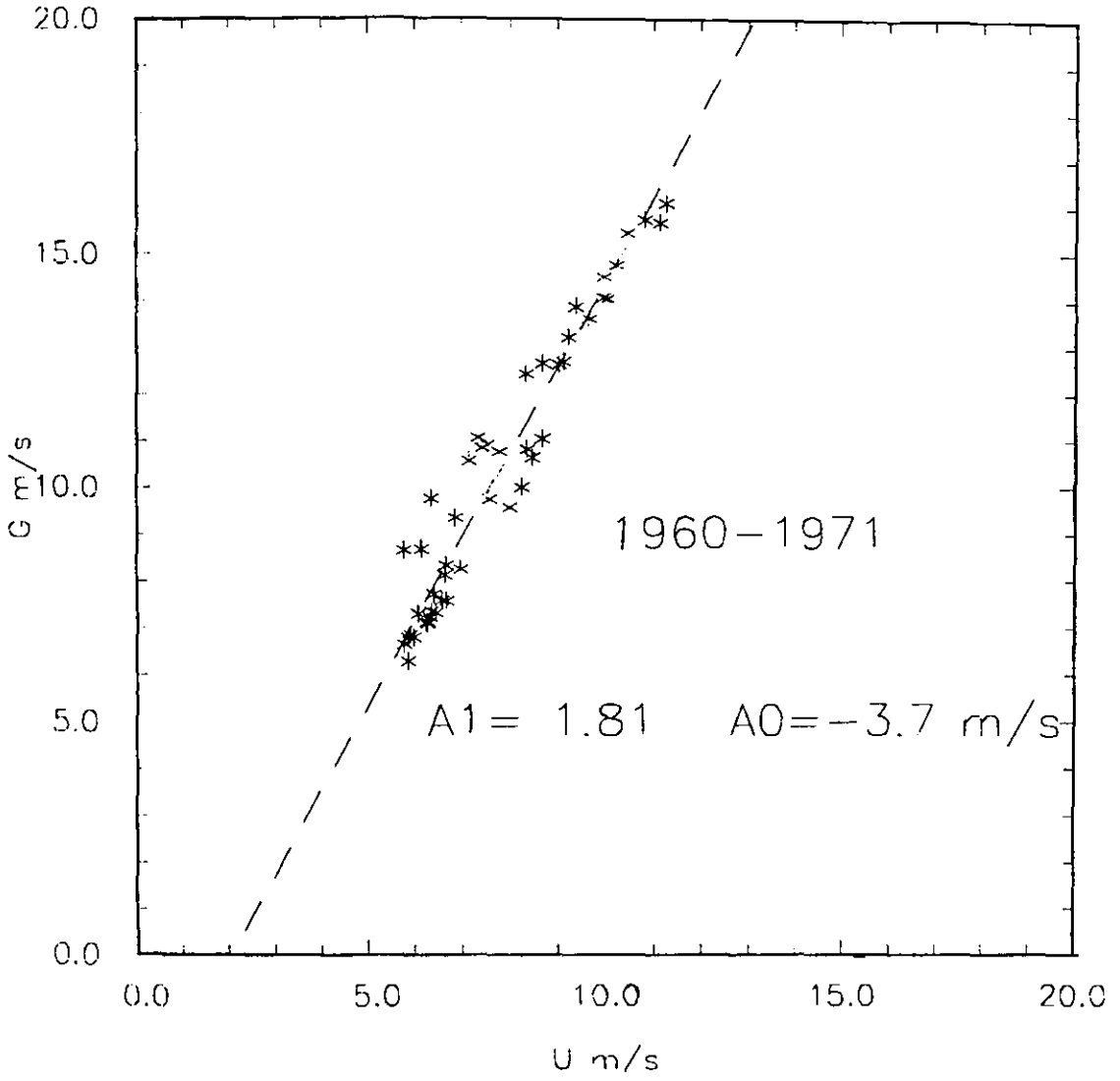

Figure 7a: Relationship between G and U for the year 1895. Additionally, the relationship for the standard period 1960 to 1971, which is regarded to be valid, is pictured as dashed line. The comparison of both relationships provides coefficients of correction for the respective year. For the year 1895 the following values result: reg. coeff$^{(1895)}$ = 1.043 and constant$^{(1895)}$ = -0.55 ms^{-1}.

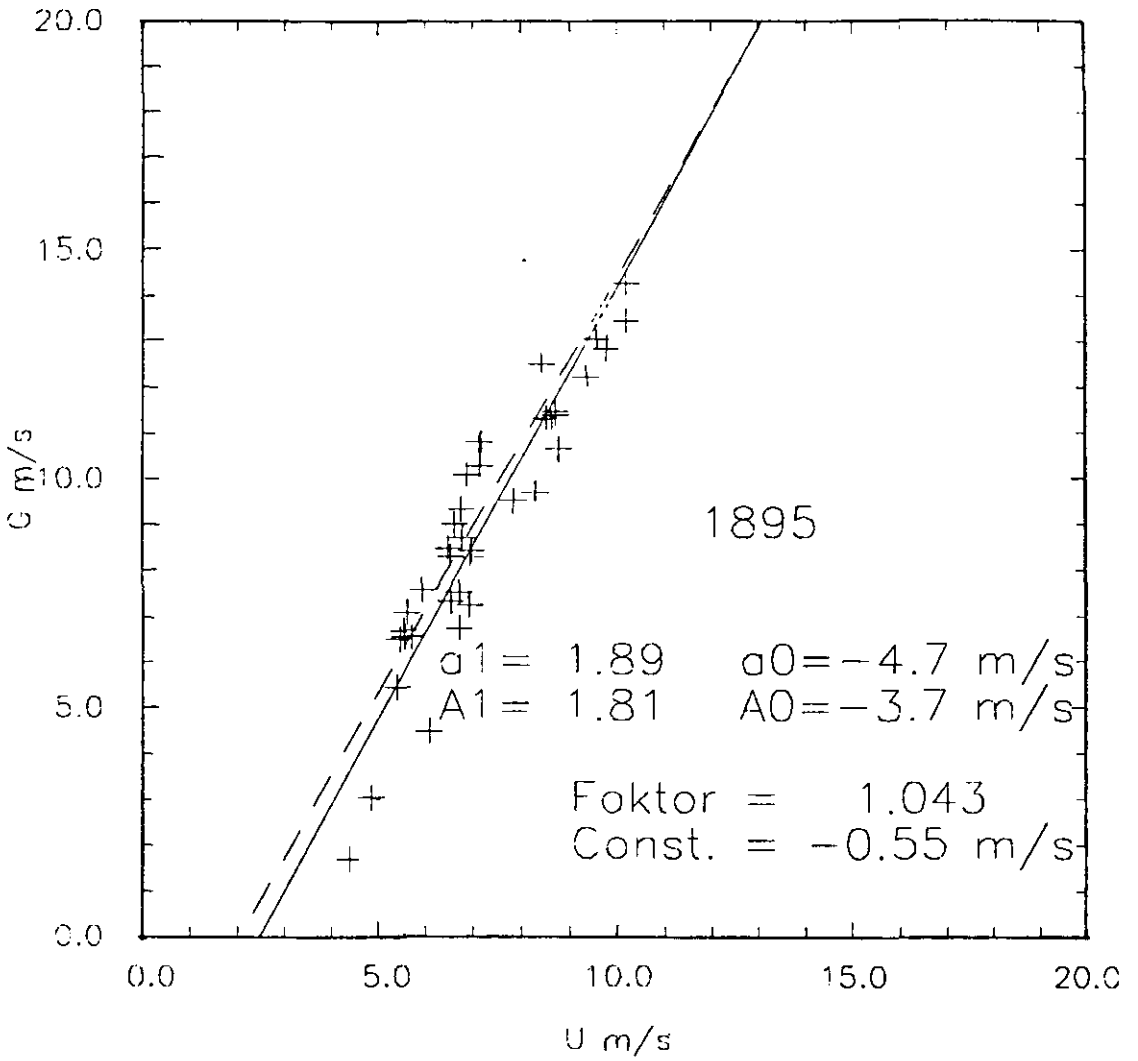

Figure 7b: As figure 7a, but for the year 1935.

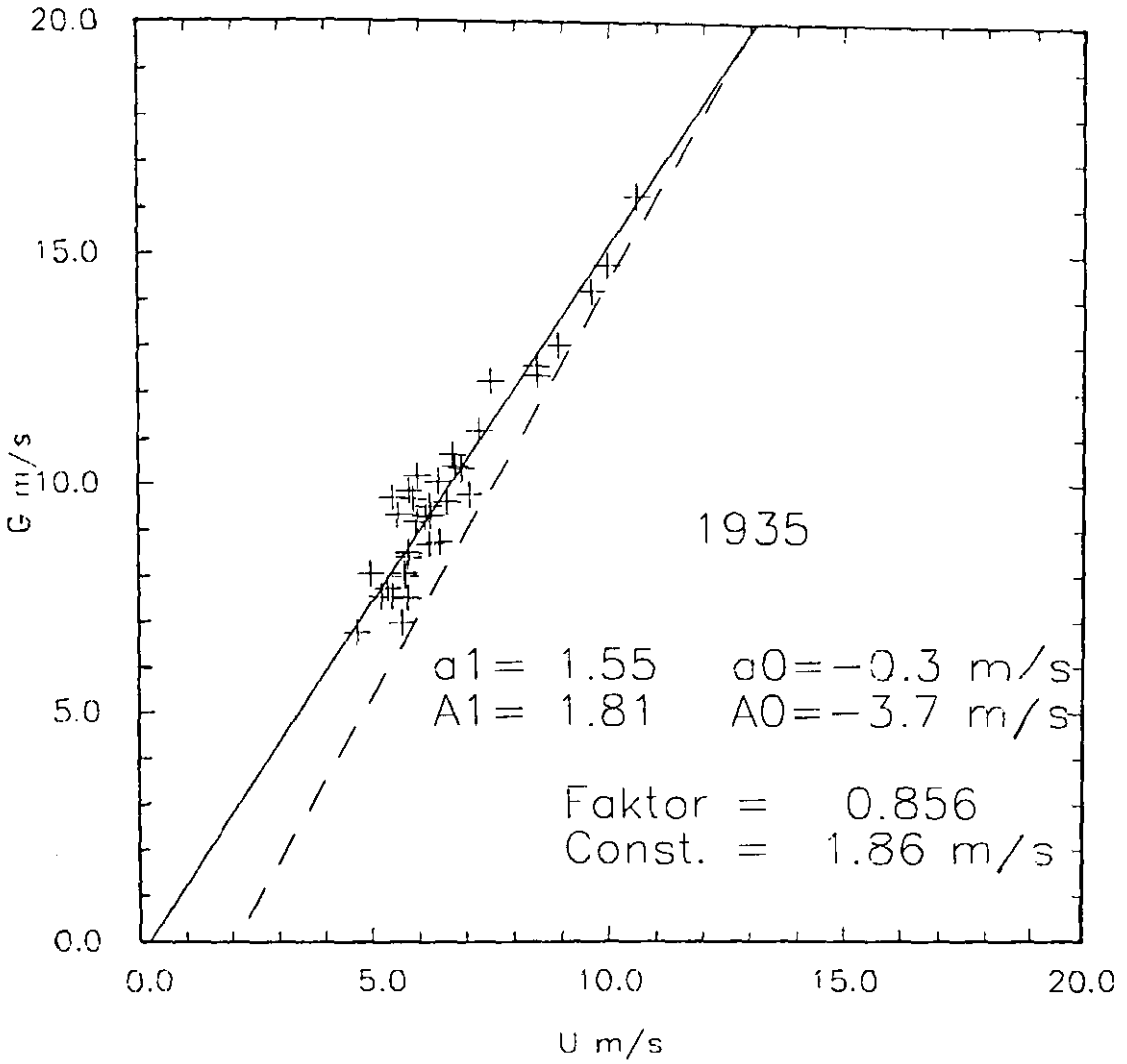

Figure 7c: As figure 7a, but for the year 1955.

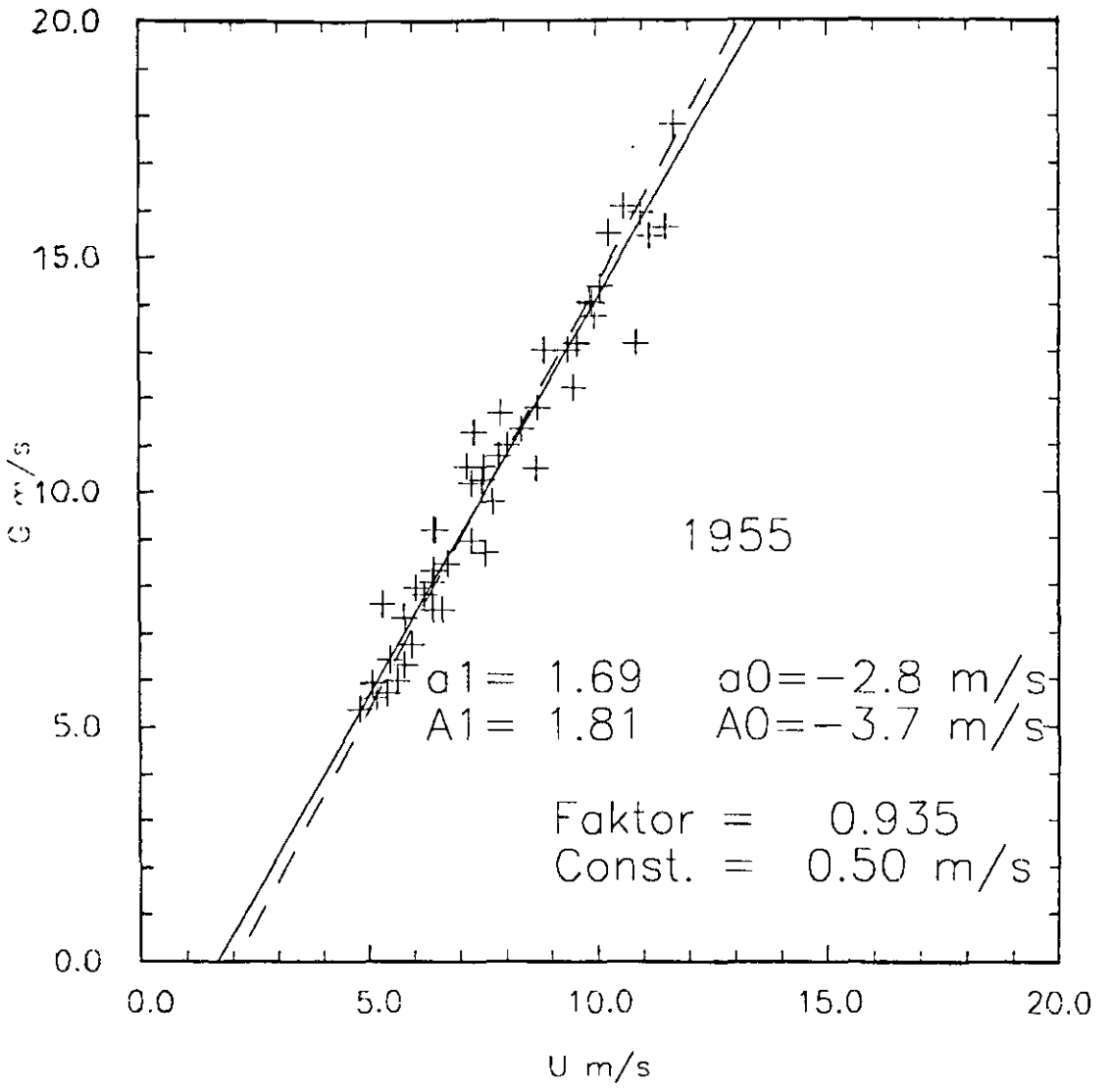

Figure 7d: As figure 7a, but for the year 1985.

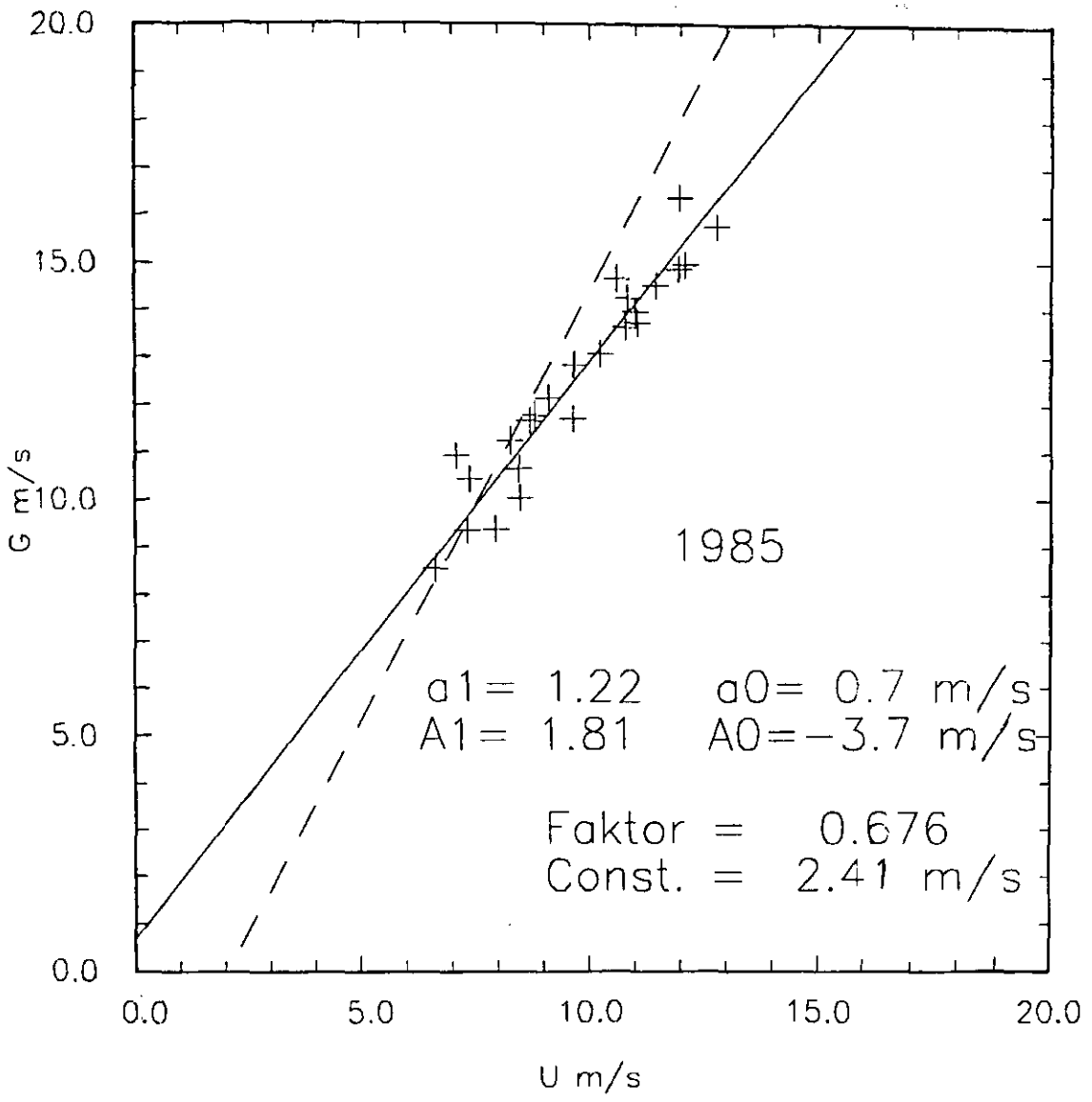

Figure 8: Time dependent Beaufort scale. The equivalent values for Beaufort 2 to 7 are figured as deviations from the equivalent scale (Lindau, 1994) valid for the standard period 1960 to 1971.

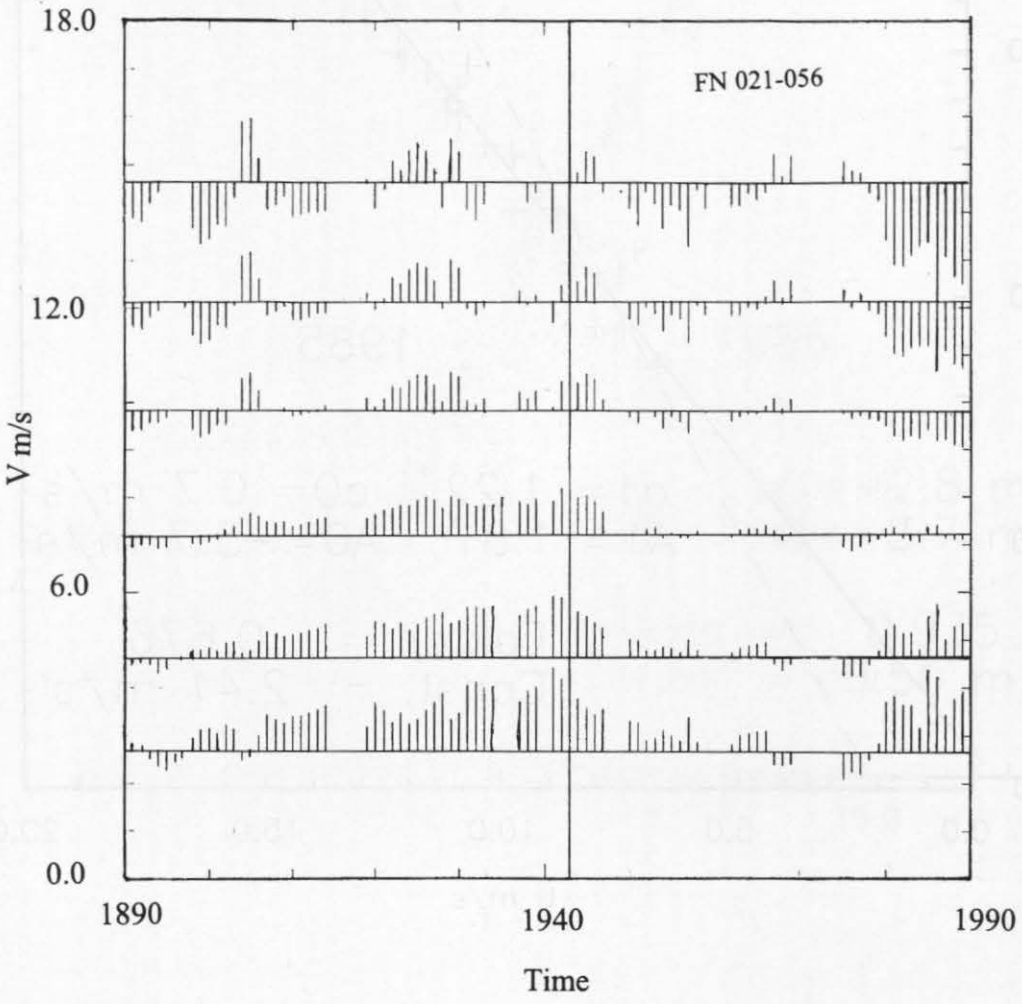

Figure 9: As figure 1, but representing the time series for Beaufort estimates converted by the time dependent scale. A positive trend of 1.02 ±0.20 cm/s/a is found for the historical period and a not significant trend of -0.11 ±0.23 cm/s/a remains for the modern period.

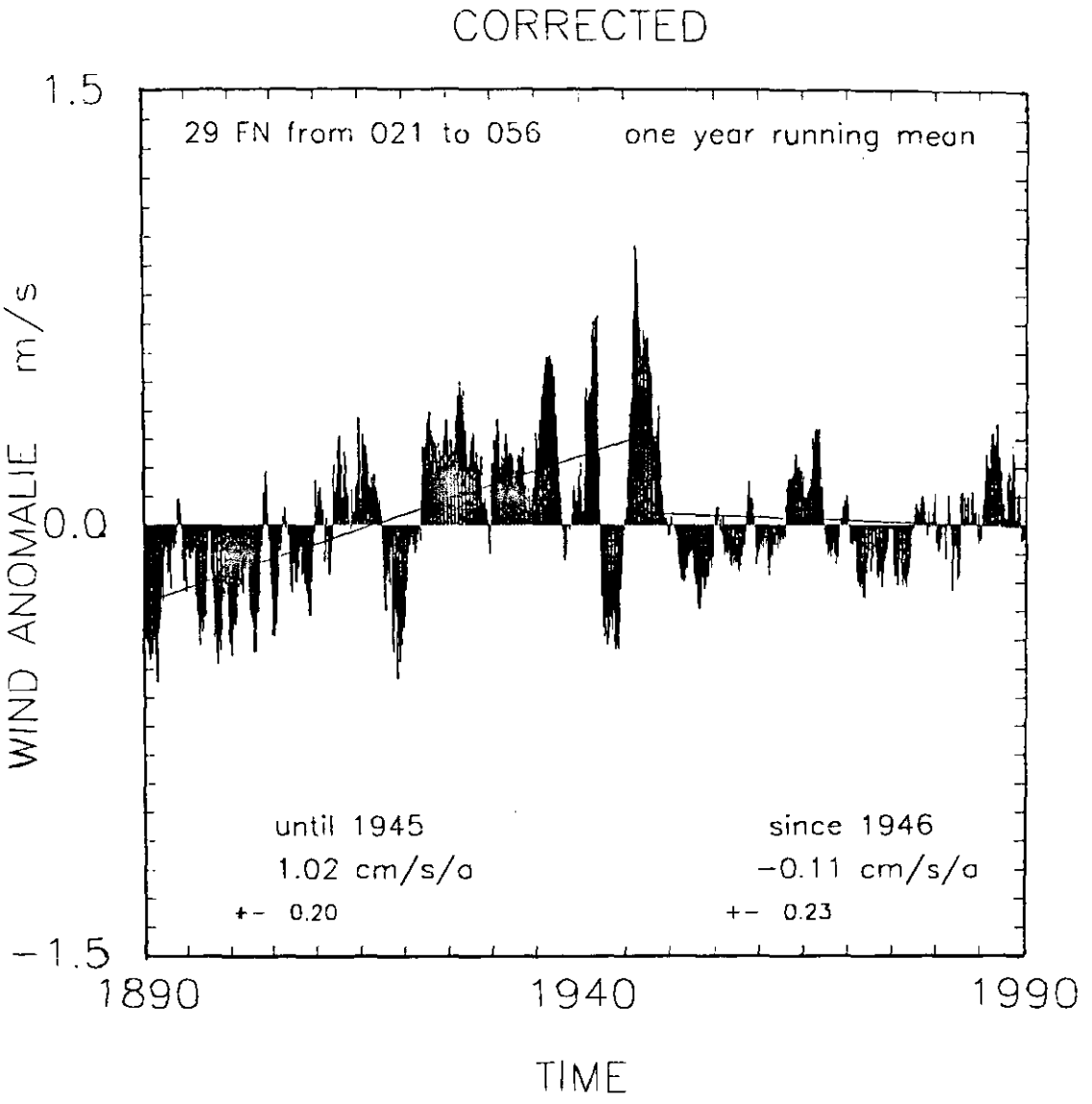

Toward a Revised Beaufort Equivalent Scale

Arlindo M. da Silva
Data Assimilation Office
NASA/GSFC, 7501 Forbes Blvd., Suite 200
Seabrook, MD 20706
e-mail: dasilva@hera.gsfc.nasa.gov

Christine C. Young and Sydney Levitus
National Oceanographic Data Center/NOAA, Washington, DC, USA

Abstract

Using individual observations from the COADS Compressed Marine Reports 5 (CMR5), separate objective analyses of estimated and measured wind speed climatology for the global oceans during the period 1970-89 is produced. Fields of annual mean estimated/measured wind speeds are used to analyze the performance of four current Beaufort equivalent scales: a) WMO Code 1100, b) CMM-IV, c) Cardone, and d) Kaufeld. This analysis identifies major biases in these scales and a method is proposed to correct individual estimated wind observations in COADS. The sensitivity of this new method on different seasons, decades and individual oceans is discussed. It is shown that this new method produces consistent estimates of measured/estimated annual mean wind speeds over the global oceans with much reduced bias compared to calculations based on previous Beaufort equivalent scales. When compared to the old WMO Code 1100 Beaufort scale estimates, our method produces higher climatological wind speeds over the global oceans and removes the long term artificial trend, with the magnitude of such corrections higher in the boreal summer.

Introduction

The complex interactions between the ocean and the atmosphere are realized through fluxes of heat, momentum and fresh water at the ocean surface. Bulk aerodynamic parameterizations of these fluxes rely strongly on the determination of wind speed a few meters above sea level. This paper further documents shortcomings in wind speed observations by the Voluntary Observing Fleet (VOF) and proposes a simple method for correcting estimated wind reports in COADS. Details of the calculation are reported by da Silva et al. (1994). Here we summarize the main results of that paper.

Wind speed reported by the VOF are either directly measured with anemometers or estimated from sea state. Instrumentation problems with anemometers are believed (or better, assumed) to be nonsystematic and hopefully cancel out when spatial/temporal

averages are taken. Although wind speeds are systematically related to anemometer height, standard surface layer similarity theory can be used to homogenize wind reports coming from ships with anemometers at different levels (e.g., Large and Pond, 1981). This homogenization, of course, requires the availability of anemometer height metadata for each wind report, which is not readily available at the moment. Following Cardone et al. (1990), an average anemometer height of 20 m is assumed throughout this study. Estimated winds are somewhat subjective and depend on the skill of the observer. Even when a correct identification of the sea state is made, the Beaufort estimate still needs to be converted to wind speed through a Beaufort equivalent scale. Since 1946 a Beaufort equivalent scale developed by Simpson (1906, 1926) combined with a well-defined description of sea state due to Petersen (1927) has been used for meteorological weather services (Isemer and Hasse 1991). This scale is commonly referred to as Code 1100.

The estimated speed included in the Comprehensive Ocean-Atmosphere Data Set (COADS) is based on the old WMO Code 1100 Beaufort equivalent scale. It is now widely accepted that the old WMO (Code 1100) Beaufort equivalent scale contains systematic errors and several alternative scales exist (WMO 1970, Cardone 1969, Kaufeld 1981, Ramage 1987).

In this study we use COADS individual reports to investigate the performance of four alternative Beaufort equivalent scales. Having documented climatological biases in all 4 current scales, we then introduce a very simple formula (eq.. 6) to correct estimated wind speeds reported in COADS. The performance of this correction for individual oceans, seasons and decades is briefly discussed (details can be found in da Silva et al., 1994, and is followed by a discussion of the impact of our estimated wind speed correction on the long term climatology and wind speed trends. We start by describing the data source and method of analysis in the next section.

Data Source and Method of Analysis

Data set

The primary data source for this study is the Compressed Marine Reports 5, product 10 of the Comprehensive Ocean-Atmosphere Data Set—COADS/CMR5 (Slutz et al., 1985). Release 1 of COADS includes data from the late 1800's up to 1979. Recently these observations have been extended to the 1980's in the so-called interim product. The Release 1a of COADS that greatly improved the data set in the 1980's was not available in time for these calculations.

For each directly measured quantity available in CMR5/COADS (zonal and meridional wind components, air and sea surface temperature, sea level pressure, etc.) observations are rejected if they do not pass the trimming procedure with a threshold of 3.5 standard deviations as outlined in Slutz et al. (1985).

Estimated versus measured winds in COADS

Flag "WI" included in each COADS/CMR5 wind observation is used to discriminate measured from estimated winds. It should be noted that this flag takes only two values: 1 for measured winds and 0 for estimated winds or unknown. It is

conceivable that some of the observations flagged as estimated/unknown could in fact be measured (see Cardone et al. [1990] for a discussion of problems with the measured/estimated indicator in a similar data set). In order to homogenize estimated winds, da Silva et al. (1994) found it necessary to bracket all COADS estimated wind speeds according to the old WMO scale (Table 1) and replace it with the appropriate equivalent wind speed.

Objective analysis

In order to eliminate spatial and temporal noise due to inhomogeneous sampling over the oceans we have objectively analyzed our fields to fill in gaps in data sparse regions and remove small scale noise. This is the same spatial resolution used in Levitus' (1982) Climatological Atlas of the World Oceans. Objective analysis is also an effective outlier removal which is beneficial to the regression analysis of section 4. Details of the objective analysis can be found in da Silva et al. (1994) and Levitus (1982).

Assessing Current Beaufort Equivalent Scales

It is well established that the old WMO (Code 1100) Beaufort equivalent scale has systematic biases and that several alternative scales have been proposed. Although all these new scales confirm that the old WMO scale underestimates low wind speeds and overestimates high wind speeds (Fig. 4), they all differ in the precise amount. This section further documents the performance of these scales by comparing anemometer-measured winds with estimated winds based on each scale, in a climatological sense. The scales considered are WMO Code 1100, WMO CMM-IV (WMO 1970), Cardone (1969) and Kaufeld (1981).

Figure 1 plots estimated against measured northern hemisphere annual mean winds for the period 1970-1989, for each of the scales described above. Wind speeds estimated with Kaufeld's scale have been converted from 25 m (average anemometer height in Kaufeld's [1981] study) to 20 m, under the assumption of neutral stability. These scatter diagrams present several measures of error and goodness of fit, viz.

$$\text{std. dev.} = \left[\frac{1}{N}\sum_i (\overline{W}_{ei} - \overline{W}_{mi})^2\right]^{1/2} \qquad (1)$$

$$\text{bias} = \frac{1}{N}\sum_i (\overline{W}_{ei} - \overline{W}_{mi}) \qquad (2)$$

$$\text{scatter} = \left[\frac{1}{N}\sum_i (\overline{W}_{ei} - \overline{W}_{mi} - b)^2\right]^{1/2} \qquad (3)$$

where $\overline{W}_{ei}$ / $\overline{W}_{mi}$ stands for climatological estimated/measured wind speed at gridpoint i and N is the total number of gridpoints. Figure 2 also shows the slope and intercept of the least square fit relating W_e to W_m in each panel.

Although the old WMO scale gives a slope very close to 1, it is clear from Fig. 2a that it underestimates wind speed with a standard deviation of almost 1 m/s. The CMM-IV Beaufort equivalent scale (Fig. lb) does a better job for wind speeds in the range 5-9 m/s but tends to underestimate (overestimate) wind speeds greater (less) than 9 m/s (5 m/s). Kaufeld's scale (Fig. lc), however, systematically overestimates wind speeds with a standard deviation of about 0.7 m/s and bias of 0.6 m/s. Like Kaufeld, Cardone's scale (Fig. ld) tends to overestimate wind speeds less than 9 m/s, but does a much better job at higher values of the wind speed; both bias and standard deviations are about half those of Kaufeld.

Correcting Estimated Winds in COADS

Our main objective is to devise a correction to the Code 1100 Beaufort equivalent scale that would bring not only average measure/estimated wind speed in closer agreement, but also produce consistent average nonlinear quantities such as the average pseudo wind stress ($\overline{P} = \overline{W^2} = \overline{W}^2 + \overline{W'^2}$). It is clear that a simple linear regression formula

$$W_{new} = x_1 W_{old} + x_2 \tag{4}$$

would bring measured/estimated wind speeds in Fig. 5a in close agreement, as discussed in the previous section; in the above formula W_{new}, W_{old} stands for the corrected and old WMO Code 1100 wind speed, and x_1, x_2 are constants to be determined. However, consistency between measured/estimated average pseudo wind stress $\overline{P}$ requires not only the mean speeds to be consistent ($\overline{W}_e = \overline{W}_m$), but also a consistency of standard deviations $\overline{W_e'^2} = \overline{W_m'^2}$. Such consistency of standard deviations cannot be accomplished with a simple linear regression. As discussed in the section above, a correction to the old WMO scale should increase low wind speeds and decrease high wind speeds. After much experimentation it was determined that such correction can be accomplished by a function of the form

$$W_{new} = x_1 W_{old} + x_2 \sqrt{W_{old}} \tag{5}$$

All of the three alternative Beaufort equivalent scales of the last section can accurately be expressed in the form of eq. (5). The constants x_1, x_2 are determined by means of a least squares fit.

Figure 3 shows the results of these computations based on northern hemisphere data, base years 1970-89. Each "row" in this diagram corresponds to a different set of constants x_1 / x_2, and each "column" corresponds to test data for a particular period

(annual, January or July). For example, the diagonal depicts estimated vs. measured wind speeds with the corrected Beaufort equivalent scale developed for that particular month.

It is clear from Figs. 3a,d,g that any of the new Beaufort equivalent scales performs better on climatological annual winds than the CMM-IV scale (Fig. 2b), the "best" among the current scales; the new January scale (middle row) performs nearly as well as the optimal annual scale with standard errors equal to 0.18 and 0.17 m/s, respectively (compare Figs. 5.a and 5.d). A close examination of Fig. 3 reveals that on January/July data the January scale comes slightly ahead of the annual scale. The July scale only outperforms the annual/January scales on the July data, but marginally so. The seasonal dependence of the scales is modest and does not warrant the use of a different scale for each month. Based on this analysis, and additional plots for other oceans, we selected the January scale as our primary scale. In this case eq. (5) reads:

$$W_{new} = 0.7870 W_{old} + 0.9547\sqrt{W_{old}} \qquad (6)$$

Notice that when this equation is applied to climatological winds the second term on the RHS should be the average of $W_{old}^{1/2}$ $\left(\overline{\sqrt{W}}\right)$ rather than the square-root of the average wind $\left(\sqrt{\overline{W}}\right)$.

The wind speed correction given in eq. (6) can be used to derive a revised Beaufort equivalent scale for use in COADS. In Table 1 the mean equivalent wind speed and respective interval of wind speeds for the WMO Code 1100 scale have been mapped using eq. (6) to produce a new corrected scale; this scale will be referred to as the UWM Beaufort climatological scale, because our method of correction is based on a climatological constraint rather than the usual method of paired observations. Figure 1 depicts the difference between this corrected scale and the other Beaufort equivalent scales. Consistent with the other scales, the UWM scale indicates that the old WMO Code 1100 scale underestimates low wind speeds and overestimates high wind speeds. However, the magnitude of the correction is generally smaller than previous alternatives to the old WMO scale.

Sensitivity Study

Da Silva et al. (1994) documents the regional temporal performance of the proposed wind speed correction in some detail. Only the main results are highlighted here.

Table 2 summarizes the relationship between measured/estimated wind speed in COADS for different months when our correction is applied. As expected, the best performance is attained for January, the base month used to derive the scale. Within 5% the results are consistent throughout the year.

Table 3 summarizes the performance of the UWM scale for 5 degree boxes around Ocean Weather Stations in the North Pacific and North Atlantic oceans. For each month from 1970 to 1989 separate monthly mean wind speeds are computed for measured and estimated wind reports. These boxes are chosen to include OWS so that a great number of anemometer measured reports are present. Monthly means with less than 30

observations for a particular month are eliminated. Notice that no objective analysis is performed. As before, the WI flag in COADS CMR5 was taken at face value, although H.-J. Isemer (personal communication) has brought to our attention apparent inconsistencies in this flag in the neighborhood of OWS. A sensitivity test eliminating dubious WI reports has been conducted and the main conclusions of this section are not affected by this tighter quality control. The most striking feature in Table 3 is the larger standard deviation (and scatter) compared to the climatological results presented in the previous sections. This increase in standard deviation is partially due to the absence of objective analysis, combined with the noisier character of monthly mean, regional data. Eleven out of the 16 boxes studied have slopes within 10% of one. Biases are generally small, although a few boxes (OWS B, E, N, and T) have biases in excess of 0.25 m/s. As an illustration of the results for a box with small slope and large intercept, Fig. 4 depicts measured vs. estimated wind speeds for the box around OWS P.

Figure 5 shows the global distribution of annual mean measured and estimated winds. Most of the large scale patterns of measured/estimated winds match quite well, surprisingly even in the data sparse regions of the southern oceans.

It is shown in da Silva et al. (1994) that our correction produces a consistent estimate of pseudo wind stress with a slope of 0.98 and small bias. However, there is a tendency to underestimate annual mean pseudo wind stress around 200 m^2/s^2.

Effect on Long Term Climatology and Trends

Figure 6 shows mean wind speed and standard deviation valid at 20 m for January, both corrected and the difference corrected minus uncorrected. In this calculation we used all quality controlled COADS data from 1945 to 1989, correcting all estimated wind speeds according to eq. (6). Consistent with previous studies, corrected speeds exceed uncorrected winds by about 0.5 m/s in parts of the North Atlantic, with smaller differences in the North Pacific. The corrected standard deviation (Figs. 6c,d) is reduced in the extra-tropics, with a more pronounced reduction (~ 0.3 m/s) in the North Atlantic ocean. The corrected standard deviation is generally increased in the tropics with magnitudes around 0.1 m/s in the eastern tropical Atlantic and Pacific oceans. Similar calculations for the month of July are given by da Silva et al. (1994). Due to the lower wind speed in July, the correction to the wind speed (not shown) is positive and greater than for January for most of the globe. Consistent with the findings of Cardone et al. (1990), we note a reduction in the linear trend for most of the globe due to our scientific Beaufort scale correction (not shown). This artificial linear trend can adversely impact studies of long term variability of the ocean-atmosphere climate system.

Concluding Remarks

Using individual observations from the COADS Compressed Marine Reports (CMR5) we have produced analyses of wind speed climatologies for the global oceans during the period 1970-89. Computing climatological wind speeds based on (anemometer) measured and (sea state) estimated ship reports we have analyzed the performance of 4 current scientific Beaufort scales: a) WMO Code 1100, b) CMM-IV

(WMO 1970), c) Cardone (1969), and d) Kaufeld (1981). Our analysis confirmed previous findings that the old WMO Code 1100 scale underestimates lower wind speeds and overestimates high wind speeds. Nevertheless, the other three so-called scientific Beaufort equivalent scales have biases of their own, with the CMM-IV being more accurate for intermediate winds (5-9 m/s). Having established the need for a new scale, we proposed the following formula to correct estimated wind speeds in COADS:

$$W_{new} = 0.7870 W_{old} + 0.9457\sqrt{W_{old}}$$

where W_{old} is wind speed given in COADS based on WMO Code 1100 scale, and W_{new} is our corrected estimate at a 20 m reference level. Notice that the above formula is valid only for individual observations and cannot be applied directly to monthly mean wind speeds. Our proposed correction performs reasonably well for all seasons, and marginally so in the southern hemisphere, where the poor sampling gives considerably more scatter compared to the northern hemisphere. For the month of January, there is also a poor correspondence between measured/estimated wind speeds in the Indian ocean. Overall, the new scale produces higher wind speeds throughout the globe, and reduced standard deviations. The magnitude of such corrections is generally larger in July compared to January. In agreement with Cardone et al. (1990), the long term linear trend is reduced for most of the globe.

It is important to notice that the validity of our correction is dependent on the reliability of flag WI in COADS/CMR5. (Flag WI allows us to discriminate measured/estimated wind observations). Recently, S. Woodruff (personal communication) has brought to our attention results of some preliminary tests in which some wind reports flagged as measured were determined to be estimated. If such inconsistencies exist in COADS/CMR5 they have been incorporated in our scale, which effectively brings measured/estimated wind speeds into agreement. To settle this question detailed information about the reporting ships is required. Although in principle it is possible to compile some of this metadata, it is a formidable task and such information is not likely to be included in COADS in the near future. As more reliable data becomes available we will update our analysis to reflect these changes. In the meantime, we claim that the corrections proposed in this paper produce a more consistent estimate of COADS wind speed over the global oceans.

Acknowledgments

This project has been supported by NSF Grant ATM 9215811. We would like to thank Scott Woodruff and Hans-Jörge Isemer for many fruitful discussions during the course of this work.

References

Cardone, V. J., 1969: Specification of the wind distribution in the marine boundary layer for wave forecasting. Report TR69-1, New York University, New York, NY, 131 pp. [NTIS AD 702 490].

Cardone, V. J., J. G. Greenwood and M. Cane, 1990: On trends in historical marine wind data. *J. Climate*, 3, 113-127.

Isemer, H.-J. and L. Hasse, 1991: The scientific Beaufort equivalent scale: Effects on wind statistics and climatological air-sea flux estimates in the North Atlantic ocean. *J. Climate*, 4, 819-836.

Kaufeld, L., 1981: The development of a new Beaufort equivalent scale. *Meteor. Rundsch.*, 34, 17-23.

Large, W. And S. Pond, 1981: Open ocean momentum flux measurements in moderate to strong winds. *J. Phys. Oceanogr.*, 11, 324-336.

Levitus, S., 1982: Climatological Atlas of the World Ocean, NOAA Prof. Paper No. 13, US Government Printing Office, Washington DC, 17 fiches, 173 pp.

Petersen, P., 1927: Zur Bestimmung der Windstärke auf See. Ann. Hydrogr., 55, 69-72.

Ramage, C. S., 1987: Secular changes in reported surface wind speeds over the ocean. *J. Climate Appl. Meteor.*, 26, 525-528.

da Silva, A. M., C. C. Young and S. Levitus, 1994: A method for correcting Beaufort estimated wind speeds in COADS. *J. Appl. Meteor.*, submitted.

Simpson, G. C., 1906: The velocity equivalents of the Beaufort scale. WMO Meteorological Office Publication No. 180, London.

Simpson, G. C., 1926: WMO Prof Note No. 44.

Slutz, R. J., S. J. Lubker, J. D. Hiscox, S. D. Woodruff, R. L. Jenne, D. H. Joseph, P. M. Steurer And J. D. Elms, 1985: COADS, Comprehensive Ocean-Atmosphere Data Set, Release 1. Climate Research Program, Environmental Research Laboratory, Boulder, CO 262 pp.

Woodruff, S., S. Lubker, R. Quayle, U. Radok and E. Doggett, 1991: Differences within and among surface marine data sets. Climate Research Division, NOAA Environmental Research Laboratory, Boulder CO, 216 pp.

World Meteorological Organization (WMO), 1970: Reports on marine science affairs. Rep. No. 3: The Beaufort scale of wind force. WMO, Geneva, Switzerland, 22 pp.

Table 1. Equivalent wind speed and intervals for WMO Code 1100 Beaufort equivalent scale and UWM Beaufort climatological scale.

		WMO Code 1100			UWM		
Beaufort Number	Descriptive Term	Interval of equivalent wind speed		Mean equivalent wind speed	Interval of equivalent wind speed		Mean equivalent wind speed
		knots	m/s	m/s	knots	m/s	m/s
0	Calm	0 - 1	0.0 - 0.2	0.0	0 - 2	0.0 - 1.0	0.0
1	Light air	1 - 3	0.3 - 1.8	0.8	3 - 5	1.1 - 3.0	1.5
2	Light breeze	4 - 6	1.9 - 3.3	2.4	6 - 8	3.1 - 4.5	3.4
3	Gentle breeze	7 - 10	3.4 - 5.4	4.3	9 - 13	4.6 - 6.7	5.4
4	Moderate breeze	11 - 16	5.5 - 8.5	6.7	14 - 18	6.8 - 9.7	7.7
5	Fresh breeze	17 - 21	8.6 - 11.0	9.4	19 - 23	9.8 - 12.0	10.4
6	Strong breeze	22 - 27	11.1 - 14.1	12.3	24 - 28	12.1 - 14.9	13.0
7	Near gale	28 - 33	14.2 - 17.2	15.5	29 - 34	15.0 - 17.7	16.0
8	Gale	34 - 40	17.3 - 20.8	18.9	35 - 40	17.8 - 20.9	19.0
9	Strong gale	41 - 47	20.9 - 24.4	22.6	41 - 46	21.0 - 24.1	22.4
10	Storm	44 - 45	24.5 - 28.6	26.4	47 - 54	24.2 - 27.8	25.7
11	Violent storm	56 - 63	28.7 - 32.7	30.5	55 - 60	27.9 - 31.4	29.3
12	Hurricane	≥ 64	≥ 32.8	34.9	≥ 61	≥ 31.5	33.1

Table 2. Performance of the UWM Beaufort climatological scale (base month: January) applied to data from several months. Slope, intercept, standard deviation (σ) and scatter are defined by equations (1) - (3).

month	slope	intercept	σ	bias	scatter
January	0.99	0.07	0.35	-0.00	0.35
April	1.03	-0.21	0.34	0.01	0.34
July	0.95	0.34	0.36	-0.01	0.36
October	1.02	-0.20	0.40	0.04	0.40
Annual	1.03	-0.24	0.18	0.01	0.18

Table 3. Interannual performance of the UWM scale near Ocean Weather Stations. Data are unanalyzed monthly means for 5° x 5° boxes around Ocean Weather Stations. Estimated/measured pairs are included only if more than 30 wind observations occur for each month. The period covered is 1970 - 89 with the maximum number of data points being 240. Slope, intercept, standard deviation (σ) and scatter are defined by equations (1) - (3).

Nearby OWS	5° x 5° box center		No. months	slope	intercept	σ	bias	scatter
A	62.5°N	32.5°W	98	0.56	4.02	1.27	0.07	1.47
B	56.5°N	50.5°W	36	1.09	-1.20	1.48	0.34	1.44
C	52.5°N	35.5°W	170	0.79	2.10	1.18	0.03	1.18
D	44.5°N	40.5°W	199	0.92	0.84	0.96	-0.04	0.96
E	35.5°N	47.5°W	215	0.91	0.56	0.93	0.26	0.89
I	59.5°N	18.5°W	133	0.95	0.58	1.32	-0.06	1.32
J	52.5°N	19.5°W	155	0.93	0.60	1.03	0.12	1.02
K	45.5°N	15.5°W	215	0.95	0.48	0.73	-0.02	0.73
L	57.5°N	19.5°W	224	0.89	0.94	1.17	0.18	1.15
M	66.5°N	2.5°E	95	0.93	0.62	1.26	0.05	1.26
N	30.5°N	139.5°W	235	0.93	0.25	0.83	0.29	0.78
P	50.5°N	144.5°W	227	0.74	2.68	0.88	-0.03	0.88
R	47.5°N	16.5°W	214	0.96	0.48	0.82	-0.04	0.82
T	29.5°N	135.5°E	223	0.79	1.29	1.03	0.39	0.95
V	34.5°N	164.5°E	180	0.95	0.58	1.10	-0.06	1.10
X	39.5°N	153.5°E	206	0.78	2.12	0.96	-0.10	0.95

Table 4. January scale applied to annual NH data by region.

Region	slope	intercept	σ	bias	scatter
N. Atlantic	1.04	-0.34	0.15	0.01	0.15
N. Pacific	1.01	-0.12	0.17	0.01	0.17
S. Atlantic	1.11	-0.79	0.26	0.01	0.26
S. Pacific	1.00	0.04	0.31	-0.05	0.30
Indian	1.08	-0.46	0.27	-0.10	0.25
Tropics	1.03	-0.23	0.22	-0.00	0.22

Figure 1: The old WMO Beaufort scale (Code 1100) and four alternative scientific Beaufort scales; CMM-IV (WMO(1970), Cardone (1969), Kaufeld (1981) and our new scale (UWM)

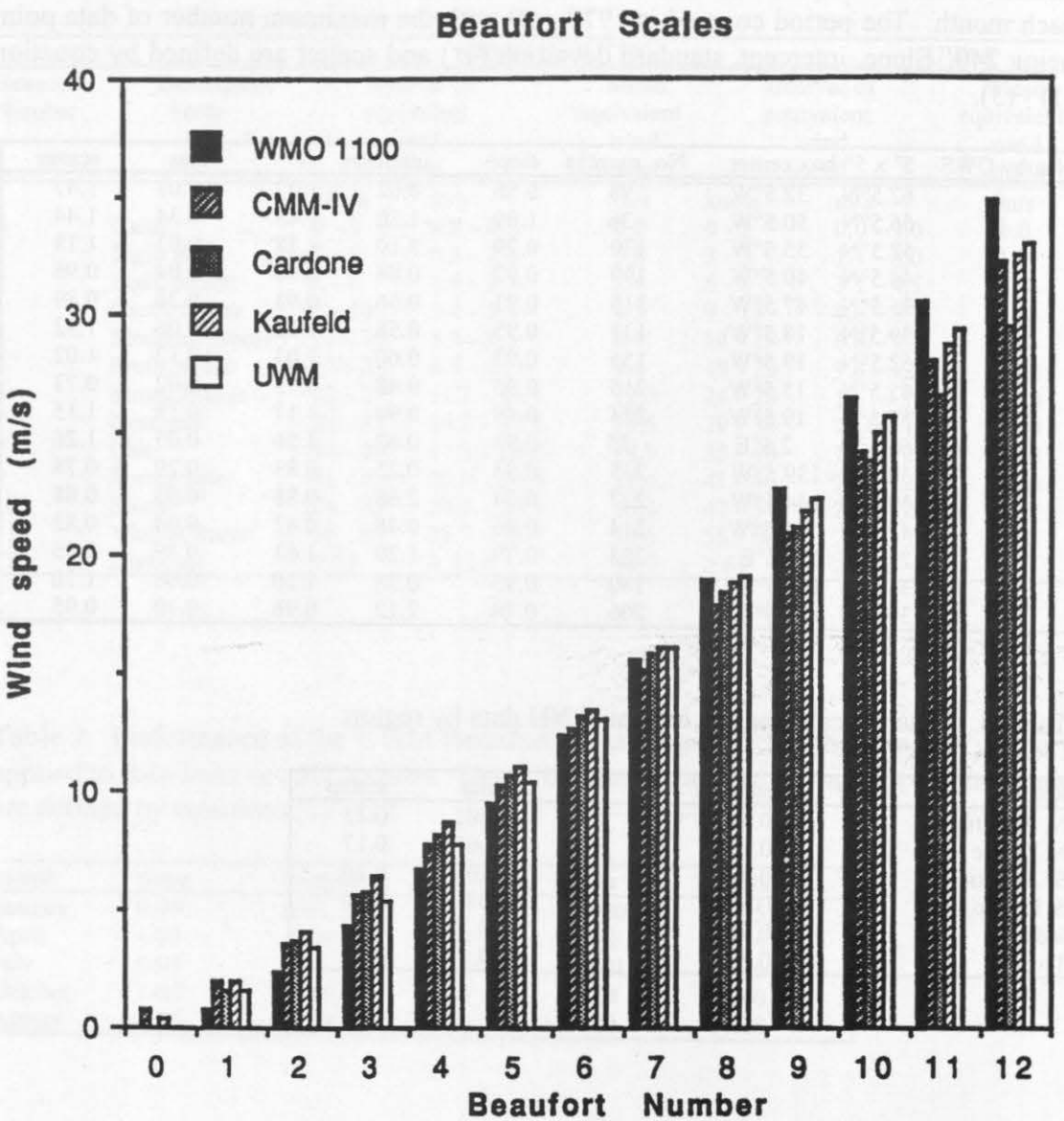

Figure 2: Analyzed estimated versus measured winds (annual mean, northern hemisphere) with estimated winds based on several equivalent Beaufort scales: a) old WMO (Code 1100), b) CMM-IV (WMO, 1970), c) Kaufeld (1981) and d) Cardone (1969). Each point in this daigram corresponds to measured/estimated winds on grid point over the northern hemisphere oceans; the horizontal grid spacing is 1° longitude by 1° latitude.

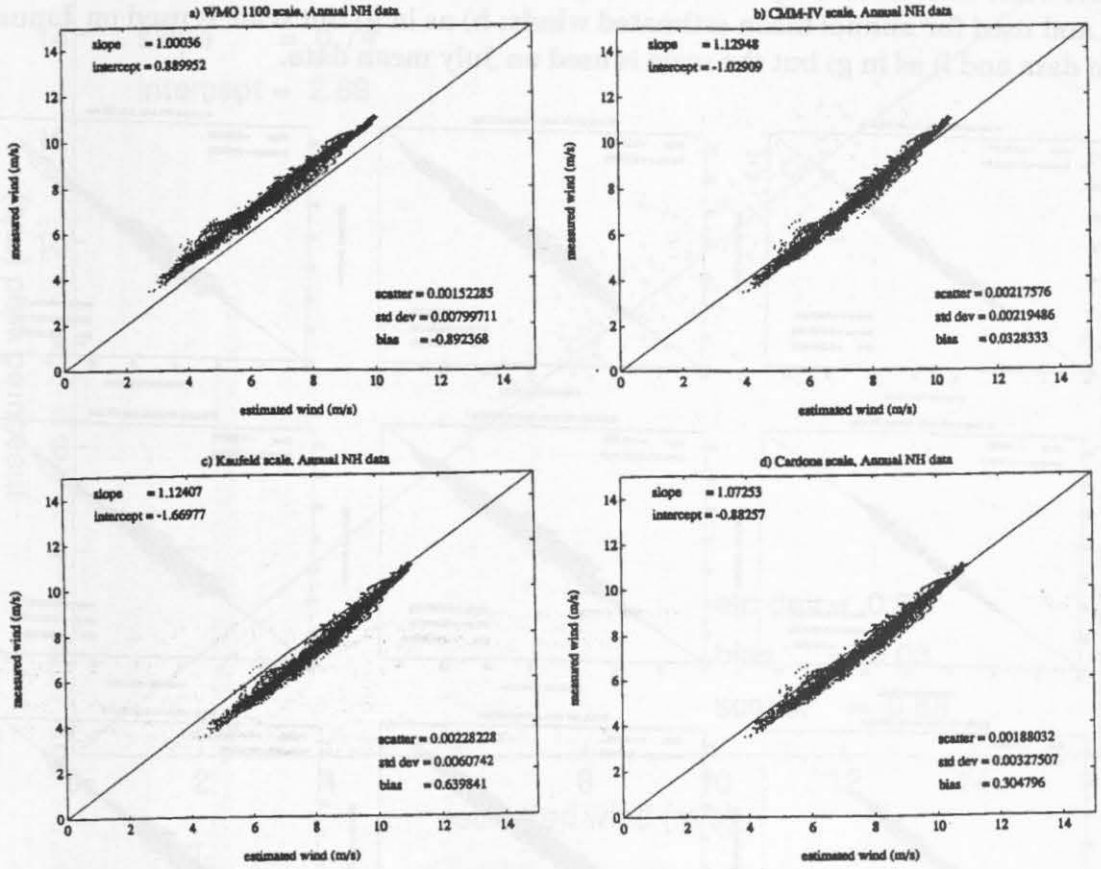

Figure 3: Analyzed estimated versus measured winds (northern hemisphere) with estimated winds based on several versions of our new Beaufort scale; a) the scale is developed based on annual mean data and used for annual mean estimated winds; b) as in a) but the scale is used on January mean data; c) as in a) but the scale is used on July mean data; d) the scale is developed based on January mean data and used for annual mean estimated winds; e) as in d) but the scale is used on January mean data; f) as in d) but hte scale is used on July mean data; g) the scale is developed based on July mean data and used for annual mean estimated winds; h) as in g) but scale is used on January mean data and i) as in g) but the scale is used on July mean data.

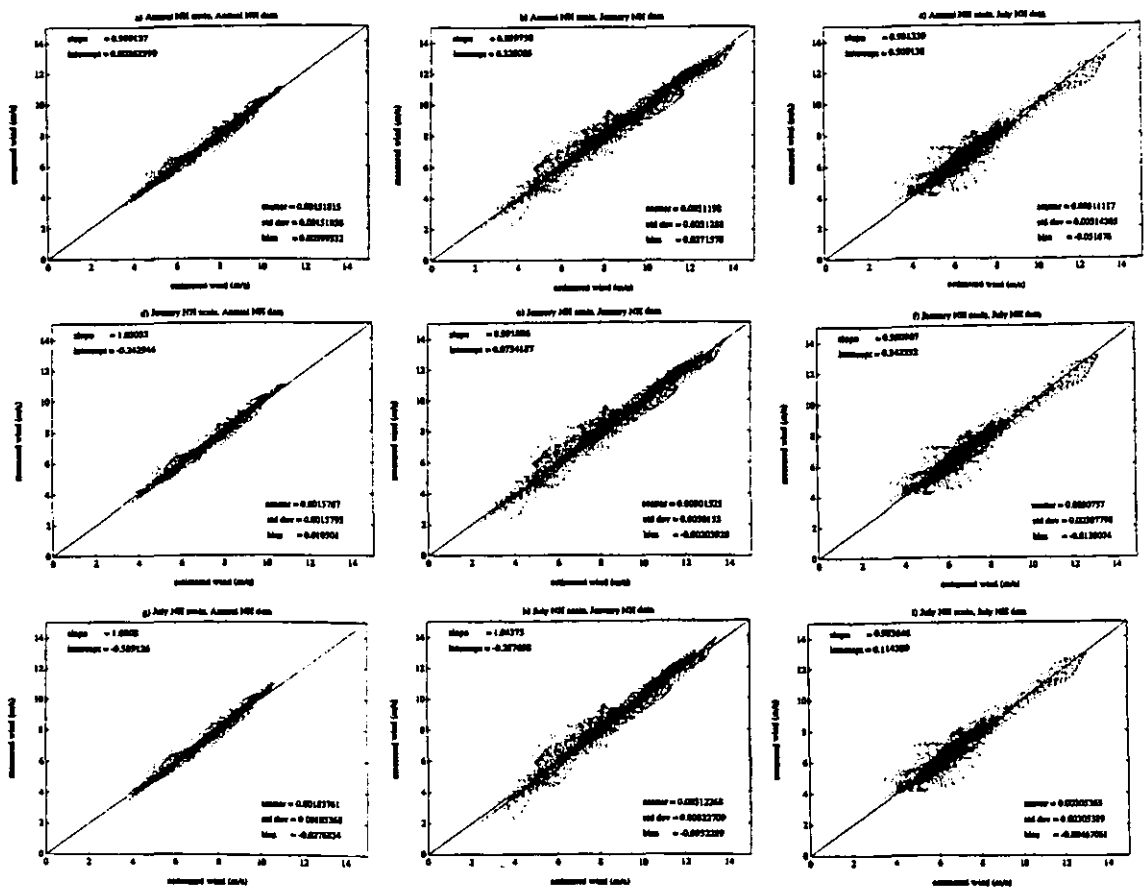

Figure 4: Estimate vs. measured winds for a 5 degree box around Ocean Weather Station Papa. Each dot corresponds to a monthly mean period 1970-89 in which more than 30 observations of each type were made inside the box.

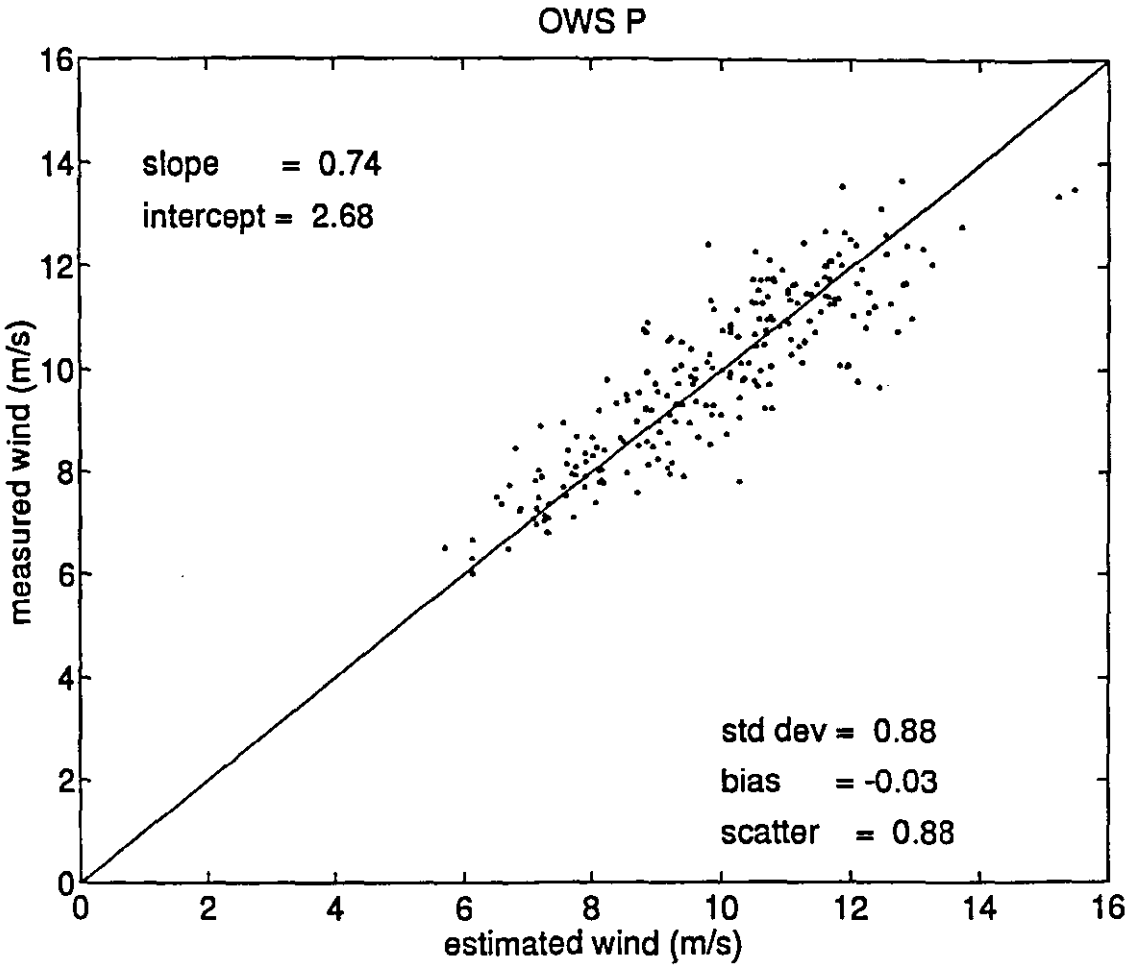

Figure 5.a: Analyzed annual estimated wind speeds over the global oceans. Our new beaufort equivalent scale has been used to produce the estimated winds. Contour interval 1 m/s.

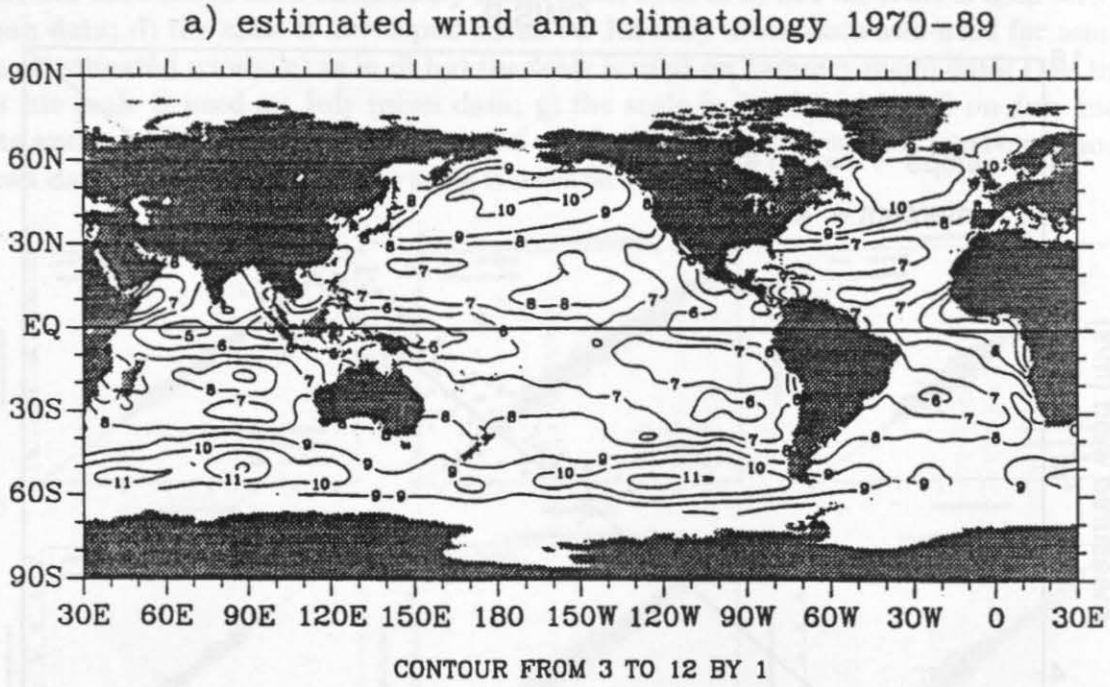

Figure 5.b: Analyzed annual measured wind speeds over the global oceans. Contour interval 1 m/s.

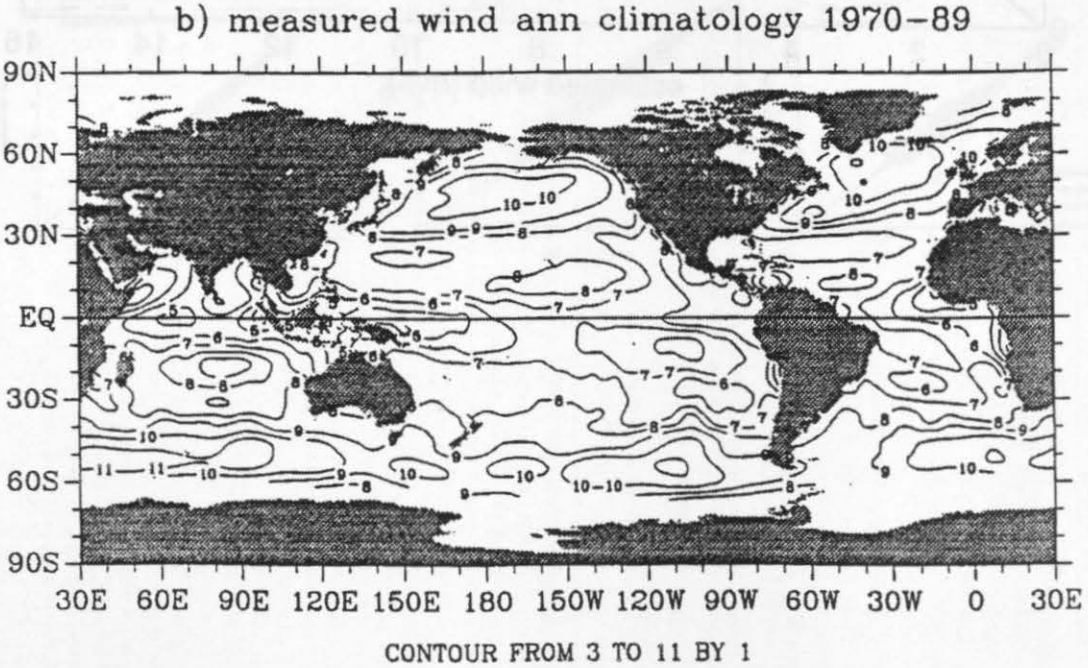

Figure 6a: January mean wind speed (1945-89) over the oceans, including both measured and estimated corrected winds; (contour interval: 1 m/s).

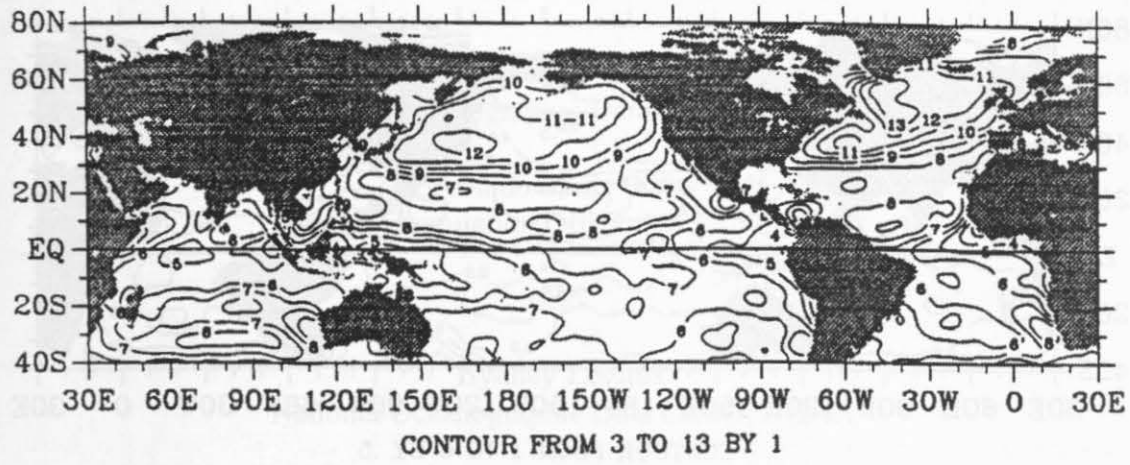

Figure 6b: January mean wind speed difference between corrected and reported wind speeds in COADS (contour interval: 0.1 m/s).

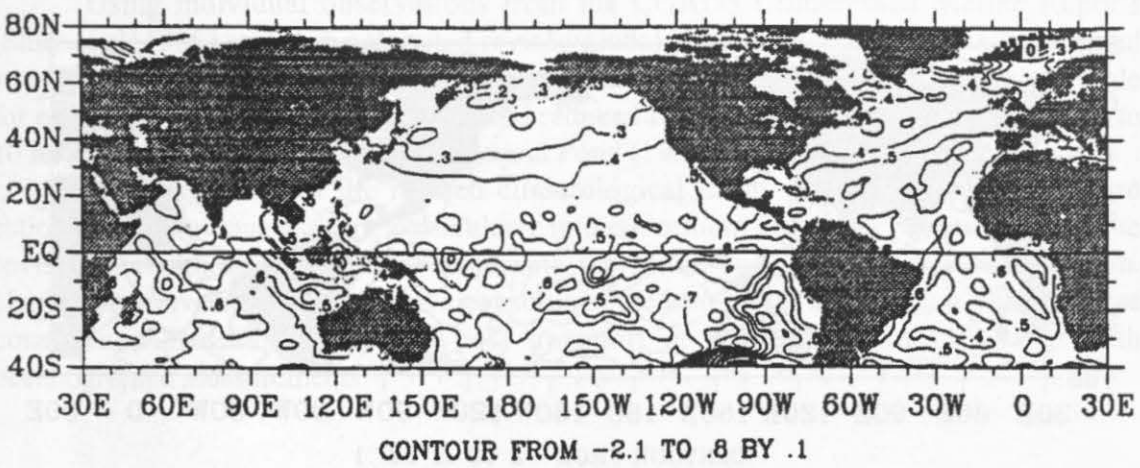

Figure 6c: January wind speed corrected standard deviation (1945-89) over the oceans, including both measured and estimated winds (contour interval: 0.5 m/s).

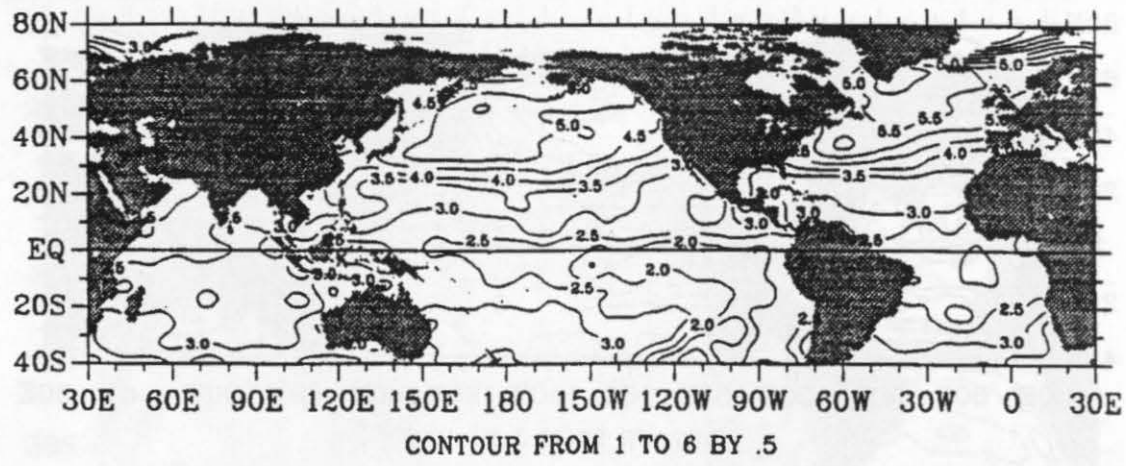

Figure 6d: January standard deviation difference between corrected and reported wind speeds in COADS (contour interval: 0.1 m/s).

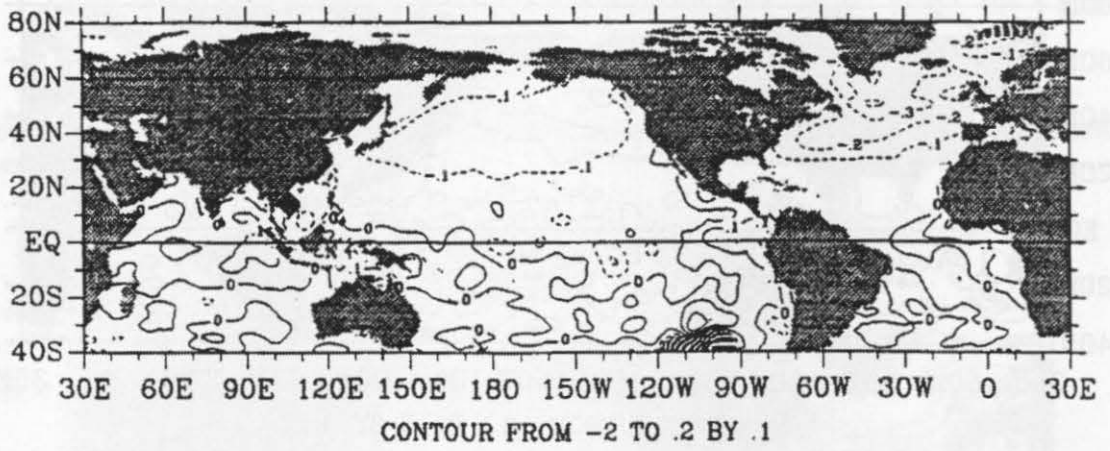

The Effect of a Revised Beaufort Equivalent Scale on Momentum and Heat Fluxes over the Global Oceans

Christine C. Young
National Oceanographic Data Center, NOAA

Arlindo M. da Silva
Data Assimilation Office, NASA/GSFC

and

Sydney Levitus
National Oceanographic Data Center, NOAA

Abstract

Using individual observations from the COADS Compressed Marine Reports (Slutz et al. 1985), we have computed revised global climatologies and anomalies of wind stress and heat fluxes. The flux computations utilize a revised Beaufort equivalent scale for estimated wind speeds, use wind speed reduced from an average anemometer height to 10 m above sea level, and include Large and Pond (1981, 1982) transfer coefficients.

The magnitude of the revised climatological mean wind stress is smaller than estimates by previous authors, particularly in the Northern Hemisphere extratropics. The revised heat fluxes appear to overestimate insolation and underestimate evaporation. Using linear inverse theory, we have constrained the heat fluxes to balance globally. These constrained heat fluxes produce heat transport in the Atlantic in agreement with oceanographic measurements.

Introduction

In a companion paper, da Silva et al. (1995, this volume) discussed the development of a new Beaufort equivalent scale. This scale was developed in an attempt to bring measured and estimated wind speeds in COADS (Slutz et al. 1985) into closer agreement. When this revised scale is applied to individual observations, the climatological wind speed increases compared to uncorrected winds, but the wind speed standard deviation decreases. When the revised scale is used for wind stress calculation, climatological wind stress decreases over large areas of the oceans. This effect is primarily due to the decrease in wind standard deviation. When the revised scale is used for latent and sensible heat fluxes, latent heat flux is slightly larger than the unrevised latent heat flux, and the revised sensible heat flux slightly smaller. In this paper we review the wind stress and heat flux products we have calculated using COADS individual observations and our revised Beaufort equivalent scale. We also describe the standard COADS Monthly Trimmed

Summaries versus our revised COADS Monthly Summaries, and we show the impact of the revised scale on wind stress and compare this resulting wind stress to that of other authors. We evaluate the impact of the new scale on heat fluxes, explain the derivation of the constrained heat flux product and compare this constrained product to the heat fluxes of other authors. The last part contains a summary of the important points of the study.

Products

The standard COADS Monthly Trimmed Summaries (MTS) are as follows (Slutz et al., 1985): Means and statistics are calculated globally in 2° x 2° latitude-longitude squares. No objective analysis is available with the standard release of COADS; the statistics are unfiltered and unsmoothed (although Oort and Pan [1986] applied an objective analysis to some of the 2° x 2° statistics). The observed quantities are winds, sea level pressure, surface sea and air temperature, specific humidity, cloudiness, among others. Derived quantities include zonal and meridional momentum and heat fluxes as well as other quantities. For any of the quantities involving wind, the WMO Code 1100 Beaufort equivalent scale is used to convert the Beaufort force wind estimates to wind speed. The derived quantities which can be used for oceanic forcing are pseudo wind stress: W_u, W_v, and pseudo heat fluxes: $W(T_s - T_a)$, $W(q_s - q)$. To properly use these fields as forcing quantities one can assume the transfer coefficients are constant or introduce wind speed/stability effects using monthly means with the so-called classical method.

The revised COADS Monthly Summaries we have produced differ from the standard MTS in several ways: only means, standard deviations, and number of observations are available on a 1° x 1° grid over the global ocean. In addition, an objective analysis has been applied to the means and standard deviations in order to fill in empty ocean squares and filter out noise. The analysis we use is a successive correction scheme with a Barnes response function—the same as used in Levitus (1982). We have the same observed quantities as the MTS and many of the same derived quantities. Our set also contains a few quantities, such as precipitation and shortwave radiation, that the MTS lack. For any quantities involving wind speed, we use our revised Beaufort equivalent scale. While the MTS provide pseudo heat and momentum fluxes, our product provides shortwave and longwave radiation to/from the sea surface in addition to latent/sensible heat flux and wind stress. These two radiation terms are not included in the MTS. Table 1 is a list of all fields we have calculated frotn the COADS individual observations.

For use as oceanic forcing terms, we have computed climatologies and anomalies of wind stress and heat fluxes using wind speed dependent and stability dependent transfer coefficients. We use the Large and Pond (1981, 1982) formulations for C_D, C_T, C_E If a wind observation is estimated, we correct it using our revised scale. We then reduce the estimated or measured wind speed observation to 10 m before computing the transfer coefficients.

Wind Stress

The bulk formulation for wind stress is as follows:

$$\tau = \rho C_D W_{10} \mathbf{u}_{10}$$

$$\mathbf{u}_{10} = (u_{10}, v_{10}), \text{ (at 10 m)}$$

$$W_{10} = \sqrt{u_{10}^2 + v_{10}^2}$$

$$C_D = C_N(W_{10}) f(Z / L), \text{ (drag coefficient)}$$

C_N = neutral drag coefficient

f = stability correction

Z = 10 m

L = Monin-Obukhov length

$$L = L(W, T_a, T_s - T_a, q_s - q)$$

Note that the drag coefficient is composed of the neutral drag coefficient and a stability correction. The neutral drag coefficient is a function of wind speed at 10 m. The stability correction is a function of the height (10 m) and the Monin-Obukov length. We convert the wind speed from the average anemometer height of 20 m to 10 m using standard surface layer similarity theory. If a wind observation was measured from a buoy, we convert the wind speed from 5 m to 10 m.

Effect of Corrections

To compare the effect of the revised Beaufort scale on wind stress, we compute two wind stress products. The first, revised or corrected wind stress, is calculated as explained above. The second, uncorrected, is computed the same as above except that the WMO Code 1100 scale is used for estimated winds and the anemometer height is assumed to be 10 m (i.e. no correction is made for height).

Figure 1 shows the global zonal means of the winter (DJF) zonal wind stress. Although the fields we calculate are global, we show only 60° S through 60° N here. This figure shows the revised wind stress as defined previously and the unrevised wind stress (in W/m^2). Notice that in large areas of the extratropics, the corrected (revised) wind stress is less than the uncorrected wind stress. Although wind speed increases when the revised scale is applied, the wind stress decreases in many areas. This is mainly due to the large decrease in the standard deviation of the wind speed.

Comparison with Other Authors

We compare our revised wind stress to the fields computed by other authors by studying the response of a simple model. The linear, barotropic model of Fanning et al. (1994) of the North Atlantic ocean using smoothed topography was forced with our revised wind stress fields. We compare the seasonal transport anomaly through the Florida Straits in response to four different wind stress estimates (part of this comparison can be found in Fanning et al. 1994). Figure 2 shows the transport anomaly at the Florida Straits as calculated from cable measurements (Larsen 1992) and as calculated in response to four different wind stress estimates:

1. Hellerman and Rosenstein (1983) who use ship winds and a rather large estimate for C_D.

2. Trenberth et al. (1990) who use ECMWF 1000 mb winds as surface winds and the Large and Pond (1981) formulation for C_D.

3. Isemer and Hasse (1987) who correct Bunker's (1976) monthly mean values of wind stress (large C_D)

4. Our corrected wind stress as explained in this paper.

The transport from the Isemer and Hasse wind stress has the largest anomaly. This is expected due to the large C_D in the Bunker data and their Beaufort scale correction which increases wind stress. Our wind stress estimate produces the smallest transport anomaly of all. This results from the relatively small Large and Pond C_D and our Beaufort/anemometer height correction which decreases wind stress over large parts of the North Atlantic. For this particular model, our corrected wind stress appears to underestimate ocean transport in the North Atlantic.

We have also compared our wind stresses, over time, to pseudo wind stresses derived by Servain and Lukas (1990) and Goldenberg and O'Brien (1981). Figure 3 shows the temporal correlation between the pseudo stress magnitudes in northern winter (DJF) over two regions: the Tropical Atlantic and the Tropical Pacific. Figure 3 is the correlation between our wind stress and the Servain and Lukas (1990) pseudo wind stress over the Tropical Atlantic. Note that several large areas have correlations exceeding 80% and correlations in most areas exceed 60%. Areas which. have lower correlations tend to be regions in which there are few observations. Temporal correlations in the Tropical Pacific (Figure 4) between our wind stress and the pseudo stress of Goldenberg and O'Brien (1981) are not as high. This is not unexpected due to the scarcity of observations in the equatorial Pacific. Farther away from the Equator, where the observation density is higher, the correlations are higher. This is particularly evident in the northern hemisphere.

Heat Fluxes

Using the COADS individual observations, we have also computed the four components of net heat flux: latent heat flux, sensible heat flux, incoming shortwave radiation, and outgoing longwave radiation. When computing latent and sensible heat flux, we use our revised Beaufort equivalent scale, reduce the winds to 10 m, and use Large and Pond's (1982) transfer coefficients.

Revised Scale and Constrained Product

An accurate estimate for net heat flux will produce a physically consistent global heat balance. Here we check the consistency of our revised net heat flux. The vertically integrated heat budget equation for the oceans is

$$\frac{\delta \mathrm{H}}{\delta \mathrm{t}} + \nabla \cdot \mathcal{H} = Q_{net}$$

where

$$\begin{aligned} \mathrm{H} &= \text{Heat content} \\ \mathcal{H} &= \text{Heat transport} \\ Q_{net} &= \text{Net heat flux at the surface} \\ &= Q_{SW} - (Q_{LW} + Q_L + Q_S) \end{aligned}$$

Integrating over many years we assume the heat storage vanishes:

$$\nabla \cdot \overline{\mathrm{H}} = \overline{Q}_{net}$$

Neglecting the heat storage, the average annual net heat flux over the global oceans must be zero:

$$\iint_{Globe} \overline{Q_{net}} dx dy = 0$$

But, because $\overline{Q_{net}}$ is computed as difference of large, uncertain terms, the condition above is not met. Figure 5 shows the mean annual net heat flux over the global ocean (in W/m^2). It is clear that the amount of outgoing (negative) heat flux is not sufficient to balance the amount of incoming (positive) heat flux.
However, "small" adjustments in the bulk formulas can produce a physically consistent net heat flux. Following the method of Isemer et al. (1989), we use linear inverse theory (Menke 1984) to introduce non-dimensional correction factors to the bulk formulas. We assign a correction factor p to each term which is likely to be a source of error:

$$Q_{SW} = p_{Tr} Q_{clear} (1 - p_c 0.62c + 0.0019\beta)(1 - \alpha)$$

$$Q_{LW} = \varepsilon\sigma T_s^4 p_e(0.39 - 0.05\sqrt{e})(1 - p_x X c^2) + 4\varepsilon\sigma T_s^3(T_s - T_a)$$
$$Q_L = p_L \rho c_p L_E C_E W(q_s - q)$$
$$Q_S = p_S \rho c_p C_T W(\theta_s - \theta)$$

We choose the transmissivity term of the clear sky radiation and the cloudiness term as likely sources of error in the shortwave formula (Q_{SW}). For longwave radiation (Q_{LW}), we choose the vapor pressure term and the cloudiness coefficient. For latent and sensible heat (Q_L, Q_S) we combine the errors likely to be found in the transfer coefficients and the difference terms and assign a single correction factor to each of the two fluxes. We assume that each error is statistically independent of the others. In the original calculation of heat flux, the factors $p_{Tr}, p_c, p_e, p_X, p_L$ and p_S as are each equal to one. The goal is to find small corrections to the *p's* so that the meridional heat transport, $\mathcal{H}$, is consistent with oceanographic measurements. We use linear inverse theory to calculate the small corrections. In order for the solution to be acceptable, the corrections to the *p's* must be smaller than the error allowance for each correction factor. We set the error limit for the latent and sensible heat flux factors to be 20%. The rest of the factors are allowed 10% error which is the approximate error for meridional heat flux measurements. As an example, we calculate the corrections so that the global meridional heat flux is constrained to zero at the southern boundary:

$$\delta p_{Tr} = -7\%$$
$$\delta p_c = +4\%$$
$$\delta p_e = +2\%$$
$$\delta p_X = -1\%$$
$$\delta p_L = +15\%$$
$$\delta p_S = +1\%$$

These corrections are smaller than the allowed error and thus are acceptable. The corrections serve to reduce shortwave radiation and increase evaporation. This finding is consistent with what Oberhuber (1988) did in order to balance his calculation of net heat flux, which was based on the classical method.

Figure 7 shows the constrained meridional heat transport using the corrections listed above. The transport (in 10^{15} W) is shown for the global ocean and for each individual ocean. Three measurements of meridional transport in the Atlantic are also shown. Our constrained Atlantic transport is within the error bars of Wunsch's (1984) and Hall and Bryden's (1982) measurements. Our Atlantic transport does not approach the measurement of Rago and Rossby (1987) who admit their measurement to be rather large. Figure 6 shows the constrained annual mean net heat flux. The negative and positive regions of net heat flux (in W/m^2) now balance out globally; the equilibrium considerations are met.

Comparison with Other Authors

The main component of the outgoing portion of net heat flux is the latent heat flux. For simplicity we compare orfly our constrained latent heat flux to other authors. Figure 8 shows zonal averages of global latent heat flux (in W/m^2) in winter for various authors. Our revised latent heat flux, labeled "UWM" is shown in comparison to Oberhuber (1988), and Esbensen and Kushnir (1981), whose data are obtained from ship observations. We also compare our flux to the latent heat flux estimated by Busalacchi et al. (1993) derived from SSM/I satellite measurements of winds with fields of temperature and moisture from the Goddard Laboratory for Atmospheres Fourth-Order General Circulation Model.

In general, our revised, constrained latent heat flux is greater than that derived by other authors. This is mainly due to the 15% increase in latent heat flux obtained when we apply the constraint parameters. The latent heat flux of the other authors only exceeds our constrained flux in two regions. The first is south of about 40°S where the derived fields are unreliable due to low observation density (with the probable exception of SSM/I). The second region in which our latent heat flux is less than the other authors' is in the northern hemisphere extratropics. Our revised latent heat flux tends to be less than Oberhuber's (1988) estimate north of around 35°N. Oberhuber used a value for Charnock's constant nearly six times the value we use. This increases his latent heat flux estimate significantly in regions where the friction velocity is high, namely north of around 30°N in the Atlantic and Pacific during the northern hemisphere winter.

Our revised latent heat flux is generally greater than that of Esbensen and Kushnir (1981), who calculated their flux using the classical method. In some cases, this method can produce latent heat flux values greater than the method using individual observations (Esbensen and Reynolds 1981). At low to moderate wind speeds, their transfer coefficients (Liu et al. 1979) tend to be much smaller than our transfer coefficients in unstable conditions, but slightly larger in neutral or stable conditions. As the winter marine atmosphere is definitely unstable north of 40° N. it appears that the Esbensen and Kushnir latent heat fluxis greater than or equal to ours north of 45° N due to either their monthly mean calculations or a difference in the data sets.

The SSM/I latent heat flux is greater than our revised latent heat flux north of 20°N. A similar pattern does not exist in the sensible heat flux which tells us that the excess is not due to a wind speed difference. The difference must lie in the analyses of temperature and/or moisture. Compared to Isemer and Hasse (1987) [comparison not shown] our latent heat flux is smaller. This is due to the same reasons that their wind speed exceeded our revised wind speed: the Large and Pond transfer coefficients that we use tend to be smaller than their coefficients and their Beaufort correction tends to increase wind speeds by a larger amount than does our correction.

Concluding Remarks

Our revised wind stress fields, computed from COADS individual observations using our revised Beaufort equivalent scale, Large and Pond transfer coefficients, and the anemometer height reduction, are smaller than previous estimates. The revised stresses

"under estimate" the transport anomaly through the Florida Straits in a linear barotropic model. However, a study in progress shows that, used in a tropical model, the revised stresses produce a realistic climatology and interannual variability of sea surface temperature in the Tropical Atlantic ocean.

Heat fluxes computed solely from the bulk formulas appear to overestimate shortwave radiation and underestimate evaporation. Thus they are not able to satisfy global equilibrium conditions. By using simple linear inverse theory we can impose small corrections upon the bulk formulas to produce heat transports in agreement with some oceanographic measurements. Our constrained latent heat flux is generally greater than the latent heat fluxes of other authors.

Acknowledgments

We would like to thank A. Fanning for kindly running his model with our revised stress. Work presented in this paper has been supported by NSF grant ATM 9215811 (AMdS/CCY) and by NOAA's Climate and Global Change Program (SL/CCY).

References

Busalacchi, A. J., R. M. Atlas, E. C. Hackert, 1993: Comparison of special sensor microwave imager vector wind stress with model-derived and subjective products for the tropical Pacific. *J. Geophys. Res.*, 98, 6961-6977.

Bunker, A. F., 1976: Computations of surface energy fiux and annual air-sea interaction cycles of the North Atlantic Ocean. *Mon. Wea. Rev.*, 104, 1122-1140.

Esbensen, S. K., and Y. Kushnir, 1981: The heat budget of the global oceans: An atlas based on estimates from marine surface observations. Oregon State University Climate Research Institute Rep. No. 29, 27 pp.

Esbensen, S. K., and R. W. Reynolds,1981: Estimating monthly averaged air-sea transfers of heat and momentum using the bulk aerodynamic method. *J. Phys. Oceanogr.*, 11, 457-465.

Fanning, A. F., R. J. Greatbach, A. M. da Silva and S. Levitus, 1994: Model-calculated seasonal transport variations through the Florida Straits: A comparison using different wind-stress climatologies. *J. Phys. Oceanogr.*, 24, 30-45.

Goldenberg, S. B., and J. J. O'Brien, 1981: Time and space variability of tropical Pacific wind stress. *Mon. Wea. Rew.*, 109,.1190-1207.

Hall, M. M., and H. L. Bryden, 1982: Direct estimates and mechanisms of ocean heat transport. *Deep-Sea Res.*, 29, 339-359.

Hellerman, S., and M. Rosenstein,1983: Normal monthly wind stress over the World Ocean with error estimates. *J. Phys. Oceanogr.*, 13, 1093-1104.

Isemer, H.-J., and L. Hasse, 1987: The Bunker Atlas of the North Atlantic Ocean. Vol. 2: Air-sea Interactions. Springer Verlag, 252 pp.

Isemer, H.-J., J. Willebrand and L. Hasse, 1989: Fine adjustment of large air-sea energy

flux parameterizations by direct estimates of ocean heat transport. *J. Climate*, 2, 1173-1184.

Large, W., and S . Pond,1981: Open ocean momentum flux measurements in moderate to strong winds . *J. Phys. Oceanogr.*, 11, 324-336.

Large, W., and S. Pond, 1982: Sensible and latent heat flux measurements over the ocean. *J. Phys. Oceanogr.*, 12, 464-482.

Larsen, J. C., 1992: Transport and heat flux of the Florida Current at 27°N derived from cross-stream voltages and profiling data: Theory and observations. *Phil. Trans. Roy. Soc. London A*, 338, 169-236.

Levitus, S., 1982: Climatological Atlas of the World Ocean, NOAA Prof. Paper No. 13, US Government Printing Office, Washington DC, 17 fiches, 173 pp.

Liu, W. T., K. B. Katsaros and J. A. Businger; 1979: Bulk parameterization of air-sea exchanges of heat and water vapor including the molecular constraints at the interface. *J. Atmos. Sci.*, 36, 1722-1735

Menke, W., 1984: *Geophysical Data Analysis: Discrete Inverse Theory*. Academic Press, 257 pp.

Oberhuber, J. M., 1988: An Atlas Based on the COADS Data Set: The Budgets of Heat, Buoyancy, and Turbulent Kinetic Energy at the Surface of the Global Ocean. Report No. 15, Max-Planck Institut fur Meteorology.

Oort, A. H., and Y.-H. Pan, 1986: Diagnosis of historical ENSO events. Programme on Long-Range Forecasting Research, No. 6, Vol. 1, WMO/TD-No. 87, World Meteorological Organization,249-258.

Rago, T. T., and H. T. Rossby, 1987: Heat transport into the North Atlantic Ocean north of 27°N latitude. *J. Phys. Oceanogr.*, 17, 854-871.

Servain, J., and S. Lukas, 1990: G1imatic Atlas of the Tropical Atlantic Wini Stress ani Sea Svrface Temperatare 19851989. IFREMER, SDP, Brest, France, 143 pp.

Slutz, R. J., S. J. Lubker, J. D. Hiscox, S. D. Woodruff, R. L. Jenne, D. H. Joseph, P. M. Steurer and J. D. Elms, 1985: COADS, Comprehensive Ocean-Atmosphere Data Set, Release 1. Climate Research Program, Environmental Research Laboratory, Boulder, CO 262 pp.

Trenberth, K. E., W. G. Large and J. G. Olson, 1990: The mean annual cycle in global ocean wind stress. *J. Phys. Oceanogr.*, 20, 1742-1760.

Wunsch, C., 1984: An eclectic Atlantic Ocean circulation model. Part I: The meridional flux of heat. *J. Phys. Oceanogr.*, 14, 1712-1733.

Table 1: Variables in the UWM/COADS data set

File Name	Units	Description
airdens.nc	kg/m^3	sea level air density
bouy5.nc	$kg/(m^{3)}$	constrained bouy flux
cloud.nc	fraction of 1.	fractional cloudiness
evaprate.nc	mm/(3 hours)	evaporation rate
fvcubed.nc	m^3/s^3	ocean friction velocity cubed
icemask.nc	(none)	icemask
latent3.nc	W/m^2	corrected latent heat flux
longrad.nc	W/m^2	outgoing longwave radiation
netheat5.nc	W/m^2	constrained net heat flux
precip6.nc	mm/(3 hours)	precipitation rate
qair.nc	g/kg	specific humidity
qs_qa.nc	g/kg	qsea minus qair
qsea.nc	g/kg	sea level specific humidity
rh.nc	%	relative humidity
sat.nc	C	sea level air temperature
sensib3.nc	W/m^2	corrected sensible heat flux
shortrad.nc	W/m^2	incoming short wave radiation
slp.nc	mb	sea level air pressure
sst_sat.nc	C	sea minus air temperatue
sst.nc	C	surface temperature
taux3.nc	N/m^2	corrected zonal wind stress
tauy3.nc	N/m^2	corrected meridional stress
u3.nc	m/s	corrected zonal wind
ua.nc	K m/s	zonal heat flux
uq.nc	m/s	zonal moisture flux
v3.nc	m/s	corrected meridional flux
va.nc	K m/s	meridional heat flux
vappress.nc	mb	vapor pressure
virtemp.nc	C	virtual temperature
vq.nc	m/s	meridional moisture flux
w3.nc	m/s	corrected wind speed
zdl.nc	(unitless)	10m/(Monin Obukov length)

Figure 1: Zonal wind stress averaged zonally over the globe (N/m^2) for boreal winter (DJF). Revised stress (Corrected, solid line) is computed using the revised Beaufort scale with anemometer height reduction to 10 m. Uncorrected (broken line) stress is computed using the WMO Code 1100 without anemometer height reduction.

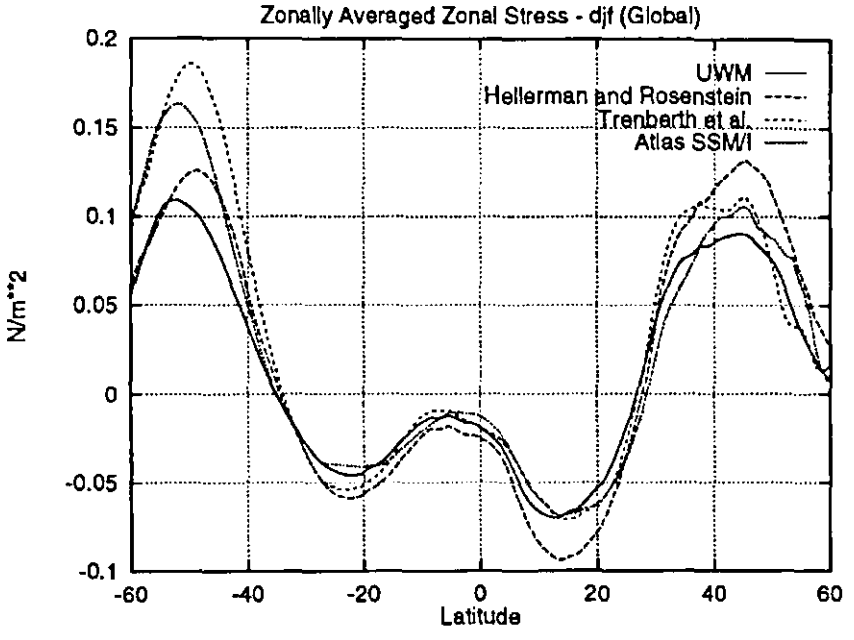

Figure 2: Transport anomaly (Sv) through the florida Straits observed from cable measurements (shown with error bars) [Larsen 1992] and from a linear barotropic model using smoothed topography. Modeled transport is in response to wind stress fields from (IH) Isemer and Hasse [1987], (HR) Hellerman and Rosenstein [1983]. (TR) Trenberth et al., [1990], and our (DS) corrected wind stress.

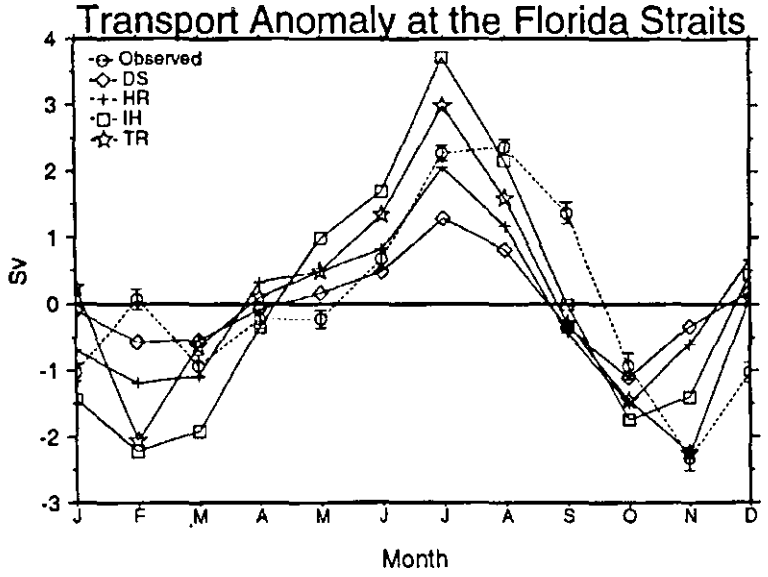

Figure 3: Correlation (%) between our revised wind stress and psuedo wind stress derived by Servain and Lukas (1990) for boreal winter (DJF).

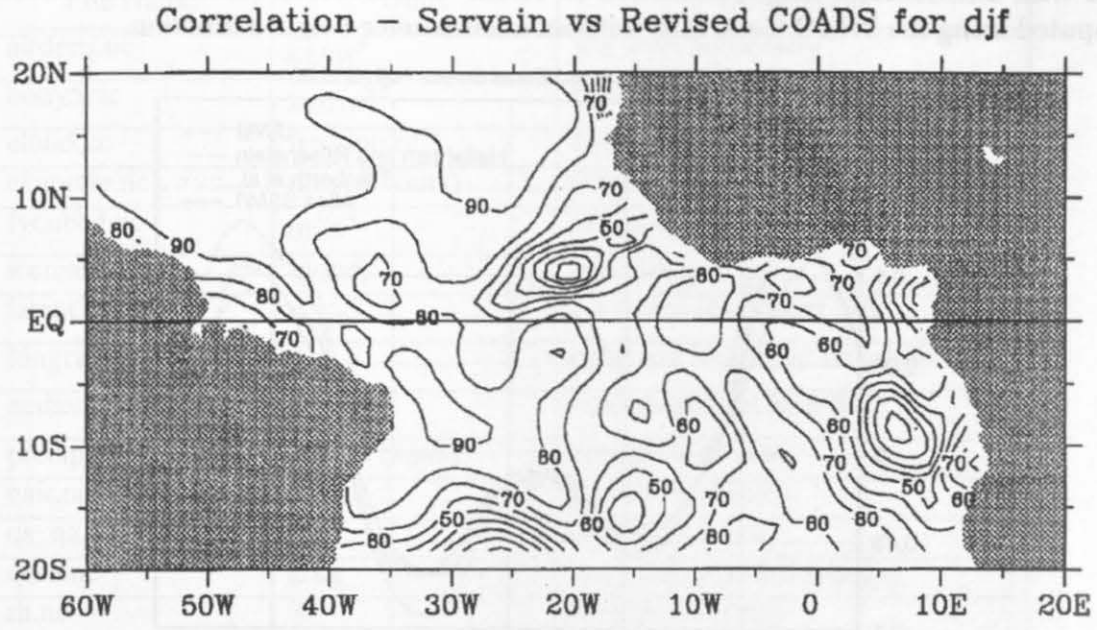

Figure 4: Correlation (%) between our revised wind stress and psuedo wind stress derived by Goldenberg and O'Brien (1981) for boreal winter (DJF).

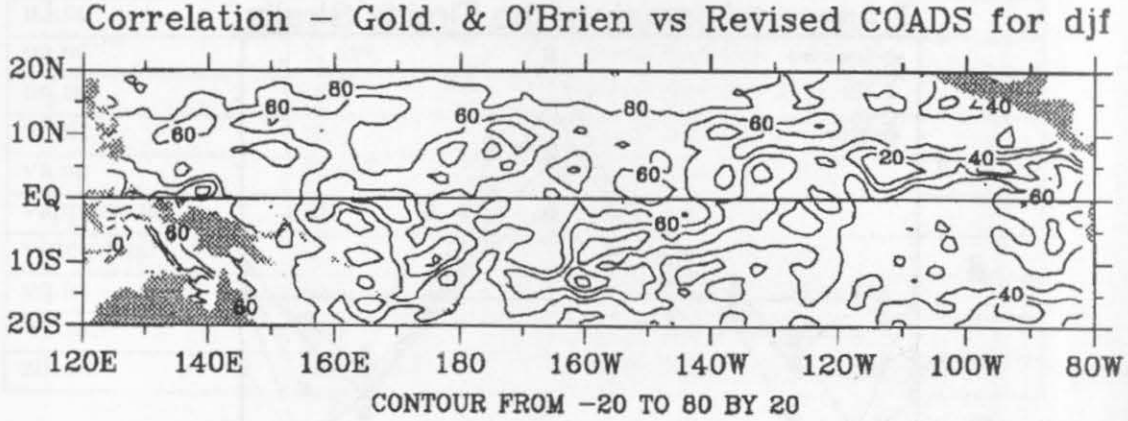

Figure 5: Revised, but unconstrained annual mean net heat flux over the global ocean (W/m^2). Heat flux is computed using the revised Beaufort scale with anemometer height reduction to 10m.

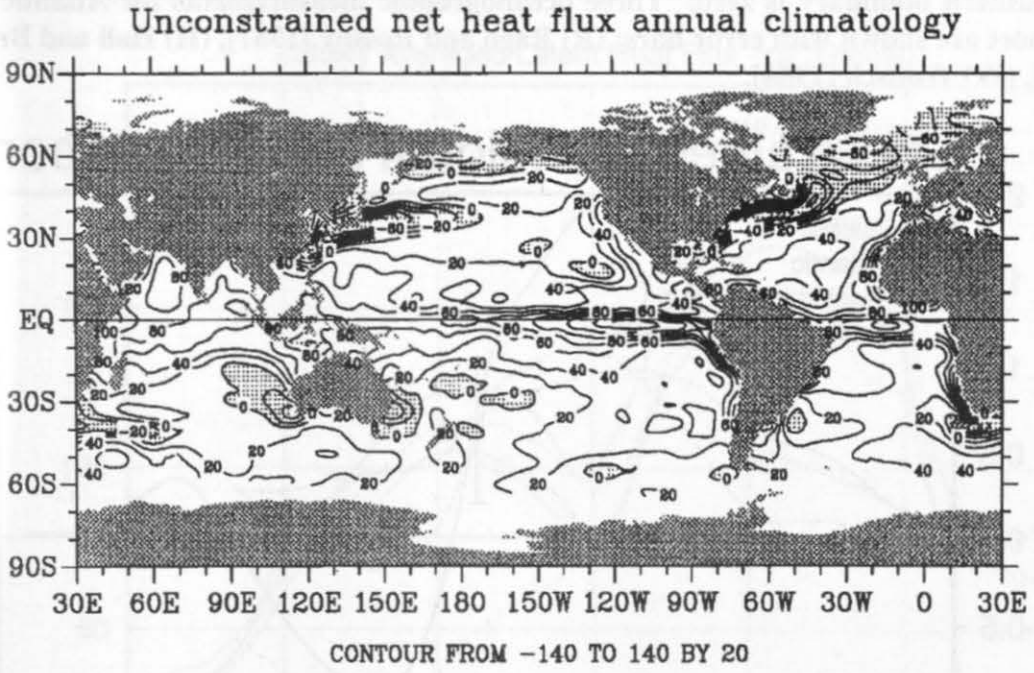

Figure 6: Revised, constrained annual mean net heat flux over the global ocean (W/m^2). Heat flux is computed using the revised Beaufort scale with anemometer height reduction to 10 m and constraineed so that the global meridional heat transport at the southern boundary is zero.

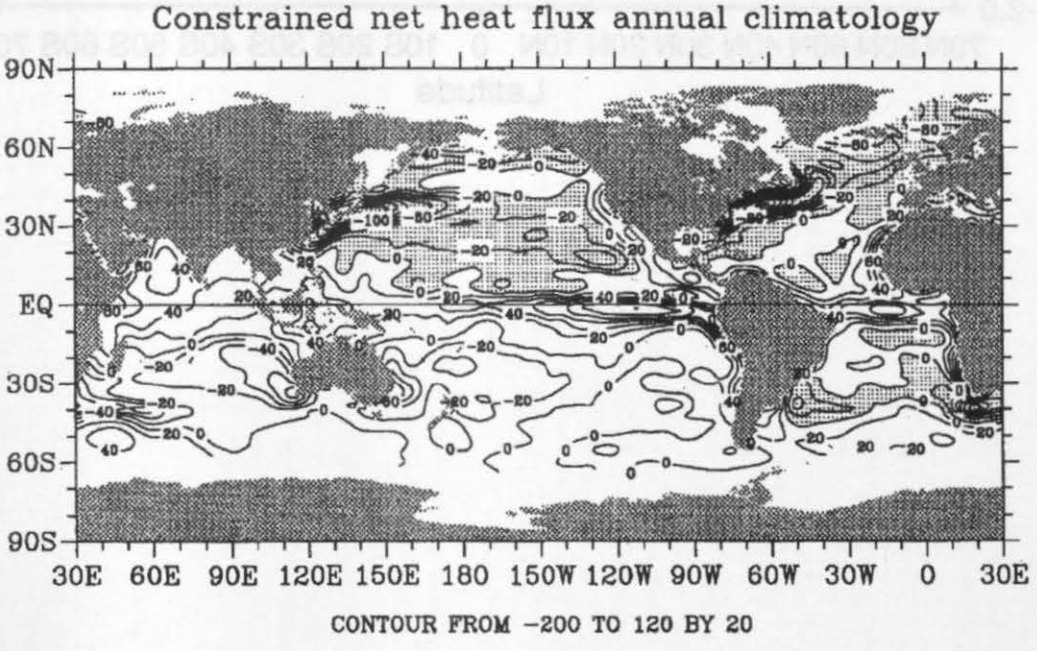

Figure 7: Meridional heat transport (1 PW=10^{15}W) calculated from constrained net heat flux. Heat flux is computed using the revised Beaufort scale with anemometer height reduction ot 10 m and constrained so that the global meridional heat transport at the southern boundary is zero. Three oceanographic measurements for Atlantic heat transport are shown with error bars: (R) Rago and Rossby [1987], (H) Hall and Bryden [1982], (W) Wunsch [1984].

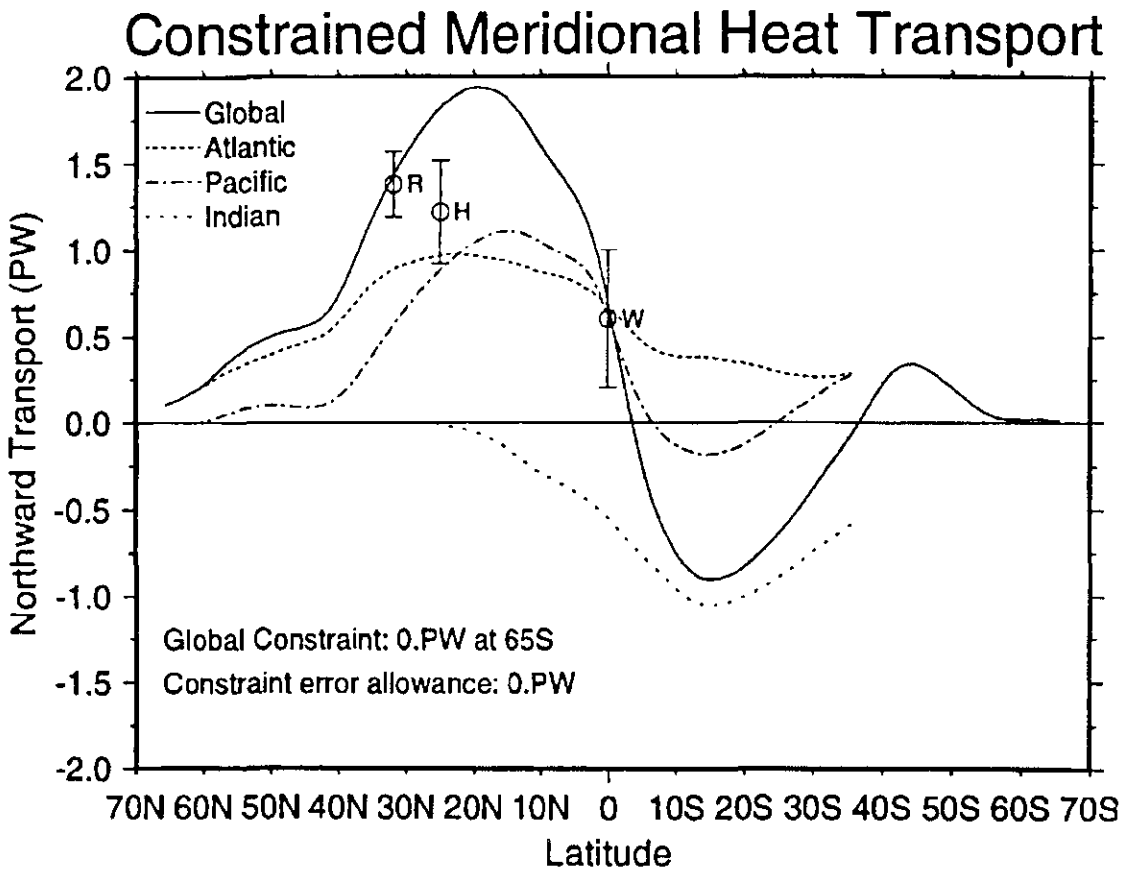

Figure 8: Zonal averages of latent heat flux (W/m^2) over the globe for boreal winter (DJF). Our revised, constrained latent heat flux [solid line] is compared to the latent heat fluxes of Oberhuber et al., (1988) [long dash], Esbensen and Kushnir (1981) [medium dash], and Busalacchi et al., (1993) [short dash].